The role of BCL-3 feedback loops in regulating NF-κB signalling

A thesis submitted to the University of Manchester for the degree of Doctor of Philosophy
in the Faculty of Engineering and Physical Sciences

2012

Thomas Walker

School of Chemical Engineering and Analytical Sciences
Integrative Systems Biology

Contents

Contents..... 1
Word count..... 9
List of figures..... 9
List of tables..... 11
Abbreviations..... 11
Abstract..... 15
Declaration & Copyright Statement..... 16
Acknowledgements..... 17

Chapter 1
Introduction..... 18

1.1. The inflammatory response..... 18
1.1.1. PAMPs: initial indicators of infection..... 18
1.1.2. The inflammatory response..... 19
1.1.3. Cytokines..... 19
1.1.3.1. The TNF family of cytokines..... 20
1.1.3.2. The TNFR family..... 20
1.1.3.3. Diverse cell types produce and are responsive to TNFα..... 21
1.1.4. Fibroblasts as inflammation mediators..... 21

1.2. NF-κB transcription factors..... 22
1.2.1. NF-κB subunits and dimer combinations..... 22
1.2.2. Canonical NF-κB signalling..... 23
1.2.3. p50 homodimers..... 25
1.2.4. Non-canonical NF-κB signalling..... 26
1.2.5. Post transcriptional modification of NF-κB factors..... 27
1.2.6. DNA sequence specific binding of NF-κB..... 27
1.2.6.1. Variant κB sites have different affinities for NF-κB dimers..... 27
1.2.6.2. The dynamic nature of κB site binding..... 28
1.2.6.3. Dynamic NF-κB DNA binding is made possible by active removal mechanisms..... 28
1.2.7. NF-κB as a transcription mediator..... 29
1.2.8. NF-κB and other cytokine induced signalling pathways..... 30

1.3. The IκB family of proteins..... 30
1.3.1. BCL-3: A distinct member of the IκB family..... 30
1.3.1.1. BCL-3..... 31
1.3.2. BCL-3 binds a specific subset of NF-κB dimers..... 31
1.3.3. Sub-cellular localisation of BCL-3..... 32
1.3.4. Post-transcriptional modification of BCL-3..... 32
1.3.5. The cellular function of BCL-3..... 32
1.3.6. BCL-3 effects on NF-κB binding..... 33
1.3.6.1. BCL-3 enhances the DNA binding abilty of p50 and p52 homodimers..... 33
1.3.6.2. Negative effects of BCL-3 on p50/p52 homodimer DNA binding..... 33
1.3.7. Functional effects of BCL-3 complexes..... 34
1.3.7.1. Negative effects of BCL-3 on transcription: HDAC recruitment..... 34
1.3.7.2. BCL-3 as a positive transcription factor..... 35

1.3.7.3. The contrary nature of BCL-3 activity…… 36
1.3.8. NF-κB mediated induction of BCL-3……..... 37
1.3.9. Anti-inflammaoty cytokines and *BCL3* expression: IL-9 and -10…….. 37
1.3.10. Negative feedback and BCL-3…….. 37

1.4. TNFα: An inducer and target of NF-κB signalling…… 38
1.4.1. NF-κB induces *TNFA* promoter activity…… 38
1.4.2. Cytokine overexpression…… 38
1.4.3. Mechanisms to reduce the extent of NF-κB signalling…….. 38
1.4.3.1. IκB negative feedback…….. 38
1.4.3.2. A20…… 39
1.4.3.3. Post-transcriptional modifcation of NF-κB……..... 39
1.4.4. Limiting *TNFA* transcript induction to inflammatory stimuli…… 40
1.4.4.1. *TNFA* mRNA stability…… 40
1.4.4.2. BCL-3 as a direct inhibitor of TNFα self induced transcription…… 40
1.4.5. The dynamic nature of the *TNFA* gene promoter…….. 40
1.4.5.1. *TNFA* promoters across species: From mouse to human…….. 41
1.4.5.2. κB sites within the human *TNFA* promoter: Spatial segregation of …….. 42
contrary roles…….. … 43
1.4.5.3. Competition at distal binding sites…….. 43

1.5. Chromatin strutre and dynamics…….. 44
1.5.1. Chromatin structure…… 44
1.5.2. Nucleosomes and transcription factor binding……..... 45
1.5.3. Nucleosome positioning…….. 46
1.5.4. Chromatin remodelling……..... 47
1.5.4.1. Nucleosome binding activity of chromatin remodelling complexes…… 48
1.5.5. Post transcriptional modification of histones……..... 48
1.5.6. Inducible HAT recruitment…… 49

1.6. RNA polymerase II dynamics and binding…….. 50
1.6.1. Pre-initiaion complex assembly…… 50
1.6.2. Core promoter elements…… 51
1.6.3. TBP induced DNA curvature…… 52
1.6.4. Nucleosome Depleted Regions (NDRs)…….. 53
1.6.4.1. Flanking nucleosomes…… 53
1.6.4.2. Histone modification and open chromatin at the TSS……..54
1.6.4.3. Sequence mediated NDRs…… 54
1.6.4.4. Inducible or constitutive chromatin marks at gene TSSs…… 55
1.6.5. The RNA polymerase II transcription cycle……55
1.6.5.1. Pre-RNAP binding transcription control…….. 56
1.6.5.2. Post-RNAP binding transcription control…… 56
1.6.5.2.1. Overcoming nucleosome obstacles…….. 57
1.6.5.2.2. Non-nucleosome mediated pausing mechanisms…… 57
1.6.5.2.2.1. Transcription initiation and promoter escape…… 58
1.6.5.3. DSIF/NELF mediated arrest…… 58
1.6.5.4. P-TEFb mediated release from pausing…… 59
1.6.5.5. P-TEFb and recruitment of RNA processing factors…… 60
1.6.5.6. RNAP backtracking and TFIIS mediated release……60
1.6.6. Functions of pre-stimulus bound and paused RNAP…… 61
1.6.7. Transcription activators – differential points of activity…… 63
1.6.8. NF-κB conducts transcription activation roles at multiple sites in the
transcription cycle……..... 63
1.6.8.1. Timing of NF-κB transcription induction……63
1.7. Aims of the work…….. 63

Chapter 2
Materials and Methods…… 65

2.1. Cell culture…… 65
2.1.1. Cell lines used…… 65
2.1.1.1. SK-N-AS…… 65
2.1.1.2. HT1080…… 65
2.1.2. Cell culture…… 65
2.1.2.1. Cell growth conditions…… 65
2.1.2.2. Adherent cell detachment…… 66
2.1.2.3. Cell sub-culturing…… 66
2.1.3. Cell stimulation with TNFα…… 66
2.1.4. Cell treatment reagents…… 66
2.1.5. Counting cells…… 67
2.1.6. Cryopreservation of HT1080 cell line…… 67
2.1.7. Cell viability assay…… 67

2.2. Quantitative real time reverse transcriptase PCR (qRT-PCR)……68
2.2.1. RNA extraction……68
2.2.2. cDNA synthesis……68
2.2.3. qRT-PCR conditions……68
2.2.4. Ct method and Statistical comparison of data…… 69

2.3. Human cell transfection…… 70
2.3.1. Plasmid transfection of HT1080 cells…… 70
2.3.1.1. ExGen500…… 70
2.3.1.2. FuGene 6…… 70
2.3.2. siRNA transfection…… 71
2.3.2.1. Lipofectamine 2000…… 71
2.3.3. BAC transfection…… 71

2.4. Live imaging of human cells…… 71
2.4.1. Cell culture…… 71
2.4.2. Micropscopy…… 72
2.4.3. Cell tracker…… 72

2.5. Western blots…… 72
2.5.1. Protein extraction…… 72
2.5.2. Protein quantification…… 72
2.5.3. SDS-PAGE…… 73
2.5.4. Blotting and blocking…… 73
2.5.5. Antibody binding and detection…… 74

2.6. Immunocytochemistry…… 76

2.7. Chromatin immunoprecipatation (ChIP)…… 77
2.7.1. Cell fixation and chromatin extraction…… 77
2.7.2. Chromatin sonication…… 77
2.7.3. Antibody binding of chromatin…… 77
2.7.4. Immunoprecipiation of chromatin, washes and elution…… 78
2.7.5. Quantification of eluted DNA fragments……78

2.8. Cloning/Molecular Biology techniques…… 81
2.8.1. Plasmid DNA extraction…… 81

2.8.2. Bacterial transformation…… 81
2.8.2.1. Glycerol stocks…… 81
2.8.3. Polymerase Chain Reaction (PCR)…… 81
2.8.3.1. Primer design…… 81
2.8.3.2. PCR conditions…… 82
2.8.4. Gel electrophoresis…… 83
2.8.5. Restriction endonucelase digests…… 83
2.8.6. Ligation reactions…… 83
2.8.7. Colony PCR…… 84
2.8.8. Quantification of nucleic acid concentration…… 84
2.8.9. Genomic DNA extraction from HT1080 cells…… 84

2.9. BCL-3 BAC characterisation and Recombineering…… 85
2.9.1. BCL-3 BAC identification and ordering…… 85
2.9.2. Transformation of SW102 cells with BACs…… 85
2.9.3. Extraction of BAC DNA…… 85
2.9.3.1. BAC maxipreps…… 85
2.9.3.2. BAC minipreps…… 86
2.9.4. Restriction endonucelase digestion and resolution of BAC DNA…… 86
2.9.4.1. SalI and NotI digestion of BAC DNA…… 87
2.9.4.2. Pulse Field Gel Electrophoresis (PFGE)…… 87
2.9.5. Southern blotting of BAC DNA…… 87
2.9.5.1. Probe amplification and biotinylation…… 87
2.9.5.2. DNA digestion and resolution…… 87
2.9.5.3. Transfer and cross linking…… 87
2.9.5.4. Hybridisation and washing…… 88
2.9.5.5. Detection…… 88
2.9.6. BAC Recombineering…… 89
2.9.6.1. Produciton of galK recombination cassette…… 89
2.9.6.2. Primary targeting: galK recombination…… 89
2.9.6.3. Secondary targeting: Venus recombination…… 90

2.10. XcmI chromatin accessibility assay…… 90
2.10.1. XcmI digestion of genomic DNA…… 90
2.10.2. Genomic DNA purification…… 91
2.10.3. PCR assay…… 91

2.11. Flow Cytometry…… 91

2.12. Mathematical simulations…… 91

2.13. Graph preparation and images…… 91

2.14. Statistics…… 92

Chapter 3
Investigating the induction dynamics of the *TNFA* and *BCL3* genes in HT1080 cells stimulated with TNFα…… 93

3.1. Introduction
3.1.1. TNFα induced transcription of the *TNFA* and *BCL3* genes via the NF-κB signalling pathway…… 93
3.1.2. IL-9 and IL-10 are potential inducers of BCL-3 expression…… 94
3.1.3. Attenuation of *TNFA* transcription…… 94

3.1.4. Differential responses of cell types to a common stimulus…… 94
3.1.5. Chapter aims…… 95

3.2. Results…… 95
3.2.1. Measurement of the response of TNFA and BCL3 transcript levels in HT1080 cells stimulated with TNFα…… 95
3.2.1.1. Quantitative reverse transcriptase PCR (qRT-PCR)…… 95
3.2.1.2. Optimisation of a qRT-PCR protocol for the detection of *TNFA* and *BCL3* gene transcripts..... 96
3.2.1.2.1. Primer design…… 96
3.2.1.2.2. Confirming the robustness of a primer set's efficiency across varied cDNA template concentrations…… 97
3.2.1.3. *TNFA* and *BCL3* transcript levels are induced in HT1080 cells by stimulation with TNFα…… 98
3.2.2. TNFα acts to induce *TNFA* and *BCL3* transcript levels via the NF-κB signalling pathway in HT1080 cells…… 99
3.2.3. IL9 and IL10 have no detectable expression in HT1080 cells…… 101
3.2.4. Observing the nuclear localisation of NF-κB subunit in response to TNFα in HT1080 cells…… 102
3.2.4.1. Dynamic imaging of sub-cellular localisation of p65-dsRed protein in HT1080 cells…… 102
3.2.4.1.1. Transfection of HT1080 cells with a p65-dsRed expressing plasmid…… 102
3.2.4.1.2. Exogenous p65-dsRed shows a rapid nuclear translocation following TNFα stimulation and a subsequent return to cytoplasmic localisation…… 104
3.2.4.2. Endogenous p65 protein also exhibits nuclear translocation…… 106
3.2.5. BCL-3 protein induction and localisation in HT1080 cells stimulated with TNFα……107
3.2.5.1. Western blot analysis of BCL-3 protein levels in HT1080 cells following TNFα stimulation…… 107
3.2.5.1.1. Optimisation of Western blot conditions…… 107
3.2.5.1.2. TNFα induces levels of BCL-3 in HT1080 cells in a delayed manner…… 108
3.2.5.2. Induced BCL-3 localises predominantly to the nucleus…… 110
3.2.6. BCL-3 has an inhibitory effect on *TNFA* transcript levels…… 110
3.2.7. Investigating the temporal binding of BCL-3 at a distal κB site (-869) in the *TNFA* promoter – using a ChIP/qPRC assay…… 111
3.2.7.1. Optimisation of ChIP reagents…… 112
3.2.7.2. Relative quantification of immunoprecipitated DNA fragments using qPCR and the Percentage Input method…… 113
3.2.7.3. BCL-3 binds at a distal κB site in the *TNFA* promoter in a manner temporally consistent with an inhibitory effect on *TNFA* transcription…… 113

3.3. Discussion…… 116
3.3.1. Incoherent Feed Forward Loop motifs…… 117
3.3.2. Interaction timings in the *TNFA*/BCL-3 I-FFL…… 120

Chapter 4
Investigating NF-κB mediated induction of *BCL3* transcription…… 121

4.1. Introduction…… 121
4.1.1. Mechanisms of NF-κB induced transcription…… 121
4.1.2. NF-κB acts at different points in the Transcription Cycle…… 121
4.1.3. Chapter aims…… 122

4.2. Results…… 122
4.2.1. TNFα induces *BCL3* transcript increases in a delayed manner relative to *TNFA* transcript levels…… 122
4.2.2. RNAP dynamics at the *TNFA* and *BCL3* genes…… 123
4.2.2.1. RNAP is bound in a paused state at the *TNFA* gene promoter in unstimulated cells – in contrast to no observed binding at the *BCL3* gene…… 123
4.2.3. RNAP exhibits TNFα induced binding at the *BCL3* promoter in a manner correlated with enhanced histone 3 acetylation…… 124
4.2.4. Transcription initiation at the *BCL3* promoter is induced by NF-κB mediated acetylation of histones…… 125
4.2.5. Differential binding timing of NF-κB subunit p65 at the *BCL3* and *TNFA* promoters…… 126
4.2.6. Assaying chromatin accessibility at a proximal κB site in the *BCL3* promoter……128
4.2.6.1. XcmI chromatin accessibility assay design and optimisation…… 128
4.2.6.2. TNFα treatment of HT1080 cells induces chromatin remodelling at a proximal κB site in the *BCL3* gene promoter…… 130

4.3. Discussion…… 133
4.3.1. TNFα induced transcription of the *BCL3* gene occurs via a sequence of events culminating in chromatin remodelling…… 133
4.3.2. A dual role for NF-κB in inducing *BCL3* transcription…… 134
4.3.3. Chromatin states as a determinant of the response rate of NF-κB responsive genes……135

Chapter 5
Modelling the temporal effects of BCL-3 on *TNFA* gene transcription……137

5.1. Introduction……137

5.2. Results……138
5.2.1. Equations…… 138
5.2.1.1. Volume of a fibroblast cell…… 138
5.2.1.2. Nuclear translocation of NF-κB……138
5.2.1.3. NF-κB induction of *TNFA* mRNA……139
5.2.1.4. NF-κB induced histone 3 acetylation state…… 142
5.2.1.5. Induced chromatin accesssibilty at the *BCL3* promoter……142
5.2.1.6. NF-κB/chromatin remodelling induced *BCL3* mRNA levels……143
5.2.1.6.1. BCL-3 inhibits *BCL3* transcript levels in HT1080 cells…… 143
5.2.1.7. *BCL3* mRNA translation……145
5.2.2. Model outputs…… 146
5.2.2.1. A linear chain of sequential and dependent events recreates chromatin modification behaviour at the *BCL3* promoter and transcript induction dynamics for the *TNFA* and *BCL3* genes…… 146
5.2.3. Secondary TNFα stimulation…… 148
5.2.3.1. BCL-3 mediates a diminished *TNFA* transcriptional response to subsequent TNFα stimuli…… 149
5.2.4. Delayed *BCL3* transcription allows an initially large magnitude of *TNFA* transcription response but with robust later inhibition…… 151
5.2.4.1. A delayed inhibitory leg of an I-FFL uncouples inhibitory response speed and magnitude…… 152
5.2.5. An I-FFL containing a delayed inhibitory leg exhibits non-linear output responses to pulsed inputs…… 154
5.2.5.1. The propensity for pulsed cytokine signalling……154
5.2.5.2. Shorter pulses of nuclear NF-κB induce prolonged *TNFA* transcript induction…… 155
5.2.5.3. Non-monotonic output of an I-FFL generated by a delayed inhibitory leg rather than differential response sensitivities…… 156

5.2.5.3.1. The *TNFA* and *BCL3* genes exhibit equal sensitivity to transcript upregulation by TNFα…… 157
5.2.5.4. *BCL3* transcription shows a limited response to pulsed inductive signals…… 159
5.2.5.5. Desensitisation of cells to continued high magnitude TNFα signalling…… 160
5.2.5.6. *BCL3* transcription exhibits reduced sensitivity to low frequency NF-κB stimulation…… 161
5.2.5.7. Cells are predicted to remain able to induce *TNFA* transcription over extended periods of low frequency NF-κB stimulation due to low BCL-3 responses to such stimulation…… 161

5.3. Discussion…… 163
5.3.1. Regulating the size of cytokine transcriptional pulse responses…… 163
5.3.2. *TNFA* transcription shows a non-monotonic response to enhanced magnitude and frequency of NF-κB signalling…… 164
5.3.2.1. Potential functionality of such a non-monotonic response in induced *TNFA* transcription dynamics…… 165
5.3.2.2. Defining the nature of localised *TNFA* transcriptional pulses…… 166
5.3.2.3. Pulse frequency as an indication of the extent of local TNFα signalling…… 166
5.3.2.4. A consideration of secreted TNFα dynamics…… 167

Chapter 6
Modelling the TNFα positive feedback loop……168

6.1. Introduction……168
6.1.1. Problems with cytokine self amplification: cytokine storms and cancer…… 168
6.1.2. Chapter aims…… 168

6.2. Results…… 169
6.2.1. Modelling the TNFα positive feedback loop…… 169
6.2.1.1. TNFα induction of *TNFA* transcription…… 169
6.2.1.2. *TNFA* transcript translation…… 171
6.2.1.3. TNFα secretion and stability in solution…… 171
6.2.2. Effects of parameters k6 and k7 on *TNFA* mRNA steady states…… 172
6.2.3. The rate of decrease in secreted TNFα (parameter k7) defines the number and nature of *TNFA* mRNA steady states the system can attain…… 175
6.2.4. BCL-3 acts to limit the number of steady states which *TNFA* mRNA can attain…… 178

6.3. Discussion…… 179
6.3.1. The stability of secreted TNFα can potentially have a profound effect on long term *TNFA* transcription…… 179
6.3.2. Further potential experimental work on secreted TNFα dynamics…… 180
6.3.3. Further considerations for TNFα stability……181
6.3.4. Active removal of secreted TNFα: natural and therapeutic methods…… 181
6.3.5. The role of BCL-3 in moderating *TNFA* mRNA steady staes…… 182

Chapter 7
Developing tools to visualise BCL-3 dynamics in live cells using a BAC expression system…… 183

7.1 Introduction…… 183
7.1.1. Live visualisation of single cell protein dynamics…… 183
7.1.1.1. Fluorescent protein tagging…… 183

7.1.2. Expression vectors…… 184
7.1.2.1. Distal enhancer elements…… 184
7.1.3. Bacterial Artificial Chromosomes (BACs)…… 184
7.1.3.1. Modifying BACs by Recombineering…… 185
7.1.3.2. Recombination system: GalK selection method in *Escherichia coli* strain SW102…… 185
7.1.3.2.1. GalK selection…… 186
7.1.4. Chapters aims…… 186

7.2. Results…… 187
7.2.1 Identification and charatcerisation of a BCL-3 BAC…… 188
7.2.1.1. Identification of a BAC containing the *BCL3* gene sequence…… 188
7.2.1.2. Characterisation of the CTD-02608C5…… 188
7.2.1.2.1. Restriction endonuclease digestion profile……188
7.2.1.2.2. Southern blot……189
7.2.2. Amplification of homology arms to introduce galK sequence to the BCL-3 BAC by homologous recombination…… 191
7.2.3. Introduction of galK sequence into BCL-3 BACs contained within SW102 *E. coli* cells…… 193
7.2.4. Secondary targeting: introduction of Venus coding sequence into the BCL-3 BAC…… 193
7.2.4.1. Production of a targeting cassette containing Venus flanked with *BCL3* gene H arms……193
7.2.4.2. Secondary recombination of Venus sequence into the BCL-3 BAC…… 194
7.2.4.3. Sequencing of the Venus gene sequence and fusion boundary with the *BCL3* gene…… 198
7.2.5. Transfection of BCL-3:Venus into human cell lines…… 199
7.2.5.1. BAC transfection of HT1080 cells…… 199
7.2.5.2. BAC transfection of SK-N-AS cells…… 200

7.3. Discussion…… 201
7.3.1. Problems with the expression of recombinant protein fusions…… 202
7.3.2. The importance of non-coding sequence in gene expression tools…… 202
7.3.3. BCL-3 in single cell expression systems…… 202
7.3.4. From cells to tissue: future applications of BAC expression tools…… 203

Chapter 8
Conclusions…… 204
8.1. Summary of conclusions derived from this work…… 204
8.2. Timing in genetic circuits…… 204
8.3. RNA polymerase II dynamics…… 205
8.4. Measuring chromatin remodelling dynamics…… 206
8.4.1. Measuring chromatin modification and states: Population and single cell studies…… 207
8.5. Regulating cytokine expression levels…… 208
8.6. Further mediators of *TNFA* transcription…… 209
8.7. Additional considerations for the work…… 210
8.7.1. Further κB sites potentially relevant to *TNFA* transcription…… 210
8.7.2. Further mechanisms negatively regulating *TNFA* transcription…… 211

Appendices……212
Appendix 1: Methods…… 212
Appendix 2: Equipment suppliers…… 213
Appendix 3: Location of qRT-PCR primers…… 216

Appendix 4: Localisation of primers amplifying proximal to TSSs of *BCL3* and *TNFA* genes…… 217
Appendix 5: Primers to amplify distal (-869) κB site in the *TNFA* promoter for ChIP assay…… 217
Appendix 6: Site of primers amplifying across XcmI/proximal κB site in the *BCL3* gene promoter…… 218
Appendix 6: Lines fitted to relative experimental time courses (fig 5A)…… 218
Appendix 8: Model code…… 219
Appendix 9: Sequencing…… 221

References…… 222

WORD COUNT: 60,115

List of figures

1.1. Overview of 'classic' canonical NF-κB signalling…… 25
1.2. The *BCL3* gene…… 31
1.3. Position and sequence of κB sites in the human *TNFA* promoter with respect to transcription start site (+1)…… 42
1.4. Nucleosome structure…… 45

2.1. Assembly of a Southern blot stack for transfer of DNA from gel to membrane…… 88

3.1. Design and verification of suitable primer sets to amplify from *BCL3* and *TNFA* cDNA molecules…… 98
3.2. TNFα stimulation of HT1080 cells induces transcript levels of both *TNFA* and *BCL3* genes…… 98
3.3. TNFα induced transcript levels of both *TNFA* and *BCL3* genes in HT1080 cells occurs via the NF-κB signalling pathway…… 101
3.4. *IL9* and *IL10* genes are not expressed in HT1080 cells…… 102
3.5. p65-dsRed exhibits rapid nuclear localisation following TNFα stimulation of HT1080 cells and subsequent reduction of nuclear localisation signal…… 105
3.6. Localisation of endogenous p65 protein, as observed by Immunocytochemistry, exhibits induced nuclear localisation following TNFα stimulation…… 106
3.7. TNFα stimulation of HT1080 cells induces BCL-3 protein levels in a delayed manner…… 109
3.8. Induced BCL-3 protein exhibits greatest accumulation in the nucleus…… 110
3.9. BCL-3 exerts a negative influence on *TNFA* transcript levels in HT1080 cells…… 111
3.10. BCL-3 binds at a distal κB site (-869) in the *TNFA* promoter in a temporal manner consistent with mediating a transcriptional inhibition of the *TNFA* gene…… 115
3.11. Genetic circuit regulating TNFα induction of *TNFA* transcription. …… …… 117
3.12. Representative graphs illustrating the output characteristics which can potentially be produced by the I-FFL motif…… …… 119

4.1. Delayed induction of *BCL3* transcript increases, relative to *TNFA* transcript increases, in HT1080 cells following TNFα stimulation…… 123
4.2. RNA polymerase II is bound at the *TNFA* gene promoter prior to TNFα stimulation but is not detected within the *TNFA* coding sequence…… 124
4.3. Binding of RNA polymerase II at the *BCL3* gene occurs in a delayed manner and correlates with the acetylation state of histone 3 at this site…… …… 126

4.4. The binding of p65 occurs at a delayed rate at a proximal region to the *BCL3* gene's TSS relative to the *TNFA* gene's TSS proximal region…….. 128
4.5. Design and optimisation of an assay to detect changes in chromatin accessibility at a proximal κB site in the *BCL3* gene promoter utilising an XcmI cleavage site at the same location…… 130
4.6. A proximal κB site in the *BCL3* gene promoter exhibits TNFα induced increases in accessibility to the XcmI restriction endonuclease…… 131
4.7. Schematic view of events constituting the induction of *BCL3* transcription following HT1080 cell stimulation with TNFα…… 134

5.1. Overview of NF-κB mediated induction of both *TNFA* and *BCL3* gene expression and subsequent inhibition of *TNFA* transcription by BCL-3…… 137
5.2. Population levels of induced nuclear p65-dsRed localisation in HT1080 cells…… 139
5.3. Schematic diagram of the binding reactions of NF-κB and BCL-3 to proximal and distal κB sites respectively in the *TNFA* gene promoter…… 140
5.4. Calculation of the half life of *TNFA* and *BCL3* transcripts…… 141
5.5. BCL-3 negatively regulates transcription of its own gene…… 144
5.6. The timing of TNFα induced transcription enabling events at the *BCL3* gene…… 147
5.7. ODE simulated induction of *TNFA* and *BCL3* transcript levels following TNFα stimulation…… 148
5.8. Secondary stimulation of HT1080 cells with TNFα…… 150
5.9. Simulated modelling of simultaneous *TNFA* and *BCL3* transcription in response to nuclear NF-κB induction…… 152
5.10. Simulation of BCL-3 inhibition of *TNFA* utilising a constant nuclear NF-κB level input…… 154
5.11. Simulated responses of *TNFA* mRNA levels produced by a model (outlined in [5.2.1.]) stimulated with varied length pulses of nuclear NF-κB levels at 60 minute intervals…… 156
5.12. TNFα dose dependent transcription responses of the *TNFA* and *BCL3* genes in HT1080 cells…. 158
5.13. An I-FFL motif with a delayed inhibitory leg can exhibit differential responses to continuous and pulsed input stimuli – demonstrated using an ODE model [5.2.1.]…… 160
5.14. *BCL3* transcription shows sensitivity to the frequency of nuclear NF-κB stimulation…… 162
5.15. Summary of the two legs comprising the I-FFL comprising NF-κB induction of both *TNFA* transcription and an inhibitor of this process: BCL-3…… 163

6.1. Overview of simplified TNFα self-amplification, as modeled in [5.2.6.1.]…… 169
6.2. Effect of varying parameters k6 and k7 on the steady states which can be achieved by *TNFA* mRNA…… 175
6.3. Rate of change in *TNFA* mRNA levels as a function of the external TNFα concentration…… 177
6.4. Effect of BCL-3 on *TNFA* mRNA steady state attainment…… 179

7.1. Schematic outline of steps involved in the introduction of *Venus* fluorescent protein coding sequence into a *BCL3* gene containing BAC using a Recombineering strategy…… 187
7.2. Characterisation of the *BCL3* gene sequence containing CTD-2608C5 BAC…… 189
7.3. Southern blot of EcoRI digested BCL-3 BAC DNA…… 191
7.4. Design and production of H arms to introduce galK sequence into the BCL-3 BAC…… 192
7.5. Cloning strategy for the production of BCL-3 H arms flanking Venus fluorescent protein coding sequence…… 194
7.6. Identification and subsequent screening of $Venus^{+}$ BCL-3 BAC containing SW102 cells…… .197
7.7. PCR confirmation of the presence of Venus sequence in a putatively identified BCL-3/Venus BAC……198
7.8. Transfection efficiency of HT1080 cells with BCL-3:Venus BAC as assayed by Flow Cytometry…… 200
7.9. Analysis of SK-N-AS cells co-transfected with BCL-3:Venus BACs and p65 expressing plasmids…… 201

List of tables

2.1. Reaction conditions for qRT-PR…… 69
2.2. Primers used in qRT-PCR……69
2.3. Buffers used in western blot assay……75
2.4. Primary and secondary antibodies used in western blots…… 76
2.5. ChIP buffers…… 79
2.6. Antibodies used in ChIP assays…… 80
2.7. Primers used in ChIP assays…… 80
2.8. Reaction conditions for BIOTAQ^{TM} PCR…… 82
2.9. Reaction condtions for High Fidelity PCR…… 82
2.10. Buffers used in Southern blot…… 89

5.1. Parameter values for an ODE representing NF-κB induction and BCL-3 inhibition of transcription at the *TNFA* gene…… 140
5.2. Parameter values for an ODE representing changes in histone acetylation at the *BCL3* promoter…… 142
5.3. Parameter values for an ODE representing changes in chromatin accessibility at the *BCL3* promoter…… 143
5.4. Parameter values for an ODE representing changes in *BCL3* transcript levels…… 145
5.5. Parameter values for an ODE representing changes in BCL-3 protein level…… 146

6.1. Parameter values for ODE representing TNFα induced transcription of the *TNFA* gene…… 170
6.2. Parameter values for ODE representing *TNFA* translation…… 171
6.3. Parameter values for ODE representing secreted TNFα levels…… 172

Abbreviations

A	Adenine
A_{260}	Absorbance at 260nm
Ab	Antibody
Ag	Antigen
AP-1	Activator protein 1
ATCC	American Type Culture Collection
ATP	Adenosine 5'-triphosphate
AU	Arbitrary Unit
BAC	Bacterial Artificial Chromosome
BCL-3	B-cell lymphoma-3 protein
Bisacrylamide	N,N'-methylenebisacrylamide
bp	Base pair
BSA	Bovine Serum Albumin
C	Cytosine
℃	Degrees Celsius
CBP	CREB binding protein

cDNA	complementary DNA
ChIP	Chromatin Immunoprecipiation
Da	Dalton
DAPI	4',6-diamidino-2-phenylindole
DNA	Deoxyribonucleic acid
DNase	Deoxyribonuclease
dNTP	Deoxynucleotide triphophate
DMSO	Dimethylsulphoxide
dsDNA	Double-stranded DNA
DsRed	*Discosoma sp.* Red Flurorescent protein
E. coli	*Escherichia coli*
EDTA	Ethylenediaminetetraacetic acid
eGFP	Enhanced Green Flureoscent protein
FAT	Factor acetyltransferase
FBS	Foetal Bovine Serum
FISH	Flurorescence *in situ* hybridisation
g	Gram
GSK-3β	Glycogen Synthase Kinase-3β
HAT	Histone Acetyltransferase
HDAC	Histone Deacetylase
HEPES	4-(2-hydroxyethyl)-1-piperaziniithanesulfonic Acid
H_2O	Water
HS	Hypersensitive site
HSP70	Heat shock protein 70
HT1080	Human fibrosarcoma cell line
Ig	Immunoglobulin
IκB	Inhibitor of Kappa B
IKK	IκB Kinase complex
IL	Interleukin
IRF1	Interferon regulatory factor 1
JNK	c-Jun N-terminal kinase
K_D	Dissociation constant
kb	Kilobase pairs
kDa	Kilodalton
L	Litre
LB	Luria Bertani
LPS	Lipopolysaccharide

LBP	LPS binding protein
mA	Milliampere
mAb	Monoclonal antibody
MAP3K	Mitogen kinase kinase kinase
MEF	Mouse embryonic fibroblast
MEM	Minimum Eagle's Medium
mg	Milligram
min	Minutes
MKK	Mitogen kinase kinase
ml	Millilitre
mM	Millimole
MNase	Micrococcal nuclease
mRNA	Messenger Ribonucleic acid
NaCl	Sodium Chloride
NEAA	Non-essential Amino Acids
NEMO	NF-κB essential modulator
NES	Nuclear Export Sequence
NF-κB	Nuclear Factor Kappa B
ng	Nanogram
NIK	NF-κB inducing kinase
NLS	Nuclear Localisation Sequence
nm	Nanometer
NP-40	Nonidet P-40
NS	Not Significant
nt	Nucleotide
OD_{260}	Optical Density at 260nm
ODE	Odinary differential equation
PAMP	Pathogen associated molecular pattern
PBS	Phosphate Buffered Saline
PCR	Polymerase Chain Reaction
PFGE	Pulse Field Gel Electrophoresis
PIPES	piperazine-N,N′-bis(2-ethanesulfonic acid)
Poly(A)	Poly Adenylation
PTM	Post transcriptional modification
qRT-PCR	Quantitative Real Time PCR
RHD	Rel Homology Domain
RIP	Receptor interacting protein

RNA	Ribonucleic Acid
RNAi	RNA interference
RNAP	RNA polymerase II
RNase	Ribonulease
rpm	Revolutions per minute
RT-PCR	Reverse Transcirptase Polymerase Chain Reaction
SDS	Sodium Dodecyl Sulphate
SDS-PAGE	Sodium Dodecyl Sulphate Polyacrylamide gel electrophoresis
SK-N-AS	Human neuroblastoma cell line
SNP	Single Nucleotide Polymorphism
SSC	Sodium citrate
ssDNA	Single-strand DNA
SW102	*E. coli* strain containing the Red phage system
T	Thymine
Taq	Polymerase derived from *Thermophilus aquaticus*
TAE	Tris-Acetate-EDTA
TBE	Tris-Borate-EDTA
TBP	TATA-box binding protein
TLR	Toll like receptor
T_M	Melting temperature
TNFα	Tumour Necrosis Factor Alpha
TNFR	Tumour Necorsis Factor Receptor
TRADD	TNFR1 associated death domain protein
TRAF	TNF receptor associated factor
TSA	Trichostatin A
U	Uracil
µF	Microfarad
µg	Microgram
µl	Microlitre
µm	Micrometre
µM	Micromolar
UTR	Untranslated Region
UV	Ultraviolet
V	Volts
v/v	Volume as a percentage of volume
W	Watt
w/v	Weights as a percentage of volume

Abstract

The role of BCL-3 feedback loops in regulating NF-κB signalling
Thomas Walker (2012)
A thesis submitted to the University of Manchester for the degree of Doctor of Philosophy

NF-κB signalling induces transcriptional upregulation of a wide array of genes in response to inflammatory signalling caused by, for example, TNFα cytokine. In addition to inducing the expression of factors which mediate an intracellular response, such stimuli also cause the expression of further signalling factors, including TNFα itself, to propagate and refine an initial stimulus. However, while such positive feedback signalling can be seen to be beneficial in amplifying potentially small initial stimuli, excessive production can cause hyper-inflammatory responses; an occurrence linked to several autoimmune diseases. Therefore, correct regulation – in regards to both too little and too much TNFα signal production – is essential for a balanced immune response.

In this thesis I have focussed on the effects of the IκB protein family member BCL-3 on *TNFA* transcription: demonstrating NF-κB dependent induction of both *TNFA* and *BCL3* genes and a subsequent negative role for BCL-3 in regulating *TNFA* transcription in the human fibrosarcoma HT1080 cell line – forming an Incoherent Feed Forward Loop (I-FFL) motif. Notably, I have shown a differential rate of induction of *TNFA* (rapid) and *BCL3* (delayed) transcript levels; demonstrating that while the *TNFA* gene has a pre-stimulus RNA polymerase II bound and poised for a rapid response, the *BCL3* promoter requires histone modification and chromatin remodelling for binding of NF-κB and RNA polymerase II. Extensive characterisation of the temporal sequence of events constituting *BCL3* promoter remodelling, mRNA plus protein levels and NF-κB nuclear localisation through live cell microscopy allowed the construction of a mathematical model which has been tested to ensure it can accurately recreate biological behaviour.

This model has been utilised to show that the delayed production of inhibitory BCL-3 produces distinct *TNFA* transcript dynamics: (i.) initially allowing a high magnitude response but coupled to later strong repression of *TNFA* expression and (ii.) producing a non-monotonic response to pulsed stimuli. This behaviour cannot be quantitatively recreated with models in which *BCL3* transcription is induced simultaneously with *TNFA* and proposed physiological benefits are outlined. Based on this work, time delays in I-FFLs are proposed as a novel mechanism to produce varied output dynamics.

Future research tools have also been developed in this work - including generation of an expression vector to visualise BCL-3 protein in live cells (utilising a BAC recombinant engineering approach) - plus further research questions and predictions regarding TNFα signalling have been raised by additional modelling work.

Declaration

No portion of the work referred to in this thesis has been submitted in support of an application for another degree or qualification of this or any other university or other institute of learning.

Copyright Statement

i. The author of this thesis (including any appendices and/or schedules to this thesis) owns certain copyright or related rights in it (the “Copyright”) and s/he has given The University of Manchester certain rights to use such Copyright, including for administrative purposes.

ii. Copies of this thesis, either in full or in extracts and whether in hard or electronic copy, may be made **only** in accordance with the Copyright, Designs and Patents Act 1988 (as amended) and regulations issued under it or, where appropriate, in accordance with licensing agreements which the University has from time to time. This page must form part of any such copies made.

iii. The ownership of certain Copyright, patents, designs, trade marks and other intellectual property (the “Intellectual Property”) and any reproductions of copyright works in the thesis, for example graphs and tables (“Reproductions”), which may be described in this thesis, may not be owned by the author and may be owned by third parties. Such Intellectual Property and Reproductions cannot and must not be made available for use without the prior written permission of the owner(s) of the relevant Intellectual Property and/or Reproductions.

iv. Further information on the conditions under which disclosure, publication and commercialisation of this thesis, the Copyright and any Intellectual Property and/or Reproductions described in it may take place is available in the University IP Policy (see http://www.campus.manchester.ac.uk/medialibrary/policies/intellectual-property.pdf), in any relevant Thesis restriction declarations deposited in the University Library, The University Library"s regulations (see http://www.manchester.ac.uk/library/aboutus/regulations) and in The University"s policy on presentation of Theses.

Acknowledgments

I'm indebted to numerous people for help in performing the work outlined in this thesis: Dean Jackson, Antony Adamson, Angela Pisco, Apolinar Maya-Mendoza, Asia Merchut-dé-Maya, Dave Spiller, Emanuela Monteiro, Hans Westerhoff, Louise Ashall, Mark Muldoon, Nick Chadwick & Pete Taylor. Work was funded by the EPSRC and carried out under the Doctoral Training Centre scheme at the University of Manchester. Thank you all.

"I feel a very unusual sensation - if it is not indigestion, I think it must be gratitude."

~Benjamin Disraeli

Chapter 1
Introduction

1.1. The inflammatory response

Mechanisms to combat infection or tissue damage are typically carried out by numerous cells recruited from regions beyond the immediate vicinity of insult; therefore initial detection of such events induces a broad primary signal production; inflammation. This widespread reaction affects aspects of the innate immune response as well as forming a stimulus for the adaptive immune response.

1.1.1. PAMPs: initial indicators of infection

Non-specific immune responses are induced following recognition of conserved molecules derived from pathogens which are distinct from host derived molecules; commonly known as pathogen associated molecular patterns (PAMPs). Such indicators of infection are recognised by Toll like receptors (TLRs); specifically a subset of the Interleukin-1 Receptor/Toll-Like Receptor superfamily containing the subgroup 2 Toll-IL-1 receptor domain (Moreland et al., 1999). PAMP varieties interact with distinct TLR family members; for example dsRNA bound by TLR3, unmethylated CpG DNA bound by TLR9 and the common experimentally utilised lipopolysaccharide – a lipid/polysaccharide composite molecule fragment of Gram-negative bacteria outer membranes – binds the TLR4 receptor in conjunction with cofactors MD-2, LPS-binding protein (LBP) and CD14 (Phelps et al., 2000). TLRs also bind host derived proteins indicative of nearby stressed or necrotic cells – damage associated molecular patterns (DAMPs), for example extracellular HSP70 (Asea et al., 2002).

Activated TLRs transduce signal through assembly of adaptors molecules: MyD88, TRAM, TRIF or TIRAP (Kagan et al., 2008). In turn, these adaptors can initiate signalling pathways such as NF-κB (through PI3K and IKKs), AP-1 (through MAP3Ks) and IRF3 (through TBK1/IKKi). Different TLRs act through some, or all, of these signalling routes. These pathways act by moderating transcription of multiple genes; mediating a direct immune responses (for example, antimicrobial compounds) or the production of signalling molecules - cytokines [1.1.3.] – which mediate a further immune response; inflammation.

1.1.2. The inflammatory response

Inflammation acts in two broadly defined ways, involving (1) induction of further innate immunity responses and (2) the recruitment, to a site of infection or injury, of active leukocytes from the circulatory bloodstream – facilitating an adaptive immune response. Such actions mediate a remedial response: the clearance of pathogens and/or repair of localised tissue. Secreted inflammatory cytokines are integral in these processes:

(1) Innate immunity: IL-1 induces the production of nitric oxide (NO) – a general regulator of immune and inflammatory cell function (Coleman, 2001). IL-12, IL-18 and IFNγ also activate NK cells; innate immunity mediating cells which exhibit cytotoxicity and the production of further cytokines (Scott and Trinchieri, 1995). In addition, TNFα can induce apoptosis of cells in the vicinity of an infection (Micheau and Tschopp, 2003).

(2) Induction of an adaptive immune response: LPS has been shown to induce the inflammatory cytokine IL-12 in human macrophage cells (Sanjabi et al., 2000); a factor which can activate the adaptive immune system by inducing T_h1 cell maturation (Shu et al., 1994). The inflammatory cytokines IL-1 and TNFα also mediate recruitment of mononuclear cells through induced expression of leukocyte adhesion molecules and vasodilation inducing compounds (Munro et al., 1989; Mark et al., 2001). Members of the TNF [1.1.3.1.] family of cytokines can also induce proliferation of T cells (Radeff-Huang et al., 2007; Croft, 2009).

Inflammatory responses also coordinate the repair of damaged tissue. Cytokines are induced in a similar manner to infections; for example the HMGB1 (high mobility group box 1) protein released by damaged cells acts via binding of the TLR4 receptor (Schiraldi et al., 2012). Once induced, TNFα contributes to wound healing through the induction of matrix metalloproteinases (MMPs) required for a selective degradation of the extracellular matrix necessary for wound healing (Han et al., 2001).

1.1.3. Cytokines

Being small protein signalling molecules, cytokines are conceptually similar to hormones – distinctions being made based on the cellular source of the signal (hormones typically having single organ/tissue origins, whereas cytokines have more numerous sources). Given the widespread pleiotropic nature of individual cytokines, classification by function can be ambiguous. Several families have been identified based on sequence homology, notable examples being the IL-1, IL-12 and TNF family of cytokines – which includes the important inflammatory mediator TNFα.

1.1.3.1. The TNF family of cytokines

At present a 19 member strong family, TNF cytokines contain characteristic C-terminal TNF homology domains responsible for binding receptors - of which at least 29 have been identified; the TNF receptor (TNFR) family [1.1.3.2.] (Aggarwal, 2003). TNF family members are largely initially expressed as type II transmembrane proteins, signalling through direct cell to cell contact; however, cleavage by protease creates a truncated soluble form capable of acting as a remote signalling molecule ('shedding'); with TNFα released by a subset of metalloproteases (Black et al., 1997; Gallea-Robache et al., 1997). Such soluble forms of TNF tend to act as trimers (Smith and Baglioni, 1987). Intriguingly, a conserved N-terminal cytoplasmic domain present in TNF family members has suggested a potential 'reverse signalling' ligand capability (Sun and Fink, 2007).

1.1.3.2. The TNFR family

The TNF binding receptor family all contain a cysteine-rich extracellular domain (CRD) responsible for ligand interaction (Chen et al., 1995). Family members are divided on the basis of possession of a death domain; an ~80 amino acid region which, when receptors are activated, bind TNFR1-associated death domain proteins (TRADDs) to induced downstream signalling pathways (not necessarily related to the eponymous death functionality) (Hsu et al., 1995; Chinnaiyan et al., 1996). While binding of a TNF trimer had historically been seen to be required for receptor trimerisation, the discovery of a domain in two TNFα binding receptors which is necessary and sufficient to mediate this process suggests pre-ligand formation of the structure (Chan et al., 2000).

TNFRs exhibit varied expression patterns, varying from few (typically immune) cell types to ubiquitous expression. TNFα binds two receptors: TNFR1 (~p60) and TNFR2 (~p80). While TNFR1 expression has been observed in many cell types, TNFR2 appears restricted to immune and endothelial cell types (Mukhopadhyay et al., 2001; Aggarwal, 2003).

The consequence of TNF-TNFR interactions are diverse and potentially contrary. TNF family members having been shown to induce apoptosis, cell survival, differentiation or proliferation through numerous signalling pathways including NF-κB, p38 MAPK, c-Jun N-terminal kinases and p42/p44 MAPKs (Aggarwal, 2003). The ability of a single cytokine species to induce differential outcomes may be due to its form or the type of receptors expressed by a recipient cell. A study has shown soluble TNFα as activating TNFR1 (p60), whereas membrane TNFα acts via TNFR2 (p80) to induce different cellular effects (Grell et al., 1995); however, additional studies also show the two receptors acting cooperatively (Mukhopadhyay et al., 2001). Differences in downstream signal transduction components between cell lines used may account for the different outcomes.

TNFRs lack intrinsic enzymatic activity, therefore activation is relayed through adaptor proteins – resulting in the formation of a multiprotein complex; as exemplified by TNFR1. As previously mentioned, TRADD proteins can bind activated receptors containing the death domain (including TNFR1) – a process allowed by the dissociation of silencer of death domain (SODD) proteins bound to the intracellular region of TNFR1 receptors (Takada et al., 2003). TRADD then facilitates binding of further factors such as FAS-associated death domain protein (FASS), TNFR-associated factor 2 (TRAF2) and receptor interacting protein (RIP), which in turn recruit proteins with enzymatic ability: IKK complexes to activate NF-κB[1.2.], MEKK1 to activate c-Jun N terminal kinase (JNK), MKK3 to activate p38 or FASS dependent recruitment of caspase-8 and caspase-3; mediators of apoptosis (Hsu et al., 1996; Chen and Goeddel, 2002; Wajant et al., 2003). The binding of additional TRAF variants to specific TNFR containing amino acid sequences gives considerable scope for TNFR variants to activate distinct pathways – although considerable overlap in the pathways induced by diverse TNFR family members does exist (Arch et al., 1998; Aggarwal, 2003).

1.1.3.3. Diverse cell types produce and are responsive to TNFα

While monocyte derived cells are undoubtedly important producers of cytokines such as TNFα (MacNaul et al., 1990; Vassalli, 1992), the experimental focus on such cell types has led to the cytokine contribution of additional cell types, notably those with non-exclusive immune function, being neglected and consequently underappreciated. As previously asserted, while the TNFα receptor TNFR2 is exclusive to hematopoietic cells, TNFR1 is widely and constitutively expressed in many cell types (Santee and Owen-Schaub, 1996) – suggesting that most, if not all, cell types are responsive to TNFα.

1.1.4. Fibroblasts as inflammation mediators

One such non-immune function exclusive cell type with a role in inflammation are fibroblasts; cells which constitute connective tissue providing structural support for tissues through synthesis of the extracellular matrix (ECM). Fibroblasts are sensitive to induction by several cytokines, for example TNFα (Sullivan et al., 2009) and IL-1 (Kaushansky et al., 1988) which can induce transcriptional activity in fibroblasts via the NF-κB signalling pathway [1.2.] (Han et al., 2001). In addition, human lung fibroblasts have been shown to express CD40 – a member of the TNFR family [1.1.3.2.] – which, when activated by its ligand displayed on the surface of T lymphocytes and eosinophils recruited to an inflammatory site, induces the production of further cytokines, again through activation of the NF-κB signalling pathway (Sempowski et al., 1997; Zhang et al., 1998). Furthermore, fibroblasts also have the ability to perceive an initial infection event directly themselves (rather than by cytokines produced by a PAMP activated immune cell); mouse embryonic fibroblasts (MEFs) have been shown to be activated by necrotic cells in a TLR2-dependent manner (Li et al., 2001).

Fibroblasts also have the ability to produce inflammatory cytokines themselves; for example, TNFα (Benderdour et al., 1998) and IL-6 (Gomes et al., 2005). Indeed, rather than simply background to an immune response raging around them, fibroblasts have been described as 'sentinel' cells – recruiting leukocytes through a broad spectrum of cytokine synthesis (Smith et al., 1997). The role of this cell type in inflammatory responses is illustrated by their potential to cause excessive inflammatory responses. Synovial fibroblasts derived from patients suffering rheumatoid arthritis display enhanced cytokine expression profiles (relative to fibroblasts derived from non-suffering patients). This enhanced cytokine profile is also stable – remaining after several cell passages and the removal of external stimuli (Pap et al., 2000; Buckley et al., 2001). Such hyperactive fibroblasts have been proposed to be the cause of chronic inflammatory conditions, causing the prolonged retention of leukocytes at tissue niches (Buckley et al., 2001).

As a note of caution, care must be taken when extrapolating previous work as 'fibroblasts' is a term encompassing a heterologous population of cells derived from different progenitor cells (ectoderm or mesoderm) (Komuro, 1990). As such, cytokine production and sensitivity previously desribed are potentially features of just a subset of fibroblasts.

1.2. NF-κB transcription factors

Several signalling pathways act to convey TNFα cytokine binding at cell surface receptors into intracellular effects; including p38 mitogen activated protein kinases (MAPKs) (Kumar et al., 2001), p42/p44 MAPKs (Schwenger et al., 1996), c-Jun N-terminal kinases (Nishitoh et al., 1998), Akt kinases (Rivas et al., 2008) and NF-κB (Kruppa et al., 1992). NF-κB has diverse roles in mediating perceived cellular stress events, with more than 150 different stimuli having been shown to induce NF-κB activity to varying degrees; including many immune response related receptors such as T- and B-cell receptors, TNFR, LTβR and Toll/IL-1R. NF-κB mediates an immune system response through upregulation of genes including cytokines, adhesion molecules and additional mediators (Ghosh et al., 1998; Li and Verma, 2002; Bonizzi and Karin, 2004; Hayden and Ghosh, 2004).

1.2.1. NF-κB subunits and dimer combinations

The NF-κB transcription factor was first discovered as a B-cell specific factor – binding at a κB site motif in the Igκ light chain enhancer sequence (Sen and Baltimore, 1986). NF-κB transcription factors bind approximately 10 bp DNA motifs called κB sites [1.2.6.] as dimer combinations of five mammalian subunits: RelA (p65), Rel-B, c-Rel (class I), p50 and p52 (class II). The p50 and p52 subunits are initially produced as precursor proteins – p105 and p100 respectively – which are subsequently

cleaved either constitutively (p105) (Moorthy et al., 2006) or in a stimulus responsive manner through non-canonical NF-κB signalling (p100) [1.2.4.].

The N terminal Rel homology domain (RHD) present in all NF-κB subunits mediates subunit dimerisation, DNA binding, nuclear localisation and also confers the ability of NF-κB dimers to interact with regulatory IκB proteins [1.3.]. While p65, Rel-B and c-Rel contain a transcription activating domain (TAD), this sequence is absent from p50 and p52; as such, homodimers of p50 and p52 are assumed to have no intrinsic transcription inducing ability (Baldwin, 1996; Vallabhapurapu and Karin, 2009). As a generalisation, RelB preferentially binds p52, or its precursor p100, (Dobrzanski et al., 1995; Yilmaz et al., 2003) whereas p65 and c-Rel form homodimers or heterodimers with p50/p52 (Karin and Ben-Neriah, 2000). Induction of such NF-κB dimer activity by cytokine signalling occurs via canonical [1.2.2.] or non-canonical [1.2.4.] pathways.

1.2.2. Canonical NF-κB signalling

A key requirement for an immune response is speed. NF-κB is able to respond quickly to stimuli as it is already present in the cell in an inactive form; consequently, there are no delays due to translational or transcriptional up-regulation. NF-κB dimers can be sequestered in the cytoplasm through interaction with cytoplasmic IκB proteins [1.3.] – an interaction which masks the NLS of the NF-κB dimer (Beg et al., 1992).

A well characterised occurrence of canonical signalling involves TNFα cytokine activation of a p50/p65 heterodimer through a signal transduction cascade (fig 1.1.). TNFα binding induces trimerisation of TNFR1 subunits which recruits and activates TNFR1 associated death domain protein (TRADD), TNF receptor-associated factor (TRAF2) and receptor interacting protein (RIP) – forming an active complex. TRAF 2 and -6 proteins have N-terminal RING domains typical of E3 ubiquitin ligases and are able to catalyse the polyubiquitination of RIP1, NEMO and themselves (Deng et al. 2000; Chen, 2005). Polyubiquitinated RIP1 is then able to bind further proteins: including the Transforming Growth Factor β-activated Kinase 1 (TAK1) complex (via TAB-2 and -3 subunits) and the NEMO subunit of the IKK complex (discussed in more detail below) (Kanayama et al., 2004). Ea et al. have proposed that the polyubiquitin chains present on the RIP1 act as a platform for the recruitment of both TAK1 and IKK complexes – with the resulting colocalisation allowing TAK1 to phosphorylate and activate the IKK complex (Ea et al., 2006). The Lys-377 residue of RIP1 is essential for this dual recruitment and co-localisation of TAK1 and IKK complexes at TNFR complexes following stimulation (Ea et al. 2006).

A downstream target of the TAK1 kinase is the IκB kinase (IKK) complex; which consists of subunits containing kinase activity; IKKα and IKKβ, plus a regulatory subunit IKKγ (NEMO) (Mercurio et al., 1997; Zandi et al., 1998). TAK1 phosphorylates serine residues within the activation loop of the IKKβ protein necessary for activation (Wang et al., 2001; Kanayama, et al., 2004). TAK1 can also act

through activation of NF-κB inducing kinase (NIK); a member of the MAP3K family of proteins (Hsu et al., 1995; Hsu et al., 1996; Malinin et al., 1997; Ninomiya-Tsuji et al., 1999). NIK phosphorylates IKKα at Ser176, consequently activating IKKα and IKKβ activity – potentially through further upstream kinase or trans-phosphorylation activity (Ling et al., 1998; Scheidereit, 2006).

Amino terminal regions of cytoplasmic IκBs (IκBα, -β and -ε) [1.3.1.] contain conserved serine residues which are phosphorylated by the IKKβ subunit of activated IKK complexes. IκB proteins phosphorylated in such a way are subsequently ubiquitinated by ubiquitin ligases (SCF/SCRF families) and are, consequently, degraded by the proteosome (DiDonato et al., 1997; Li et al., 1999; Krappmann and Scheidereit, 2005). Such degradation of IκB exposes the NF-κB nuclear localising signal allowing the factor to enter the nucleus and initiate a transcriptional response (Li and Verma, 2002; Hayden and Ghosh, 2004). Such a response includes the cytoplasmic IκB genes themselves (Sun et al., 1993; Hoffmann et al., 2002; Kearns et al., 2006). These IκB proteins contains both nuclear targeting and nuclear export signals, consequently newly produced protein is able to shuttle into the nucleus, bind NF-κB and cause its nuclear export – a negative feedback loop [1.4.3.1.]. The delayed nature of IκB induction can cause an oscillation in NF-κB between nucleus and cytoplasm (Nelson et al., 2004). TNFα has also been shown to induce degradation of IκBα via phosphorylation of tyrosines, by c-Src, in murine bone marrow macrophages (Abu-Amer et al., 1998).

While such signalling has predominantly been demonstrated with p50/p65 NF-κB dimers, observed binding between cytoplasmic IκBs (IκBα, -β, -ε) and p65 or c-Rel containing dimers [1.3.] and the inducible degradation of all such IκBs (albeit at different rates) suggests this mechanism may be a general one for regulating p65 or c-Rel-dependent transcription (Wu and Ghosh, 2003).

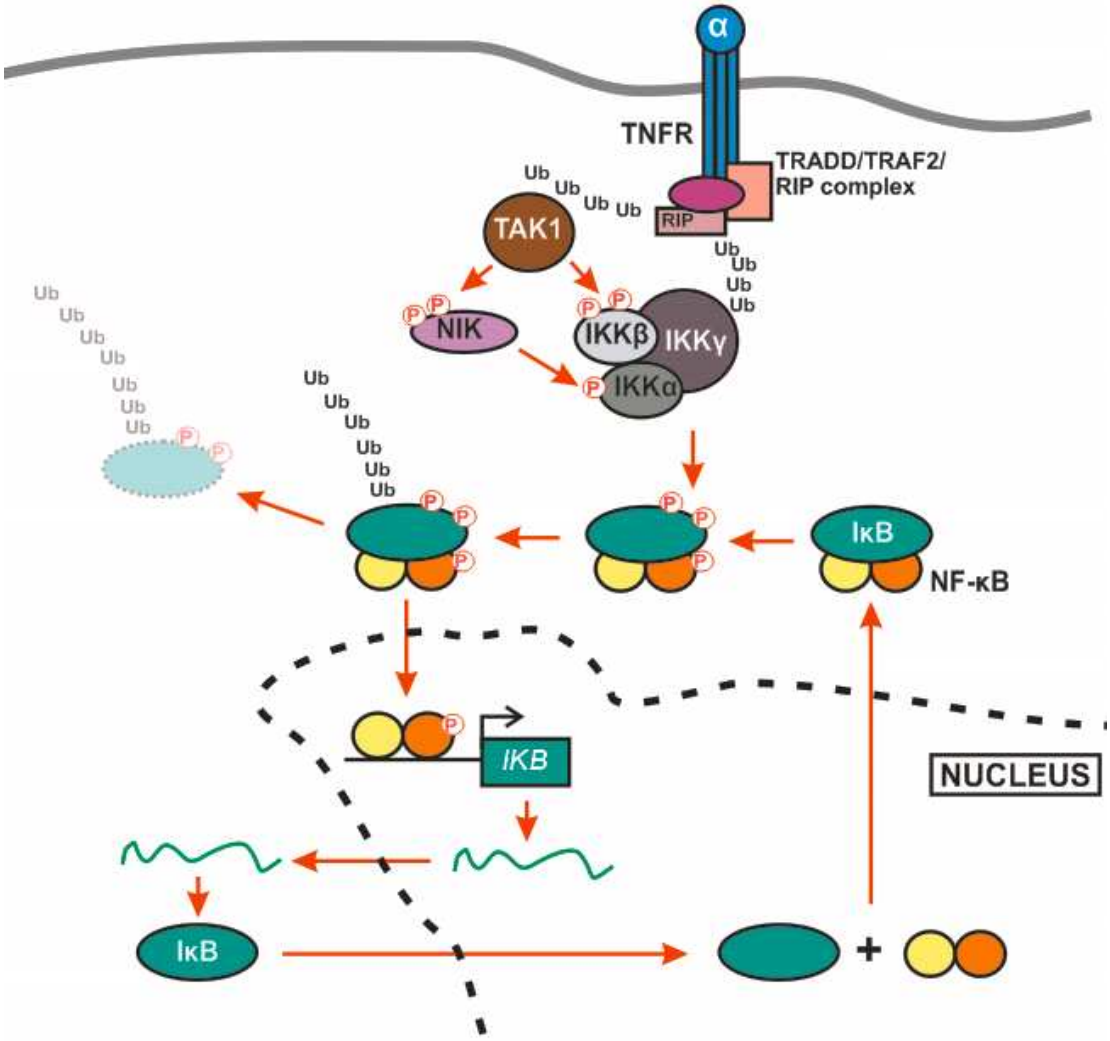

Figure 1.1. Overview of 'classic' canonical NF-κB signalling. Phosphorylation and ubiquitination events are representative and not numerically accurate.

1.2.3. p50 homodimers

Homodimers of the transcriptionally inactive p50 NF-κB subunits have been observed in the nucleus in the absence of inductive stimuli (Collart et al., 1990; Zhong et al., 2002) – potentially due to their inability to bind cytoplasmic localised IκB family members [1.3.] and consequently available NLS (Latimer et al., 1998). While nuclear, the activity of these homodimers (which lack TADs [1.2.1.]) is assumed to be negligible – until the induction of cofactors which can provide transcription inducing activity; such as BCL-3 – as discussed in a later section [1.3.7.2.].

Notably, however, dimers in which p50 is bound to its unprocessed precursor p105 are observed as cytoplasmic complexes, potential due to the ankyrin repeat sequence present within the p105 protein sequence (not present in the cleaved p50 protein) (Naumann et al., 1993). The production of p50 has been shown to occur in a co-translational manner, with dimerisation of nascent p105 molecules produced from the same mRNA molecules – indeed this dimerisation has been shown to be essential for stable p50/p105 production (Lin et al., 2000). Furthermore, while processing of one of the p105 dimer constituents occurs spontaneously, the resulting complex appears stable and resistant to further processing; forming a p50/p105 heterodimer. As such, a restriction on p50 nuclear localisation appears to be imposed as the protein is produced (Lin et al., 2000) – although constitutive processing has also been observed (Palombella et al., 1994). Such restrictions appear important; notably, transgenic mice expressing p50 produced without the p105 precursor are chronically inflamed (Ishikawa et al., 1998).

Such restrictions will limit p50 homodimers in resting cell nuclei, with levels potentially induced by stimuli. Phosphorylation of p105 at Ser927 and Ser932 by activated IKKβ causes ubiquitination and complete degradation of p105 (rather than partial degradation to p50) (Cohen et al., 2004); an event, which while not producing p50 homodimers from the original p50/p105 complex may free this original p50 monomer to form a homodimer which another such freed p50 molecule. Alternatively, selective degradation of p105 molecules in the p50/p105 heterodimers may also occur (Orian et al., 1999).

The two activation dependent modifications of p105 – complete degradation or limited processing – can both be induced by activated IKKβ enzyme. Phosphorylation of C-terminal Ser927 and Ser932 residues in the p105 protein (within its IκBγ region) lead to recruitment of $SCF^{\beta\text{-}TCP}$ ubiquitin ligase, ubiquitination of lysine residues and consequent degradation. Alternatively, IKKβ can also induce p105 processing (to p50) in an $SCF^{\beta\text{-}TCP}$ independent manner (Cohen et al., 2004), relying on a Glycine-Rich Region (GRR) of the protein to halt processive degradation by the 26S proteosome (Orian et al., 1999). Mechanisms determining the relative occurrence of these processing routes are unknown, however phosphorylation of p105 by the Glycogen Synthase Kinase-3β (GSK-3β) stabilises full length p105 in resting cells – with TNFα mediated inhibition of the enzyme facilitating p105 degradation in response to the cytokine (Demarchi et al., 2003).

1.2.4. Non-canonical NF-κB signalling

As previously noted [1.2.1.], RelB forms dimers which p52 which, when present in its precursor p100 form, inhibits activity of RelB. Induction of independent IKKα homodimers due to phosphorylation, through NIK activated by a subset of stimuli, causes subsequent phosphorylation of p100 molecules bound to RelB – causing recruitment of $SCF^{\beta TrCP}$, polyubiquitination of Lysine 855 and resulting processing to produce p52 (Fong and Sun, 2002; Amir et al., 2004; Shao-Cong, 2011). The produced

RelB/p52 is then able to enter the nucleus. Less data is available regarding the presence and localisation of p52 homodimers. As constitutive processing of p100 to p52 occurs at low levels, pre-stimulation levels of p52 homodimer is presumably low; potentially relying on non-canonical signalling to induce levels (Betts and Nabel, 1996).

1.2.5. Post transcriptional modification of NF-κB factors

In addition to post transcriptional modifications (PTMs) which moderate NF-κB activity by inactivation of its IκB inhibitors [1.2.2.], PTMs, notably phosphorylation, can also directly affect NF-κB activity (Perkins, 2006). Such modifications can occur either simultaneously with IKK mediated phosphorylation of IκB proteins (IKKβ; p65 Ser-536) or by independent kinases (PKC; p65 Ser-311) (Sakurai et al., 1999; Duran et al., 2003). The effects of NF-κB PTMs are diverse: including mediating transcription inducing ability (through acetylation of p65 Lys-310) (Chen et al., 2002) or sub-cellular localisation of NF-κB (phosphorylation at p65 Ser-276) (Gao et al., 2008). Dephosphorylation of nuclear NF-κB can also act as a mechanism to limit its activity duration per activation event. Therefore, an ideal scenario would refer not to generic NF-κB dimer combinations but to specifically modified sub-populations with a more refined range of activities.

1.2.6. DNA sequence specific binding of NF-κB

1.2.6.1. Variant κB sites have different affinities for NF-κB dimers

The κB site motif has a loose consensus sequence: GGGRNNYYCC (in which R is a purine; Y is a pyrimidine and N is any base). From various studies it is apparent that κB variants have distinct preferences for binding NF-κB dimers of different composition and that single base pair changes are sufficient to mediate large changes in affinity. Several κB sites have also shown preferential affinity for distinct NF-κB dimers. A κB site within the *IL8* gene promoter binds p65, c-Rel and p52 but does not bind p50/65 or p50 homodimers. Conversely sites within the ICAM-1 gene promoter bind p50 homodimers and p50/65 exclusively (*in vitro*) (Ledebur and Parks, 1995).

Oeth et al. noted that a κB site within the human *TF* gene promoter bound c-Rel and p52 homodimers with far greater affinity than complexes containing p50. The authors were able to show that this property was due to a variation from the classic κB consensus sequence at position one (from G→C; 5'-CGGAGTTTCC-3') as a single base pair substitution here to G drastically improved the ability of p50 containing dimers to bind (Oeth et al., 1994). NF-κB dimers containing p50 have a preference for a run of three Gs at the 5' end of the binding site – a sequence which has been shown to directly interact with the protein using crystallography (Kunsch and Rosen, 1993). Consequently, p50 homodimers favour palindromic κB sequences of the form 5'-GGGxxxxCCC-3'. In contrast, large scale random

oligonucleotide screens have identified a slightly different consensus sequences for p65 and c-Rel homodimers (Kunsch et al., 1992).

While preferentially binding different κB sites, p50 homodimers and p50/65 heterodimers can bind at the same κB sites; a fact, which given the potentially contrary effects on transcription the two dimers have, has implications for competitive binding at the same site. However the relative binding affinities will vary depending on the κB sequence. Urban and Baeurle (1990) separated the pentameric half sites of κB sequence GGGACTTTCC (AB) and produced palindromic AA (GGGACGTCCC) and BB (GGAAATTTCC) sites. Homodimers of p50 preferentially recognised AA sites followed by AB then BB, whereas p50/65 heterodimers only significantly bound AB sites – but with approximately twice the affinity of p50 homodimers at this particular motif sequence.

1.2.6.2. The dynamic nature of κB site binding

The ability of κB sites to bind multiple NF-κB dimer combinations creates mechanisms to moderate the effect of NF-κB dimers on gene expression. Individual κB sites can bind multiple NF-κB types in a sequential manner or several NF-κB dimers can be observed bound in no temporal order (Saccani et al., 2001; Saccani et al., 2003). Feedback mechanisms where initial NF-κB dimers are replaced by a different NF-κB dimer combination the presence of which they have induced provides a mechanism to limit or maintain induction levels. For example, decreases in IκBα promoter activity levels are observed over time as inducing p50/65 dimers are replaced by increasing levels of p50/c-Rel dimers – which have a poor transcriptional activity in this context. At the IL-12p40 promoter, delayed increases in RelB containing dimers, in place of p65 containing dimers, correlate with a decrease in RNAP occupancy of the promoter – consequently the promoter is resistant to subsequent LPS inductions – as RelB containing dimers inhibit further binding by p65 (Saccani et al., 2001; Saccani et al., 2003).

Several studies have reported p50 homodimer binding at a κB site pre-stimulus and being replaced by transcription inducing NF-κB dimers upon stimulation (Kang et al., 1992). Such binding has been proposed to limit basal transcription levels at such genes from residual transcription inducing NF-κB present in the nucleus at low levels in the absence of stimuli.

1.2.6.3. Dynamic NF-κB DNA binding is made possible by active displacement

The dynamic nature of NF-κB binding appears to be in contrast to the high binding affinity exhibited between the factor and κB sites – typically between 10^{-13}-10^{-10} M (Urban and Baeuerle, 1990; Chen-Park et al., 2002). However, Bosisio et al. used in vivo techniques to show that p65 exhibits highly dynamic binding. Utilising an array of 384 κB sites transfected into a cell containing GFP tagged p65, the authors were able to visualise bound p65 as a fluorescent bright spot. Using lasers to remove GFP activity from 90% nuclei but leaving the array bound GFP intact, the authors observed the rate of p65-

GFP dissociation from the DNA – Fluorescence Loss in Photobleaching (FLIP). After 20 seconds, less than 1% of p65 remained bound. The authors suggested a mechanism of active removal of NF-κB to account for this rapid dissociation – showing that a p65 mutant protein with reduced susceptibility to proteosome degradation remained bound for an enhanced time period (Bosisio et al., 2006). A further mechanism for limiting NF-κB binding duration is post transcriptional modification. The p65 NF-κB factor acts as a transcriptional activator by recruiting Histone Acetyl Transferases (HATs) to promoter sequences – however these same proteins act as Factor Acetyl Transferases (FATs) and acetylate p65 itself. Acetylation, by factors PCAF and p300, at Lysines 122 and 123 reduce DNA binding ability of the p65 containing dimer – reducing the half life of the DNA-protein complex (Kiernan et al., 2003).

Overall, the rapid change in NF-κB bound at DNA suggests the establishment of a dynamic equilibrium between bound and free nucleoplasmic NF-κB – i.e. the occupancy levels of κB sites reflects the nuclear concentrations of NF-κB dimer combinations. The rapid dissociation and turnover of DNA bound NF-κB suggests that changes in the nuclear ratios of NF-κBs can be quickly reflected in promoter occupancy (Bosisio et al., 2006). Such rapid changes prevent the prolonged binding of transcription inducing NF-κB complexes at promoters and allow regulatory versions of the transcription factor to intercede.

1.2.7. NF-κB as a transcription activator

Certain NF-κB dimers, notably containing p65, act as a transcription activator by targeting, and facilitating assembly, of a coactivator complex including coactivators such as p300, CBP, p/CAF and p160 proteins. Such recruitment may be direct, for example p65 can directly bind the CBP and p300 proteins (Perkins et al., 1997; Zhong et al., 1998), or indirect – CBP is able to bind p160 and p/CAF coactivators (Sheppard et al., 1999).

Such coactivators contain histone acetyltransferase activity (Ogryzko et al., 1996; Yang et al., 1996); with hyperacetylated histones being conducive to transcription amenable chromatin structure – this theme is discussed in greater detail in a later section [1.5.]. In addition, a direct interaction has been shown between p300 and the RNAP holoenzyme (Nakajima et al., 1997; Cho et al., 1998). Specific roles may be provided by individual coactivators; for example, Sheppard et al. show the HAT activity of the p/CAF but not CBP is required for NF-κB dependent transcription from a reporter construct. Such selective functions of individual coactivators may be a general feature of NF-κB activity, or may be varied at other promoters or cell types. Post transcriptional modification also regulates the ability of NF-κB to interact with coactivators; most strikingly the requirement for phosphorylation of p65 (as mediated by a cytoplasmic induction event) necessary for interaction with CBP/p300 – in the absence of this phosphorylation p65 is associated with an HDAC complex (Zhong et al., 2002).

1.2.8. NF-κB and other cytokine induced signalling pathways

In addition to inducing NF-κB signalling, cell simulation with TNFα also activates the AP-1 family of transcription factors. Indeed, such activation even occurs via a partially conserved signalling cascade: with TRAF2 proteins recruited by an activated TNFR complex activating NF-κB via an NIK dependent route [1.2.2.] and also c-Jun N-terminal kinases (JNKs) via an NIK independent route (Song et al., 1997). As such, it appears that no inflammation signalling pathway is likely to be induced alone; with transcription of induced genes reliant on multiple types of TFs.

While often implied as acting on its own to induce transcription, NF-κB dimers have documented interactions with a range of other TFs. For example, a cooperative interaction between NF-κB and JunD enhances transcription of the *CCND1* gene (Toualbi-Abed et al., 2008) and both NF-κB and c-Jun are required for recruitment of p300 to the *OPN* gene in murine macrophages (Zhao et al., 2011). In addition, the ribosomal protein S3 (RPS3) is able to bind p65 subunits and enhance its binding at κB sites – acting as a functional, non RHD containing, subunit of NF-κB complexes which is required for binding at a subset of genes. The RPS3 protein is itself activated by stimulus dependent nuclear localisation, although this occurs in an NF-κB independent manner (Wan et al., 2007).

1.3. The IκB family of proteins

1.3.1. BCL-3: A distinct member of the IκB family

BCL-3 is a member of the IκB multigene family – a group of genes which have a well documented role in binding and modifying the activities of NF-κB/Rel transcription factors. Family members can be broadly divided into three categories: cytoplasmic IκBs which undergo stimulus dependent degradation – see [1.2.2.] - (IκBα, -β and –ε); precursor IκBs which are cleaved to form Rel subunits p50 and p52 (p100/IκBδ and p105/IκBγ) and nuclear IκBs (IκBζ, BCL-3 and IκBNS) (Manavalan et al., 2010).

Members of the family all contain 5-7 copies of a centrally located 33 amino acid consensus ankyrin repeat which confers the ability to interact with Rel Homology (RH) domains present in NF-κB dimers [1.2.1.] (Sedgwick and Smerdon, 1999). A nuclear localisation sequence is also contained within the ankyrin repeats (which is masked by binding to NF-κB dimers in cytoplasmic IκBs) (Sachdev et al., 1998). Differences are apparent in the structures of nuclear and cytoplasmic IκBs; notably the lack in nuclear IκBs of both a C-terminus PEST region and N-terminal amino acid residues responsible for signal induced phosphorylation and consequent degradation (Jacobs and Harrison, 1998; Kearns et al., 2006). A broad summary can be made that cytoplasmic/precursor IκBs are controlled post-

transcriptionally (i.e. by degradation) whereas active nuclear IκBs levels are due to induced transcription.

While less well defined, roles for IκBδ and IκBγ (which are contained within the precursor molecules p100 and p105) have been shown in regulating NF-κB dimers; either acting as fully independent IκB molecules or through stimulus induced partial degradation to p50 or p52 molecules which can subsequently pass to the nucleus (Savinova et al., 2009).

1.3.1.1. BCL-3

The B-cell lymphoma 3 (*BCL3*) gene was identified due its propensity to cause B-cell lymphoma following translocation into the immunoglobulin alpha locus (Zhang et al., 1994). The gene is located on chromosome 19, contains 9 introns and is 12,340 bp in length. A notable feature is the two large first introns, which are 2.2 and 4.9 kb respectively. The gene possesses two CpG islands: one situated at the first intron and another within the 3' coding sequence of the gene. The BCL-3 protein consists of 454 amino acids and contains seven of the ankyrin repeats typical of an IκB protein (fig 1.2.) (McKeithan et al., 1995).

Mice defective for BCL-3 have increased mortality when infected due to a reduced ability to mount immune responses; notably succumbing to bacterial infections due to lack of a T helper 1 immune response and exhibit an impaired T-dependent antibody response when infected with influenza (Franzoso et al., 1997).

Figure 1.2. The *BCL3* gene. Boxes denote exons, line representes introns. Pink boxes represent UTR sequence.

1.3.2. BCL-3 binds a specific subset of NF-κB dimers

While all IκB family members bind NF-κB dimers in general, preferences are shown for specific dimer combinations. Cytoplasmic IκBs have a requirement for the presence of p65 or c-Rel for significant binding (NF-κB subunits with transcription activation domains) (Zabel and Baeuerle, 1990; Kerr et al., 1992; Fujita et al., 1993). In contrast, BCL-3 exhibits a strong preference for binding p50 and p52 homodimers, with several studies showing BCL-3 to have a very limited, or non existent, affinity for p65 or c-Rel homodimers and p50/65 heterodimers (Kerr et al., 1992; Wulczyn et al., 1992; Fujita et al., 1993; Nolan et al., 1993). Wulczyn et al. showed the sequence of p50 necessary for BCL-3 interaction

is very similar to the region involved in homodimerisation. The same authors also demonstrated a propensity for complex formation when p50 and BCL-3 proteins are mixed (Wulczyn et al., 1992). *In silico* studies suggest a mechanistic explanation for distinct NF-κB binding partners based on the number and distribution of flexible amino acid residues at regions within and adjacent to the conserved ankyrin repeats (Manavalan et al., 2010).

1.3.3. Sub-cellular localisation of BCL-3

BCL-3 is often described as a 'nuclear IκB', with the majority of literature reporting exclusive or predominantly nuclear localisation. These include NIH 3T3 cells (Nolan et al., 1993), NTera-2 cells (Bours et al., 1993), COS-1 cells (Zhang et al., 1994) and murine thymic cells (Caamano et al., 1996). In contrast to these observations, in Hep G2 cells BCL-3 localises to the cytoplasm following cytokine induction (Brasier et al., 2001).

In terms of a functional consequence of BCL-3 localisation, the protein has been shown to force the localisation of p50 homodimers either to the cytoplasm (Brasier et al., 2001) or the nucleus (Zhang et al., 1994) – dependent on BCL-3 localisation in the cell line used. Conversely, additional studies have shown p50 mutants lacking a NLS as able to re-locate BCL-3 from predominantly nuclear localisation to the cytoplasm – suggesting that p50 in this case was the driving force for complex location and not vice versa (Nolan et al., 1993; Zhang et al., 1994). Localisation discrepancies between cell lines may be accounted for by effects on BCL-3 localisation mediated by PTMs. Polyubiquitination of lysine 63 has been shown to be essential for the nuclear localisation of BCL-3 in murine cells. Induced nuclear localisation of the deubiquitinase enzyme CYLD - under stimulation with O-tetradecanoylphorbol-13 acetate (TPA) or UV light, for example - acts to remove such modifications from the BCL-3 protein and induce cytoplasmic localisation (as a mechanism to reduce cell proliferation via BCL-3 induction of the cyclin D1 gene) (Massoumi et al., 2006).

1.3.4. Post-transcriptional modifications of BCL-3

The BCL-3 protein exhibits hyper-phosphorylation, notably at its C-terminal domain. While the kinases responsible are largely unknown – although GSK3 has been shown to act on particular serine residues in this region (Viatour et al., 2004) – phosphorylation is essential for BCL-3 function: moderating DNA binding (Nolan et al., 1993; Bundy and McKeithan, 1997) and through inducing subsequent polyubiquitination of the protein necessary for sub-cellular localisation (Massoumi et al., 2006).

1.3.5. The cellular function of BCL-3

While the specific binding of BCL-3 to p50 and p52 homodimers has been well documented, the effects of this interaction are less well defined. BCL-3 has a wide ranging and even potentially contradictory role in the transcription of κB dependent genes; with the ability to act as both a transcription

cosuppressor and coactivator in a highly context-dependent manner. As such, a generalised overview of activity is impossible and instead examples of the different characters of BCL-3 are outlined below.

1.3.6. BCL-3 effects on NF-κB DNA binding

The common binding of consensus κB sites by various NF-κB dimer combinations suggests competition. Such competition will be functionally relevant if transcription inducing NF-κB dimers (e.g. p50/p65) are prevented from binding by a dimer that lacks any transcription influencing ability (e.g. p50 or p52 homodimers). BCL-3 binding to such p50 or p52 homodimers has both positive [1.3.6.1.] and negative [1.3.6.2.] influence on DNA binding.

1.3.6.1. BCL-3 enhances the DNA binding ability of p50 and p52 homodimers

Mouse macrophage cells with defective BCL-3 genes exhibit reduced p50 DNA binding both *in vitro*, through EMSAs, and *in vivo* - with ChIP experiments demonstrating reduced levels of p50 at both the *TNFA* and *CXCL2* promoters in this mutant cell line (Carmody et al., 2007). Rather than by enhancing the affinity of p50 homodimers for DNA, BCL-3 acts by protecting DNA associated p50 homodimers from polyubiquitination and subsequent degradation; allowing p50 homodimers to bind for an enhanced period of time (Carmody et al., 2007). Caamano et al. were able to show enhanced p50 homodimer binding to κB sites in murine thymic cells overexpressing BCL-3 (Caamano et al., 1996). Further studies have shown BCL-3 to enhance p52 homodimer DNA binding, and demonstrated the importance of BCL-3 phosphorylation status on its activity. Bundy and McKeithen showed that only phosphorylated BCL-3 enhances p52 homodimer binding to κB sites in the presence of excess non-target DNA. Interestingly, phosphorylated BCL-3 was shown to have a relatively low affinity for p52 homodimer already bound to κB DNA motifs – therefore the authors suggested a model whereby BCL-3 causes dissociation of p52 homodimer bound to non-specific DNA, yet is somehow released when κB sites are bound. As such, BCL-3 was proposed to act by freeing p52 from non-specific DNA binding, therefore allowing κB sites to be bound more rapidly (Bundy and McKeithan, 1997).

1.3.6.2. Negative effects of BCL-3 on p50/p52 homodimer DNA binding

In contrast to previously described work [1.3.6.1.], Nolan et al. (1993) showed a decreasing ability of p50 to bind DNA in the presence of increasing amounts of BCL-3 – with BCL-3 also shown to induce dissociation of p50 homodimers pre-bound at DNA. Such behaviour has been shown for other IκB family members IκBα and IκBβ; which can actively dissociate bound p50/65 heterodimers from DNA, reducing the half life of the protein-DNA complex from 45 to less than 10 minutes (Zabel and Baeuerle, 1990). The cellular effects of BCL-3 mediated removal of p50/p52 homodimer from DNA was developed in an earlier study (Franzoso et al., 1993). Expression of increasing BCL-3 was able to counteract the negative effects of p50 overexpression on p65 induced transcription (Franzoso et al.,

1993). From this data, the authors suggested BCL-3 acts to prevent p50 homodimers from competing with p65 containing dimers for binding, with consequent transcription inducing effects.

This apparently contradictory ability of BCL-3 to both enhance and inhibit p50/p52 DNA binding may be explained by concentration and phosphorylation-dependent activity. As mentioned previously [1.3.4.], the phosphorylation state of BCL-3 can influence its activity; consequently, BCL-3 derived from differing cell lines, or even from different species, may have intrinsically different behaviour. Furthermore, BCL-3 activity has been suggested to be concentration-dependent; for example, Fujita et al. demonstrated that BCL-3 only inhibited p50 DNA binding when added in a greater than ten fold molar excess (Fujita et al., 1993). It is of particular note that many BCL-3 studies have employed overexpression as a method. A consequence of this may be abnormally high BCL-3 protein levels causing non-standard behaviour – particularly the inhibition of p50/p52 homodimer DNA binding.

1.3.7. Functional effects of BCL-3 complexes

As previously described, BCL-3 can positively influence the binding of p50 or p52 homodimers at κB DNA motifs [1.3.6.]. Such a binding event can act in a passive manner by preventing binding of other NF-κB dimers. However, bound BCL-3 can also instigate several active mechanisms to influence transcription. Such functions are notably diverse; with BCL-3 having the capability to act as a transcription corepressor and costimulator, depending on the cellular and gene context.

1.3.7.1. Negative effects of BCL-3 on transcription: HDAC recruitment

The heterodimer of p50 or p52 plus p65 acts a transcriptional activator due to transactivating domains provided by p65 (Schmitz et al., 1995) – a domain lacking in p50 or p52 subunits. As both hetero- and homodimers bind the same κB site, p50/p52 homodimers have been proposed to act as transcription inhibitors through competitive binding with p50/65 – as such any factor which affects p50/p52 binding will have implications for p50/65 induced transcription.

While BCL-3 containing complexes can cause inhibitory effects by passively competing for binding with transcription inducing NF-κB complexes, the protein can also have a more direct negative effect. This is mediated by recruitment of HDAC (Histone Deacetylase) complexes to κB site containing loci by BCL-3 and/or p50. Zhong et al. noted DNA bound p50 homodimers in complex with HDAC-1 in nuclear extracts of unstimulated Jurkat cells (Zhong et al., 2002). Addition of TSA (a HDAC activity inhibitor) caused up-regulation of a subset of κB dependent genes – inferring that HDAC activity at these loci in resting cells was responsible for their low basal expression. Furthermore, ChIP experiments showed HDAC-1 and p50 to be present at the TSA sensitive IL-6 promoter (Zhong et al., 2002). The activation of genes inhibited in this manner through NF-κB signalling was shown to occur

via replacement of the inhibitory p50-HDAC-1 complex with CBP/p300 recruiting p65 containing NF-κB dimers and mediated histone acetylation and transcription up-regulation (Zhong et al., 2002).

The above studies make no mention of BCL-3, however as previously outlined BCL-3 plays an integral role in stabilising p50 homodimers at DNA and consequently seems likely to have a role in mediating stable and constant HDAC-1 recruitment to κB sites. In support of this, Wessels et al. showed that decreases in *TNFA* gene promoter activity caused by BCL-3 expression could be reversed by TSA in mouse macrophage cells – i.e. through inhibition of HDAC activity (Wessels et al., 2004). In addition, BCL-3 and HDAC-1 co-immunoprecipitated from nuclear extracts following LPS stimulation. Therefore, it would appear that a p50/BCL-3 complex is responsible for recruiting HDAC-1 to specific κB sites – although BCL-3 may not directly interact with HDAC-1 but may mediate recruitment by stabilising p50 homodimers bound at DNA (Wessels et al., 2004).

1.3.7.2. BCL-3 as a positive transcriptional factor

Studies have also revealed further roles for BCL-3 and an ability to act as a direct transcriptional inducer itself. Dose-dependent induction of genes have been observed in response to transfection of plasmids expressing BCL-3 in conjunction with either p50 or p52 expressing plasmids – with *in vitro* studies conducted in parallel confirming the presence of a BCL-3 containing complex at such induced genes (Bours et al., 1993; Fujita et al., 1993). A well-documented direct positive transcriptional role for BCL-3 occurs at the cyclin D1 promoter. Here, p52 and BCL-3 act in a synergistic manner to induce expression of the cyclin D1 gene through binding at a proximal κB site in the gene's promoter (Guttridge et al., 1999; Westerheide et al., 2001; Barre and Perkins, 2007).

The role of BCL-3 as a stimulatory transcriptional factor is supported by the identification of transactivating domains in the BCL-3 protein sequence. Mutational analysis of putative transactivating domains confirmed their functionality – with such mutant proteins still able to bind p52 but lose a previously demonstrated ability to induce transcription (Bours et al., 1993). In addition to binding p50 and p52, BCL-3 has also been shown to interact with other nuclear factors at κB sites, most notably Tip60 – a histone acetylase (Dechend et al., 1999). Tip60 enhances p50/BCL-3 mediated transcription in a dose-dependent manner leading to a proposed function for BCL-3 as an adaptor linking p50/p52 homodimers bound at κB sites to transcription activating complexes and/or chromatin remodelling factors (Dechend et al., 1999). BCL-3 also associates with general transcription factors TFIIB, TBP and TFIIA as well as transcription co-activator CBP/p300 via the BCL-3 binding protein (B3BP) (Na et al., 1998; Na et al., 1999).

1.3.7.3. The contrary nature of BCL-3 activity

One possibility for the potentially contradictory variation in BCL-3 activity is an artifact of experimental procedure. For example, BCL-3 has been shown to act in a concentration-dependent manner [1.3.6.2.] – as many of the studies outlined above have relied upon overexpression through transfection of additional BCL-3 (and other gene) copies this may create an abnormally high BCL-3 concentration in the cell and cause behaviour not seen in a physiological context. In addition, the form of NF-κB subunit used may also have an influence on results. The p50 NF-κB subunit is produced from a proteolytic digestion of precursor p105 – when p50 is expressed in experiments, DNA corresponding to the truncated p50 protein is used but different studies used different coding sequences. In particular, Fujita et al. noted that XbaI truncated fragments commonly used in expression constructs do not form proteins corresponding to endogenous p50 size *in vivo* (Fujita et al., 1993).

Alternatively, differing observed BCL-3 behaviour may reflect diverse activity at different sequence sites. Perkins et al. suggested that the sequence of the κB site bound may influence the activity of the NF-κB complex (Perkins et al., 1992). The authors showed that while a dimer of p52/p65 was able to bind reporter gene-linked promoters containing various κB sequence varients, only a canonical κB site facilitated transcription. It was hypothesised that due to the different sequences involved, p65 binding was differential and the conformations induced affected its ability to bind components of the transcription initiating complex. Escalantes et al. were able to show a conformational change in a p50/65 dimer bound at two different κB sites using structural crystallography. The authors suggested that this allosteric interaction between κB site and dimer may account for the different activity of p50/65 when bound at variations of the consensus κB sequence (Escalante et al., 2002). In addition, computational modelling predicts multiple potential conformations of BCL-3 bound to p50 homodimers; these different conformations may have differential abilities – both intrinsic and with regard to interaction partners (Manavalan et al., 2010). Such a scenario could plausibly occur with BCL-3, with different κB sites inducing differential activity on the bound BCL-3 protein complexes.

Furthermore, it is important to consider that NF-κB factors bound at DNA are not acting in isolation – the binding of additional classes of transcription factor may be required for cooperative activity. Yao et al. showed that tandem arrangements of a fragment of the human *TNFA* promoter containing both κB and CRE sites was able to confer LPS inducibilty on a basal promoter – however tandem arrays of either motif individually did not (Yao et al., 1997). As such, the sequences surrounding a κB site are also important in determining the context dependent activity of NF-κB dimers bound there – potentially BCL-3 may only exhibit certain behaviour if accompanied by an adjacent co-factor.

Potentially due to all these reasons, it appears likely that BCL-3 is a very versatile protein with context dependent activities which varies in different cell types and at different κB site locations within the genome. Consequently, cell signalling events that upregulate BCL-3 levels can have a diverse and wide ranging effect within the cell and no assumptions should be made about BCL-3 activity at a particular κB site based on precedence at other locations in the genome.

1.3.8. NF-κB mediated induction of BCL-3

BCL3 gene induction in response to cytokine stimuli such as TNFα and IL-1 has been well documented – with levels of both mRNA and protein induced in an NF-κB-dependent manner (Brasier et al., 2001; Ge et al., 2003). Two κB sites have been identified in the *BCL3* gene promoter region; κB1 (-861) and κB2 (-96). While both have been shown to bind p65, the more proximal site (κB2) is necessary and sufficient for NF-κB mediated induction of BCL-3 (Brasier et al., 2001). Further κB sites which mediate NF-κB induction of *BCL3* transcription have also been identified in intronic sequence. Ge et al. identified candidate regulatory sequences through evolutionary conservation and DNAse hypersensitivity – including two regions in the second *BCL3* intron (Ge et al., 2003). Inclusion of these regions in sequences driving expression of a reporter gene significantly increased induced expression. Further work identified a κB site within the intron which largely mediated this inductive ability and which was shown to bind p50/p65 heterodimers (Ge et al., 2003).

It must also be noted that binding sites for several other TFs – including AP-1 and STAT3 – have also been identified in the BCL-3 promoter region; although functionality of these putative binding sites is largely unproven. However, IL-4 has been shown to induce *BCL3* expression via AP-1 sites in a murine T cell line (Rebollo et al., 2000).

1.3.9. Anti-inflammatory cytokines and *BCL3* expression: IL-9 and -10

The anti-inflammatory cytokines IL-9 and IL-10 have also been shown to induce transcription of the *BCL3* gene – via the STAT pathway in the case of IL-9 (Richard et al., 1999; Kuwata et al., 2003). Expression of IL-9 and IL-10 has itself been shown to be induced by inflammatory cytokines, including via NF-κB signalling (Wanidworanun and Strober, 1993; Zhu et al., 1996; Chen et al., 2008). Furthermore, induced BCL-3 protein has been shown to feedback and induce transcription of the *IL10* gene through direct binding at the promoter (Wessells et al., 2004; Massoumi et al., 2009); although an inhibitory role for BCL-3 in *IL10* transcription has also been described (Riemann et al., 2005).

1.3.10. Negative feedback and BCL-3

A further important influence on BCL-3 levels is its apparent autoinhibitory activity – with induced *BCL3* gene expression inhibited in a dose-dependent manner by transfection of BCL-3 expressing plasmid in HepG2 cells (Brocke-Heidrich et al., 2006). Sites of this autoinhibition have been identified within the

BCL3 gene promoter and also within intronic sequence. ChIP analysis confirmed the binding of both p50 and BCL-3 within the BCL3 gene's second intron – in a region containing a previously mentioned κB site which mediated NF-κB induced expression of *BCL3* (Brocke-Heidrich et al., 2006) [1.3.8.].

1.4. TNFα: an inducer and target of NF-κB signalling

1.4.1. NF-κB induces *TNFA* promoter activity

As already outlined, TNFα induces NF-κB nuclear translocation [1.2.2.], allowing the binding and activation of numerous downstream genes, including the *TNFA* gene itself. Several κB sites have been identified in both the mouse and human *TNFA* gene promoter sequence which are capable of binding NF-κB dimers and are able to confer LPS responsiveness on a basal promoter (Collart et al., 1990; Ziegler-Heitbrock et al., 1993). Essentially, TNFα forms a positive feedback loop.

An advantage of such a loop is that the effects of transient signals can be maintained over a substantial period of time. The positive feedback loop can also amplify the effects of a relatively small TNFα response - for example produced by few PAMP perceiving cells [1.1.1.] early in infection – into a large and rapid immune response before pathogenic agents can establish and mutliply. However, these advantages can also be viewed in a different light: a continuous or prolonged inflammatory response can have disastrous consequences for cells.

1.4.2. Cytokine overexpression

NF-κB induced by TNFα upregulates many integral cellular processes – including cell division and anti-apoptosis – processes which in excess will be deleterious for the cell. The overexpression of TNFα in humans is manifest as a number of medical conditions, including autoimmune diseases, diabetes, septic shock, chronic inflammation and cachexia (Hotamisligil et al., 1994; Schattner, 1994; Marc et al., 1995; Roulis et al., 2011). In light of such extremely adverse consequences for overexpression, mechanisms to limit NF-κB induction of *TNFA* transcription are of considerable importance. These mechanisms must ensure that while sufficient TNFα is produced to provoke an appropriate inflammatory response the extent of this response does not have adverse effects for the cell.

1.4.3. Mechanisms to reduce the extent of NF-κB signalling

1.4.3.1. IκB negative feedback

One feedback mechanism has already been introduced – NF-κB upregulation of its own inhibitory IκB factors [1.2.2.]. Three IκB variants having been described in such an NF-κB inhibitory capacity: IκBα, -β and –ε (Hoffmann et al., 2002; O'Dea et al., 2007; Kim et al., 2009)[1.3.]. While all three IκBs act

generally to bind and sequester NF-κB in the cytoplasm, Hoffman et al. described more refined and discrete roles for the individual IκBs (Hoffmann et al., 2002). The authors observed IκBα to act in a more rapid manner, both in terms of initial degradation in response to signalling and then in re-appearance following NF-κB induction. NF-κB and IκBα levels engage in oscillatory behaviour once initial IκBβ and -ε had degraded. However, this behaviour disappeared following the delayed reappearance of the IκBβ and -ε forms – with a stabilised NF-κB nuclear level of approximately half maximum nuclear occupancy level occurring. This data is in accordance with phenotypes of MEF cells in which two of the three IκB forms had been mutagenised; cells possessing only IκBβ or –ε versions exhibited no oscillatory levels of nuclear NF-κB – leading the authors to hypothesise that IκBα is responsible for oscillatory behaviour and -β and - ε variants cause a gradual dampening of the long term NF-κB response. The effect appears to be due to transcriptional response speed – while IκBβ is unable to compensate for IκBα loss in an IκBα$^{-/-}$ mutant mouse, expression of IκBβ under an IκBα promoter in the same mutant background prevents early postnatal death and mice survive with no major apparent abnormalities (Cheng et al., 1998). This complementation and the apparent normalised response of thymocytes to NF-κB stimulation suggests that it is the transcriptional timing which functionally distinguishes IκBα from IκBβ (Cheng et al., 1998). Coupling this with the Hoffman et al. data suggests that temporally distinct activation of IκB forms serves different purposes in moderating the NF-κB response – from oscillation generation to later dampening. It must be noted that this activity may be cell type specific, as Ashall et al. reported that an siRNA mediated knock down of IκBε in human SK-N-AS neuroblastoma cells had no effect on NF-κB oscillations (Ashall et al., 2009). Stochastic and delayed IκBε production has also been proposed as a mechanism to promote heterogeneous, out of phase NF-κB oscillation across a cell population (Paszek et al., 2010).

1.4.3.2. A20

A further negative feedback occurs through the deubiquitinating enzyme A20. A20 removes the activating polyubiquitin signals from lysine 63 residues in components of the TNFα-TNFR signal transduction pathway, including TRAF6, TRAF2 and NEMO [1.2.2.] (Chen, 2005; Hutti et al., 2007). NF-κB not only increased A20 cellular levels through transcriptional induction (Opipari et al., 1990; Krikos et al., 1992) but activated IKKβ (a subunit of the TNFα transducing IKK complex [1.2.2.]) phosphorylates and activates A20 (Hutti et al., 2007). The importance of A20 in reducing inflammatory effects is seen in A20$^{-/-}$ mice that are hypersensitive to LPS and TNFα and suffer excessive whole body inflammation. A further deubiquitinating enzyme, CYLD, which can act to attenuate NF-κB signalling, has also been identified (Kovalenko et al., 2003).

1.4.3.3. Post-transcriptional modification of NF-κB

PTM of NF-κB components are also able to reduce their transcription inducing activity. Examples include targeted degradation of p65 by the ubiquitin ligase SOCS-1 (Ryo et al., 2003), reduced DNA

binding affinity of p65 as a result of acetylation by CBP/p300 (Kiernan et al., 2003) or conversely the phosphorylation of Thr-254 in p65 causes binding by Pin1 protein, which inhibits association with IκBα and therefore prolongs p65 nuclear presence (Ryo et al., 2003; Perkins, 2006).

1.4.4. Limiting *TNFA* transcript induction to inflammatory stimuli

While the inhibitory effects outlined above [1.4.3.] will decrease the magnitude of NF-κB response they may not be sufficient to completely attenuate it; SK-N-AS human neuroblastoma cells induced with an initial TNFα stimulus are able to maintain an extended nuclear NF-κB oscillatory response, at least over a 10 hour experimental time course (Nelson et al., 2004; Ashall et al., 2009). While NF-κB signalling may persist, cellular mechanisms also exist to limit the expression of specific downstream genes. Such mechanisms concerning the *TNFA* gene are discussed below.

1.4.4.1. *TNFA* mRNA stability

TNFA mRNA contains AU rich elements (AREs) in its 3' UTR region – a sequence which mediates instability or reduced translation efficiency of mRNA when bound by ARE binding proteins such as tristetaprolin (TTP) (Shaw and Kamen, 1986; Lai et al., 1999). While LPS stimulation is able to induce TTP expression (Zhu et al., 2001), the p38 MAPK signalling pathway inactivates TTP – resulting in enhanced TNFA mRNA stability (Deleault et al., 2008; Kratochvill et al., 2011). Inhibition of the p38 MAPK pathway, for example by the anti-inflammatory cytokine IL-10, therefore induces instability in *TNFA* mRNA (Rajasingh et al., 2006).

1.4.4.2. BCL-3 as a direct inhibitor of TNFα self induced transcription

Overexpression of BCL-3 in murine macrophage cells inhibits upregulation of *TNFA* promoter activity in a κB site-dependent manner. This, coupled with co-precipitation of p50 plus BCL-3 with the *TNFA* promoter in the same macrophage cells, led the authors to conclude that a p50/BCL-3 complex mediated attenuation of promoter activity (Wessells et al., 2004). In addition, murine BCL-$3^{-/-}$ cells have a decreased ability to attenuate induced *TNFA*; as occurs in wild type cells. Such inhibited *TNFA* transcript levels correlate well with observed increases in BCL-3 protein levels and suggests BCL-3 as a good candidate to attenuate long term *TNFA* gene activation through its ability to recruit HDAC enzymes to the murine *TNFA* promoter (Wessells et al., 2004).

1.4.5. The dynamic nature of the *TNFA* gene promoter

As previously outlined, the binding of NF-κB factors to κB sites is a dynamic event, able to influence expression of associated genes [1.2.6.2.]. Such dynamic changes are also apparent at the *TNFA* promoter. Collart et al. noted that two forms of NF-κB dimer bind the murine *TNFA* promoter at a sequence contained a (-510) κB site: a 'constitutive' binding complex (p50 homodimer) and an inducible binding complex (p50/p65) (Collart et al., 1990). Overexpression of p50 was subsequently

shown to inhibit activation of the gene, whereas p65 overexpression enhanced activation, and basal expression, in murine macrophage cells (Baer et al., 1998).

The authors identified four κB sites in the mouse promoter and showed that one (which corresponds to the -510 site in Collart et al.) was sufficient to mediate repression caused by p50 overexpression; the same site was also shown to bind the p50/p65 complex. Temporal analysis following LPS stimulation showed initially almost exclusive p50/p65 binding, however over time p50 homodimers became the predominantly bound NF-κB variant, an event correlated with decrease in *TNFA* transcript levels (Baer et al., 1998).

1.4.5.1. *TNFA* promoters across species: From mouse to human

Given the similarity of sequence between mouse and human *TNFA* promoters, work conducted in mice should have considerable application in human cell work (Shakhov et al., 1990). The human *TNFA* promoter also has multiple κB sites which are summarised in the diagram below. It must be noted that the naming of the κB sites in this context may not be the same as in original cited literature – a consensus has been imposed for clarity (fig 1.3.).

Furthermore, in addition to κB sites which have been extensively studies with regard to their effect on *TNFA* transcription (κB sites 1-4 in fig. 2.1), many additional κB sites exist in genomic sequence surrounding the gene which do bind NF-κB. Such sites are increasingly being identified on a global scale through the use of ChIP-seq methodology. Sites shown in figure 1.3 were identified in such a manner; with p65 bound DNA following cell stimulation with TNFα (Rao et al., 2011). Distal sites in the genome can interact with RNA polymerase II at a gene's core promoter through DNA looping, as discussed in [1.6.1.]. However, the proximity of *TNFA* to neighbouring genes – *LTA* and *LTB* – means that the function of such κB sites, in relation to *TNFA* transcription, is not necessarily clear. Further functional studies in the regard will therefore be necessary.

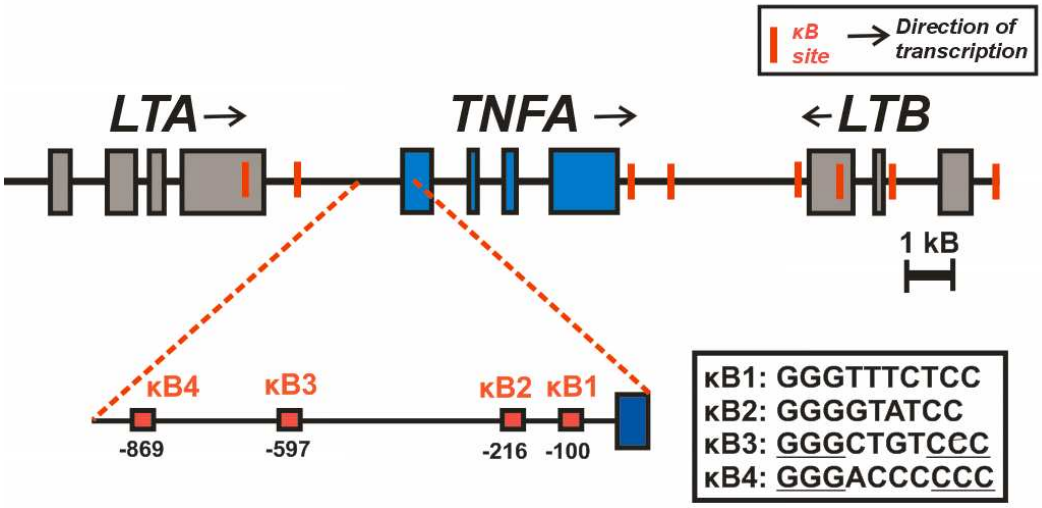

Figure 1.3. The position of κB sites in the vicinity of the *TNFA* gene. *TNFA* and two adjacent genes are shown. The position and sequence of κB sites in the human *TNFA* gene promoter, with respect to transcription start site (+1), are shown in close-up. Numeral values relate to 5' base of each κB site. Palindromic sequence is underlined.

Just as occurs at the mouse *TNFA* promoter, human cells also exhibit binding of both p50 homodimer and p50/65 heterodimers at κB sites. The timing of different complex occupancy is also similar – with a p50 homodimer binding at κB3 site in unstimulated cells and subsequently being replaced by a p50/65 complex following LPS induction. This change in binding is inhibited when NF-κB movement is blocked by addition of dithiocarbamites with an associated lack of *TNFA* transcript increase (Ziegler-Heitbrock et al., 1993).

Udalova et al. have shown that a SNP occurring naturally 863 bases upstream of the *TNFA* transcriptional start site causes an increase in *TNFA* promoter activity in human monocyte cells. This single base pair change is of particular relevance as it occurs within a κB site (κB4; fig 1.2.) and changes its ability to bind both p50 homodimers and p50/65 to almost exclusive p50/65 binding. A mutant promoter fused to luciferase shows identical expression levels to wild type promoter fusions in unstimulated cells. However, while a wild type promoter is induced approximately 20 fold by LPS, the mutant promoter shows an 80 fold increase. The authors attribute this increase to the reduced ability of p50 homodimers to bind the *TNFA* promoter and reduce transcriptional activity (Udalova et al., 2000). Furthermore, binding of p50 homodimers at distal regions in the human *TNFA* promoter has been shown to inhibit induction of transcription in response to secondary LPS stimulation in macrophage cells (Liu et al., 2000).

Information previously outlined relating to the p50 homodimer requirements for DNA binding [1.2.6.1.] are particularly pertinent to the observations of Udalova et al. Here, a κB site, which strongly (perhaps

preferentially) bound p50 homodimers (GGGACCCCCC), lost this ability when the final C base was mutated to A – destroying the palindromic nature of the site and hence, therefore, p50 affinity (Udalova et al., 2000). As p50 homodimers are mediating a negative effect on *TNFA* promoter activity in this context, the reduced affinity of the κB site would be hypothesised to lead to increased promoter activity – as the authors observed.

1.4.5.2. κB sites within the human *TNFA* promoter: spatial segregation of contrary roles

Analysis of the κB sites within the human *TNFA* promoter segregates into two groups; two proximal κB sites with little symmetry (κB1 and -2) and more distal sites with strong symmetry (κB3 and -4) (fig 1.2.). Based on this observation, a potential hypothesis would be that p50 homodimers can bind predominantly at the distal κB sites and weakly, or not at all, at the more proximal sites.

While it appears that p50 homodimers act at the more distal κB sites to mediate transcription attenuation, there is evidence in the literature that the most proximal κB site alone is responsible for p50/65 mediated transcription upregulation. Multiple studies have shown this site as necessary and sufficient to confer responsiveness of the *TNFA* promoter to LPS stimulation, with correlated binding of p50/p65 dimers (Goldfeld et al., 1990; Yao et al., 1997; Liu et al., 2000; Tsytsykova et al., 2007). As such, a tentative segregation of the contrary roles of κB sites in the *TNFA* promoter can be drawn: proximal sites mediate p50/65 upregulation of transcription whereas more distal sites bind p50/BCL-3 preferentially and mediate down regulation of promoter activity.

1.4.5.3. Competition at distal binding sites

While the literature summarised above suggests that p50/65 mediate their transcriptional stimulatory role at κB proximal sites there is good evidence to suggest that the dimer also binds at more distal sites (Udalova et al., 1998). Notably, the -869 κB site in Udalova et al. was able to bind p50/65 – however the functionality of this binding was not addressed. While the authors showed that a single base pair substitution drastically reduced p50 homodimer binding, p50/65 binding levels were not significantly affected – suggesting that the increase in promoter activity caused by this mutation is due to decreased p50 mediated inhibition not enhanced p50/65 mediated activation. An equivalent situation is also apparent in mice. Here a distal κB site located at approximately -800 has been shown to bind p50/65 dimers with high affinity (as well as p50 homodimers) - yet in contrast to other more proximal κB sites, this site cannot confer LPS inducibility to a basal promoter (Drouet et al., 1991). This is in accordance with work showing proximal κB sites are solely responsible for NF-κB mediated transcriptional increases (Yao et al., 1997; Liu et al., 2000).

The question is therefore raised as to the function of p50/65 binding at distal κB sites. One possible hypothesis is that p50/65 levels, increased in the nucleus in response to stimuli, act to out compete

binding of p50/BCL-3 complexes at the κB site – preventing their inhibitory activity. Induced BCL-3 levels (in response to NF-κB [1.3.8.]) can later displace binding of these complexes. In this manner, p50/65 would act in two ways to promote *TNFA* transcription: (i.) directly at proximal sites to recruit transcriptional machinery and (ii.) indirectly at distal sites to prevent inhibitory p50/BCL-3 complexes binding.

Numerous additional TF binding sites are present within the *TNFA* promoter; including a proximal AP-1 site which, in contrast to other sites in which NF-κB and c-Jun act synergistically [1.2.8.], independently contributes to inducing transcription in response to LPS stimulation (Liu et al., 2000). However, mutagenesis studies targeting the proximal most κB site have demonstrated that NF-κB signalling, even if not the sole driver of induced *TNFA* transcription, is a major component in this process (Yao et al., 1997). However, it must be noted that in disagreement with the studies outlined above, Tsytsykova et al. proposed an NF-κB independent activation of *TNFA* transcription in LPS stimulation of murine T-cell lines – suggesting that NF-κB acts rather through an, unspecified, mechanism stabilising *TNFA* mRNA levels (Tsytsykova et al., 2007).

1.5. Chromatin structure and dynamics

1.5.1. Chromatin structure

At its lowest order of packaging, DNA is wound around histone octamers (two each of H2A, H2B, H3 and H4) to form a nucleosome. Interaction between histone surface lysines and arginines and phosphate groups in the DNA molecules backbone facilitate strong interactions, with 147bp DNA wound ~1¾ times around the histone core (Davey et al., 2002). N-terminal arms of histone molecules protrude from the nucleosome core; acting as sites for covalent modification of nucleosomes and induced alterations in DNA-histone interaction (discussed further in [1.5.5.]) (Davie, 1998). Repetition of the nucleosome structure forms the base unit of chromatin, with H1 histones acting as linkers between adjacent nucleosomes through interaction with the histone octamer and linker DNA (the ~15-80 bp DNA which links two adjacent nucleosomes) and facilitating further packaging of chromatin into 30nm fibres (Allan et al., 1980). An overview of nucleosomes structure is shown in fig 1.4.A.

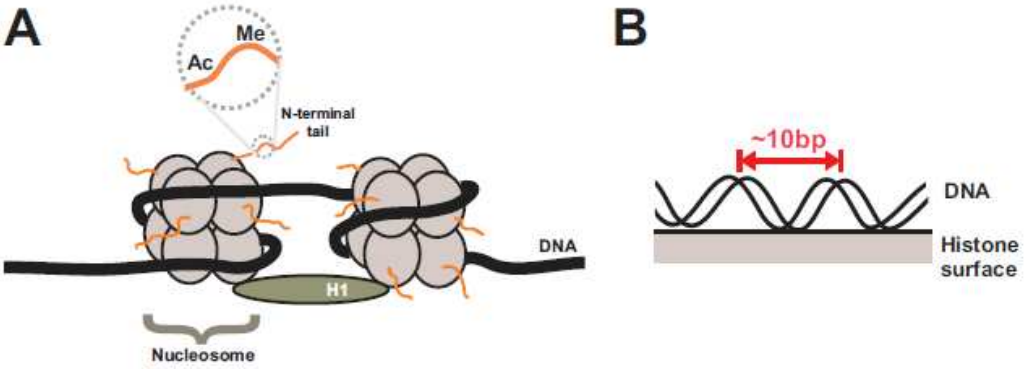

Figure 1.4. Nucleosome structure. Diagrammatical representation (scales and sizes purely representative) of two adjacent nucleosomes linked by H1 with N-terminal tails (and potential PTMs) shown (A) plus a greater resolution view of the association of a DNA helix with histone proteins (B).

1.5.2. Nucleosomes and transcription factor binding

The close association between DNA and histone in a nucleosome has long been assumed to preclude TF binding to this DNA sequence, with accessible DNA confined to nucleosome free or nucleosome linker regions (Beato and Eisfeld, 1997). However, such an assertion is perhaps too simplistic – with more subtle interactions between nucleosome bound DNA and other DNA binding proteins.

Notably, some TFs ('initiator' or 'pioneer' factors) are able to bind nucleosome associated DNA. The DNA helix executes a complete turn approximately every 10bp – therefore DNA situated at intervals of 10 bp occur on the same side, or rotational position, on the DNA. Rotational setting defines the orientation of an individual base with respect to the histone surface. When DNA is wound round a histone octamer core, certain positions are outwards facing with respect to the histone surface – consequently these bases will be most accessible to TF binding (fig 1.4.B). The rotational positioning of DBEs (DNA Binding Elements) therefore has a strong role in determining their functionality while nucleosome associated – notably small (2-3bp) shifts in the positioning of DBE within a nucleosome can significantly reduce binding (Li and Wrange, 1995; Wong et al., 1997). In addition to favourable rotational positioning, DBE sites which are bound when nucleosome associated have a tendency to be at the borders of histone associated sequence; potentially due to looser DNA-histone binding at this region (Albert et al., 2007).

TFs which bind DNA at a narrow sequence length increase the chance that the entirety of this sequence will be on the outward face of histone associated DNA (in an appropriate rotational position) – hormone receptors are a good example of this binding type. In contrast, TFs with larger numbers of DNA contact points falling across the whole circumference of the DNA strand will be unable to bind when one DNA face is inaccessible due to histone binding. Interestingly, factors that bind naked DNA

with high affinity, caused by relatively large numbers of DNA contact points, tend to have poor affinity for nucleosomal DNA and make poor pioneer factors (Luisi et al., 1991; Perlmann, 1992; Eisfeld et al., 1997). Notably, p50 homodimers are able to bind nucleosome associated DNA with almost the same affinity as naked DNA, with binding occurring without observed perturbation of the nucleosome structure (Angelov et al., 2004).

Furthermore, DNA binding in nucleosomes has been shown to be a dynamic relationship – with rapid spontaneous site exposure caused by periodic DNA unwrapping from the histone core. This process occurs on average every ~250 ms in a progressive manner and takes approximately 10-50 ms to complete; creating windows of time in which normally histone bound DNA is exposed (Li et al., 2005). Binding of factors at these spontaneously available regions of DNA can then, effectively, hold the chromatin open and allow subsequent binding of additional factors in a non-contact cooperative manner. Competition will likely exist between these newly bound factors and re-binding of the DNA by histones, however if such factors can recruit nucleosome remodelling complexes [1.5.4.] to the site this will ensure an opportunistic binding at temporarily exposed DNA can be propagated into a prolonged binding event with functional consequences (Polach and Widom, 1995; Polach and Widom, 1996; Li and Widom, 2004). The probabilistic binding of sites in such a manner will be reliant on factors such as binding affinity and nuclear concentration.

1.5.3. Nucleosome positioning

Nucleosomes are therefore able to strongly influence (even if not completely occlude) the DNA binding of non-histone proteins [1.5.2.], therefore nucleosome positioning within the genome, relative to gene sequences, will influence expression. The curvature of DNA when wrapped around a histone core is problematic for such an intrinsically rigid molecule (Mills and Hagerman, 2004). Low energy binding requiring runs of AT dinucleotides (which are more amenable to curvature) on one side of the DNA molecule, i.e. occurring periodically every ~10bp (the DNA helix completes a full turn every ~10bp (Wang, 1979) fig 1.3.B) (Ioshikhes et al., 1996). This sequence requirement suggests nucleosome positioning is intrinsically encoded within the genome. However, non-sequence factors will also play a role – discrepancies between predicted and observed global nucleosome positions are notable, as are altered nucleosome positions in two cells types derived from the same organism (Segal et al., 2006). In addition, while, in global studies, nucleosomes can show one major position, a large proportion exhibit multiple positions; either as a result of several energetically favourable local sites or due to dynamic nucleosome repositioning in response to stimuli - chromatin remodelling (Schones et al., 2008).

1.5.4. Chromatin remodelling

Several TFs are shown to act via recruitment of ATP-dependent chromatin remodelling complexes capable of altering nucleosome structure or position within a localised region. Five major eukaryotic chromatin remodelling families exist: SWI/SNF, ISWI, INO80, SWR1 and NuRD/Mi-2/CHD – the first two of which are best characterised; with their abilities often extrapolated across the families (Saha et al., 2006). Activities of the family members can be broadly divided into two functional outcomes: ensuring the even spacing of nucleosomes during chromatin assembly or, contrarily, disrupting an ordered nucleosome array into a new configuration (a function largely attributed to the SWI/SNF family) (Ito et al., 1997; Schnitzler et al., 2001). All families members contain a catalytic domain (SWI2/SNF2-family ATPase subunit) possessing ATPase and DNA-translocation activity (Saha et al., 2006; Clapier and Cairns, 2009) with differences in activity and specificity mediated by variation in additional domains or subunits (discussed below).

The exact mechanism, and exact nucleosome changes, caused by chromatin remodellers is still debated. Broadly this process consists of initial binding to both nucleosome core and DNA, an ATP-dependent conformation change in structure which exerts a torsion force capable of breaking nearby DNA-histone interactions and potentially exerts a pulling force on the DNA, causing it to translocate relative to the histone surfaces ('sliding') and potentially assume a new position when DNA-histone interaction reform at this new conformation (Saha et al., 2005; Saha et al., 2006). Alterations in position can be very localised, potentially just ~20bp (Métivier et al., 2003). An alternative hypothesis (the two may co-exist) posits that remodellers act purely by altering DNA-histone contacts and forming alternative, stable, nucleosome conformations, i.e. with no associated movement of DNA relative to the nucleosome (Narlikar et al., 2001; Bouazoune et al., 2009). An extreme version of this altered DNA-histone contact is complete nucleosome eviction; with SWI/SNF complexes responsible for dissociation of nucleosomes from the *pho8* gene promoter during gene induction in *Saccharomyces cerevisiae* (Brown et al., 2011). Chromatin remodellers can also act through modifying the structure of nucleosomes. The SWR1 remodelling complex can catalyse the exchange of histone variant H2AZ for the conventional H2A – altering nucleosome structure with implications for transcription initiation [1.6.4.1.] (Mizuguchi et al., 2004).

The activity of chromatin remodelling complexes is able to reconfigure nucleosomes into a less stable arrangement (relative to resting state) and as such might be assumed to be a transient event. However, binding of human SWI/SNF persists, even in the absence of ATP, following the remodelling event and can act to stabile the new nucleosome conformation - therefore prolonged changes in chromatin structure can be effected (Guyon et al., 2001). Indeed, an active mechanism, utilising ISWI remodelling complexes, has been shown as required to reverse SWI/SNF nucleosome repositioning (Schnitzler, 2008).

1.5.4.1. Nucleosome binding activity of chromatin remodelling complexes

Additional functions of chromatin remodellers are provided by further domains (i.e. non-ATPase) present either in the same subunit or in a varied plethora of subunits which can constituent such complexes. Such functions include non-specific DNA binding through high mobility group (HMG) domains (Thomas and Travers, 2001) and the ability of SWI/SNF complex subunits to bind actin and actin related proteins (ARPs) (Olave et al., 2002).

Interaction with nucleosomes is also a key function which is required to recruit remodelling complexes to their site of activity. This is predominantly provided by bromodomains – protein regions which bind acetylated lysines; notably those in N-terminal histone tails [1.5.1.]. Such domains are contained within the ATPase containing subunit of SWI/SNF complexes (notably the BRG1 protein) or provided by separate subunits in the case of other chromatin remodelling families (Hassan et al., 2002; Shen et al., 2007).

Variation in the bromodomain structures which recognise sequence flanking acetylated lysines allows bromodomains contained within different subunits to bind specific histone tail modifications (Zhang et al., 2010). Multiple bromodomains can be clustered on a single protein (polybromo) or through aggregation of several subunits – a scenario which allows the modular construction of diverse complexes capable of binding specific acetylated lysine combinations, known as the 'histone code'.

Chromatin remodelling subunits can also bind methylated lysine residues in histone tails through chromodomains (Sachdev et al.,1998) or methylated DNA via methyl CpG binding domains (MBD) (Clapier and Cairns, 2009). Plant homeodomains (PHDs) in remodelling subunits can also bind methyl-lysines, for example in the BPTF subunit of dNURF binding H3K4me3 (Wysocka et al., 2006). Nucleosome interactions can also be mediated by the HAND-SANT-SLIDE domain combination. SANT domain binds unmodified histone tails, SLIDE domains bind nucleosome associated DNA – with binding of both domains coordinating general DNA and histone binding and subsequent activation of the ATPase domain (Wysocka et al., 2006).

1.5.5. Post translation modification of histones

As outlined in [1.5.4.1.], chromatin remodelling complexes are able to bind covalent marks made on histone tails. The deposition of such marks is therefore a mechanism to recruit specific remodelling complexes to gene promoters or enhancer elements.

Many TFs possess histone acetyltransferase (HAT) activity capable of acetylating specific amino acids; for example, the Gcn5 yeast HAT family specifically acetylate lysine 14 in histone 3 (H3K14) and lysines 8 and 16 in histone 4 (H4K8/16) (Kuo et al., 1996) or p300 which can acetylate at

H3K9/14/27/36/37 (Sterner and Berger, 2000; Luebben et al., 2010; Szerlong et al., 2010). HAT activity is opposed by histone deacetylases (HDACs), which also exhibit specific activity, for example HDAC1 (human) and Rpd3 (yeast) HDAC complexes preferentially deacetylate H4K5/12 (Rundlett et al., 1996). While recruitment of HATs to a specific site is well characterised – relying on induced TF binding, discussed in [1.5.6.] – antagonistic HDAC recruitment is less well defined; the proteins are assumed to be either ubiquitously chromatin associated, recruited by specific factors – such as BCL-3 (Jamaluddin et al., 2005) - or recruited by the same mechanisms as HATs in a negative feedback motif [1.5.6.] (Dokmanovic et al., 2007).

Methylation of the histone N-terminal tail is caused by histone methyltransferases (HMTs) which either target arginines (the PRMT family) or lysines (SET domain and Dot1/DOT1L families) with mono-, di- or tri-methylations (Voelkel and Angrand, 2007; Wu et al., 2010). While methylation marks are notoriously stable, they can be dynamically removed; as in the inflammation dependent removal of methyl groups from H3K9 (Saccani and Natoli, 2002). Mechanism for methyl group removal are poorly defined; however, arginine and lysine demethylases have been identified (Chang et al., 2007; Shi, 2007) or alternatively whole histones may be replaced with unmethylated versions (Voelkel and Angrand, 2007).

1.5.6. Inducible HAT recruitment

As noted previously, chromatin remodelling complexes contain bromodomains [1.5.4.1.], which have been shown to be necessary for recruitment to nucleosomes (Awad and Hassan, 2008; Chatterjee et al., 2011). Such changes are induced through stimulus specific recruitment of HATs to a particular gene promoter or enhancer site. HATs generally act as cofactors which are targeted to nucleosome sites through interaction with transcription activators (Utley et al., 1998). The initial binding activator is usually a pioneer factor; which are well suited to binding within nucleosome dense areas [1.5.2.]. Subsequent recruitment of a chromatin remodelling complex creates more amenable conditions for binding of a secondary transcription activator or elements of the RNAP pre-initiation complex (Archer et al., 1991; Hebbar and Archer, 2003). Steroid hormone receptors – notably the glucocorticoid receptor (GR) and estrogen receptor (ER) – are paradigmatic for this mechanism; being able to bind nucleosome associated DNA and interact with multiple HATs and arginine methyltransferases (Hager et al., 2000; Lee et al., 2001). HATs can also be recruited by numerous other transcription factors, including NF-κB [1.2.].

Chromatin marks typically don't occur in isolation, being deposited in a sequential manner; for example at the human pS2 gene promoter at which ERα binding initially causes H3K14ac and H4R3me2 modifications, followed by H3R17me2 and H4K16ac - culminating in recruitment of SWI/SNF remodelling complexes (Métivier et al., 2003). Modification of diverse histone tail amino acids may

reflect the recruitment of multiple HAT/methyltransferase (each with potential different substrates) in a manner dependent on previous covalent modifications; with, for example, bromodomains being widely present within HATs (Dhalluin et al., 1999). Multiple acetylated sites may be necessary for stable binding by chromatin remodelling complexes; which can contain multiple bromodomains. While a general requirement for histone acetylation has been shown for chromatin remodelling complex binding, data on specific residue acetylation is less well defined – however histones 3 and 4 appear the predominant targets; with the yeast Rsc4 remodelling complex shown to bind H3K14ac (Kasten et al., 2004) plus Bgr1 and Snf5 (both SWI/SNF subunits) binding at H4K8ac and H3K56ac respectively (Xu et al., 2005; Shahbazian and Grunstein, 2007).

In addition to recruiting HATs to promoter sites, nuclear receptors can also recruit HDACs. Such recruitment occurs via nuclear receptor corepressors, such as SMRT and NCoR, and has been shown to occur following a successful transcription event (i.e. when components of the PIC leave the promoter during transcription initiation). The consecutive HAT and then HDAC recruitment creates cyclical patterns of histone acetylation at this site. Removal of the acetylation events which causes initial nucleosome movement is not in itself sufficient to cause a return to the initial conformation – this requires independent recruitment of a further chromatin remodelling complex – but it does prevent further transcription permissive movement of the nucleosome unless HATs are re-recruited by a continued transcription inducing signal (Alland et al., 1997; Lee et al., 2001). Such corepressor molecules (SMRT, NCoR and CoREST) can also bind to unacetylated histone tails (non-acetylated H4K5 is a particular requirement) via SANT domains – recruiting various HDAC complexes to the site (Yu et al., 2003). Acetylation of histones can therefore act not only through HAT recruitment but through inhibition of HDAC binding. HDAC recruitment can also occur independent of initial histone tail covalent marks, for example by the BCL-3 protein (Jamaluddin et al., 2005).

1.6. RNA polymerase II dynamics and binding

The previous section predominantly concerned TF binding at DNA, but chromatin states also affect the binding of RNAP to core promoter sites – a topic addressed in the following sections.

1.6.1. Pre-initiation complex assembly

RNA polymerase II (RNAP) is unable to bind autonomously to eukaryotic promoters and requires the assistance of several general transcriptions factors (GTFs) which make up the Pre-Initiation complex (PIC). The six general transcription factors which make up the PIC – TFIIA/B/D/E/F and H – each contribute different functional abilities to facilitate RNAP binding plus the conformational changes required in both protein and DNA for the successful start of transcription. Initial protein-promoter

contact occurs via core promoter sequence elements [1.6.2.] binding TFIID, a process enhanced by TFIIA (Emami et al., 1997). Successful establishment of TFIIA/TFIID at core promoter sites initiates a sequential assembly of further factors; next TFIIB binds and subsequently interacts with, and recruits, TFIIF and RNAP (Buratowski et al., 1989; Ha et al., 1993). The next component to bind is TFIIE which in turn recruits and activates TFIIH for roles in promoter escape and transcription initiation (discussed in greater detail later [1.6.5.2.2.1.]) (Ohkuma et al., 1995). Binding and activation of PIC components is mediated by the activity of co-factors which are often provided in a transcription inducing stimulus dependent manner – as discussed in [1.6.5.1.].

In addition, a subset of general transcription factors have also been observed to associate with RNAP independent of DNA binding – forming a holoenzyme complex (Conaway and Conaway, 1993; Malik and Roeder, 2000). This complex avoids the step wise assembly at promoter sites and can pre-form GTF interactions prior to gene induction, with formation mediated by a Mediator complex of proteins which can also facilitate interaction with transcription activator factors (Hengartner et al., 1995; Badi and Barberis, 2001).

Increasing numbers of DNA regulatory elements are found far from the gene promoters they act on (Bulger and Groudine, 2010). Techniques such as chromatin conformation capture (3C) show direct interaction between such elements and core promoters (Sajan and Hawkins, 2012). The mechanism of chromatin looping required for such long range interactions is still not fully understood. However, the process does require the cohesion protein, which binds at sites occupied by the CCCTC binding factor (CTCF) and stabilises DNA looping by facilitating cohesion of *cis* DNA sequences. The transcription coactivator mediator is also required for the stable formation of DNA loops (Nativio et al., 2009; Kagey et al., 2010).

1.6.2. Core promoter elements

Sequence elements of the core promoter are responsible for binding elements of the PIC. A central tenant of core promoter studies has been the TATA box sequence situated 25-30bp upstream of the TSS which recruits the TFIID, specifically the TBP (TATA box binding protein) subunit component (Smale and Kadonaga, 2003). While TATA box related work has perhaps been the focus of research, TATA-less promoters are actual the more common situation, though interactions at this promoter type are less well defined. TBP has been observed binding at non-TATA sequence (Martinez et al., 1995; Smale and Kadonaga, 2003), furthermore Downstream Promoter Elements (DPEs) – situated at +23 to +32 – can also act in TATA-less promoters to recruit TFIID, via interaction with TAF40 and -60 TFIID subunits (Burke and Kadonaga, 1997). DPE alone is insufficient to recruit TFIID – recruitment additionally requires Initiator sequence a set distance from the DPE site. Initiator (Inr) sequences occur at the TSS and are constituted by AC dinucleotides at +1/-1 sites respectively within a pyrimidine

rich region. TFIID binds this sequence via TAF1 and -2 subunits, provided additional interaction sites are provided by TATA box or DPE sequence (Smale and Kadonaga, 2003). Basal transcription factor TFII-I can also interact with Inr sites (Roy et al., 1997).

While TFIID is the major factor in recognising core promoter element, TFIIB is also able to bind a specific DNA region - the TFIIB Recognition Element (BRE). TFIIB ensures correct polar binding of TBP to TATA box elements by binding downstream – TBP binds TATA boxes in both orientations and is therefore unable to autonomously specify correct directionality of the PIC assembly (Bell et al., 1999; Tsai and Sigler, 2000). While the TFIIB-BRE interaction has been shown to promote PIC assembly in *Archaea*, its role in humans is less clear - even potentially inhibitory to transcription in some circumstances (Lagrange et al., 1998; Smale and Kadonaga, 2003).

Not all TFIID recruitment elements are sequence based. Trimethylated histone 3 lysine 4 (H3K4me3) are also able to bind the TFIID component subunit TAF3 (Vermeulen et al., 2007). This interaction is affected by additional modification of histone residues – with acetylation of histone 3 lysines 9 and 14 enhancing binding and dimethylation of histone 3 arginine-2 acting in an inhibitory capacity. It is unclear if this chromatin mark is sufficient to act as the sole recruiter of TFIID or merely acts as a stabilising force for TFIID bound at sequence elements. However, it can be speculated that such interactions may play an important role in RNAP promoter binding and may account for promoters where no distinct sequence element responsible for RNAP recruitment have been discovered.

1.6.3. TBP induced DNA curvature

TBP binding induces a conformational change in DNA and sharp kinking at the ends of the TATA box sequence altering both the trajectory of adjacent DNA and curvature of internal sequence (Kim et al., 1993; Kim et al., 1993; Pardo et al., 2000). The distortion of DNA in a TBP context is potentially inconsistent with the structural constraints placed on DNA conformation in a tightly wound nucleosome structure [1.5.3.] – making the binding of TBP to a nucleosome complex unlikely. Indeed, inclusion of TATA boxes within nucleosome sequence has a strong inhibitory effect on transcription initiation – *in vitro* nucleosome associated TATA boxes bind TBP poorly unless induced into a new conformation by the introduction of SWI/SNF chromatin remodelling complexes [1.5.4.] (Imbalzano et al., 1994). Thus TATA boxes are clearly far more accessible when in non-occluded DNA.

However, even location of TATA boxes in linker sequence (DNA sequence between nucleosomes) may not be sufficient; experimental movement of the *S. cerevisiae STE6* gene TATA box into linker sequence did not reduce transcription repression. The relatively short linker sequence at this location (~15bp) is a potential further inhibitory factor – with the possibility that flanking nucleosomes with so little interconnecting sequence are unable to accommodate the topological changes ('writhing') which

accompanies the severe TBP induced DNA bending (Patterton and Simpson, 1994) or simply the substantial size of the PIC. Genome wide studies in *S. cerevisiae* have predicted an average linker distance of ~13bp – the unlikelihood of such short sequence accommodating PIC formation suggests the necessity for areas of reduced nucleosome density (Nucleosome Free or Depleted Regions; NFR/NDR) – in fact a relative paucity of nucleosomes is considered a hallmark of transcription initiation sites.

1.6.4. Nucleosome Depleted Regions (NDRs)

TSSs of highly expressed genes are closely linked with Nucleosome Depleted Regions (NDRs). Global studies at single nucleosome resolution in *S. cerevisiae, Drosophila* and human cell lines identify start sites commonly occurring in significant sized nucleosome denuded regions (~130bp) bookended by consistently positioned nucleosomes (Yuan et al., 2005; Ozsolak et al., 2007; Mavrich et al., 2008; Schones et al., 2008). Regions of such size are too small to accommodate nucleosome formation (which incorporate 147bp of DNA) – therefore strict and stable positioning of these flanking nucleosomes may act to prevent intercalation of an extra nucleosome at this site, maintaining the NDR status (Ozsolak et al., 2007). Chromatin related landmarks and sequence elements have been associated with NDRs, these features are outlined in the following sections.

1.6.4.1. Flanking nucleosomes

NDRs are characterised, and perhaps caused by, differential compositions of their flanking nucleosomes in comparison to those packaging the bulk of the genome. Two histone variants are enriched in flanking nucleosomes:

(i.) H2A.Z

H2A.Z nucleosome inclusion imposes profound structural changes in the complex – including a decrease in nucleosome stability and enhanced potential for loss of H2A.Z–H2B histone dimers (in comparison to H2A-H2B dimers) (Redon et al., 2002). This facilitates nucleosome ejection by chromatin remodelling complexes – a notable example being at the inducible *PHO5* promoter (Redon et al., 2002). While this may be a factor, it does not explain the frequently observed continual presence of H2A.Z at NDRs. In this context, H2A.Z may act as a sentinel against an encroaching compact nucleosome state. The H2 variant histone has a defined role in inhibiting the spread of chromatin silencing Sir proteins in yeast. The distribution of H2A.Z correlates well with gene silencing state and cells with mutated H2A.Z genes demonstrating abnormal spread of chromatin inhibitory complexes into previously open chromatin regions along with loss of active chromatin marks (Meneghini et al., 2003). Sites need to be predisposed to incorporate H2A.Z – chromatin marks have been hypothesised to provide this function, for example H4K16ac (Meneghini et al., 2003). The SWR1

chromatin remodelling complex is also implicated in H2A.Z deposition, being itself recruited by bromodomain containing protein Bdf1 (Raisner et al., 2005).

(ii.) **H3.3**

A further histone variant associated with active gene promoters is H3.3. While the exact functional significance of H3.3 has not been explicitly defined, it has been mapped along with H2A.Z to promoter NDRs – forming a double variant nucleosome. Studies on the detection of double variant nucleosome regions have suggested that the relative instability of these nucleosome in general, and particularly under physiological ion extraction techniques, lead to regions of double nucleosome presence appearing to be devoid of nucleosomes due to experimental artifacts. As such, the nucleosome 'free' or 'depleted ' regions (NFR/NDRs) are perhaps more accurately regions of differentially composed nucleosomes – which are more amenable to DNA access. Lower strength interaction between DNA in these nucleosomes and/or periodic spontaneous dissociations from DNA would lead to enhanced access of components of transcription machinery at these sites. The presence of double variant nucleosomes may act at these sites to prevent the binding of more 'conventional' and stable nucleosomes, maintaining the site as binding amenable even if not totally exposed (Jin et al., 2009; Lickwar et al., 2012).

1.6.4.2. Histone modifications and open chromatin at the TSS

Histone composition is not the only epigenetic demarcation of open chromatin regions at TSSs; post-transcriptional modifications also play a role – potential through interactions with chromatin remodelling complexes as outlined previously [1.5.4.]. Acetylation of histone 3 K9 and K14 occurs in a tightly localised manner at promoter and enhancer sequences – acetylation 'islands' – marking these regions as differentially accessible between cell types (Roh et al., 2005). Significantly, sharp distribution peaks of these modifications occur within 500bp of TSSs (just 1-2% of the total genome) of active genes across many cell types, correlating well with differential gene expression profiles (Liang et al., 2004; Koch et al., 2007).

Liu et al. utilised single nucleosome resolution studies to determine histone modifications at nucleosomes immediately flanking the TSS, in contrast to previous work which used probes sheared to sizes of ~300-500bp in microarray studies (a length of sequence potentially covering multiple nucleosomes) (Liu et al., 2005). This study showed hypoacetylation of certain lysine residues (H2BK16, H4K4, and H4K16) at TSS flanking nucleosomes whereas surrounding nucleosomes were highly acetylated. Small subsets of modification combinations were seen, potentially due to the ability of specific histone modification to recruit further enzymes to modify the nucleosome (Fischle et al., 2003).

1.6.4.3. Sequence mediated NDRs

Two particular repetitive sequences can cause NDRs:

(i.) AT tracts: In contrast to the ~10bp periodic AT dinucleotides which form DNA structure conductive to histone binding [1.5.3.], DNA molecules consisting of continuous AT rich tracts have physically rigid properties poorly suited for the considerable bending required for DNA to wind around a histone core (Anderson and Widom, 2001; Sekinger et al., 2005).

(ii.) **CpG islands:** CpG islands are formed by the concentrated occurrence of CpG dinucleotides; a relatively rare motif in the genome but observed in concentrated regions proximal to many gene promoters (Smale and Kadonaga, 2003; Saxonov et al., 2006). The particular nature of sequence in CpG islands destabilises the assembly of nucleosomes and renders promoters in which they occur vulnerable to nuclease attack even in the absence of transcription inducing stimuli – potentially due to constitutive presence of chromatin remodelling complexes (BRG1 has been observed) at these sites (Ramirez-Carrozzi et al., 2009). CpG islands also occur in close conjunction with relatively high levels of acetylated histone 3 and H3K4me3 – further contributors to NDRs - although the cause and effect relationship between these genomic features are uncertain (Hargreaves et al., 2009).

1.6.4.4. Inducible or constitutive chromatin marks at gene TSSs

The occurrence of such NDRs, or the position of TSSs relative to a gene promoter's NDR, will determine the requirement for chromatin remodelling prior to PIC assembly (Ioshikhes et al., 2006). Sites at which TSS are not immediately accessible require induced chromatin remodelling for RNAP binding (Albert et al., 2007) whereas sites with stable NDRs and accessible TSSs not only lack this requirement but can also have constitutive RNAP binding. This constitutive, stimulus-independent binding of RNAP at promoters does not necessarily result in constitutive transcription. While many promoters regulate transcription occurrence by preventing RNAP-DNA contact unless stimulated [1.6.5.1.], RNAP binding does not necessarily mean immediate progression to full elongating capacity; additional activator factors are usually required. The complex multi-step transcription cycle governing the binding of RNAP and progression to an actively transcribing molecule provides many different stages and mechanisms for regulating transcription – as outlined below [1.6.5.].

1.6.5. The RNA polymerase II transcription cycle

The RNAP transcription cycle occurs in eight major stages. RNAP access to DNA must be ensured (1), possibly requiring nucleosome remodelling prior to PIC assembly (2). Once RNAP is fully bound, transcription initiation can occur (3), followed by early elongation stages (4) with early nascent RNA production and promoter escape potentially followed by proximal RNAP pausing. Full escape from the promoter potentially requires further RNAP C-terminal domain (CTD) phosphorylation (5) before

elongation can occur along the entire gene length (6). Transcription termination (7) can be followed by a re-start of the entire cycle (8) (Fuda et al., 2009). Each stage transition is a potential rate limiting step, requiring additional activator factors – provided by transcription activating signals - for completion. In different genes, transcription is restricted at varied points in the transcription cycle; broadly defined as pre- and post-RNAP binding.

1.6.5.1. Pre-RNAP binding transcription control

A well established paradigm for transcription activation involves the assisted binding of the PIC at TSSs by a coactivating transcription factor - setting in motion an inevitable ordered sequence of events which culminates in production of a functional transcript (Kadonaga, 2004). As such, observation of RNAP/PIC at a gene's promoter is expected to correlate with transcript production, a relationship observed at >75% genes in a human fibroblast cell line (Kim et al., 2005). At these genes, transcriptional control is exerted at the assembly of the PIC [1.6.1.]; either via a requirement for component assembly or the production of amenable chromatin conditions:

(i.) Coactivator mediated PIC assembly

Coactivator enhanced binding of virtually every stage of PIC assembly has been observed. This includes induced isomerisation of the TFIID/TFIIA complex necessary for TFIIB binding (Chi and Carey, 1996) and direct interaction between transcription factors, such as Sp1 or ERα, and PIC components in a manner which enhances their recruitment to the PIC (Burley and Roeder, 1996; Sabbah et al., 1998). Post transcriptional modifications of TFIID can also be required for further PIC component binding (Segil et al., 1996).

(ii.) The PIC and chromatin remodelling

As outlined previously [1.6.3.], PIC binding has a particular requirement for highly accessible chromatin structure – with RNAP binding strongly associated with NDRs [1.6.4.]. Creation of NDRs can be induced through chromatin marks, notably acetylation, at TSS adjacent sites [1.6.4.2.]; an occurrence closely linked to the recruitment of chromatin remodelling complexes [1.5.4.1.]. Notably, a recent study has linked the production of a dynamic NDR with the acetylation of histone 3 and dimethylation of H3K4 at nucleosomes flanking the induced NDR (Andreu-Vieyra et al., 2011).

1.6.5.2. Post-RNAP binding transcription control

Constitutive binding of RNAP at promoter sites followed by pausing is increasingly seen as a common state of transcription regulation – largely based on the widespread observation of RNAP bound at the promoters of genes with no substantial associated presence in the gene coding region or functional

transcript production. Up to 30% of a cell's genes have been shown to exhibit such behaviour in human embryonic stem cells, the phenomena has also been observed in *Drosophila* and murine cell lines (Kim et al., 2005; Guenther et al., 2007; Price, 2008; Rahl et al., 2010; Min et al., 2011).

Stimulus-independent binding of RNAP is made possible by stable NDRs; forming a constrictively amenable binding site for PIC components at a subset of genes [1.6.4.]. Notably, the experimental disruption of a nucleosome which usually occludes the core promoter of the *S. cerevisiae rnr3* gene permitted spontaneous PIC formation, even in the absence of transcription inducing signal (Zhang and Reese, 2007), suggesting amenable chromatin conditions may be all that are required for PIC/RNAP binding at some genes. However, PIC assembly in such cases does not necessarily lead to transcription. Transition to latter stages in the transcription cycle (transcription initiation and elongation) can be blocked by numerous factors, requiring the activity of stimuli induced cofactors to relive such obstacles – as outlined in the following sections.

1.6.5.2.1. Overcoming nucleosome obstacles

While chromatin remodelling is not necessarily required for RNAP binding at TSSs contained within NDRs, it may be necessary for the enzyme to progress into the coding region of the gene, as nucleosome structures might restrict elongation until they are remodeled into a more amenable state. Notably, arrested RNAP molecules are often positioned in contact with the +1 nucleosome (i.e. the nucleosome immediately downstream of the TSS) (Mavrich et al., 2008), with disruption of this nucleosomes structure abolishing RNAP pausing (Brown et al., 1996).

Stimulus induced disruption of +1, and other immediately downstream, nucleosomes at RNAP promoter paused sites has been observed via covalent chromatin modifications, resulting in chromatin remodelling and induction of elongating RNAP. Such mechanisms include localised recruitment of SWI/SNF subunit BRG1 (in response to heat shock stimuli via HSF1) (Corey et al., 2003) and the *Drosophila* Set1 methyltransferase. The latter acts to increase H3K4me3 at regions downstream of promoters containing paused RNAP; a modification which is bound by the histone 3.3 exchange factor CH1 which can act, in this manner, to directly destabilise nucleosomes in this region (Konev et al., 2007; Ardehali et al., 2011) or act through the recruitment of FACT complexes (facilitates chromatin transcription), which are capable of displacing a single dimer of H2A/H2B from nucleosomes – a further destabilising event (Orphanides et al., 1998; Orphanides et al., 1999). Reductions in histone-DNA interactions have strong association with a permissive elongation environment (Bondarenko et al., 2006); further histone modifications linked to transcription elongation – for example acetylation of H3K56 – are associated with decreased DNA-histone affinity (Neumann et al., 2009) and may be required for paused RNAP to overcome nucleosome obstacles to its transcribing progress.

1.6.5.2.2. Non-nucleosome mediated pausing mechanisms

While nucleosomal barriers appear to be a strong factor in causing RNAP pausing at many genes this is not necessarily a consensus mechanism for all sites. In striking contrast to nucleosome mediated pausing at the human *HSP70* gene, the *Drosophila Hsp70* gene recreates endogenous RNAP pausing in cell free systems in the absence of nucleosome formation (Benjamin and Gilmour, 1998). Pausing at the c-myc gene has also been shown to be nucleosome independent. Differential mechanisms clearly therefore exist to generate a paused RNAP, even between homologous genes. While the functional effect of these different mechanisms may be equivalent, the differential molecular event required for releasing a paused RNAP from each mechanism has implications for the speed and type of response needed for transition to productive elongation.

1.6.5.2.2.1. Transcription Initiation and Promoter Escape

Release of RNAP from its initial PIC to process along gene coding region requires breaking of bonds to the core promoter sequence, melting of the DNA and the initiation of a nascent RNA molecules – a process which, at least initially, is unstable and prone to abortive transcription (Mason and Lis, 1997; Tang et al., 2000). The general transcription factor TFIIH is essential for this process, via both its kinase and helicase activities, (Serizawa et al., 1993; Moreland et al., 1999; Roeder, 2005)

Notably, TFIIH is able to phosphorylated the C-terminal domain (CTD) of RNAP (a 52 heptapeptide repeat of the sequence $YS^2PTS^5PS^7$) at serine 5, a modification broadly associated with the initiation transition phase and is required for the recruitment of capping enzymes, elongation factors and chromatin modifying factors necessary for efficient progression of the RNAP (Helenius et al., 2011). Addition of a 7-methylguanine 5'ppp5'N cap to the growing (~25-50nt) RNA chain is a multistep process catalyzed by RNA triphosphatases, RNA guanyltransferases and methyltransferase enzymes – Capping Enzymes (CEs) (Shuman, 2000). Assembly of these enzymes occurs on the CTD tail of RNAP with binding controlled at the level of serine 5 residue phosphorylation (Ghosh et al., 2000; Pei et al., 2001; Fabrega et al., 2003). Successful transcript capping is required for continued transcript production; in addition to stabilising the transcript, the methyl cap CEs bound at RNAP CTD mediates an interaction with elongation factor hSPT5 (Wen and Shatkin, 1999) and is necessary and sufficient for R Loop Formation (RLF) through non-catalytic activity of the guanyltransferase domain (Kaneko et al., 2007). Transcriptional R Loops are the hybrid structure of nascent RNA paired to the DNA template strand. The physiological role of CE in RLF has been suggested to prevent the overextension of RNA:DNA hybrid length and thus ensure processivity of the RNAP complex (Kaneko et al., 2007).

1.6.5.3. DSIF/NELF mediated arrest

In addition to CEs, putative elongating complexes require additional bound factors to fully initiate; factors which are targets for regulatory inhibition. The DSIF complex consists of human homologs of

S. cerevisiae Spt4 and -5 proteins and while this complex alone is associated with elongation, in conjunction with the NELF complex plays an inhibitory role which holds RNAP in an arrested state – notably at *Drosophila* heat shock genes, where paused RNAP can be seen associated with DSIF and NELF. Heat shock induction – and associated end of RNAP pausing – is associated with the loss of NELF but not DSIF (Wu et al., 2003). DSIF is able to enhance elongation *in vitro* and has homology to bacterial elongation factors (Wada et al., 1998). In addition, DSIF has also been seen associated with RNAP within gene coding sequences, i.e. associated with elongating complexes, consistent with the idea of DSIF acting in an elongation promoting manner unless associated with NELF (Andrulis et al., 2000; Aida et al., 2006).

Interaction of the DSIF/NELF unit with arrested RNAP occurs via DSIF direct binding of the RNAP molecule (Yamaguchi et al., 1999) but also requires a greater than 18nt transcript for stable binding. DSIF interacts with RNA through subunit SPT5 and the NELF complex also contain RNA recognition motifs (RRMs) (Fujinaga et al., 2004; Missra and Gilmour, 2010). NELF inhibits elongation through this binding of an emerging transcript via an RNA recognition element (Wu et al., 2003) or potentially via interactions with the RNAP clamp domain (Missra and Gilmour, 2010). DSIF/NELF also act via inhibition of TFIIS – a basal transcription factor with a role in facilitating the end of RNAP arrest (Palangat et al., 2005) [1.6.5.6.].

1.6.5.4. P-TEFb mediated release from pausing

Positive Transcription Elongation factor b (P-TEFb) acts to inhibit DSIF/NELF mediated arrest in a kinase activity dependent manner. The protein phosphorylates serine 2 of the RNAP CTD tail; the functional effect of this modification has been suggested to enhance recruitment of Capping Enzymes and associated positive effects on elongation (Shim et al., 2002; Peterlin and Price, 2006). P-TEFb mediated phosphorylation of RNAP CTD has also been shown to reduce DSIF-RNAP binding which would abolish the inhibitory influence of DSIF/NELF complexes – although this induced dissociation of DSIF is in contrast to studies mentioned above reporting a continued DSIF–RNAP association well into elongation (Wada et al., 1998). Another target for P-TEFb is the C-terminal region of SPT5 subunit of DSIF. Phosphorylation of residues in this region acts as a switch between elongation negative and positive status – potentially by inducing release of the inhibitory NELF complex (Sims et al., 2004; Yamada et al., 2006). The NELF complex itself is also a target of P-TEFb. Phosphorylation of the NELF-E/RD subunit inhibit the complex's RNA binding capacity and associated inhibitory effect of this function (Fujinaga et al., 2004).

Recruitment of P-TEFb to arrested RNAP sites is carried out by a diverse array of activators, for example P-TEFb shows HSF dependent recruitment to heat shock loci upon stimulation (Andrulis et al., 2000; Lis et al., 2000). A further factor shown to recruit P-TEFb is c-myc – a transcription factor

able to bind at E-box elements and observed to localise at TSSs enriched with this sequence (Rahl et al.). A wide range of activators appear to function via P-TEFb recruitment – another example being the androgen receptor (Lee et al., 2001).

1.6.5.5. P-TEFb and recruitment of RNA processing factors

In contrast to studies showed a paused RNAP unable to progress beyond the first ~50 bp of transcript, Hargreaves et al. showed pre-bound RNAP existing in its serine 5 phosphorylated CTD form is able to elongate (albeit at a lower level) and produce full length transcripts. Crucially, however, these transcripts are in an unspliced form – and are consequently not able to provide a template for protein synthesis (Hargreaves et al., 2009). This work suggests P-TEFb may act to promoter successful transcription by mediating recruitment of splicing machinery to the transcribing RNAP molecule. Notably, hyperphosphorylated RNAP CTD tails have previously described roles in early stages of splicing machinery assembly (Hirose et al., 1999).

Further roles for P-TEFb independent of its direct role in elongation release have also been described. While addition of the P-TEFb kinase activity inhibiting drug flavopiritol decreases the density of elongating RNAP molecules on some genes, no such effect is seen at the *Drosophila Hsp70* gene following induction, despite an observed inhibitory effect of the drug in the fold induction of the gene transcript levels. P-TEFb mediated transcript induction at this gene appears to occur through facilitating correct processing of the 3' end of the transcript. Incorrectly processed transcripts are rapidly degraded – accounting for the drop in gene induction (Ni et al., 2004). P-TEFb dependent phosphorylation of RNAP CTD serine 2 has been shown to be responsible for co-transcriptional recruitment of polyadenylation factors at certain yeast genes – knock downs of kinase subunits of P-TEFb again result in transcript instability (Ahn et al., 2004).

1.6.5.6. RNAP backtracking and TFIIS mediated release

Another significant landmark in RNAP procession occurs at 25-50nt into the nascent transcript. Paused RNAP molecules occur in conjunction with a transcriptional bubble and short transcripts of 25-50nt (Rougvie and Lis, 1988; Rasmussen and Lis, 1995). Rather than RNAP coming to a halt at the sequence point at which pausing occurs at, occurrences of 'back-tracking' of the enzyme are observed – with the RNAP molecule and associated transcription bubble moving back along the DNA and RNA sequence to a site upstream of the leading edge of the RNA molecule (Samkurashvili and Luse, 1998).

Movement of RNAP to this retreated state occurs with a repositioning of both DNA and RNA sequence within the protein. Crucially the catalytic site of the RNAP enzyme is now positioned at an internal site within the RNA molecule and not at the 3' hydroxyl end required for the growing synthesis of the

transcript – consequently arrested complexes lose catalytic activity (Komissarova and Kashlev, 1997). Foot printing studies at these paused sites show interconversion between the active and retreated states of RNAP – suggesting RNAP advance is a discontinuous process with additions to the growing RNA transcript only possible when the RNAP enzyme is in the amenable ternary complex isoform (Komissarova and Kashlev, 1997; Komissarova and Kashlev, 1997). Factors which influence the dynamic equilibrium between the two RNAP states will be able to affect an influence on the rate and likelihood of transition to a longer RNA chain and successful elongation.

One such proposed factor is an inherent property of the RNA chain being produced. 'Sliding Clamp' models have been proposed, with the bi-directional movement of RNAP along template DNA settling at a location which maximizes the ~8bp RNA:DNA hybrid interaction strength and consequently the ternary complex stability (Landick, 1997). This model predicts pausing to be caused by relatively low RNA:DNA sequence affinity at the pause site initially destabilises a processive RNAP complex. In *Drosophila* cells RNA transcripts at paused promoters can be attributed to particular sequence properties – with the hybridisation strength of DNA:RNA hybrid being a strong factor in the elongation efficiency of the transcribing RNAP. Paused transcripts show blocks of bases with high melting temperature from +20 to +35 positions followed by a trough region of far lower melting temperature which is predicted to destabilise the elongation complex and cause stalling and potential backtracking of the RNAP to the high melting temperature region (Nechaev et al., 2010). While sequence mediated stability of ternary complexes has been demonstrated to play a role in promoting pausing at many genes, back-tracking of RNAP molecules also occurs in a sequence independent manner. In such cases, the length of the nascent transcript rather than the sequence content has been hypothesised to stabilize the ternary complex – with a fully fledged and stable elongation complex not being formed until ~50nt have been transcribed (Samkurashvili and Luse, 1998).

Stable ternary complex at the retreated position is unable to resume transcription due to the discrepancy between the position of RNAP on the DNA template and 3' end sequence of RNA being misaligned. Re-initiation can be induced by cleavage of RNA corresponding to backtracked sequence to effectively re-align the RNAP catalytic site and bound DNA template with the 3' end of sequence corresponding RNA molecule. RNAP possesses intrinsic nuclease activity however this activity is greatly enhance by general transcription factor TFIIS (Izban and Luse, 1992; Reines et al., 1992). Inhibition of TFIIS interaction with RNAP is a site of action for negative elongation factors DSIF/NELF. Notably, DSIF/NELF are causative RNAP arrest factors at the *Drosophila Hsp70* gene, with stimulus mediated inhibition of these factors and associated release of RNAP form arrest not able to occur in the absence of TFIIS (Palangat et al., 2005).

1.6.6. Functions of pre-stimulus bound and paused RNAP

The occurrence of pre-stimulus bound, and paused, RNAP is well documented, with growing mechanistic insight into release of the enzyme by various transcription activators. Several functions of bound RNAP are outlined in the following sections.

(i.) Transcription response speed

Paused RNAP has the potential to respond to inductive signals at a faster rate than RNAP which required stimulus dependent PIC assembly (Roh et al., 2006). Following an inductive heat shock, elongation at the polymerase arrested *Drosophila Hsp70* gene is detected after just 10 seconds and reaches maximal amplitude within three minutes (Lee et al., 1992). Global studies have identified genes with promoter paused RNAP as response genes; including heat shock proteins, DNA damage response factors genes and elements of signalling cascade pathways (Kim et al., 2005; Gilchrist et al., 2012; Sawarkar et al., 2012). The required rapid response to these cell threatening processes is well suited by a poised RNAP transcriptional response.

(ii.) Variation in promoter response rate to the same stimuli

A transcriptional 'response' to extra-cellular stimuli involves a large number of genes – typically not deployed at a single time point but at several temporal stages. Macrophage cells respond to inflammatory stimuli through transcriptional upregulation across a wide range of genes. Genes at which transcription can be induced without requiring protein synthesis are categorised as 'primary response genes' in contrast to those which do – 'secondary response genes'. Primary response genes can be further sub-categorised into early and late based on their relative response rates. This temporal categorisation is determined by whether transcription requires chromatin remodelling (Wu et al., 2010) or not (early) (Ramirez-Carrozzi et al., 2006). Thus the chromatin status of gene promoters is a large factor in determining the response rate of a gene. Allowing RNAP to progress to a later stage in the transcription cycle before halting progression results in transition to initial productive transcription in a shorter time frame. Consequently, staggered response times of stimuli induced genes can be controlled though the chromatin landscape at promoters.

Differential responsiveness of gene promoters allows a single stimulus to induce genes at varying rates. A notable example of this is TNFα stimulation of NF-κB transcription activation factor which has been shown to induce a sub-set of 74 genes in three categories – early, middle and late – peaking at 1, 3 and 6 hours respectively after stimulation (Tian et al., 2005). Early response genes were enriched for paracrine response functions to propagate and refine the initial inflammatory stimulus. However it is particular striking that these early genes peak at ~1 hour and then sharply decline – indicative of active inhibitory mechanisms also induced by the same inflammatory stimuli. This observation emphasises the point that the activation of genes is not a solitary event but occurs within a framework

of multiple additional gene inductions. Many of these induced gene products will interact and regulate each other – forming a gene regulatory network.

1.6.7. Transcription activators – differential points of activity

A common theme running through the above account of the transcription cycle and control points is that transcription activator factors can act in a wide variety of different ways and at different stages of the cycle. Activator factors can act at transcription initiation and elongation separately. Factors such as Sp1 can facilitate initiation of RNAP complexes but not elongation, whereas factors such as Tat can act to transition to elongation but only if initiation has already occurred (Tang et al., 2000). Some transcription activators are capable of acting at multiple sites in the transcriptional cycle; a notable example being NF-κB.

1.6.8. NF-κB conducts transcription activation roles at multiple sites in the transcription cycle

NF-κB assists in the assembly of the PIC through interactions with numerous TAF components of the TFIID general transcription factor. Interactions have been observed between NF-κB subunit p65 and TBP plus $TAF_{II}105$, $hTAF_{II}28$, $hTAF_{II}80$ and $hTAF_{II}250$ (Guermah et al., 1998; Yamit-Hezi et al., 2000; Silkov et al., 2002). In addition, NF-κB also has a well documented role in post-PIC transcription induction. For example, at the A20 promoter Sp1 transcription factor facilitates PIC formation and induced NF-κB is responsible for progression to a fully elongating stage (Ainbinder et al., 2002).

NF-κB can act to recruit P-TEFb to activate previously bound but paused RNAP [1.6.5.5.]. Inflammation induced NF-κB activation in LPS activated macrophages recruits histone acetyl transferase P/CAF which causes the hyperacetylation of histone 3 and 4 in adjacent nucleosomes – notably at residues H4K5/8/12. The modified nucleosome is now bound by bromodomain containing factor Brd4 which in turn can recruit P-TEFb (Jang et al., 2005; Sharma et al., 2007; Hargreaves et al., 2009). TNFα activated NF-κB further acts at the IL-8 gene promoter in humans via P-TEFb release of RNAP into elongation (Barboric et al., 2001).

1.6.8.1. Timing of NF-κB transcription induction

The different stages of the transcription cycle NF-κB activates at is a potential explanation for the varied transcription response times of the genes it induces. ChIP studies have shown simultaneous binding of NF-κB at ‘early’ and ‘late’ genes – genes which reach maximal induction at ~1 and ~6 hours of induction respectively. Differential transcription mediating mechanisms induced by NF-κB may

explain this timing discrepancy – although it must be noted that a role for addition co-activators may also cause this effect (Tian et al., 2005).

In contrast, other studies have shown differential timing of NF-κB activity due to delayed binding. Saccani et al. noted two 'waves' of NF-κB binding in LPS stimulated macrophages. The authors utilised NF-κB ChIP to define two categories of NF-κB bound promoter; constitutively immediate access promoters and those bound later which required a stimulus dependent modification of chromatin to make NF-κB binding sites accessible (Saccani et al., 2001). Delayed NF-κB action in this case is caused by its own delayed binding rather than RNAP, although the time delay shares the same cause – recruitment of chromatin remodelling complexes. In both cases the chromatin 'landscape' of the promoter prior to induction has a profound effect on the promoter induction kinetics.

1.7. Aims of the work

Work in this thesis aims to investigate the role that BCL-3 plays in the control of transcription at the *TNFA* gene. In particular, this control will be in the context of transcription induced by TNFα stimulation of the NF-κB signalling pathway – the induction of both *TNFA* and *BCL3* genes having previously been shown to be induced in this manner.

The role NF-κB can play in simultaneously inducing transcription of a gene (*TNFA*) and an inhibitor of this process (*BCL3*/BCL-3) is of particular interest. The work will attempt to identify the relative response rates of these two genes and investigate differential RNA polymerase II and/or chromatin dynamics. The effect of differential chromatin states at gene promoters and any potential effect on the output characteristics of genetic motifs this can produce is a strong focus of the study.

A further aim of the work is to produce mathematical models in parallel to experimental work. It is intended that such models will generate hypotheses for further testing. Models will also be used to test the kinetics of BCL-3 induction in response to diverse patterns inflammatory stimuli, in light of its role in inhibiting *TNFA* transcription.

The work will predominantly utilise population level assay. However, a further aim of the work is to consider developing the work into single cell studies – with the production of appropriate tools and reagents – as appropriate.

Chapter 2

Materials and Methods

General details regarding buffers are given in Appendix 1. Supplier details and catalogue numbers for reagents and equipment are provided in Appendix 2.

2.1. Cell culture

2.1.1. Cell lines used

Two adherent human cell lines were used in this work: HT1080 and SK-N-AS.

2.1.1.1. SK-N-AS

SK-N-AS cells are a human neuroblastoma cell line and were obtained from Mike White's Laboratory (University of Liverpool). SK-N-AS cells have low motility and are therefore well suited for long time course, live cell imagining experiments. In addition, several previous studies have characterised the NF-κB signalling pathway in response to TNFα stimulation in this cell line (Nelson et al., 2004).

2.1.1.2. HT1080

HT1080 (CCL-121; ATCC®) cells are a human fibrosarcoma cell line derived from connective tissue, containing an activated N-ras oncogene. As HT1080 cells grow as an adherent monolayer and have previously been shown to be amenable to DNA transfection, they were considered a good candidate for cell imaging studies involving the expression of fluorescent tagged proteins from DNA vectors. HT1080 cells also grow rapidly, making experiments which required large quantities of cells (for example ChIP) feasible. Previous studies have also shown HT1080 cells to be relatively resistant to induced cell death via TNFα signalling and the cells also have a measurable NF-κB signalling pathway output in response to TNFα stimulation (the inflammatory cytokine used in this study) (Wang et al., 1996).

2.1.2. Cell culture

2.1.2.1. Cell growth conditions

Cells were cultured in T75 flasks (Corning Life Sciences) in Minimum Essential Medium Eagle with Earle's salts, L-glutamine and $NaHCO_3$ (hereafter referred to as MEM; Sigma-Aldrich) supplemented with 10% Foetal Bovine Serum (FBS; Fisher Scientific UK Ltd) and 1x NEAA (Sigma-Aldrich). Cells

were grown at 37℃ in 5% CO_2. For some experimental purposes, cells were also grown in 6 well plates (Corning Life Sciences) or 100mm culture dishes (Fisher Scientific UK Ltd).

2.1.2.2. Adherent cell detachment

Adherent cell lines must be removed from cell surfaces (which mimic the extra cellular matrix) prior to transference to a new vessel or use in experiments. MEM was initially removed from culture vessels, the cells were then washed with PBS (w/o Ca or Mg; Sigma-Aldrich) which was subsequently removed and the cells incubated with trypsin-EDTA (1ml and 3ml for 6 well plates and T75 flasks respectively; Sigma-Aldrich) at 37℃ in 5% CO_2, for 5 minutes. After this time, trypsin activity was neutralised by addition of MEM and the cells, now in suspension, were either diluted in more fresh MEM for further culture [1.2.3.] or transferred to a 15ml tube (Corning Life Sciences) and pelleted by centrifugation (230 x g, 5 minutes) facilitating the removal of MEM and resuspension in appropriate solution for subsequent experimental work. All solutions used had previous been warmed in a 37℃ water bath.

2.1.2.3. Cell sub-culturing

Cells were grown until approximately at 75% confluence in T75 flasks, as in [1.2.1], and then detached through trypsin treatment [1.2.2.]. A volume of 7ml of MEM was used to neutralise trypsin activity and, following mixing, 1 ml of this solution was placed into a new T75 flask and a further 9 ml of fresh MEM added – creating a 1/10 dilution of cells. All solutions used had previous been warmed in a 37℃ wate r bath. The number of sub-culturing events (or passages) cell populations have undergone was recorded. HT1080 cell lines were maintained up to passage 50, after which point growth rates were observed to be decreasing.

2.1.3. Cell stimulation with TNFα

Cell cultures were stimulated with 10ng/ml human recombinant TNFα (Merck Biosciences) unless otherwise stated. The reagent is provided in a lyophilized form which was resuspended in sterile PBS to a final concentration of 10µg/ml, divided into aliquots and stored at -80℃.

2.1.4. Cell treatment reagents

Cells were treated with the following chemicals at times and concentrations indicated in the relevant Results section. NF-κB SN50 Cell-Permeable Inhibitor Peptide (Calbiochem) [3.2.2.] was provided in a lyophilized form and was resuspended in water and stored at -20℃. Actinomycin D and Trichostatin A (TSA) (both from Sigma-Aldrich) were resuspended in 100% ethanol (Sigma-Aldrich) and stored at -20℃ in the absence of light. Actinomycin D was us ed at 5µg/ml final concentration and incubated with cells for one hour prior to beginning the experimental time course. TSA was used at varied concentrations [4.2.4.], with cells pre-incubated for 12 hours prior to the experiment start.

2.1.5. Counting cells

A Millipore Scepter^{TM} handheld automated cell counter was used to count cells. Adherent cells were trypsinised and resuspended in growth media [1.2.2.], then further diluted in growth media until cell density fell within the operational range of the cell counter ($0.5x10^6$-$1.5x10^6$ cells per ml).

2.1.6. Cryopreservation of HT1080 cells

Adherent HT1080 cells were detached by treatment with trypsin [1.2.2.] and resuspended in 5ml of MEM. Cell density per volume was calculated [2.1.5] and the cells were pelleted by centrifuging (1,500 rpm, 5 minutes). Media was then removed and cells were resuspended in freezing medium - MEM plus 5% DMSO (v/v; Sigma-Aldrich) – to a concentration of $1x10^6$ cells per ml. Following mixing, an aliquot of 1ml of the solution was placed into freezing storage vials (1.2ml CryoPure tubes; Sarstedt). Vials were placed at -20 ℃ for 1 hour, then at -80 ℃ overnight before being transferred to liquid nitrogen for long term storage.

To defrost previously cryopreserved cells stocks, vials were partially thawed until only a central portion of the contained solution was still in ice form. This liquid/ice mix was rapidly placed in a 10ml volume of growth media which was then heated until the cell stock solution became fully defrosted. Thawing in a larger volume dilutes the concentration of DMSO cells are exposed to when defrosting (DMSO makes cell membranes partially permeable) and enhances the survival rate of cells. The solution was then spun at RT at 110xg for 5 minutes and the resulting pellet resuspended in 10ml MEM (to further remove traces of DMSO from the media). This solution was then transferred to a T75 flask for cell growth as normal [as in 1.2.1.].

2.1.7. Cell viability assay

Cells were detached as in [1.2.2.] and resuspended in MEM. A 50µl volume of cell suspension was mixed with an equal volume of Trypan Blue solution (0.4%; Sigma-Aldrich) and introduced slowly into a haemocytometer slide chamber (both slide and coverslip having previously been cleaned with ethanol and dried) until the chamber was full. Cells were then allowed to settle for 1 minute. A light microscope was focussed on the haemocytometer grid and used to count cells in the four large corner squares. The density of cells resuspended in MEM was adjusted to keep cells numbers per large square at 100-200 – with number above this range proving difficult to count. Cell viability was calculated using the following equation: Percentage viability = 100x(Total number of cells – cells which had taken up blue dye)/total number of cells.
Viability was calculated for each of the four squares counted and a mean value was calculated.

2.2. Quantitative real time reverse transcriptase PCR (qRT-PCR)

2.2.1. RNA extraction

Cells were detached by the addition of typsin [1.2.2.] and resuspended in 5ml MEM before being collected as a pellet by centrifugation (1300 x g for 10 minutes). RNA was extracted from this cell pellet by using either the E.Z.N.A.® Total RNA kit (Omega Bio-Tek, Inc) or RNeasy Mini kit/QIAshredder spin column kit (both from Qiagen) by following the manufacturer's instructions in both cases. RNA was ultimately eluted, from columns used in both kits, in 50µl of RNase-free water and treated with DNaseI (New England Biolabs) to remove any residual genomic DNA (44µl eluted RNA, 5µl 10x DNase I reaction buffer, 1µl DNase I - incubated for at least 3 hours at 37℃ then heat inactivated at 75℃ for 20 minutes). RNA was eithe r immediately used for cDNA synthesis [2.2.2.] or stored at -80℃.

2.2.2. cDNA synthesis

Extracted RNA was converted to cDNA using Applied Biosystem's High Capacity cDNA Reverse Transcription kit, with 2µg of RNA used per reaction, by following the manufacturer's instructions. Produced cDNA was stored at -20℃.

2.2.3. qRT-PCR conditions

PCRs were quantified using SYBR Green I reagent – a dye which fluoresces when bound to double strand DNA but not in solution. Consequently, when present in a PCR mixture the cumulative increase in fluorescence intensity at the end of each reaction cycle can be used to measure the rate of the dsDNA product produced by the PCR in real time. The following reaction mixture was used (per reaction):

0.3µl……..Forward primer (10µM),
0.3µl……..Reverse primer (10µM),
1.9µl……..dH_2O,
7.5µl……..Power SYBR® Green PCR Master mix (Applied Biosystems),
5µl…….cDNA (1/10 dilution of cDNA produced in [2.2.] – made up to 5µl volume with dH_20),
15µl……..Total

Reactions were carried out in 96 well PCR plates sealed with an adhesive polyolefin cover (both Starlab Ltd) and gently spun down (110g for 2 minutes) to accumulate reaction mixtures in the bottom of the plate's wells. Care was taken to ensure that the reaction, following addition of SYBR Green mix,

was shielded from light as much as possible. Reactions were run on an Applied Biosystem 7300 Real Time PCR System, using reaction conditions outlined in table 2.1.

Table 2.1. Reaction conditions for qRT-PCR. Fluorescence was measured at the end of Step 3 at every cycle.

Step	Temperature	Time (seconds)	Number of cycles
1	50	120	1
2	95	600	1
3	95 60	15 60	40

Primers used for individual qRT-PCRs were all designed to be functional at 60℃ (sequences in table 2.2.) [2.8.3.1.]. Prior to use, primer activity was checked by PCR [2.8.3.] and gel electrophoresis [2.8.4.] to ensure that no production of additional, non-specific, reaction products or primer dimers occurred. Furthermore, following each qRT-PCR, reaction mixes were run out on a 1% agarose gel to visualise PCR product and ensure that only the required DNA product was produced, and measured, in the reaction. Reaction output was recorded using Applied Biosystem's 7300 System SDS Software version 1.3.1 and data was output into an excel spreadsheet for analysis [2.4.].

Table 2.2. Primers used in qRT-PCR.

Gene target	Sequence		Melting temperature (℃) *
CYCA	FOR	GACCCAACACAAATGGTTCC	62.5
	REV	TCGAGTTGTCCACAGTCAGC	64.9
TNFA	FOR	CTCTTCTGCCTGCTGCACTT	65.0
	REV	GCTGGTTATCTCTCAGCTCCA	63.9
BCL3	FOR	CCCTATACCCCATGATGTGC	62.6
	REV	GGTGTCTGCCGTAGGTTGTT	65.3

* Melting temperatures calculated using the 'nearest neighbour' method and given to one decimal place. ** Sequence from Ashall et al 2009. Primers used for ChIP quantification are outlined in section [2.7].

2.2.4. Ct method and Statistical comparison of data

The Comparative C_T method (or $2^{-\Delta\Delta CT}$ method) was used to obtain the relative level of gene transcript in a population of cells in comparison to the level in another reference population of cells – which in this

study, unless otherwise stated, were cells unstimulated with TNFα (i.e. time point zero in stimulation time courses) (Schmittgen and Livak, 2008). The increase in reporter dye fluorescence levels (above basal levels) was plotted (by AB 7300 Systems SDS software) against PCR cycle number, determining the cycle number at which fluorescence levels reach an experimentally set threshold level (0.2 RFU). This is the C_T value. Values are normalised for variation, in initial cDNA concentrations, by parallel sample analysis with primers amplifying internal reference gene cyclophilin A (*CYCA)*. C_T values calculated for *CYCA* for a sample are subtracted from the target gene C_T value. The difference between this value and one calculated in the same manner from an additional sample extracted from a reference population of cells is determined:

$\Delta\Delta C_T$= Sample (C_T target gene - C_T cyclophilin A) – Reference sample (C_T target gene - C_T cyclophilin A).

As increase in PCR product is exponential, using this value as the negative exponent of 2 gives the initial fold difference in cDNA levels between the two cell populations:

Fold change =$2^{-\Delta\Delta CT}$.

An inherent assumption in this method is that the reaction efficiencies of the target and control primer sets are equal. To confirm the suitability of this method for data analysis, relative primer set amplification efficiency was tested by performing the reaction with all primer sets used on serial dilutions of template cDNA solution. If efficiencies are constant, C_T values should not alter significantly – see [3.2.1.2.2.].

2.3. Human cell transfection

2.3.1. Plasmid transfection of HT1080 cells

2.3.1.1. ExGen500

Transfection of plasmids with ExGen 500 *in vitro* Transfection reagent (Fermentas) was conducted according to the manufacturers suggested protocol. Reactions were carried out in either 6 well plates or 35mm dishes containing a 3ml volume of growth media, with 9.9µl of ExGen 500 used per transfection reaction. Optimisation of the protocol for transfection of particular plasmids is outlined in the Results section [3.2.4.1.1.].

2.3.1.2. FuGene® 6

FuGene® 6 Transfection Reagent (Roche Applied Science) was used according to the manufacturer's suggested protocol for HT1080 cells. Specifically, cells were transfected when approximately 50%

confluent, with a 3:1 ratio of Reagent:DNA used. A quantity of 1µg DNA per plasmid was used and further optimisation of the protocol is outlined in [3.2.4.1.1.].

2.3.2. siRNA transfection

2.3.2.1. Lipofectamine™ 2000

Cells were seeded into dishes one day prior to transfection, resulting in a confluence of 30-50% at the time of transfection. A combination of three sequence specific BCL-3 targeting siRNAs were used (BCL3HSS -55100965, -55184300 and -184299; Invitrogen) in equal amounts to a total quantity of 350 pmol of siRNA per transfection. Stealth RNAi siRNA Negative control Duplexes (Invitrogen) were simultaneously transfected into equivalent, but separate, cell populations. Appropriate sequence variants of the negative control siRNAs were selected on the basis of GC content (siRNA GC content correlates negatively with RNAi efficiency due to reduced dissociation of the double stranded siRNA duplexes). Therefore a ratio of 'High' to 'Medium' GC content negative control siRNAs of 2:1 was used to correspond to the three aforementioned BCL-3 siRNAs, again to a total siRNA quantity of 350pmol per transfection.

Lipofectamine™ 2000 reagent (Invitrogen) was used to transfect cells following the manufacturer's protocol. Following addition of transfection reagent, cells were left for 24 hours, at 37℃ in 5% CO_2, before growth media was changed, then left for a further 24 hours before being treated with TNFα. Following stimulation, cells were detached by treatment with trypsin [1.2.2.] and centrifuged (1700 x g, 10 minutes). The resulting pellet was resuspsended in growth medium and the cell suspension then split into two – one half volume being used for RNA extraction and subsequent conversion to cDNA for use in qRT-PCR [2.2./2.3.] and the other half used for protein extraction and analysed by western blot [2.5].

2.3.3. BAC transfection

BAC DNA was transfected with ExGen500 [2.3.1.1.] with volumes and DNA quantities varied experimentally; see [7.2.5.1.]/[7.2.5.2.].

2.4. Live imaging of human cells

2.4.1. Cell culture

Cells were grown and imaged in 35mm glass based dishes (Iwaki). While undergoing imaging, dishes were maintained in sealed environments with conditions of CO_2 (5%) and temperature (37℃) conductive for continued cell survival.

2.4.2. Microscope

Cells were imaged with a Zeiss LSM 710 confocal laser scanning microscope, 40x oil immersion objective lens and using a macro operating within the Leica LSM software package to observe multiple field positions per experimental time course (Rabut and Ellenberg, 2004); dsRed was excited with 543nm green Helium Neon laser and detected with a 570nm long-pass filter; EGFP was excited with a 488nm Argon ion laser and detected with a 505-550nm band-pass filter.

2.4.3. Cell tracking

CellTracker version 0.6 software (DTI Beacon Project, University of Manchester) was used to mark cell and nuclear boundaries of a single cell captured in consecutive time course microscopy images (Shen et al., 2006). The program measured average fluorescence intensity for total cell and nuclear areas and output these values, along with the corresponding time, into an excel spreadsheet.

2.5. Western blots

2.5.1. Protein extraction

HT1080 cells were grown, stimulated and detached as described in [1.2.2.]. A pellet of the cells was produced by centrifugation at 7000 x g for 10 minutes, the pellet was then resuspended in 30µl of PBS supplemented with 10µl of 4x Protein extraction buffer (see table 2.3.). Solutions were then incubated at 100℃ for 5 minutes, vortexed for a further five minutes and spun at 8500 x g for 10 minutes and the resulting supernatant removed and stored on ice for immediate use or at -20℃ for longer term storage.

2.5.2. Protein quantification

The total protein concentration of a sample was determined using the Bradford assay – a colorimetric assay which uses the change in absorbance of Coomassie Brilliant Blue G-250 dye when bound to proteins as an indicator of the protein concentration of a solution. The amount of total protein in a sample extracted by cell lysis [5.1.] was determined by comparison with standard values measured using known concentrations of BSA protein. A range of BSA concentrations (0, 1.25, 2.5, 5, 10,15 and 20µg/µl) were produced by diluting 2mg/ml BSA in 800µl H_2O supplemented with 1µl of 1x protein extraction buffer. A volume of 200µl Bradford dye reagent (Biorad Protein Assay Kit II) was added, the solution was then thoroughly mixed and 300µl final volume used per well in a 96 well plate with each sample measured in triplicate. Absorbance at 630nm was measured with an ELx800 Absorbance Microplate Reader using KCjunior™ software (both from BioTek UK). Data was output into an excel spreadsheet and plotted in Graph Prism 5 software – plotting BSA concentration (x axis) against OD_{630nm} absorbance (y axis). The software was used to plot a straight line of best fit using the formula

y=mx+c (m is gradient; c is y axis intercept value). Protein samples solutions were measured simultaneously on the same plate as the BSA standards (1µl protein sample + 799µl H_2O + 200µl Protein Assay Reagent – 300µl total reaction mixture measured in triplicate). The formula derived from BSA standards was used to determine the concentration of protein sample based on its output absorbance value.

2.5.3. SDS-PAGE

Whole protein cell extracts were separated by size on polyacrylamide gels by electrophoresis, utilising SDS to remove secondary structures and negatively charge each peptide (charge conferred by SDS is proportional to mass and not dependent on an individual peptides amino acid composition). Polyacrylamide gels were made between glass plates (0.75mm spacer plate Mini-PROTEAN 3 Multi-Casting Chamber; BioRad) which were washed with 70% ethanol and dried immediately prior to use. Initially, a 12% Resolving gel solution (see table 2.3.) was poured into the vertically arranged gel plate chamber immediately after addition of TEMED (the acrylamide polymerising reagent). This Resolving gel was poured to a height 0.5-1.0cm below the bottom of the gel combs with a layer of isopropanol (2-propanol; Simga-Aldrich) subsequently introduced to lie on top of the gel layer to maintain anaerobic conditions necessary for polymerisation. After 20 minutes, the isopropanol was removed and a 5% Stacking acrylamide gel (see table 2.3.) solution poured into the plates, filling the volume between the plates once the gel comb was put in place. The gel was then left a further 20 minutes to set.

Once solidified, acrylamide gels were assembled and run in a Mini-PROTEAN 3 Electrophoresis Module (BioRad Laboratories) in 1x Running buffer (see table 2.3.). The appropriate amount of protein to run per gel lane was experimentally determined (dependent on the primary antibody used), with equal amounts of total cell protein run in each lane. For loading, equal volumes of protein sample were mixed with 2x Gel loading buffer (see table 2.3.). If there were not a sufficient number of protein samples to fill all lanes in a gel, 1x Protein extraction buffer (diluted with PBS) was used in place of protein samples and loaded in the same manner. In addition, a volume of 5µl of ColorPlus Prestained Protein Marker (New England Biolabs) was also run to determine the size of proteins. Gels were run at 120V for approximately 2 hours.

2.5.4. Blotting and blocking

Protein samples resolved by SDS-PAGE were then transferred to a Nitrocellulose membrane (Sigma-Aldrich) for subsequent detection of a specific protein by antibody binding. Run polyacrylamide gels were washed and pre-incubated for 5 minutes in Transfer buffer (table 2.3.) and placed into a Trans-Blot SD Semi-Dry Transfer Cell (Bio-Rad Laboratories) in a stack comprising of the membrane, Extra Thick Blot Paper (Bio-Rad Laboratories) and a nitrocellulose membrane. All components were soaked in Transfer buffer prior to assembly and care was taken to avoid bubbles forming between layers of the

stack. The Semi-Dry Transfer Cell was run at 100mA for 2 hours. To confirm the equal transference of protein in all lanes, membranes were incubated for 5 minutes in Ponceau S staining solution (table 2.3.), followed by washing once with 1% acetic acid and two washes with water. Ponceau S reversibly stains protein and allows visualisation and inspection of whole cell protein lysates. Membranes were then blocked by incubation, on a shaking platform at RT, in 20ml of Blocking buffer (table 2.3.) with 5% Skim Milk powder (Sigma-Aldrich) for one hour.

2.5.5. Antibody binding and detection

Primary antibodies were used which bound BCL-3 and β-actin proteins (see table 2.4.). Membranes were incubated with a primary antibody (one antibody per membrane) diluted 1/500 (BCL-3) or 1/10,000 (β-actin) in Blocking buffer with 1% Skim Milk powder. Antibodies were incubated at RT on a rocking platform overnight. Membranes were then washed, first with water, then three further washes with Blocking buffer on a rocking platform at RT (each wash lasting 15 minutes). Membranes were subsequently incubated with secondary antibodies conjugated with horseradish peroxidase (HRP) which were complementary to the class and species of animal in which the primary antibody had been raised (table 2.4.). After one hour of incubation, membranes were rinsed with water, then a further four washes with Blocking buffer (10 minutes per wash). After the completion of the washes, excess liquid was removed and membranes were covered with 0.75ml of chemiluminescence substrate solution produced by combining equal volumes of solutions A and B from UptiLight^{TM} HS HRP WB Substrate. This substrate, when cleaved by the immobilised peroxidase enzymes attached to secondary antibodies, generates light, giving an indication of protein presence and quantity. The substrate solution was left on the membrane for two minutes, excess fluid was removed and the membrane sealed in a thin transparent plastic film. Emitted light was then detected by Kodak® Biomax® XAR (Sigma-Aldrich), which was exposed to the membrane (in the absence of light) for varied periods of time, followed by development of the film. Gel bands were semi-quantified using ImageJ software (http://rsbweb.nih.gov/ij/).

Table 2.3. Buffers used in Western blot assay

Buffer	Reagent
4x Protein extraction buffer	200mM Tris-Cl pH6.8 400mM DTT 8% SDS
Resolving gel	1.5M Tris pH 8.8……..2.5ml Acrylamide/bis (30%)…….4ml Water……3.3ml SDS (10%)……..100µl APS (10%)*……..100µl TEMED…….4µl **TOTAL……10ml** (sufficient for 2 gels)
Stacking gel	1M Tris pH6.8…….630µl Acrylamide/bis (30%)……830µl Water……3.4ml SDS (10%)……..50µl APS (10%)*……50µl TEMED……5µl **TOTAL……5ml** (sufficient for 2 gels)
10x Running buffer	0.25M Tris……30.2g 2M Glycine……..150g Made up to 1l with H_2O and made to pH8.3. Final solution is diluted in H_2O with 0.1% SDS.
2x Gel loading buffer	0.2% bromophenol blue 20% glycerol
Transfer buffer	1x Running buffer……160ml Methanol……..40ml
Ponceau S stain	0.1% Ponceau S (w/v) in 1% acetic acid.
Blocking buffer	PBS……400ml Tween® 20……..0.4ml

*APS is made fresh before each experiment.

Table 2.4. Primary and secondary antibodies used in Western blots

Protein	Primary antibody	Secondary antibody
BCL-3	C terminus binding (C14) Rabbit, polyclonal (sc-185, Santa Cruz Biotechnology,).	Goat Anti-Rabbit IgG (H+L)-HRP Conjugate (Cat # 172-1019; Bio-Rad Laboratories)
β-actin	Mouse, monoclonal (A1978; Sigma-Aldrich).	Goat Anti-Mouse IgG (H+L)-HRP Conjugate (Cat # 172-1011; Bio-Rad Laboratories).

2.6. Immunocytochemistry

Cells were grown on cover slips (22mm diameter; Scientific Laboratory Supplies Ltd) in 6 well plates and then fixed with 4% paraformaldehyde (Electron Microscopy Sciences) for 10 minutes, followed by washing with PBS. Cell and nuclear membranes were made permeable by incubation with 1% Triton X-100 (Sigma-Aldrich) for 15 minutes, then washed three times with PBS, followed by three further washes with PBS+ (PBS, 0.1% Tween-20, 1% BSA). Cover slips were incubated with PBS+ for 30 minutes (Blocking step) prior to incubation overnight at 4℃ overnight with a primary antibody (p65: #3034; Cell Signalling Technology or BCL-3: as in table 2.4.) diluted 1:500 in PBS+. The cover slips underwent further washes (three times PBS followed by three times PBS+) and then incubated with a 1/1000 dilution (in PBS+) of Cy^{TM}3-conjugated AffiniPure Donkey Anti-Rabbit IgG (H+L) secondary antibody (Jackson Immuno Research Laboratories, Inc.) for 30 minutes in a covered manner to exclude light (following this step care was taken to limit light exposure). Excess secondary antibody was removed by further washes (three times PBS, three times PBS+). The cover slip was then placed face downwards on a drop of VECTORSHIELD Mounting Medium with DAPI (Vector Labs) on a slide (76x26mm; Thermo Scientific) and the edges of the cover slip sealed with nail varnish. Slides were stored in the dark at 4℃ and imaged within 48 hours. Images were taken on a Zeiss Axiovert 200M widefield fluorescence microscope with a 40x objective, HBO 100 mercury lamp and using the microscope's fluorescence filters sets 'TRITC' for Cy3 (excitation filter bandwidth 546/12) and 'DAPI' for DAPI (excitation filter bandwidth 365/10nm) detection.

2.7. Chromatin Immunoprecipitation (ChIP)

ChIP is used to determine the occurrence of a protein bound at a particular DNA sequence of interest by immunoprecipitating specific proteins from a whole cell extract using antibodies and subsequently using PCR to detect DNA sequences of interest which have co-precipitated with the protein (and which are consequently assumed to be bound by it). The following protocol was adapted from Carey et al. (Carey et al., 2009).

2.7.1. Cell fixation and chromatin extraction

Cells were grown in 100mm dishes (Fisher Scientific Laboratories UK Ltd) and fixed by incubation with 1% formaldehyde (Sigma-Aldrich) at RT for 10 minutes with shaking. After this time the reaction was quenched with glycine (Fisher Scientific), added to a final concentration of 125mM, for five minutes. Cells were then washed twice with cold PBS and detached by cell scraping in PBS supplemented with Roche cOmplete, EDTA Protease inhibitor cocktail tablets (one tablet per 50ml of solution). The resulting cell containing solution was collected and pelleted by spinning at 230 x g for 10 minutes at 4℃. Cells were resuspended in Cell Lysis buffer (see table 2.5.) and incubated for 10 minutes on ice. Cell nuclei were then collected by spinning at 100 x g for 10 minutes at 4℃, the supernatant was then carefully removed and the remaining pellet of nuclei resuspended in 1 ml of Nuclear Lysis buffer (see table 2.5.) followed by incubation on ice for a further 10 minutes.

2.7.2. Chromatin sonication

Chromatin was sonicated using a Cole Palmer Ultrasonic processor probe sonicator (at 30% amplitude; 6mm probe). Cells were incubated on ice during sonication and each sonication burst transferred 20 Joules of sonic energy to the chromatin solution. A one minute pause was left between each sonication burst, with the number of bursts required to fragment chromatin to a required size being experimentally determined [3.2.7.2.]. The success of sonicaiton was assayed each time by removal of a small volume of sonicated chromatin volume (25µl from 1ml) which was subsequent treated with 1µl RNAse A (20mg/ml; Invitrogen) and incubated at 37 ℃ for at least 3 hours. Proteinase K (1µl from a 10mg/ml stock; Sigma-Aldrich) was further added to this reaction which was incubated overnight at 55℃ and subsequently run out on a 1% agarose gel to confirm that chromatin had been fragmented to below a required size.

2.7.3. Antibody binding of chromatin

A volume of the sonicated chromatin solution corresponding to 100µg DNA was used per antibody; concentration was determining using a nanodrop [2.8.8.] with the RNAse/proteinase k treated chromatin sample described in [7.2.]. Total volume was made up to 300µl with ChIP dilution buffer

(table 2.5.) and the chromatin was pre-cleared with Protein G Agarose/Salmon Sperm DNA beads (Millipore); 50µl added with a large bore pipette tip and incubated for 2 hours at 4℃ with rotation. Beads were removed by centrifugation (1000 x g at 4℃ for 5 minutes) and 250 µl of the resulting supernatant was collected. A 1% volume of each of the chromatin solutions was removed at this point and stored at -20℃ until later in the protocol – this total volume of input chromatin is later used to quantify relative levels of chromatin precipitated by specific antibodies and is hereafter referred to as 'Input'. Each of the remaining chromatin solution volumes was incubated with 10µg of relevant antibody at 4℃ under rotation overnight (antibodies used are listed in table 2.6.).

2.7.4. Immunoprecipitation of chromatin, washes and elution

A volume of 50µl of protein G bead solution was then added to the sample and incubated, again with rotation at 4℃, for 2 hours at which point the beads were centrifuged as before and supernatant carefully removed and discarded. The beads (with bound chromatin) are washed four times with High Salt buffer (see table 2.5.) – each wash consisting of resuspending the beads in High Salt buffer, rotating at RT for 10 minutes followed by centrifugation (1000 x g, RT, 2 minutes) and removal of supernatant. The beads were then washed twice as before but using TE buffer (table 2.5.) in place of High Salt wash solution. The beads, and also the previously extracted 1% Input sample, were finally resuspended in 300µl of ChIP Elution buffer (table 2.5.) with gentle flicking and incubated with 1 µl of proteinase k (10mg/ml) for 2 hours at 55℃, and then further overnight at 65℃ to reverse protein-DNA cross linking. Beads were finally removed from the solution by spinning at 10,000 x g for 10 minutes, with the DNA containing supernatant then removed and purified using a Qiagen PCR Purification kit with the manufacturer's recommended protocol. DNA was finally eluted in 50µl nuclease-free H_2O and stored at -20℃.

2.7.5. Quantification of eluted DNA fragments

PCR was used to detect the occurrence of a particular sequence of interest in DNA molecules extracted by immunoprecipitation (primers given in table 2.7.). The relative occurrence of a sequence was expressed as the PCR signal amplified from immunoprecipated DNA as a percentage of PCR signal amplified from initial total chromatin (Input). Relative quantification was performed using qPCR, with reactions and methodology used as in [2.3.] with the exception that a volume of 5µl of sonicated genomic DNA eluted from the ChIP [7.3.] was used in place of 5µl of cDNA.

C_T values [see 2.4.] are determined for primer sets amplifying from DNA fragment populations produced by antibody immunoprecipitation and also from the 1% Input samples. To adjust 1% Input values to 100% Input, 6.644 is subtracted from 1% Input C_T values ($Log_2100=6.644$). The percentage

of DNA fragments retained by immunoprecipiation with a particular antibody was determined using the following formulas:

Y= C_T value (100% Input) - C_T value (Immunoprecipitated DNA);
Percentage of Input = 100x2$^{(Y)}$.

C_T values were determined in triplicate per sample (technical replicates) and the mean value was used in Percentage of Input calculations. Each ChIP experiment was replicated with three separate cell populations (biological replicates), individual Percentage of Input values were calculated for each biological replicate and mean and standard deviation values were subsequently calculated.

Table 2.5. ChIP buffers

Buffer	Composition
Cell Lysis buffer	5mM PIPES pH8.0 85mM KCl 0.5% Nonidet P-40 Store at 4℃.
Nuclear Lysis buffer	50mM Tris-Cl pH8.0 10mM EDTA 1% SDS
Dilution buffer	16.7mM Tris-Cl pH8.0 167mM NaCl 1.2mM EDTA 0.01% SDS 1.1% Triton X-100 Store at 4℃.
High Salt wash	50mM HEPES pH7.9 500mM NaCl 1mM EDTA 0.1% SDS 1% Triton X-100 0.1% deoxycholate Store at 4℃.
TE buffer	1mM EDTA pH8.0 10mM Tris-Cl pH8.0

Elution buffer	50mM Tris-Cl pH8.0 10mM EDTA 1% SDS

Table 2.6. Antibodies used in ChIP assays.

Antibody	Cat. No.	Supplier
Anti-Mouse IgG*	12-371	Millipore
Ant-BCL-3 C terminus (polyclonal)	sc-185	Santa Cruz Biotechnology
Anti-NF-κB p65 C terminus (polyclonal)	06-418	Millipore
Anti-RNA polymerase II clone CTD4H8 (monoclonal)	05-623	Millipore
Anti-acetyl histone 3 (polyclonal)	06-599	Millipore

* Negative control

Table 2.7. Primers used in ChIP assays.

Sequence amplified	Primer name	Sequence	Melting temperature (℃)*
For amplifying a distal κB site in the *TNFA* promoter [3.2.7.](Appendix 5).	Distal κB site	FOR 5'-GGCTCTGAGGAATGGGTTAC-3'	62.7
		REV 5'-GAGGTCCTGGAGGCTCTTTC-3'	64.5
TNFα gene TSS** (Appendix 4)	TNF TSS	FOR 5'-GGACAGCAGAGGACCAGCTA-3'	65.7
		REV 5'-GTCCTTTCCAGGGGAGAGAG-3'	64.2
BCL-3 gene TSS** (Appendix 4)	BCL-3 TSS	FOR 5'-GGGCCAGAAAGACAAAAACA-3'	61.8
		REV 5'-CCCAGGGGTTTCCTGGAC-3'	65.0

* Melting temperatures were calculated with the 'nearest neighbour' method and are given to one decimal place. ** TSS = Transcription Start Site.

2.8. Cloning/Molecular Biology techniques

2.8.1. Plasmid DNA extraction

Bacterial cells were grown with shaking (200rpm) overnight at 37℃ in 5ml of LB Broth (Sigma-Aldrich) growth media. Resulting bacterial cells in solution were centrifuged to a pellet (at 1700 x g for 10 minutes) and plasmid DNA extracted with a QIAprep Spin Miniprep kit (Qiagen) following the manufacturer's instructions. Plasmid DNA was finally eluted into 30-50µl nuclease-free water.

2.8.2. Bacterial transformation

Plasmids were introduced into MAX Efficiency® DH5α™ Competent *Escherichia coli* cells (Invitrogen) following the manufacturer's protocol. Briefly, competent cells, stored at -80℃, were thawed on ice and aliquoted into pre-chilled eppendorf tubes in 50µl volumes. Plasmid DNA (with a volume <10% total reaction volume) was introduced to the cells (without mixing) and incubated on ice for 5 minutes. Reaction mixtures were then rapidly exposed to 42℃ water baths for 45 seconds, placed back on ice for 2 minutes before 0.95ml of SOC media (Appendix 1) was added to the cells. Following incubation for 1 hour at 37℃ with shaking (200 rpm), 10% and 90% volumes of the transformed cell mixes were spread onto LB agar plates (see Appendix 1) with appropriate antibiotic selection (Appendix 1) and incubated overnight at 37℃. Single colonies were then selected for further growth in liquid LB culture for plasmid extraction [as in 8.1.].

2.8.2.1. Glycerol stocks

For long term storage, transformed bacteria were stored at -80℃ in glycerol. Bacterial cell cultures were grown in LB liquid media supplemented with appropriate antibiotic until mid-logarithmic growth phase (OD_{600} 0.4-0.6) then 0.5ml of this culture was mixed with 0.5ml of filter-sterilised 80% glycerol solution in vials (1.2ml CryoPure tubes; Sarstedt) for storage.

2.8.3.Polymerase chain reactions (PCR)

2.8.3.1. Primer design

Primers were designed using Primer3 software (v.0.4.0; http://frodo.wi.mit.edu/) and output primer sequences checked for self-annealing and annealing within the primer pair with PCR Primer Stats Sequence analysis tool (http://www.bioinformatics.org/sms2/pcr_primer_stats.html). When primers were used to add restriction endonculease cleavage sites to the ends of PCR fragments, such sequences were added at the 5' end of the primer with a further six base pairs added to form the 5' terminal end of the primer sequence, i.e. 5'-X-X-X-X-X-X- Restriction site -Complementary primer sequence -3' (where X represents any nucleotide base pair, although care was taken to ensure this sequence did not self anneal or form primer dimers). This added 5' sequence acts to enhance

subsequent restriction endonuclease cleavage efficiency – many enzymes requiring sequence either side of the cut site for optimal performance. Oligonucleotide primers (Invirgoen Life Technologies) were received in a lyophilised form and resuspended in nuclease-free water to form a 100µM stock solution (required volume provided by manufacturer) and further diluted 1/10 to produce a working primer solution. Primers used for individual PCRs are detailed in the relevant Results section and sequences are given in Appendices 3-6. Reactions were performed on an Eppendorf Mastercycler (Eppendorf UK Limited; Cambridge UK) and either immediately visualised using gel electrophoresis or stored at -20℃.

2.8.3.2. PCR conditions

PCRs were catalysed with either BIOTAQ^{TM} DNA Polymerase (Bioline Reagents Ltd,) or Phusion High-Fidelity DNA Polymerase (M0530S; New England Biosciences). Phusion DNA polymerase was used in reactions where the amplified DNA fragment was subsequently use to express protein and consequently high fidelity of amplified DNA sequence was required. Reactions were set up for both enzymes in accordance with the manufacturer's recommendations, with the amount of plasmid determined experimentally for each reaction. Reaction conditions for BIOTAQ^{TM} and Phusion enzymes are outlined in tables 2.8 and 2.9 respectively.

Table 2.8. Reaction conditions for BIOTAQ^{TM} PCR.

Step	Temperature (℃)	Time (seconds)	Number of cycles
Initial denaturing	94	180	1
Denaturing Annealing Extension	94 Varied* 72	15 30 Varied**	25-40***
Final extension	72	300	1

Table 2.9. Reaction conditions for High Fidelity PCR.

Step	Temperature (℃)	Time (seconds)	Number of cycles
Initial denaturing	98	180	1
Denaturing Annealing Extension	98 Varied* 72	10 30 Varied**	25-40***
Final extension	72	300	1

*Appropriate annealing temperatures were experimentally determined per primer pair (55-60℃). **Extension time varied between reactions and calculated at 30 seconds per 1kb of sequence to amplify. *** Number of reaction cycles was varied dependent on the specific reaction involved.

2.8.4. Gel electrophoresis

Agarose gels were made to 1% (w/v) by dissolving agarose powder (Lonza) in TAE electrophoresis buffer (see Appendix 1) with heating. The solution was subsequently cooled to 50℃ in a water bath and SafeView Nucleic Acid Stain (NBS Biologicals Ltd; Huntingdon UK) was introduced at 5µl stain per 100ml gel solution to visualise DNA molecules (the dye fluoresces when bound to nucleic acid and excited with appropriate wavelength light of 290-320nm). Cooled and solidified gels were run in 1x TAE buffer within a horizontal gel electrophoresis tank at 50-100V. To approximate the size of gel fragments run in a gel, HyperLadder^{TM} I (for fragments 1,000-10,000bp) or HyperLadder^{TM} I (for fragments <1,000bp) (both Bioline Reagents Ltd) were run in adjacent lanes to DNA samples. DNA samples are added with 1x DNA Loading buffer (see Appendix 1). Gels were imaged using the Bio-Rad Gel Doc^{TM} XR^{+} system and Image Lab^{TM} Sotware (Bio-Rad, Hertfordshire, UK).

2.8.5. Restriction endonuclease digests

Restriction enzymes were used with appropriate (i.e. manufacturer recommended) buffers and were obtained from either Roche or New England Biolabs (complete list of enzymes in Appendix 1). BSA was also added (to a final concentration of 100µg/ml) where necessary. Approximately 0.5µg of purified DNA was incubated with 0.5µl restriction endonuclease, buffer (to 1x concentration) and nuclease-free H_2O in a 20µl reaction. Reactions were incubated overnight at 37℃ (this temperature is optimum for all enzymes used in this work). In the case of double digestions (i.e. digestion of a DNA molecule with two restriction endonucleases), if a common buffer was available in which both restriction enzymes exhibited 100% activity then the reactions were carried out simultaneously in a single reaction. When enzymes did not share a compatible buffer, the digestions were carried out sequentially over two separate overnight reactions, with DNA being purified with a Qiagen PCR Purification kit prior to digestion with the second enzyme. Digestions were ultimately purified with Qiagen PCR Purification kit for PCR fragments or QiaQuick Gel Extraction kit for digested plasmids (to remove uncut plasmid from the reaction mixture) following the manufacturers recommended protocol and eluting DNA in 30-50µl of nuclease-free water.

2.8.6. Ligation reactions

T4 DNA Ligase (New England Biolabs) enzyme was used to fuse cohesive ends of plasmid and insert PCR derived DNA fragment molecules cut with common restriction enzymes. Plasmid and PCR fragments cut with restriction endonucelases [2.8.5.] were mixed in a 3:1 molar ratio (insert:plasmid) to produce a total DNA quantity of ~100ng. A volume of 2µl of 10x T4 DNA Ligase buffer (New England

Biolabs) and 1µl of T4 DNA Ligase were added to this DNA mixture, which was made up to 20µl total volume with nuclease-free H_2O and incubated overnight at 16℃. The reaction was then stopped by heating to 65℃ for 10 minutes, cooled on ice and finally 1µl was used to transform competent *E. coli* cells [2.8.2.].

2.8.7. Colony PCR

E. coli colonies growing on selective media agar plates (see Appendix 1) following transformation with a ligation mixture [8.6] were screened for successfully ligated plasmids with colony PCR. Cells from a bacterial colony were removed with the tip of a pipette and subsequently expelled into 5µl of dH_2O in a PCR reaction tube This mixture was then heated at 95℃ for 10 minutes and used as template in a PCR reaction. Primer sets which amplify the insert region were used to screen colonies and PCR outputs were resolved and visualised with agarose gel electrophoresis.

2.8.8. Quantification of nucleic acid concentration

Concentrations of nucleic acids in solution (1µl volume) were quantified using a NanoDrop 2000 (Thermo Scientific) micro-volume spectrophotometer. The amount of nucleic acid is calculated by sample absorbance of 260nm light (A_{260}) - one unit of A_{260} corresponds to 50µg/ml of dsDNA or 40µg/ml of ssRNA. Sample contamination (with, for example, protein or organic molecules) was determined by the ratio of sample absorbance at 260nm and 280nm ($A_{260/280}$). Pure RNA has an $A_{260/280}$ of 2.0 (values over 1.5 were considered acceptable) and pure DNA has an $A_{260/280}$ of 1.8 (values over 1.4 were considered acceptable).

2.8.9. Genomic DNA extraction from HT1080 cells

Protocol was adapted from (Laird et al., 1991). Cells were grown in a 6 well plate and lysed, following removal of MEM and washing with PBS, in 0.5ml of Lysis buffer at 37℃ for 2 hours. The Lysis buffer used consisted of 100mM Tris-Cl (pH 8.5; 5ml), 0.5M EDTA (0.5ml), 5M NaCl (2ml), Proteinase K (20mg/ml; 0.25ml), nuclease free H_2O (make volume up to 50ml). The salt concentration of the solution was adjusted by addition of sodium acetate (pH 5.2) to a final concentration of 0.3M, followed by addition of an 0.7ml volume of isopropanol and thorough mixing. Precipitated DNA was subsequently collected by centrifugation (15,000 x g, 20 minutes, 4℃) and the supernatant removed. The pellet was then washed by resuspension in 70% ethanol and centrifugation (15,000 x g, 20 minutes, 4℃), the resulting pellet being air-dried and resuspended in nuclease-free water with incubation at 37℃ for a further two hours.

2.9. BCL-3 BAC characterisation and Recombineering

2.9.1. BCL-3 BAC identification and ordering

The genomic location of the BCL-3 gene was found using the Ensembl database (www.ensembl.org) and suitable BACs spanning this region identified using the USSC Genome Bioinformatics website (http://genome.ucsc.edu/) and ordered from Invitrogen. Characterisation and annotation of BAC sequence was conducted in SimVector 4.01.

2.9.2. Transformation of SW102 *E. coli* cells with BACs

Bacteria from a single SW102 colony were grown in 5ml LB media containing tetracycline (12.5µg/ml) overnight at 32℃ with shaking. One millilitre of this culture was subsequently diluted in 50ml of LB media (with tetracycline) and cells grown until OD_{600} reached 0.4-0.6. Bacterial cultures were then cooled on ice for 2 minutes; the culture was then equally split into two pre-chilled 50ml tubes and spun for 5 minutes at 2500 x g in a centrifuged cooled to 4℃. Supernatant was removed and the bacterial pellet resuspended in 10ml cold dH_2O. Two further washes of the bacterial culture in 10ml cold dH_2O were conducted, followed by a switch to resuspension in 1ml of cold dH_2O and three further washes. Finally, the bacterial cell pellet was resuspended in 40µl cold dH_2O. Alternatively, for longer term storage, the water was layered on top of the pellet and stored at -80℃. When required for use, the pellet/water was gently thawed and resuspended. To introduce BACs to the bacteria, 100ng BAC DNA was added to the competent SW102 cells and incubated on ice for 5 minutes before transference to a pre-chilled Electroporation cuvette (1mm; Geneflow). Bacteria were electroporated in a BioRad Gene Pulser® II Elecroporation System at -25µF, 1.8kV and 200ohms. Cuvettes were then immediately placed on ice and rapidly rescued in 1ml of SOC media (see Appendix 1) followed by incubation for 90 minutes at 32℃ with shaking. Volumes of 10 and 90 % of the resulting bacterial cultures were plated on LB agar plates containing tetracycline (12.5µg/ml) plus chloramphenicol (5µg/ml) and incubated at 32℃ for 24 hours. Glycerol stocks of BCL-3 BAC transformed SW102 cells were created as before [2.8.2.1.].

2.9.3. Extraction of BAC DNA

BACs were amplified in bacterial cultures and extracted using either BAC Maxipreps [2.9.3.1.] (used for higher quantity of greater purity BAC DNA) or Minpreps [2.9.3.2.] (used for diagnostic checks of BAC DNA during the recombineering process).

2.9.3.1. BAC Maxipreps

Bacteria containing the required BAC were grown in 5ml LB cultures at 32℃ overnight with appropriate selective antibiotics. The total volume of this culture was subsequently used to grow SW102 bacteria in 1 litre volumes of LB media overnight (again with appropriate antibiotics). A Machnerey-Nagel

Nucleobond kit was used to extract BAC DNA using the manufacturer's recommended protocol. Elution was performed with pre-warmed elution buffer (65℃) in a volume of 100-200 µl, which was subsequently aliquot into smaller volumes and stored at -20℃ (care was taken to limit free-thaw cycles).

2.9.3.2. BAC Minipreps

Cells from a single bacterial colony transfected with BAC DNA, and grown on an appropriate antibiotic resistance agar plate, were cultured overnight at 32℃ with shaking (200rpm). An 0.5ml volume was extracted from this mix to make glycerol stocks [see 2.8.2.1.] and the remaining culture was spun down at 2500 x g for 10 minutes. The resulting pellet was resuspended in 250µl of P1 buffer (with RNAse added; Qiagen), then 250µl buffer P2 (Qiagen) was added and the solution mixed by inversion six times. A volume of 350µl of buffer N3 (Qiagen) was then added and the solution again inverted six times, followed by centrifuging at 10,000 x g for 20 minutes at 4℃. The resulting supernatant was removed and mixed with 650µl of cold isopropanol (previously stored at -20℃) and the reaction left for at least 2 hours at -20℃. Precipitated BAC DNA was then collected by centrifugation (10,000 x g for 20 minutes at 4℃). The resulting pellet was washed with 70% ethanol, air dried, resupended in 50µl nuclease-free water and stored at -20℃.

2.9.4. Restriction endonculease digestion and resolution of BAC DNA

Restriction endonuclase digestion of BAC DNA generates large DNA fragment sizes which cannot be resolved by standard gel electrophoresis, requiring the use of Pulse Field Gel Electrophoresis (PFGE) instead. This technique periodically switches the orientation of the electric field applied to the gel about its main longitudinal axis. As a consequence, DNA fragments do not move in a straight line but are constantly forced to change migration direction, something smaller fragments do more efficiently than large fragments and can therefore move more rapidly through the gel. To further enhanced resolution, gels are run at low voltage (6V) over long periods of time (16 hours) – requiring cooling and circulation of running buffer.

2.9.4.1. SalI and NotI digestion of BAC DNA

A volume of 26.5µl of BAC DNA (extracted by BAC miniprep [2.9.3.2.]) is used in a 30µl total reaction volume with 0.5µl of high fidelity restriction endonuclease SalI-HF or NotI-HF (high fidelity enzymes are used in this reaction; both enzymes from New England Biolabs) and 3µl of 10x NEBuffer 4 (New England Biolabs). NotI-HF digestions additionally included 1x BSA (New England Biolabs). Reactions were incubated at 37℃ for at least 12 hours:

2.9.4.2. Pulse Field Gel Electrophoresis (PFGE)

A 1% agarose gel (w/v; Pulse Field Certified Agarose; BioRad) produced using 0.5x TBE buffer (see Appendix 1) was run in 0.5x TBE buffer chilled to 14℃ in a CHEF DRII PFGE apparatus (Biorad). Samples were run at 6 V/cm, with a 1-6 second switching time for 16 hours. Two DNA markers were used to approximate digested fragment sizes: Mid Range PFG marker I and Mid Range PFG marker II (both New England Biolabs). After running, gels were soaked in 0.5x TBE buffer supplemented with SafeView Nucleic Acid Stain (5µl per 100ml buffer; NBS Biologicals Ltd) with shaking for at least one hour and subsequently analysed with a Bio-Rad Gel Doc^{TM} XR^{+} system and Image Lab^{TM} Sotware (Bio-Rad).

2.9.5. Southern blotting of BAC DNA

2.9.5.1. Probe amplification and biotinylation

The experimental design of DNA fragments used as probes in Southern blots, plus the primers used to amplify the regions, are described in chapter 7 [7.2.1.2.2.]. PCR reactions were run with BIOTAQ^{TM} DNA polymerase as in [8.3.1.]. A volume of 34µl probe PCR fragment containing 100ng probe DNA (diluted in dH_2O) was boiled for 5 minutes and placed on ice. The following reagents - all part of NEBlot Phototope Kit (New England Biolabs) - were subsequently added (in this order):

- 10µl 5x labelling mix
- 5µl biotinylated dNTP mixture
- 1µl Klenow Fragment.

The reaction was incubated for 2 hours at 37℃ and terminated by addition of 5µl 0.2M EDTA (pH 8.0). Probes solutions were then purified with a Qiagen PCR purification kit (following the manufacturer's protocol), eluted in 20µl TE (10mM Tris-HCl, 1mM EDTA), boiled for 5 minutes to denature probe and stored at -20℃.

2.9.5.2. DNA digestion and resolution

BAC DNA (100ng) was digested overnight with EcoRI restriction enzyme with appropriate buffer (New England Biolabs). The digested DNA was subsequently run on a 0.8% agarose gel at 60V for 6 hours. A Biotinylated 2-Log Ladder was simultaneously run on the gel (1µl per lane; New England Biolabs). Once run, gels were soaked in 0.25M HCl for 15 minutes to depurinate and then rinsed with dH_2O and left in 0.4M NaOH.

2.9.5.3. Transfer and cross linking

DNA was transferred from the gel to a Nitrocellulse membrane (Sigma-Aldrich) using a transfer apparatus assembly ('Southern blot stack') shown in fig 2.1. and were left overnight. Membranes were then washed first in 1M Na_2HPO_4 and then 2x SSC (both washes were less than 5 minutes). DNA

molecules were then UV cross-inked to the membrane using a Stratalinker UV Crosslinker (1 minute exposure, 30W source).

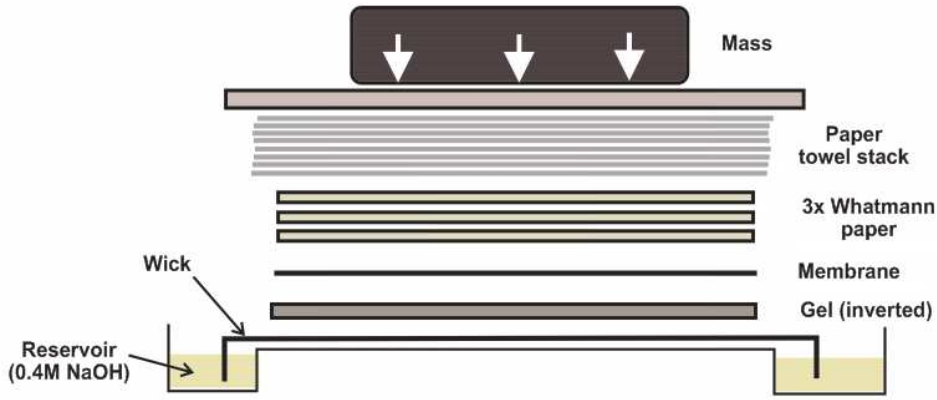

Figure 2.1. Assembly of a Southern blot stack for the transfer of DNA from gels to membranes.

2.9.5.4. Hybridisation and washing

Membranes were incubated with Hybridisation buffer (see table 2.10.) for 1 hour at 68℃. Buffer was then drained and replaced with Hybridisation buffer supplemented with 100ng of the appropriate biotinylated probe described in [2.9.5.1.]. Membranes were incubated with agitation in this solution overnight at 68℃. Sequential washes (all at 68℃) followed to remove non-specific probe binding: initially a 30 minute wash in 1x Wash Solution I (table 2.10.) followed by three 30 minute washes in Wash Solution II (table 2.10.).

2.9.5.5. Detection

Membranes were then blocked, at 68℃, in pre-warmed blocking solution for 20 minutes and then incubated with Streptavidin diluted 1/1000 in Blocking solution for 10 minute with shaking at RT. Membranes were then washed twice, 5 minutes each, in Wash Solution III (table 2.10.) and then incubated in Biotinylated Alkaline Phosphatase diluted 1/1000 in Blocking solution for 10 minutes at RT. The membrane was then washed; once in Blocking solution, then twice in Wash Solution IV (all washes were for 5 minutes), This was followed by incubation with CDP Star reagent diluted 1/100 in CDP Star buffer (25ml volume) for 10 minutes at room temperature (all solutions from Starlab). Membranes were then exposed to Kodak® Biomax® XAR film (Sigma-Aldrich) in the absence of light and the film was subsequently developed.

Table 2.10. Buffers used in Southern blots

Buffer	
20x SSC	87.6g NaCl 44.12g Sodium Citrate ($Na_3C_6H_5O_7$) Dissolve in 500ml ddH_2O and pH to 7.0.
Hybridisation buffer	0.5M Na_2HPO_4 7% SDS 10mM EDTA Add ddH_2O to 1 litre.
Wash Solution I	100mM Na_2HPO_4 0.1% SDS Add ddH_2O to 1 litre.
Wash Solution II	30mM Na_2HPO_4 0.1% SDS Add ddH_2O to 1 litre.
Blocking solution	125mM NaCl 25mM sodium phosphate (2.4g Na_2HPO_4; 1.0g NaH_2PO_4). 5% SDS Add ddH_2O to 1 litre.
Wash Solution III	Blocking solution diluted 1/10 with ddH_2O.
Wash Solution IV (10x)	100mM Tris-HCl 100mM NaCl 10mM $MgCl_2$ Add ddH_2O to 1 litre, pH to 9.5.

2.9.6. BAC Recombineering

2.9.6.1. Production of galk recombination cassette

The design of primers to amplify appropriate DNA homology regions (H arms) for recombination and associated cloning strategy are outlined in [7.2.2.]. High fidelity Phusion DNA polymerase enzyme was used [2.8.3.2.] to amplify H arms, which were subsequently introduced to appropriate plasmid vectors using ligation and bacterial transformation techniques previously described in [2.8.6.] and [2.8.2.]. Subsequent production of DNA 'cassettes' containing H-galk-H and H-Venus-H was conducted using PCR and High fidelity Phusion DNA polymerase. Multiple PCRs were performed and the resulting DNA recombination cassette containing reaction mixtures purified and pooled by passage through a single column in a Qiagen PCR purification kit. Reactions were subsequently digested overnight with DpnI restriction endonuclease to remove residual plasmid and again purified with a Qiagen PCR purification kit.

2.9.6.2. Primary targeting: Galk recombination

Transformation competent SW102 cells containing the BCL-3 BAC were produced as for the original SW102 cells [2.9.2.]. A 100ng quantity of H-galk-H cassette DNA [2.9.6.1.] was added to the competent cells and introduced by elecroporation as before [2.9.2.]. Bacterial cells were rescued in SOC media as before; however, following incubation at 32℃ with shaking for one hour, bacterial cells

were washed three times with 1M M9 salt solution (Appendix 1) to remove SOC traces. Each wash involved spinning at 2500 x g for five minutes (RT), removal of supernatant and resupsension in 1ml of 1M M9 salt solution. Following these washes, 10 and 90% of the bacterial culture were then plated on M63 minimal plates containing galactose and chloramphenicol (Appendix 1) and incubated at 32℃ for two days. Any resulting single colonies were streaked on MacConkey plates (containing galactose and chlorampehnicol; see Appendix 1) and incubated overnight at 32℃. Positive single colonies (coloured bright pink indicating metabolism of galactose due to successful incorporation of the galk gene into the BAC) were tested for further, unwanted, recombination events in the BAC sequence by comparing SalI and NotI restriction endonuclease digests [2.9.4.1.] with original (i.e. not having undergone recombineering) BCL-3 BAC DNA. Bacteria containg BACs with unaltered digestion profiles were stored as glycerol stocks.

2.9.6.3. Secondary targeting: Venus recombination

Transformation competent SW102 cells containing BCL-3 BAC (with incorporated galk cassette sequence produced in [2.9.6.2.]) were made as in [2.9.2.]. Transformation protocol was as for galk [2.9.6.2.] with the exception that 200ng H-Venus-H cassette DNA was used, cells were rescued in 10ml SOC following electroporation and subsequently incubated for 4.5 hours at 32℃ with shaking. In addition, bacteria were plated on M63 plates containing Deoxygalactose (DOG) and glycerol in place of galactose (see Appendix 1). Colonies which grow on this plate are again streaked on MacConkey plates, however colonies which are negative for galactose metabolism (i.e. having lost the galk gene sequence; colonies are white/pale pink) are selected. Cells are screened with PFGE for correct BAC structure, as in [2.9.5.2.], and stored as glycerol stocks.

2.10. XcmI chromatin accessibility assay

2.10.1. XcmI digestion of genomic DNA

Cells in a 6 well plate were grown to approximately 75% confluence and were stimulated with TNFα for experimentally determined lengths of time [4.2.6.2.] and detached with trypsin [2.1.2.2.]. The resulting cell suspension was pelleted by centrifugation (4℃ 2500 x g, 10 minutes) and washed twice with cold PBS. Cell membranes were then lysed with 1ml of Cell Lysis buffer (5 mM PIPES pH 8.0; 85 mM KCl; 0.5% Nonidet P-40) incubated on ice for 10 minutes and released cell nuclei spun down to a pellet (4℃ 1000 x g, 10 minutes) and re-suspended in 100 µl NEBuffer 2 (New England BioLabs Ltd). A volume of 9.5µl of this nuclei suspension was incubated with 0.5µl XcmI restriction endonuclease (2.5U; New England Biolabs) for 30 minutes at 37℃. The reaction was stopped by subsequent heating to 65℃ for 20 minutes.

2.10.2. Genomic DNA purification

Reaction mixes volumes were briefly centrifuged to collect sample and then made up to 100µl with Nuclear Lysis buffer (500mM Tris-Cl pH8.0; 10mM EDTA; 1% SDS) and incubated on ice for 10 minutes. Genomic DNA was further purified by isopropanol precipitation. Sodium acetate (pH 5.2) was added to a final concentration of 0.3M, followed by 700µl isopropanol and mixing. The sample was then centrifuged (15,000 x g, 30 minutes, 4℃) to collect precipitated DNA, which was then washed with 1ml of 70% ethanol and centrifuged to re-pellet (15,000 x g, 15 minutes, 4℃). The resulting pellet was air dried (approximately 10 minutes) and resuspended in 50µl nuclease-free water.

2.10.3. PCR assay

Varying quantities of genomic DNA were used as a template in PCRs with primers XcmIsiteFOR (GGGCCAGAAAGACAAAAACA) and XcmIsite REV (CCACTCACCGGGGTAGTAAA) and BIOTAQ™ DNA Polymerase, as in [8.3.1.]. The PCR was run at 94℃ for 3 minutes followed by 25 cycles of 94℃ 15 seconds/58℃ 15 seconds/72℃ 30 seconds. Varyi ng amounts of PCR product were run on a 1% agarose gel and band intensity was measured using Bio-Rad Image Lab 3.0 software (Bio-Rad Laboratories Ltd).

2.11. Flow Cytometry

Detached SK-N-AS and HT1080 cells [2.1.2.2.] were resupsended in Hank's Balanced Salt Solution (HBSS) supplemented with 5% FBS and analysed in a FACSCalibur unit with CellQuest™ Pro Software (both from BD Biosciences). Samples were stimulated with an argon laser (488nm) and fluorescent signal detected in channel FL-1 for Venus (filter wavelength 530/30nm) and channel FL-2 for dsRed (filter wavelength 585/40nm). Gating of cell populations was conducted as outlined in [7.2.5.2.] using forward and side scatter.

2.12. Mathematical simulations

Mathematical simulations were carried out using MATLAB R2007b (MathWorks, Massachusetts, USA) and data was output in an excel spreadsheet format.

2.13. Graph preparation and images

Numerical data outputs from MATLAB or experiments were displayed as graphs and analysed (curve fitting) using GraphPad Prism 5 (v5.03) (GraphPad Software, La Jolla USA). Images were arranged using CorelDRAW x3 (v13.0.0.576) (Corel, Ottawa, Canada).

2.14. Statistics

Use of non-parametric tests was impossible due to sample sizes (typically three replicates), therefore parametric tests – either Students t test or ANOVA – were used; assuming a normal distribution of data. Logarithmic transformations were used to enhance normal distribution (Personal Communication; Dr Mark Muldoon, Department of Mathematics, University of Manchester).

Chapter 3

Investigating the induction dynamics of the *TNFA* and *BCL3* genes in HT1080 cells stimulated with TNFα

3.1. Introduction

TNFα stimulated cell signalling pathways induce the initial expression of hundreds of genes which, rather than responding in a passive manner to the stimuli, also subsequently act to modify the cell's response by either inducing the expression of further genes or by limiting the expression of those already induced. A consideration of the induced expression of a gene is therefore more properly considered as part of a web of interactions, including regulatory feedback loops, rather than as a simple linear induction by an initial stimulus.

Such induced targets include further signalling molecules, such as TNFα itself. This chapter address the characterisation of TNFα induced transcription of the *TNFA* gene, in addition to the potential inhibitor *BCL3* gene, in the human fibrosarcoma cell line HT1080.

3.1.1. TNFα induced transcription of the *TNFA* and *BCL3* genes via the NF-κB signalling pathway

The binding of TNFα at cell membrane receptors induces nuclear transcription events via two signalling pathways: MAPK mediated activation of transcription factors or induced nuclear localisation of NF-κB transcription factors [1.2.]. A proximal κB site in the *TNFA* promoter (fig 1.2.) has been shown to be responsible for LPS induced expression the gene; with observed binding of NF-κB constituent sub-units p50 and p65 at this site (Collart et al., 1990; Liu et al., 2000) and LPS sensitivity conferred on a core promoter by adjacent positioning of tandem arrays of this κB site (Drouet et al., 1991). While c-Jun was also observed to bind at a proximal site in the *TNFA* promoter, the positive effect of this factor was shown to be relatively modest in comparison to NF-κB (as assayed by equimolar expression of dominant negative forms of each factor) and no synergistic interaction was observed between the two factors (Liu et al., 2000). NF-κB also induces expression of *BCL3* through the binding of a proximal κB site in the gene's promoter (Brasier et al., 2001) and also an intronic κB site (Ge et al., 2003) [1.3.8.].

3.1.2. IL-9 and IL-10 are potential inducers of *BCL3* expression

In addition, the anti-inflammatory cytokines IL-9 and IL-10 have also shown to induce *BCL3* expression via STAT activation pathways (Zhu et al., 1996; Kuwata et al., 2003). Expression of the *IL9* gene itself has been shown to be NF-κB dependent (Zhu et al., 1996; Chen et al., 2008) and *IL10* expression is induced by TNFα through an unknown pathway (Wanidworanun and Strober, 1993). BCL-3 itself also has a documented role in binding *IL10* promoter sequence and inducing expression of the gene (Wessells et al., 2004; Massoumi et al., 2009) [1.3.9.].

3.1.3. Attenuation of *TNFA* transcription

A distal site in the *TNFA* promoter has the reported ability to bind both p50/p65 heterodimers and p50 homodimers – with binding of p50 homodimers associated with transcription attenuation and the conferred insensitivity of the promoter to subsequent stimulation events (Liu et al., 2000; Udalova et al., 2000) [1.4.5.]. Competitive binding of different Rel dimer combinations at a common κB site is a proposed mechanisms for controlling induction of gene transcription [1.2.6.2.] and as BCL-3 has a documented role in stabilizing p50 homodimer binding at DNA, induction kinetics of this factor appear likely to play a key role in attenuation of *TNFA* transcription. Indeed, several studies have shown BCL-3 as having a role in inhibition of *TNFA* transcription (Kuwata et al., 2003; Wessells et al., 2004).

3.1.4. Differential responses of cell types to a common stimulus

Work concerning NF-κB signalling and also *TNFA* and *BCL3* gene studies has been conducted in various cell types – consequently, these interactions and expression may be significantly different in the cell line used in this study (HT1080 human fibrosarcoma cell). Cell types, even when derived from a common organism, have the potential for considerable variation. With regards to TNFα signalling, differential expression levels of receptor proteins or components of the signal transduction pathway may alter a cell's sensitivity to a particular quantity of TNFα stimulation. Notably, high levels of variation have been seen in the expression of the TNFα receptor TNFR-1 between cell types (Al-Lamki et al., 2008). In addition, human cell lines are derived from different individuals with consequent differential genetic make-up. Natural genetic variation is able to cause significant differences in gene expression levels (Cowles et al., 2002; Kim et al., 2005). Varied chromatin states are also seen in different cell type genomes – a feature which can influence the *de novo* binding of transcription factors to DNA and therefore confer differential sensitivity of a gene in two cell types to the same signal. Notably, comparisons of two mouse cell lines – mammary (3134) and pituitary (AtT-20) cells – showed only an 0.78% overlap in accessible genomic sequence (as assayed by DNase I sensitivity) with a consequent highly differential binding pattern of GR following stimulation of cells (John et al., 2010).

3.1.5. Chapter aims

The potential variety between cell types means that work regarding NF-κB signalling and *TNFA*/*BCL3* transcription elucidated in different cell types must be confirmed and consolidated in the cell type used in this study (HT1080 cells). The following assertions were therefore addressed in this chapter:

- TNFα stimulation induces both *TNFA* and *BCL3* transcript levels via the NF-κB pathway.
- BCL-3 protein levels increase in response to TNFα and localise to the nucleus.
- IL-9 and IL-10 are expressed in HT1080 cells; and are (a.) induced by BCL-3 and/or (b.) induce *BCL3* transcription themselves.
- Nuclear localisation of NF-κB is rapidly induced in response to TNFα, with levels continuing to oscillate between nucleus and cytoplasm thereafter.
- BCL-3 inhibits *TNFA* transcription.
- The BCL-3 protein is able to bind at the *TNFA* gene promoter.

3.2. Results

3.2.1. Measurement of the response of *TNFA* and *BCL3* transcript levels in HT1080 cells stimulated with TNFα

To determine the effect of TNFα stimulation on *TNFA* and *BCL3* transcript levels in HT1080 cells over time, quantitative reverse transcriptase real time PCR (qRT-PCR) was performed. A note on acronyms: in this thesis qRT-PCR is taken to mean quantitative (real time) reverse transcriptase PCR; that is, PCR performed on cDNA template produced by reverse transcriptase. This is in contrast to qPCR which is quantitative (real time) PCR performed on DNA template which is not derived by reverse transcriptase (genomic DNA, for example).

3.2.1.1. Quantitative reverse transcriptase PCR (qRT-PCR)

PCRs allow amplification of selective DNA sequence through the extension of experimentally designed short, single strand DNA primers complementary to a DNA sequence which is provided as a template. Use of primers complementary to the sense and anti-sense strands flanking a region of interest creates a chain reaction – with new sequence produced in one cycle acting as template in subsequent reaction cycles. DNA fragments are therefore exponentially produced – with a doubling of PCR produced DNA fragments per cycle (assuming the reaction is 100% efficient). Consequently, it is possible to infer the

concentration of initial template molecule from the rate of increase in absolute DNA molecules per reaction cycle. Introduction of SYBR Green dye to the qRT-PCR reaction – a molecule which fluoresces when bound to double strand DNA – allows measurement of the increase in PCR product at the end of every reaction cycle, i.e. in real time. The rate of reaction is measured by the time taken (in reaction cycles) to attain a threshold level of fluorescence above basal levels – the C_T value.

RNA extracted from populations of cells is converted to PCR amenable cDNA molecules by a reverse transcriptase enzyme catalysed extension of random primers. Primers designed to be complementary to a gene of interest can be used to selectively amplify sequence from a heterologous pool of cDNA molecules produce in this manner and allow a measure of the initial quantity of template to be obtained (using qRT-PCR, as above).

3.2.1.2. Optimisation of a qRT-PCR protocol for the detection of *TNFA* and *BCL3* gene transcripts

3.2.1.2.1. Primer design

To measure the output of a PCR reaction relating to amplification from a specific cDNA molecule, primers must be used which exclusively amplify the desired sequence and which do not produce primer dimers (self annealing of primers) – both of which would produce non-specific double strand DNA. Primers designed against exon sequences within the *TNFA* and *BCL3* genes [2.8.3.1.] were tested in PCRs [2.8.3.2.] using cDNA produced from unstimulated HT1080 cell populations [2.1.1.2.] and resolved using gel electrophoresis [2.8.3.].

An example of potential primer pairs to amplify from *BCL3* cDNA is shown in figure 3.1.A. Primer sets were discarded if they produced primer dimers (‡; lane 2), non-specific PCR products (#; lanes 3 and 4) or failed to amplify any sequence. A primer sequence was selected on the basis of producing a single, strong band (lane 6) which produced no primer dimers even when a reaction was performed in the absence of DNA template (replaced in the reaction with dH_20).

A further potential cause of qRT-PCR product contamination is amplification from genomic DNA sequence which persists in extracted RNA samples and subsequent reverse transcriptase reactions. To prevent this scenario, extracted RNA samples were treated with DNase I [2.2.1.] and also primers were designed to amplify across introns. Consequently, PCR products amplified from cDNA (in which introns are excised) and genomic DNA exhibit differential sizes, as shown in figure 3.1.B. The presence of genomic DNA amplified PCR product in qRT-PCRs was screened for by resolving completed qRT-PCR reactions on agarose gels to ensure that only cDNA produced fragments were present.

3.2.1.2.2. Confirming the robustness of a primer set's efficiency across varied cDNA template concentrations

Levels of cDNA (and consequently RNA) molecules extracted from cell populations were measured as relative level changes when compared to unstimulated cells using the Comparative C_T method [2.2.4.]. Detectable transcript levels of both transcripts in unstimulated cells was therefore necessary and was confirmed by performing initial tests of primer suitability [3.2.1.2.1.] using cDNA extracted from unstimulated cell populations (fig 3.1.A).

A requirement for the Comparative C_T method is that the difference in C_T value between control primers amplifying from the Cyclophilin A gene (*CYPA*) and primers amplifying from the transcripts of interest (C_T(gene of interest) - C_T(*CYPA*)) is constant across the potential range of cDNA template concentrations used, i.e. that the primer set amplification efficiencies are the same.

To confirm the suitability of the primer sets selected for both *TNFA* and *BCL3* transcripts, template cDNA quantities used was varied about the conventional quantity used - 0.5µl cDNA (produced from 2µg RNA as in [2.2.2.]) in a 15µl reaction volume – also using 5, 0.05 and 0.005µl volumes of cDNA (from the same unstimulated HT1080 cell population) in a 15µl reaction. Triplicate reactions were conducted using *TNFA*, *BCL3* and *CYPA* primer sets per sample and ΔC_T values between *TNFA* or *BCL3* primers sets and *CYPA* primer set calculated for each concentration of cDNA used. Values were plotted against $\log_{10}$ of the amount of cDNA volume used per reaction (fig 3.1.C). Assuming no change existed in the relative efficiency of *TNFA* or *BCL3* and *CYPA* primers, the ΔC_T calculated per dilution of cDNA for each primer should remain constant, i.e. points should be fit by a horizontal straight line. A horizontal line was fitted to each primer set - at ΔC_T 7.273 for TNFα (R^2=0.928) and 8.451 for BCL-3 (R^2=0.913) – and no significant difference was seen between data points for either primer set ($P>0.05$) (fig 3.1.C). Primer sets were therefore adjudged to be robust enough to accurately assess *TNFA* and *BCL3* transcript levels across a range of potential cDNA template amounts.

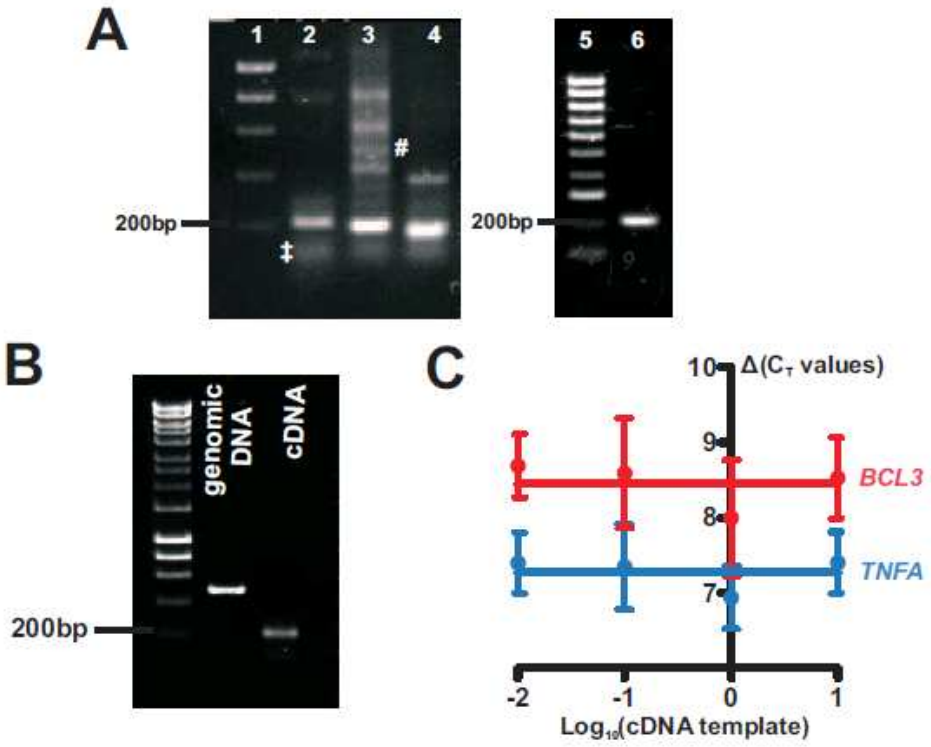

Figure 3.1. Design and verification of suitable primer sets to amplify from *BCL3* and *TNFA* cDNA molecules. (A) PCR products produced by potential *BCL3* primer sets amplifying from cDNA produced from an unstimulated HT1080 cell population (lanes 2, 3, 4 and 6). #: non-specific product; ‡: primer dimer; Lanes 1 and 5 are ladder; 200bp sizes are marked. (B) The differential PCR product size produced by a selected *BCL3* primer pair (lane 6 in A) when amplifying from cDNA and genomic DNA - caused by using primer sequences which are complementary to different exons. (C) The efficiency of selected *TNFA* and *BCL3* primer sets and control *CYPA* primer set does not vary in amplification across a range of cDNA template concentrations. Log_{10} cDNA levels correspond to the dilution of cDNA in dH_2O used in qRT-PCR reactions relative to standard amounts [2.2.3.]. ΔC_T value corresponds to difference in C_T value measured for either *TNFA* or *BCL3* primer set and primers amplifying *CYPA* sequence (i.e. C_T(*TNFA* or *BCL3*) – C_T(*CYPA*)). Straight lines were fitted with the constraint that gradient = 0 (i.e. horizontal).

3.2.1.3. *TNFA* and *BCL3* transcript levels are induced in HT1080 cells by stimulation with TNFα

The fold induction of both *TNFA* and *BCL3* transcript levels was determined, relative to basal levels in unstimulated cells (t=0), at 30, 60, 90, 180, 450 and 900 minutes after stimulation with 10ng/µl TNFα cytokine. Transcript levels of both genes were induced, with *TNFA* transcripts exhibiting a rapid induction peaking at 90 minutes and then rapidly declining to near basal levels (left axis; fig 3.2A). *BCL3* transcripts showed qualitatively similar behaviour but peaked at a later time, 180 minutes, and persisted at relatively higher levels over an extended time scale (right axis; fig 3.2.A). The rates of increase in transcript level over the time intervals observed is shown for *TNFA* (fig 3.2.B) and *BCL3* (fig 3.2.C). Maximal induction rates for *TNFA* transcripts occurred at an earlier time interval than *BCL3*

(30-60 minutes compared with 60-90 minutes) accounting for the difference in maximal peaks in relative transcript levels between the two genes.

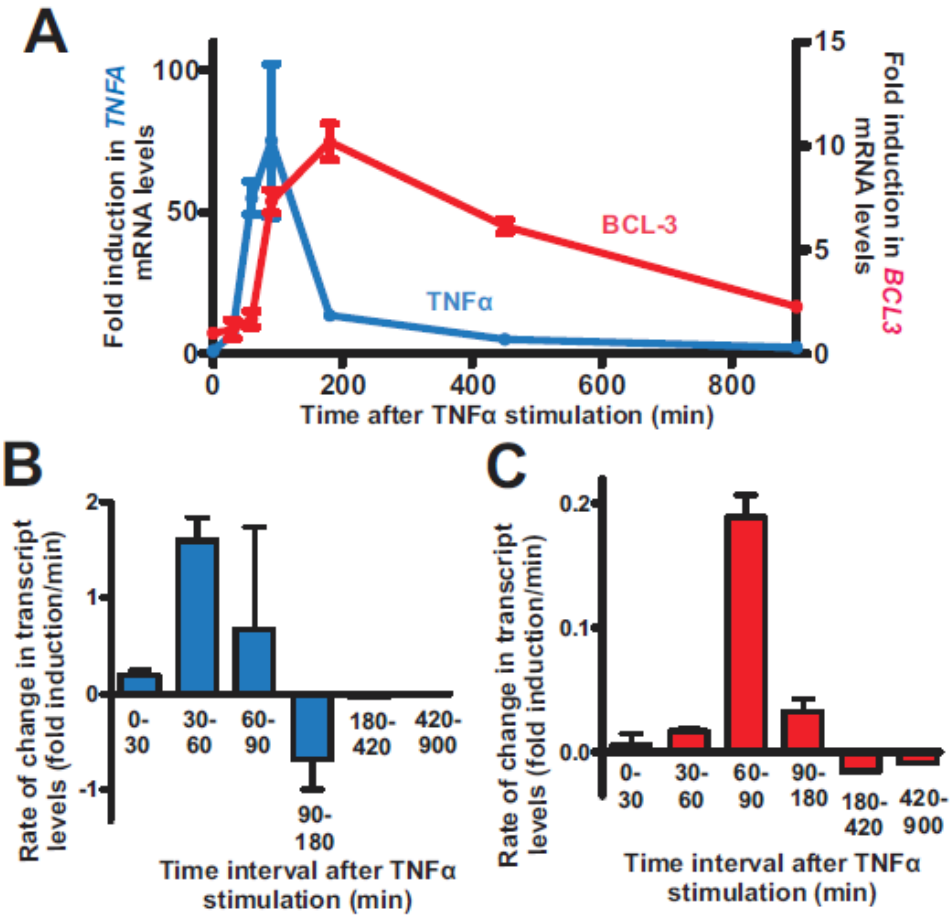

Figure 3.2. TNFα stimulation of HT1080 cells induces transcript levels of both *TNFA* and *BCL3* genes. (A) The induction of both *TNFA* and *BCL3* transcript levels increases in response to stimulation of HT1080 cell populations with TNFα (at t=0). Fold inductions are relative to levels at t=0 independently for *TNFA* (left axis) and *BCL3* (right axis). The rate of change in *TNFA* (B) and *BCL3* (C) transcript levels calculated between time points in the induction time course shown in A. NS: Not Significant; * P<0.05.

3.2.2. TNFα acts to induce *TNFA* and *BCL3* transcript levels via the NF-κB signalling pathway in HT1080 cells

The effect of TNFα on transcription is potentially mediated by multiple signalling pathways [1.1.3.2.]. To determine whether TNFα stimulation acts to induce *TNFA* and *BCL3* transcript levels in HT1080 cells via the NF-κB signalling pathway, the pathway was inhibited with SN50. This small cell permeable inhibitor peptide contains the nuclear localisation signal peptide sequence (NLS) of the p50

protein and consequently is able to inhibit nuclear translocation of p50 containing NF-κB dimers (including the conventional p50/p65 heterodimer) by competing for binding to nuclear membrane translocation machinery (Lin et al., 1995).

To ensure that cells remained viable when pre-treated with SN50 and subsequently subjected to an inflammatory cytokine stimulus, cells were pre-treated with 30 and 50μg/μl SN50 for one hour then stimulated with TNFα, again for one hour, and assayed for viability using trypan blue staining [2.1.7.]. Cells pre-treated with 50μg/μl SN50 showed a significant decrease in viability ($P<0.05$) following a one hour TNFα stimulation when compared to cells which were only stimulated with TNFα (fig 3.3.A). In contrast, pre-treatment with 30μg/μl SN50 showed no such viability decrease ($P>0.05$) (fig 3.3.A). This viability is potentially due to a previously identified role for NF-κB signalling in suppressing TNFα induced apoptosis (Van Antwerp et al., 1996).

Cells which were pre-treated with 30μg/μl SN50 for one hour showed significantly ($P<0.05$) lower levels of induction of both *TNFA* and *BCL3* transcript levels in response to 60 and 180 minutes of TNFα stimulation respectively (fig 3.3.B). The use of different stimulation times for each transcript reflects the different induction dynamics of each gene in response to TNFα (see fig 3.2.A). The lack of total abolishment of transcript level stimulation in this case is assumed to be due to incomplete inhibition of NF-κB nuclear transition at this concentration of inhibitor. LPS induced human monocytic THP-1 and murine endothelial LE-II cell lines have both exhibited an approximately 50% decrease in DNA binding of NF-κB when pre-treated with the same concentration of SN50 (30μg/ml) (Lin et al., 1995). The use of higher SN50 concentrations is prevented in this study by increased cell death at such levels (as previously shown – fig 3.3.A). Therefore, while NF-κB is shown to have a significant role in TNFα induced increases in *TNFA* and *BCL3* transcript levels; these data can not definitely rule out roles for additional signalling pathways.

SN50 acts via interaction with a nuclear transport localisation complex (specifically, the importin-α/importin-β heterodimer) which facilitates movement through nuclear pores – thus inhibiting the nuclear import of the p50 protein whose NLS the SN50 peptide contains through competition. However, contrary to early assumptions of NF- κB specificity, this blocking of nuclear transport machinery also affects other transcription factors such as AP-1 and members of the NFAT family (Boothby, 2001; Orange and May, 2008). Such a generalised activity would potentially prevent any observed effect of SN50 on gene transcription being attributed exclusively to NF-kB. While the peptide has been shown to be more selective in terms of its inhibition target (i.e inhibiting NF-κB but not AP-1 or NFATs) at lower concentrations such as 37.5 μg/ml (30 μg/ml was used in this study), further proof of this specificity in HT1080 cells would improve the validity of any results utilising this reagent (Ray, 2001). Such proof could be obtained by quantifying the nuclear presence of transcription factors

following induction with TNFα – potentially with immunocytochemistry or by assaying concentrations of protein from nuclear extracts.

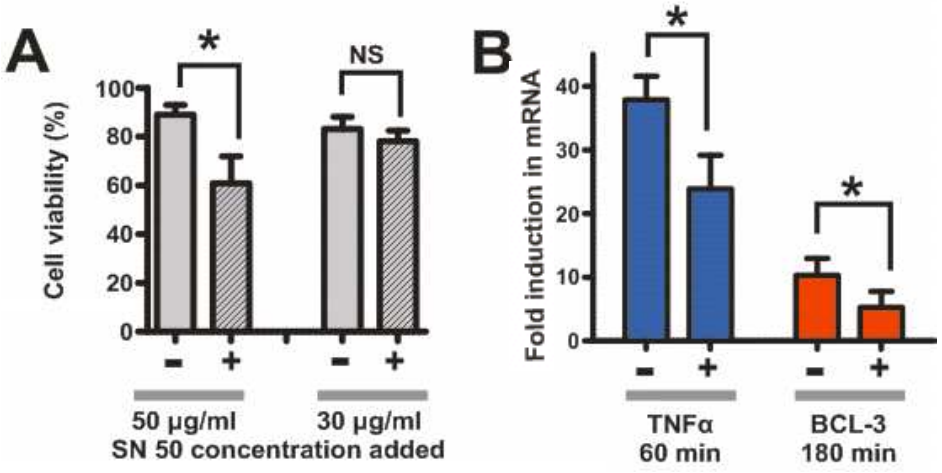

Figure 3.3. TNFα induced transcript levels of both *TNFA* and *BCL3* genes in HT1080 cells occurs via the NF-κB signalling pathway. (A) Viability of cell populations treated with (+) and without (-) 30 and 50µg/ml of SN50 for 1 hour prior to stimulation with TNFα for a further hour. (B) Pre-treatment of cells with 30 µg/ml of SN50 for 1 hour significantly reduces the subsequent TNFα induced increases in *TNFA* and *BCL3* transcript levels after 60 and 180 minutes respectively. * P<0.05; NS: Not Significant.

3.2.3. *IL9* and *IL10* have no detectable expression in HT1080 cells – even following TNFα stimulation

IL-9 and IL-10 anti-inflammatory cytokines have previously documented roles in inhibiting TNFα in a BCL-3 dependent and independent manner, with expression of both IL-9 and IL-10 themselves induced by TNFα through BCL-3 up-regulation [1.3.9.]. However, work has almost exclusively been conducted in immune cell lines such as macrophages and monocytes – therefore levels and induction of these factors in HT1080 cells was investigated.

Primers were designed against exon regions of each gene. However, despite having proved activity of these primers when amplifying from genomic DNA template (fig 3.4.A), no PCR product was observed from cDNA produced from HT1080 cells stimulated with TNFα for time points up to 1,440 minutes (fig 3.4.B). Therefore, these cytokines were adjudged to have no influence on *BCL3* expression in monocultures of HT1080 cells.

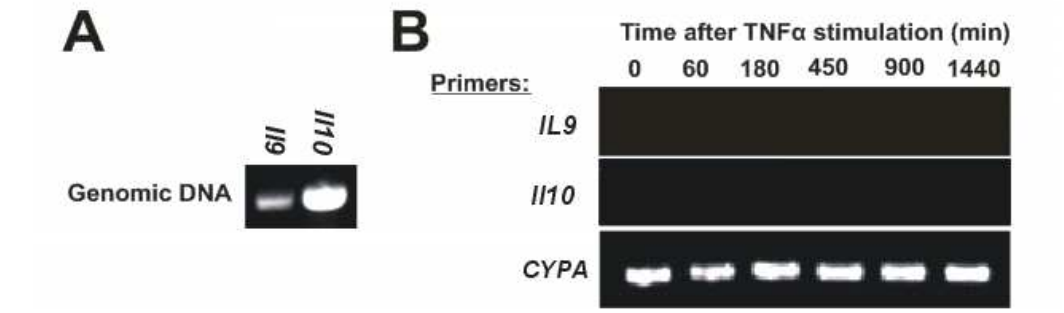

Figure 3.4. *IL9* and *IL10* genes are not expressed in HT1080 cells. In contrast to the produced PCR products amplified from *IL9* and *IL10* exon sequence from a genomic DNA template (A), no PCR product is seen amplified from cDNA produced from HT1080 cells stimulated with TNFα for varying lengths of time (B). *CYPA* acts as a positive control for the presence of cDNA.

3.2.4. Observing the nuclear localisation of NF-κB subunit p65 in response to TNFα in HT1080 cells

The NF-κB sub-unit p65 has previously been shown to reside in the cytoplasm of cells prior to TNFα stimulation and rapidly localise to the nucleus following TNFα induced degradation of IκB factors responsible for cytoplasmic sequestration of NF-κB dimers [1.2.2.]. This behaviour has notably been shown in SK-N-AS cells (Nelson et al., 2004; Ashall et al., 2009) but also in additional cell lines such as RAW264 (Zheng et al., 1993) and a primary cultured human umbilical vein endothelial cell line (Fuseler et al., 2006). Nuclear residence of NF-κB factors is later curtailed by the active removal by members of the IκB protein family, which are themselves induced by NF-κB signalling (Arenzana-Seisdedos et al., 1995) [1.2.2.].

3.2.4.1. Dynamic imaging of sub-cellular localisation of p65-dsRed protein in HT1080 cells

The rate at which p65 enters the nucleus and the duration of its occupancy will dictate the transcriptional responses of induced genes – consequently continuous live cell imaging of HT1080 cells expressing p65-dsRed under the control of a human CMV immediate early promoter (hCMV-IE) was utilised (Nelson et al., 2002).

3.2.4.1.1. Transfection of HT1080 cells with a p65-dsRed expressing plasmid

Initial transfection of HT1080 cells with 0.5µg p65-dsRed plasmid per 35mm dish of HT1080 cells [2.3.1.] resulted in high levels of observed cell death (cells detached and were apparent in the growth media) and cells which did survive this transfection, and showed dsRed signal, were rapidly killed by treatment with TNFα. Transfection with decreasing quantities of plasmid either exhibited similar results (0.25 µg) or no observed transfected cells (0.1 and 0.025µg). To ensure the ExGen500 transfection reagent used was not responsible; cells were simultaneously incubated with ExGen500 and a further

(non-p65 sequence containing) plasmid; with comparatively low levels of cell mortality. Transfection was also conducted with FuGene6 [2.3.1.2.] transfection reagent – which produced comparable levels of cell death. It was therefore likely that over-expression of p65 (in addition to endogenous levels and driven by a constitutive promoter) led to an enhanced and non-stimulus induced inflammatory cells stress response which caused cell mortality. Such a situation is likely to have been exacerbated by additional inflammatory stimuli; accounting for death of cells which do survived transfection with subsequent TNFα stimulation.

To counteract the excess p65-dsRed, a plasmid expressing IκBa-EGFP – a factor responsible for cytoplasmic sequestration of p65 [1.2.2.] - under the control of the same hCMV-IE promoter (Nelson et al., 2002) was co-transfected in equal quantity (0.5μg) Cells were also transfected 48 hours prior to stimulation with TNFα – allowing time for plasmid levels to decrease and reduce expression levels of p65-dsRed protein at the point of inflammatory stimulation. In addition, two 35mm dishes of cells were co-transfected and after 24 hours trypsinised and combined into a single dish before experimental stimulation 24 hours later. This step was included due to previous observations of poor proliferation of HT1080 cells when they were plated at too low a density – potentially due to a requirement for paracrine signalling between fibroblast cells for continued proliferation, as demonstrated for Fibroblast growth factor 7 (FGF7) in human breast cells (Palmieri et al., 2003). Furthermore, low cell densities have previously been shown to reduce expression of vascular endothelial growth factor (VEGF) in HT1080 cells (Mukhopadhyay et al., 1998). Overexpression of p65 could therefore potentially cause a double stress on cells – an increased inflammatory response and also, through increased cell death mediated by this effect, cause a lower cell density which acted as a further stress to cells. Co-transfection of p65-dsRed and IκBa-EGFP along with pooling of transfected cells to increase density increased the ability of cells to withstand TNFα stimulation and allowed observation over a prolonged time course.

While IκBa-EGFP was expressed in cells, this protein was not imaged. This was necessitated by the unexpected high level of motility exhibited by HT1080 cells (an example is shown in fig 3.5.A) which required large numbers of cells to be analysed in a single experiment to ensure that even a small proportion remained within microscopy frame for a significant length of time (success rates were typically ~25% of cells imaged remaining in frame for >30 minutes). Measurement of two emission wavelengths would have doubled the time taken to cycle between cells per time point. This, along with the increased number of cells which had to be visualised, would increase the time span between images captured of a single cell – an undesirable situation given the rapidly changing localisation dynamics of p65 protein.

3.2.4.1.2. Exogenous p65-dsRed shows rapid nuclear translocation following TNFα stimulation and a subsequent return to cytoplasmic localisation

Cell were initially imaged in the absence of TNFα for at least 30 minutes to observe p65-dsRed levels in resting cells – with cells exhibiting predominantly cytoplasmic localisation (t=-15; fig 3.5B). Following stimulation with TNFα (at t=0), increased p65-dsRed was observed in the nucleus (t=5; fig 3.5B), with levels increasing until fluorescence signal was predominantly localised in the nucleus (t=35; fig 3.5B). Following this peak, nuclear levels dropped and cytoplasmic levels increased until cells reached pre-stimulation distributions (t=151; fig 3.5B).

To obtain relative quantification of dsRed levels in the nucleus and cytoplasm, images from the time course experiment were marked with nuclear and cytoplasmic boundaries for each cell (examples are shown in fig 3.5.C) in the CellTracker program and used to extract dsRed signal levels from each cell compartment. Nuclear levels of dsRed signal were normalised against total cell fluorescence, with 15 cells analysed and shown in fig 3.5.D. A rapid increase in nuclear localisation of p65-dsRed was seen in all cells following TNFα addition (t=0) in agreement with previous analysis conducted in SK-N-AS cell (Nelson et al., 2004). However, in contrast to this study, no significant subsequent nuclear translocation was seen once the protein had left the nucleus - the characteristic oscillatory behaviour characterised in that study. In addition, the average nuclear occupancy of p65-dsRed in HT1080 cells was measured at 140.27±41.79 minutes (mean±standard deviation) in contrast to ~100 minutes in SK-N-AS cells (Nelson et al., 2004). The cause of this single nuclear translocation in HT1080 cells, in contrast to repeated nuclear translocation in SK-N-AS cells, is unclear. However, it is apparent that HT1080 cells are able to inherently limit NF-κB response to an initial TNFα stimulus, whereas SK-N-AS cells carry out a response over a prolonged period of time - up to 10 hours post stimulation – following an initial TNFα stimulus (Nelson et al., 2004). Studies in a further cell line – GH3 (derived from a rat anterior pituitary tumour) – show heterogeneous p65 oscillations; with cells in a TNFα induced population showing both sustained oscillations and a sole initial p65 nuclear movement (Friedrichsen et al., 2006). Therefore, NF-κB responses, while occurring in diverse cell types, vary in their exact nature between cells. The underlying cause of this variation is unknown, but the importance of characterising NF-κB responses in a cell line of choice rather than an assumption of uniform behaviour is emphasised by this work.

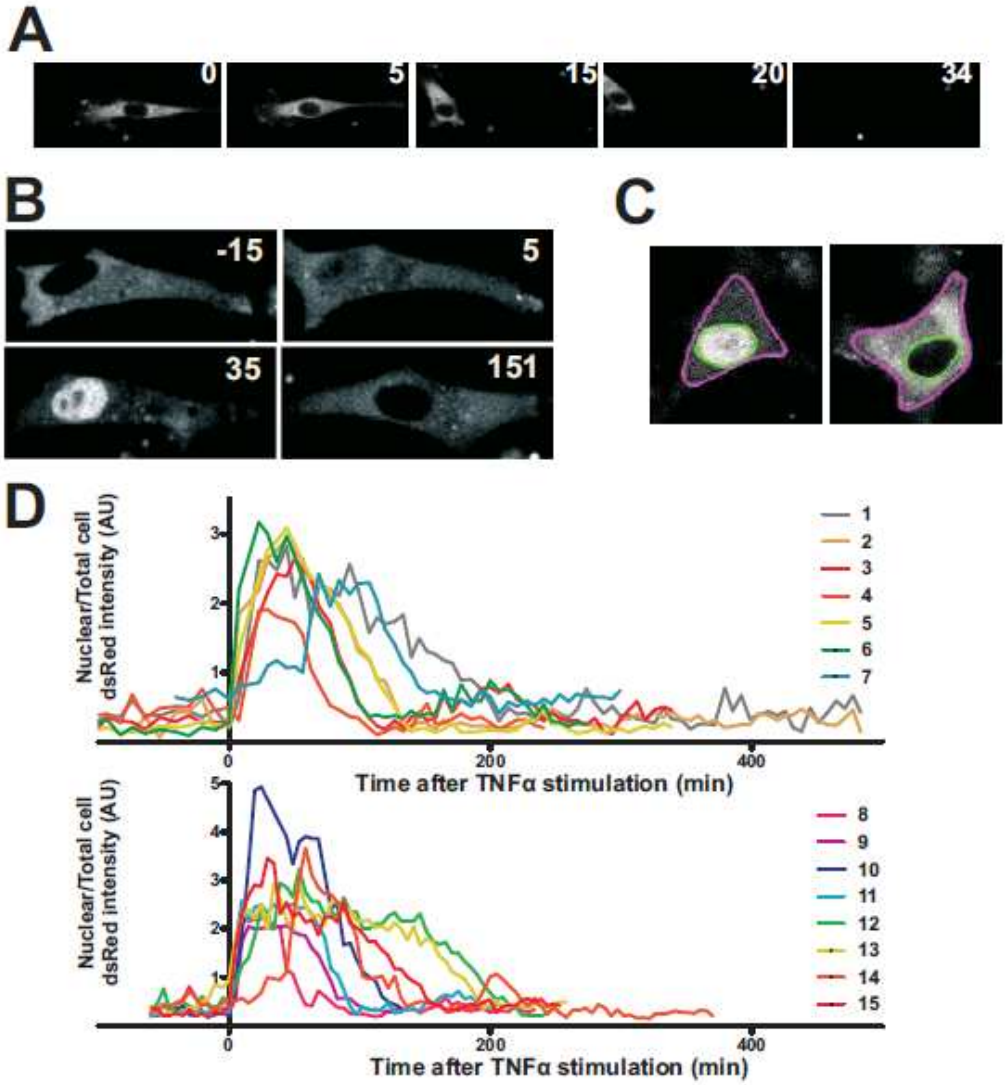

Figure 3.5. p65-dsRed exhibits rapid nuclear localisation following TNFα stimulation of HT1080 cells and subsequent reduction of nuclear localisation signal. (A) Motion of a single HT1080 cell in a constant visual field over time illustrating the difficulty in obtaining data on protein localisation in a single cell over an extended time period. Numbers relate to time following first image (0). (B) HT1080 cells transfected with plasmids expressing p65-dsRed from a constitutive promoter show cytoplasmic localisation of the protein prior to TNFα stimulation and rapid nuclear localisation post-stimulation. Protein eventual reverts back to a cytoplasmic localisation. Numbers relate to minutes relative to the time of TNFα stimulation. (C) Visual segregation of areas relating to nucleus and cytoplasm using the CellTracker program used to assess fluorescence levels in cell regions in a concatenated series of images produced from a single cell imaged over an extended time course. Two examples of cell are shown. Pink line: cell boundary; Green line: nuclear boundary. (D) Induced nuclear localisation of p65-dsRed in 15 single cells following TNFα stimulation expressed as a ratio of nuclear to total cell florescence (AU) over time post-TNFα stimulation.

3.2.4.2. Endogenous p65 protein also exhibits nuclear translocation

While live cell imaging of p65-dsRed expressing cells allows a continuous analysis of cells over an extended time course, it utilises cells which are over-expressing a p65 protein which additionally has been modified by fusion with the dsRed protein. To confirm that dynamics of this protein fusion accurately reflects endogenous p65, localisation of this protein was analysed at several time points using Immunocytochemistry with a primary antibody which binds p65 and a secondary antibody conjugated with Cy3 fluorescent dye [2.6.].

Cells which had not been stimulated with TNFα exhibited characteristic predominant cytoplasmic localisation (t=0; fig 3.6.A), with increased nuclear localisation seen following TNFα stimulation of cells (t=45; fig 3.6.A). Cells were stimulated with TNFα for 0, 45, 90, 180 and 240 minutes and nuclear levels observed and normalised against whole cell fluorescence levels using CellTracker as before [3.2.4.1.2.]. Nuclear levels were observed to be significantly increased (relative to unstimulated cells; t=0) after 45 and 90 minutes of stimulation ($P<0.01$), however no significant difference in nuclear levels was seen at later time points (180 and 240 minutes; fig 3.6.B). This is in agreement with the previous p65-dsRed localisation studies: with a rapid initial nuclear localisation followed by a return to cytoplasmic localisation and no further nuclear movement of the protein.

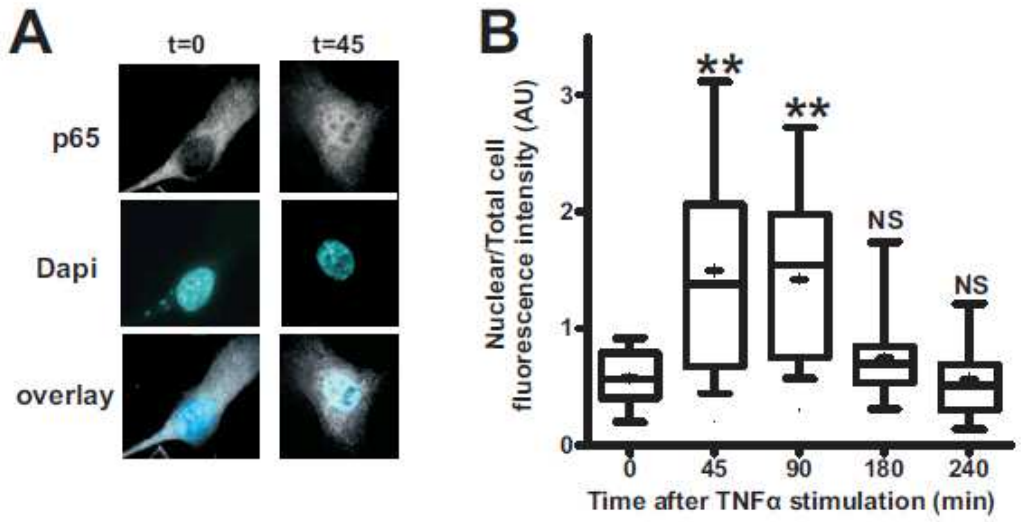

Figure 3.6. Localisation of endogenous p65 protein, as observed by Immunocytochemistry, exhibits induced nuclear localisation following TNFα stimulation.
(A)Immunocytochemistry performed with primary antibodies binding p65 (*#3034; Cell Signalling Technology*) in an unstimulated HT1080 cell shows exclusively cytoplasmic location. In contrast, an HT1080 cell stimulated with TNFα for 45 minutes exhibits enhanced nuclear presence of p65. Cells shown are considered representative of cell populations at these time points. The localisation of cell nuclei was confirmed by staining with DAPI. (B) Nuclear presence of endogenous p65 in cells (n=20 at each time point) normalised against whole cell fluorescence levels over time post- TNFα stimulation. Significance relates to comparisons with unstimulated cell levels (at t=0). NS: Not Significant; **

P<0.01. +: mean value. Horizontal lines in the box correspond to the lower and upper quartiles plus the median value. Whiskers cover 10-90% percentile of cells.

3.2.5. BCL-3 protein induction and localisation in HT1080 cells stimulated with TNFα

While previous qRT-PCR work [3.2.1.] had shown an induction in *BCL3* transcript levels in HT1080 cells in response to TNFα stimulation, it was also important to determine if this also related to an increase in protein level. Increases in mRNA level do not necessarily directly correlate to increases in protein level – restrictive mechanisms may be applied at the level of translation or on protein stability. A Western blot performed with antibodies binding BCL-3 was utilised to detect relative protein levels over a time course following TNFα stimulation.

3.2.5.1. Western blot analysis of BCL-3 protein levels in HT1080 cells following TNFα stimulation

3.2.5.1.1. Optimisation of western blot conditions

Whole cell protein was extracted by lysis [2.5.1.] and quantified based on OD_{630nm} value measurements compared to standard values calculated from serial dilutions of BSA in a Bradford assay [2.5.2.]. BSA concentrations were plotted against corresponding OD_{630nm} values and a straight line fitted of the form y=mx+c (where 'm' is line gradient and 'c' is y axis intercept value) which was rearranged to express the protein content of an unknown samples as a function if its OD_{630nm} value (fig 3.7.A) and subsequently used to calculate whole cell protein levels extracted from cells.

To determine the optimum quantity of whole cell protein to run per SDS-PAGE lane for the detection of BCL-3, serial dilutions of whole cell lysate extrated from an HT1080 cell population was run – with amounts corresponding to 10, 20, 30, 50, 75 and 100µg whole cell protein per lane. Western blotting performed with an ant-BCL-3 antibody displayed in increase in signal as whole cell protein levels increases (fig 3.7.B). Semi-quantification of band intensities using densitometry [2.5.2.] showed an initial linear increase in signal, with detection saturated at higher whole cell protein levels (fig 3.7.B). The quantity of 30 µg whole cell protein per lane was chosen as (a.) it occurs on the linear increase in sensitivity to increasing BCL-3 levels and (b.) it occurs early on this linear increase and therefore has scope to accurately detect increases in BCL-3 level - which is assumed to occur in cells which are stimulated with TNFα (cells used in this characterisation were unstimulated with TNFα). Quantities of protein run to check β-actin were run at 1/10 the amount run for BCL-3 (although following the same ratio of dilutions) as the efficiency of this antibody is such that signal levels produce causes bleaching of films when developed.

3.2.5.1.2. TNFα induces levels of BCL-3 in HT1080 cells in a delayed manner

BCL-3 run out by SDS-PAGE resolves at approximately 50kDa (fig 3.7C) as previously reported (Bundy and McKeithan, 1997). A second, marginally smaller band was also seen in some Western blots – corresponding to a previously identified non-phosphorylated form of BCL-3 (Bundy and McKeithan, 1997). The lack of this band in some gels may be due to insufficient resolution between the two bands (they exhibit similar size) or simply that levels are not sufficiently high to be constantly recognised (the band appears to be faint when present).

Following TNFα stimulation of HT1080 cells, low levels of BCL-3 are initially seen which do not noticeably increase above basal levels until 180 minutes (fig 3.7.D). Such delayed induction of BCL-3 correlates well with its proposed role in inhibiting *TNFA* transcript levels (which reach maximum levels at 90 minutes and are significantly decreased by 180 minutes – fig 3.2.A). Levels of BCL-3 remain high following stimulation, with levels remaining elevated with no noticeable decreases up to 900 minutes after TNFα stimulation (fig 3.7.D).

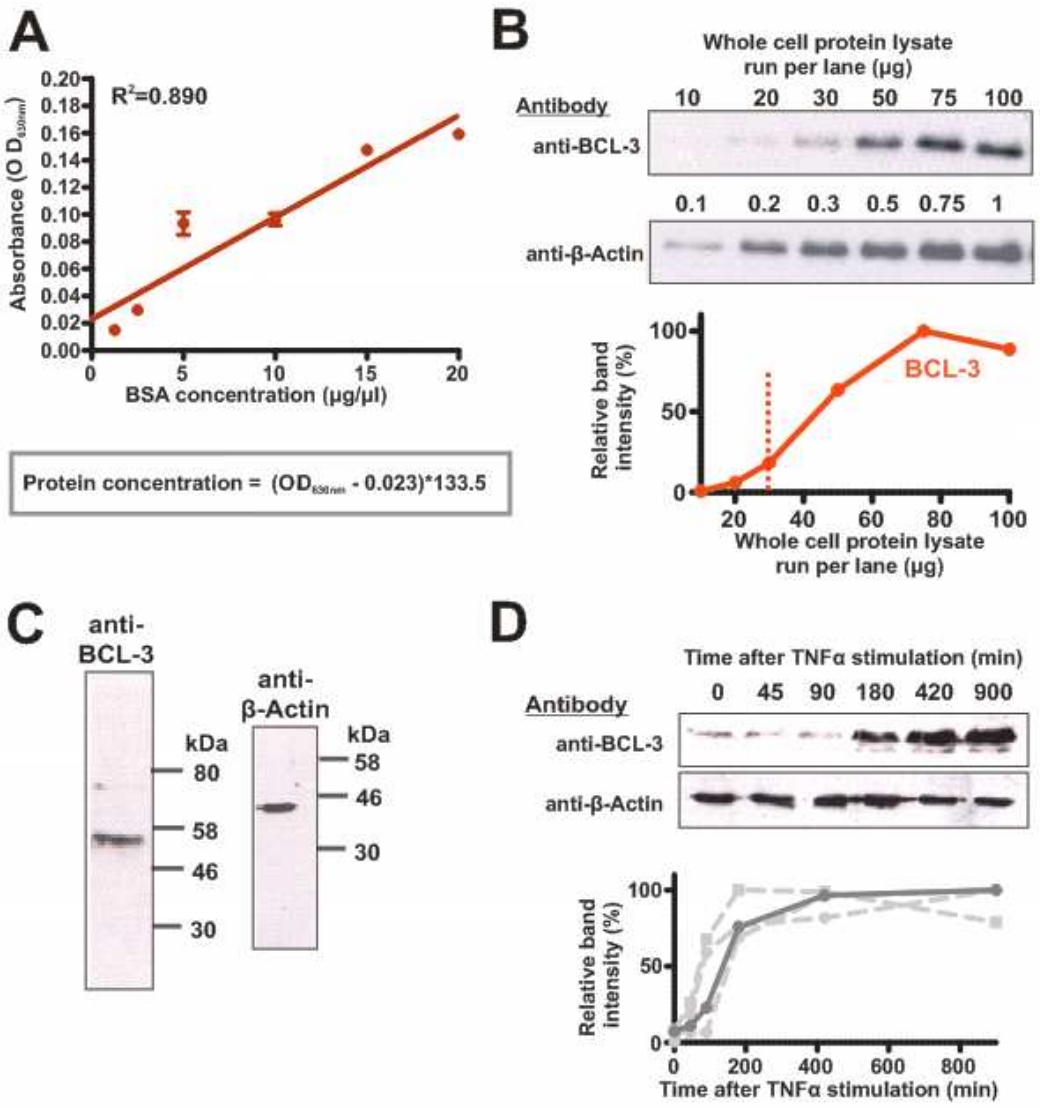

Figure 3.7. TNFα stimulation of HT1080 cells induces BCL-3 protein levels in a delayed manner. (A) Bradford assay standard graph constructed using serial dilutions of BSA standards and corresponding OD_{630nm} readings (n=3). Straight line fitted (R^2=0.890) using equation y=mx+c (where m is 133.5 and c is 0.023). This equation is adapted to calculate total protein lysate concentration extracted from a corresponding OD_{630nm} measurement. (B) Determination of an optimum quantity of whole cell protein lysate to run per lane for detection by anti-BCL-3 antibody (sc-185; Santa-Cruz Biotechnology) and anti-β-actin (A1978; Sigma-Aldrich). Quantities relate to whole cell lysate as determined by OD_{630nm} readings and standard curve shown in A. Semi-quantification of BCL-3 signal was determined by densitometry with 30µg chosen for use in experiments as approximately linear increases in signal are observed at this quantities (vertical red dashed line). (C) Detection of BCL-3 and β-Actin protein resolved by SDS-PAGE at approximately 50 and 40 kDa respectively. Protein sizes were determined by comparisons with ColorPlus Prestained Protein Marker, Broad Range 7-175kDa (New England Biolabs). (D) Western blot performed to detect BCL-3 protein (sc-185, Santa Cruz Biotechnology) on 30µg /lane whole cell lysates extracted from HT1080 cell populations at various times post-TNFα stimulation. Equality of total protein levels run confirmed with 0.3ng/lane β-actin control (A1978; Sigma-Aldrich). Relative band intensity calculated from three replicates (each shiwn as pale dashed grey line) with avegae value shown (darker, solid grey line).

3.2.5.2. Induced BCL-3 localises predominantly to the nucleus

To confirm the localisation of BCL-3 protein, Immunocytochemistry was carried out on cells stimulated with TNFα for 180 minutes (to maximize signal) [2.6.]. The strongest signal for anti-BCL-3 antibody (and secondary Cy3 conjugated secondary antibody) occurred in the nucleus, although presence in the cytoplasm was also observed (fig 3.8.). This localisation, while in contrast to a general widespread description of BCL-3 as an exclusively nuclear protein, has previously been observed in other cell types such as NIH 3T3 (Nolan et al., 1993) and NTera-2 cells (Bours et al., 1993).

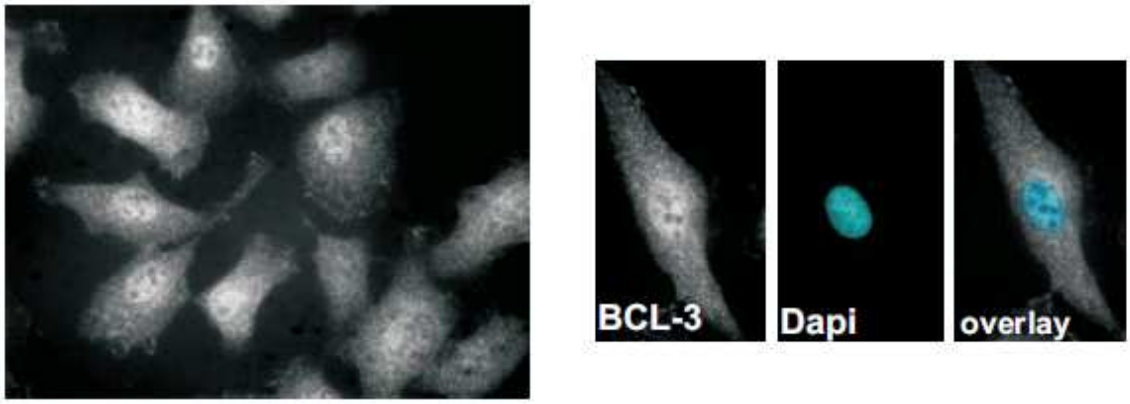

Figure 3.8. Induced BCL-3 protein exhibits greatest accumulation in the nucleus. The localisation of endogenous BCL-3 protein (sc-185, Santa Cruz Biotechnology) in HT1080 cells stimulated with TNFα for 180 minutes as determined by Immunocytochemistry. While signal is observed in the cytoplasm, the protein is predominantly seen to be localised to the nucleus – as confirmed by nuclear staining with DAPI.

3.2.6. BCL-3 has an inhibitory effect on TNFα transcript levels

The sharp decrease in *TNFA* transcript levels, as shown in fig 3.2.A, correlates with the delayed increase in *BCL3* transcript levels – suggesting an inhibitory mechanism. BCL-3 has previously been shown to inhibit TNFα transcription [1.4.4.2.] and this role was hypothesised in HT1080 cells. This inhibitory relationship was investigated by overexpressing BCL-3 through transfection of a plasmid constitutively expressing the *BCL3* under the control of the CMV promoter (Brasier et al., 2001). After a 60 minute stimulation with TNFα, cells transfected with the *BCL3* over-expression plasmid [2.3.1.1.] exhibited a greater than 60 fold higher average increase in *BCL3* transcript levels than untransfected cells (both induced populations were compared to *BCL3* levels in untransfected, unstimulated cells) (fig 3.9.A). This was associated with a more than ten fold reduction in the level of *TNFA* transcript levels induced in the same cell populations (fig 3.9.A).

Furthermore, HT1080 cells in which BCL-3 transcript levels are inhibited with anti-BCL-3 siRNA [2.3.2.] showed a significantly higher (P<0.05) fold increase in *TNFA* transcript levels, relative to untransfected cells, following 180 minutes of TNFα stimulation (fig 3.9B). A successful decrease in BCL-3 gene transcript levels and protein was confirmed by qRT-PCR (fig 3.9.B) and Western blot (fig 3.9.C; BCL-3 levels are 40.57±4.98% of untransfected cells as measured by densitometry). The sensitivity of *TNFA* transcript level increases to BCL-3 levels indicate that a previously shown negative role for BCL-3 in regulating *TNFA* transcript levels is present in HT1080 cells.

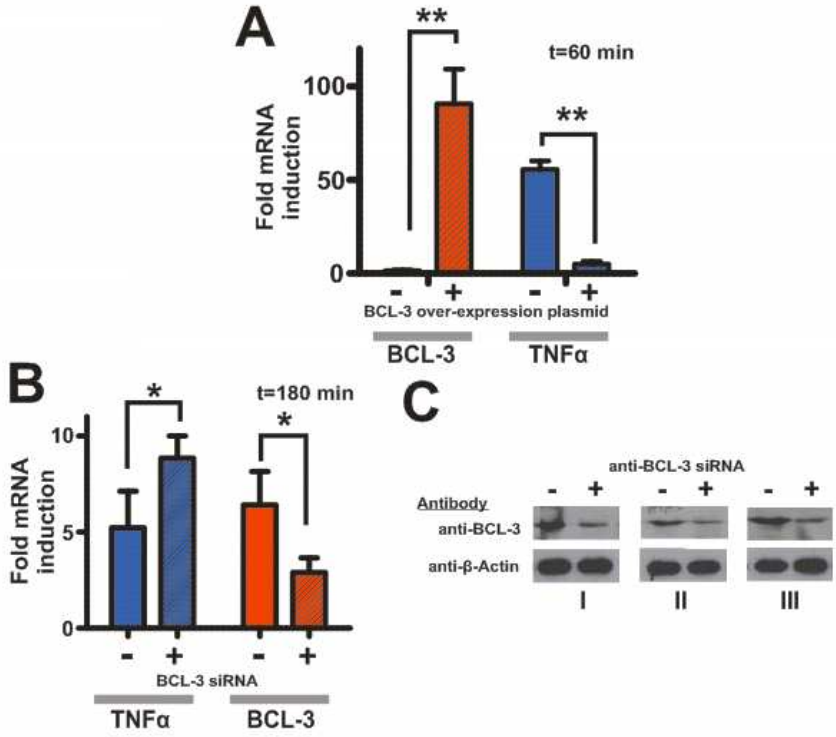

Figure 3.9. BCL-3 exerts a negative influence on *TNFA* transcript levels in HT1080 cells.
(A) HT1080 cells transfected with a plasmid expressing the *BCL3* gene from a constitutive promoter exhibit a significant increase in *BCL3* transcript levels in cells stimulated with TNFα for 60 minutes and an associated significant decrease in *TNFA* transcript levels at this time. Conversely, cells transfected with anti-BCL-3 siRNAs show a significant decrease in *BCL3* transcript levels in cells stimulated with TNFα for 180 minutes and an increase in *TNFA* transcripts at this time (B). An observed knock-down in BCL-3 protein levels in cell populations transfected with these siRNAs was confirmed by western blotting (C). I, II and III represent replicate numbers. *P<0.05; **P<0.01.

3.2.7. Investigating the temporal binding of BCL-3 at a distal κB site (-869) in the *TNFA* promoter – using a ChIP-qPCR assay

To confirm that BCL-3 is acting to inhibit *TNFA* transcript levels via transcription inhibition, rather than on transcript stability, the presence of the protein at the *TNFA* promoter was assayed using ChIP [2.7.].

ChIP is a method of determining whether a particular DNA sequence is bound by a protein of interest. Chromatin is fixed with formaldehyde and fragmented into short fragments of DNA by sonication and proteins, along with bound DNA sequence, can be selectively precipitated by use of antibodies. The protein and DNA are then split and primers used on the pool of DNA fragments precipitated to determine the presence of a sequence of interest. In this study, qPCR has been used to obtain a measure of enrichment in DNA fragments precipitated by anti-BCL-3 or anti–p65 antibodies compared against fragments precipitated by mouse anti-IgG antibody (which would exhibit no specific binding against human proteins).

3.2.7.1. Optimisation of ChIP reagents

A distal κB site (-869) in the *TNFA* promoter has previously been shown to mediate *TNFA* transcript down-regulation through binding of p50 homodimers at this site and is therefore a potential site for BCL-3 activity - as BCL-3 binds DNA indirectly via p50 homodimers and has been shown to be important in the stable binding of DNA by p50 homodimers [1.3.2.].

Primers were designed to amplify sequence proximal to, and encompassing, this κB site (-869) (fig 3.10.A). To prevent detection of sequence precipitated by protein bound at the nearest adjacent κB site (-597), chromatin needed to be sonicated to <350bp – a size less than the distance between the downstream primer used in the assay and the adjacent -597 κB site; meaning DNA fragments could not contain both the -597 κB and sequence required for the primer pair to bind (see diagram in fig 3.10.A).

To consistently obtain chromatin fragments of the required size (<350bp), paraformaldehyde fixed and extracted chromatin was sonicated for varying numbers of pulses by a probe sonicator [2.7.2.], with aliquots removed at varying numbers of pulses and treated with RNase A and proteinase K before being run out on an agarose gel to check fragment size [2.8.4.]. The sonicated sample was incubated on ice for one minute in between pulses due to observed increases in sample temperature when pulses were applied at greater frequency (increased sample temperature may lead to dissociation of protein and DNA). Fifteen pulses applied in this manner were observed to constantly produce <350bp fragmented samples (two independent extracted and sonicated samples are shown in fig 3.10.B; lanes 3 and 4). While fewer pulse numbers were observed to produce DNA fragment populations below this size, on occasions residual larger fragment sizes were observed (Ø; fig 3.10.B lane 6). To ensure that a constant sonication treatment could be applied to all samples, 15 pulse treatments were therefore used and sufficient fragmentation confirmed for every sample used by testing an aliquot of total sonicated chromatin in this way prior to starting the ChIP protocol,

3.2.7.2. Relative quantification of immunoprecipitatated DNA fragments using qPCR and the Percentage Input method

The detection and relative quantification of DNA fragments containing the -869 κB sequence (more exactly, the primer binding sequence) was conducted using qPCR performed on DNA fragment populations precipitated by anti-BCL-3, -p65 and -IgG (negative control) antibodies.

C_T values produced by qPCR conducted using antibody precipitated pools of genomic DNA fragments were normalised against the initial amount of total sonicated chromatin used per experiment (i.e. before antibody precipitation) – known as the Input sample [2.7.5.]. To obtain comparable qPCR efficiencies from Input and immunoprecipated genomic DNA samples amplified using the same primers, quantities of template DNA needed to be similar. This required a dilution of Input chromatin – which would contain a far greater amount of both primer specific and non-specific DNA fragments. To determine the most appropriate percentage of Input sample to use, qPCR was conducted with dilutions of Input (10, 1, 0.1 and 0.01%) alongside reactions using precipitated DNA samples. C_T values were subsequently compared and 1% Input chromatin ('0' value in fig 3.10C which is plotted on a logarithmic scale) fell within the range of maximal (33.20) and minimal (29.48) C_T values obtained from precipitated DNA samples.

C_T values obtained from antibody precipitated DNA samples were expressed as a percentage of the C_T value obtained from initial Input samples (C_T value for 1% Input adjusted to 100% Input [2.7.5.]). Significant qPCR C_T values were obtained by comparison with DNA precipitated with negative control mouse anti-IgG antibody [2.7.3.].

3.2.7.3. BCL-3 binds at a distal κB site in the *TNFA* promoter in a manner temporally consistent with an inhibitory effect on *TNFA* transcription

The occupancy of BCL-3 and p65 proteins at the -869 κB site was tested after 60 minutes (a time at which *TNFA* transcript levels are increasing; fig 3.2A) and 180 minutes (a time at which *TNFA* transcripts levels have dramatically decreased from maximal levels; fig. 3.2.A) after TNFα stimulation. BCL-3 is bound at significant levels (in comparison to an IgG negative control) at 180 minutes but not 60 minutes – a binding pattern which correlates with its proposed role in inhibiting *TNFA* transcription at this time (fig 3.2.A). Significant binding of p65 was not observed at either time point. The lack of significant p65 binding at this site is in contrast to work reported in Udalova et al. who reported binding competitive binding of p50/p65 heterodimers and p50 homodimers at this κB site (Udalova et al., 2000). However, while the authors show p50 homodimer binding at this site mediates *TNFA* transcription attenuation, they do not show any functionality of p50/p65 binding. Further work showing

that a proximal κB site (-100) in the *TNFA* promoter is necessary and sufficient for NF-κB mediated induction of TNFA transcription (Yao et al., 1997) indicates that any p50/p65 binding at the distal -869 κB site is unlikely to have a direct effect on *TNFA* transcription, although it may act indirectly by competing for binding with an inhibitory p50 homodimer/BCL-3 complex. Alternatively, the similarity between optimum κB site sequence for p50/p65 and p50 homodimer binding [1.2.6.1.] may lead to non-specific binding of factors which have no functional role.

The absence of any observed p65 binding at the distal (-869) κB site in this study may reflect a low level of binding which falls below the sensitivity of this assay or reflect differential binding of p65 in HT1080 cells (this study) and Mono Mac 6 monocytes cells (Udalova et al. 2000). While this cannot be due to a non-permissive chromatin binding states (as BCL-3 is observed binding at the site), it is possible that additional factors required for stable p65-container dimer binding at this location are deficient in HT1080 cells.

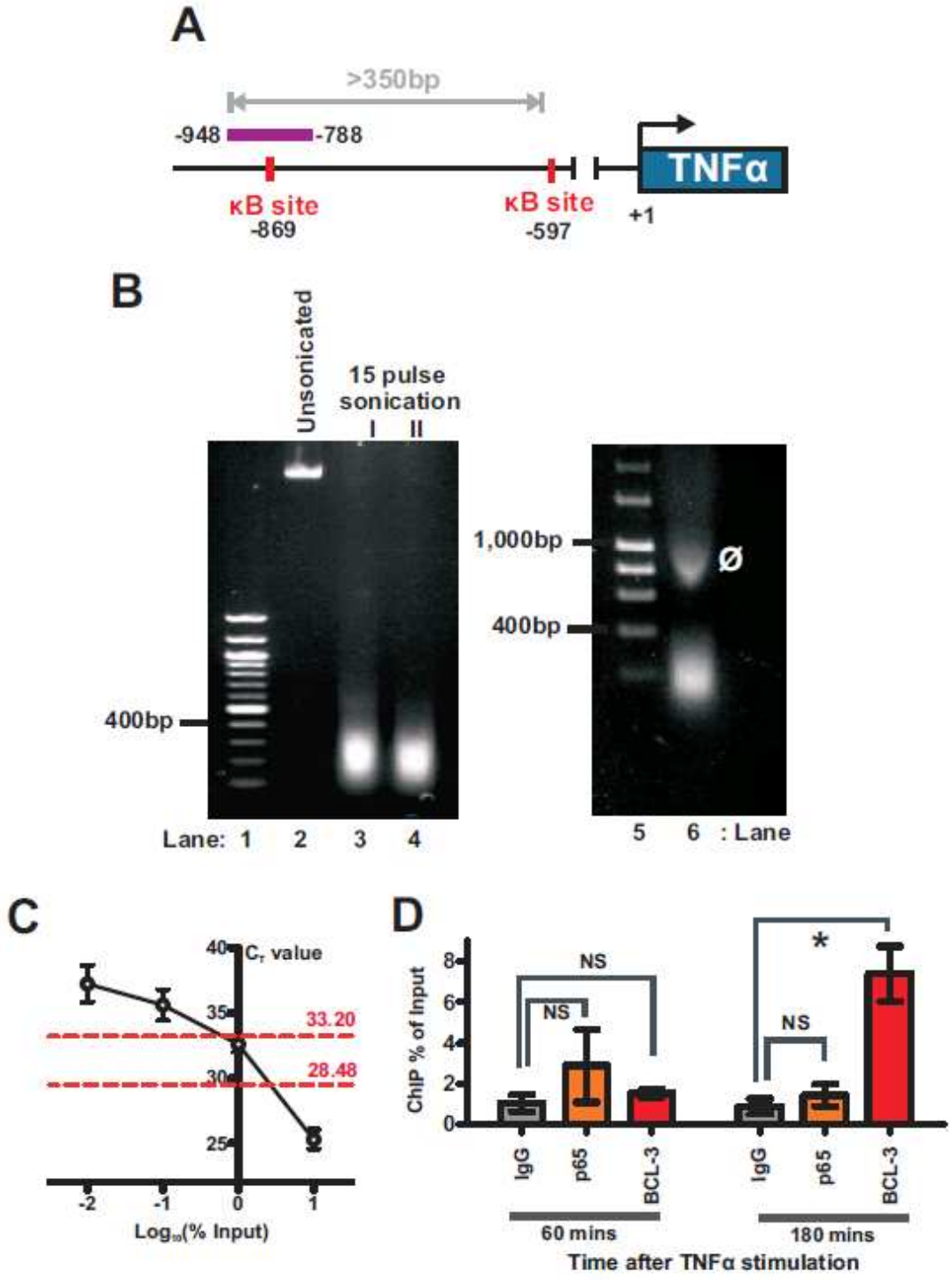

Figure 3.10. BCL-3 binds at a distal κB site (-869) in the *TNFA* promoter in a temporal manner
(A) Location of primer amplified sequence (purple bar) amplifying a distal κB site (-869) in the *TNFA* promoter and the proximity of the closest adjacent κB site (-597) to the upstream primer site necessitating the use of sonicated chromatin fragments <350bp to preclude the inclusion of protein bound at this site in the ChIP assay. (B) Formaldehyde fixed chromatin sonicated with 15 pulses (two

replicates: I & II) from a Cole-Palmer pulse sonicator [2.7.2.]. Chromatin samples were treated with RNase A and proteinase K prior to running on a 1% agarose gel. (C) C_T values produced by qPCR from a range of Input (i.e. total chromatin) percentages (expressed as log_{10}) in a qPCR reaction performed with primers shown in A. Red dashed lines relate to the upper and lower C_T values obtained by qPCR with the same primers on template DNA precipitated with ant-BCL-3 and anti-p65 antibodies showing the suitability of 1% Input as an appropriate standard for use in this experiment. (D) BCL-3 exhibits significant binding at a distal κB (-869) in the *TNFA* promoter of HT1080 cells after 180 minutes of TNFα stimulation. Levels of immunoprecipated chromatin are expressed as a percentage of total Input chromatin as measured by qPCR. Chromatin was precipitated with anti-BCL-3 (sc-185; Santa-Cruz Biotechnology), anti-p65 (06-418; Millipore) and anti-IgG (12-371; Millipore) antibodies. Significance relates to a comparison with IgG negative control levels. NS: Non Significant; *P<0.05. Error bars show standard deviation.

3.3. Discussion

Work in this chapter has concerned confirming, in HT1080 cells, previous studies conducted in diverse cell types regarding the NF-κB mediated up-regulation of *TNFA* and *BCL3* genes and a role for BCL-3 in inhibiting *TNFA* transcription.

TNFα mediated up-regulation of *TNFA* and *BCL3* transcript levels has been confirmed and shown to occur via the NF-κB signalling pathway, however no expression of the anti-inflammatory cytokines IL-9 and IL-10 was observed at the RNA level [3.2.1.3.][3.2.2.][3.2.3.]. In keeping with previous work, p65 containing NF-κB complexes reside in the cytoplasm of resting HT1080 cells but exhibit rapid nuclear localisation following TNFα stimulation [3.2.4.]. However, in contrast to previous studies conducted in a neuroblastoma cell line, only a single nuclear increase and subsequent decrease in NF-κB levels were observed. BCL-3 protein levels have also been shown to increase after approximately 180 minutes of TNFα stimulation [3.2.5.1.2.] with the protein showing strongest localisation in the nucleus [3.2.5.2.]. Finally, BCL-3 has been shown to have an inhibitory effect on *TNFA* transcript levels in HT1080 cells [3.2.6.] and binds at a distal κB site (-869) in the *TNFA* promoter at a delayed time consistent with this effect being mediated by inhibition of *TNFA* transcription [3.2.7.3.]. A summary of the interactions defined is shown in figure 3.11.A.

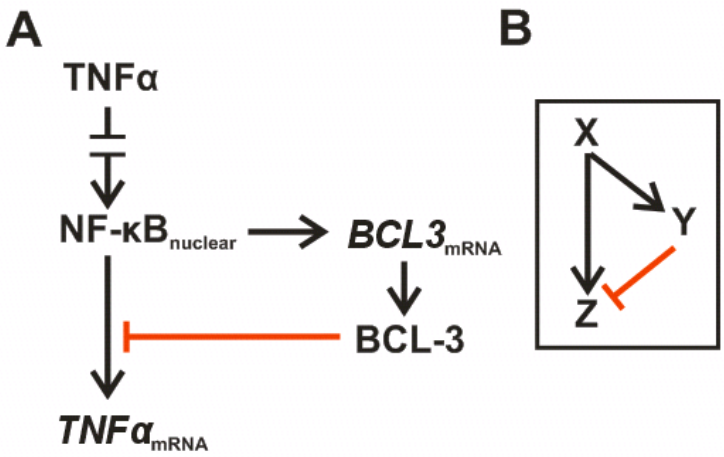

Fig 3.11. Genetic circuit regulating TNFα induction of *TNFA* transcription. (A) Representation of NF-κB mediated transcriptional induction of both *TNFA* and *BCL3* genes and subsequent inhibition of *TNFA* transcription by BCL-3 – as experimentally confirmed in HT1080 cells. (B) Schematic of a theoretical Incoherent Feed Forward Loop (I-FFL).

Notably, the NF-κB induction of *TNFA* and *BCL3* with subsequent inhibition of *TNFA* transcription by BCL-3 resembles an Incoherent Feed Forward Loop motif (as conceptually shown in fig 3.11B) – a motif in which a common stimulus (NF-κB/X) induces both an output (*TNFA* transcription/Z) and also an inhibitor of this output (BCL-3/Y).

3.3.1. Incoherent Feed Forward Loop motifs

Network motifs are particular arrangements of interactions between components which occur in networks at a far greater frequency than would be expected from a purely randomised network (Milo et al., 2002). Widespread evolutionary selection for such motifs in transcription networks suggests a benefit, i.e. that they produce useful behaviour within a network.

Incoherent Feed Forward Loops (I-FFLs) are so-called because an inductive signal acts as both a positive and, indirectly, a negative effect on the same output. While the parallel and antagonistic pathways within an Incoherent Feed Forward Loop (I-FFL) may appear counter-intuitive, the motif has been shown to produce several characteristic behaviours when stimulated:

(i.) Pulse generation

An initial positive induction of output (Z in figure 3.11.B) in response to input stimulus (X in fig 3.11.B) is later inhibited once a parallel induced inhibitor component (Y in fig 3.11.B) reaches sufficient levels. This creates a transient response to a continuous stimulus or 'pulse' like behaviour (Mangan and Alon, 2003).

(ii.) Accelerated response time

The simultaneous induction of an inhibitor (Y) allows an inductive signal (X→Z) to occur at a greater rate; as later inhibition of output by the inhibitor ensures that an initially high level of output is not sustained. In contrast, in the absence of an inhibitor, induction rates of output must be

significantly lower to produce the same final steady state level of output (as illustrated in fig 3.12.A). The time to reach a set level of output (red dashed line in fig 3.12.A) is therefore less in an induction pathway incorporating an I-FFL – an accelerated response without high levels of output over an extended period of time (Mangan et al., 2006).

(iii.) Rate sensing capability

Further studies have also reported an I-FFL synthetically created in *E. coli* is able to sense the rate of increase in input (X) signal that cells were exposed to (Basu et al., 2004). Here signal induced the positive and inhibitory pathways in a proportional manner, consequently slower increases in input created both slower increases in output and inhibition. Rapid increases in input therefore produced high amplitude output responses which were inhibited rapidly, whereas slower levels of input increase resulted in a slower and lower magnitude output but which was inhibited at a later time (as illustrated in fig 3.12.B).

(iv.) Non-monotonic response

I-FFLs can also produce a non-monotonic response of steady state output levels (Z) as input levels (X) increase. That is, induction of cells with low levels of input result in a sustained output level but once input levels cross a threshold level, output levels are inhibited (Kaplan et al., 2008). This behaviour is caused by differing sensitivities of the positive and negative I-FFL pathways to input. Use of a low input level can stimulate the more sensitive positive pathway; causing output levels to be induced and, as the less sensitive inhibitory pathway is not induced at this input level, maintained. Use of input level above a threshold level also induces the inhibitory pathway and consequently output levels are reduced (as illustrated in fig 3.12.C).

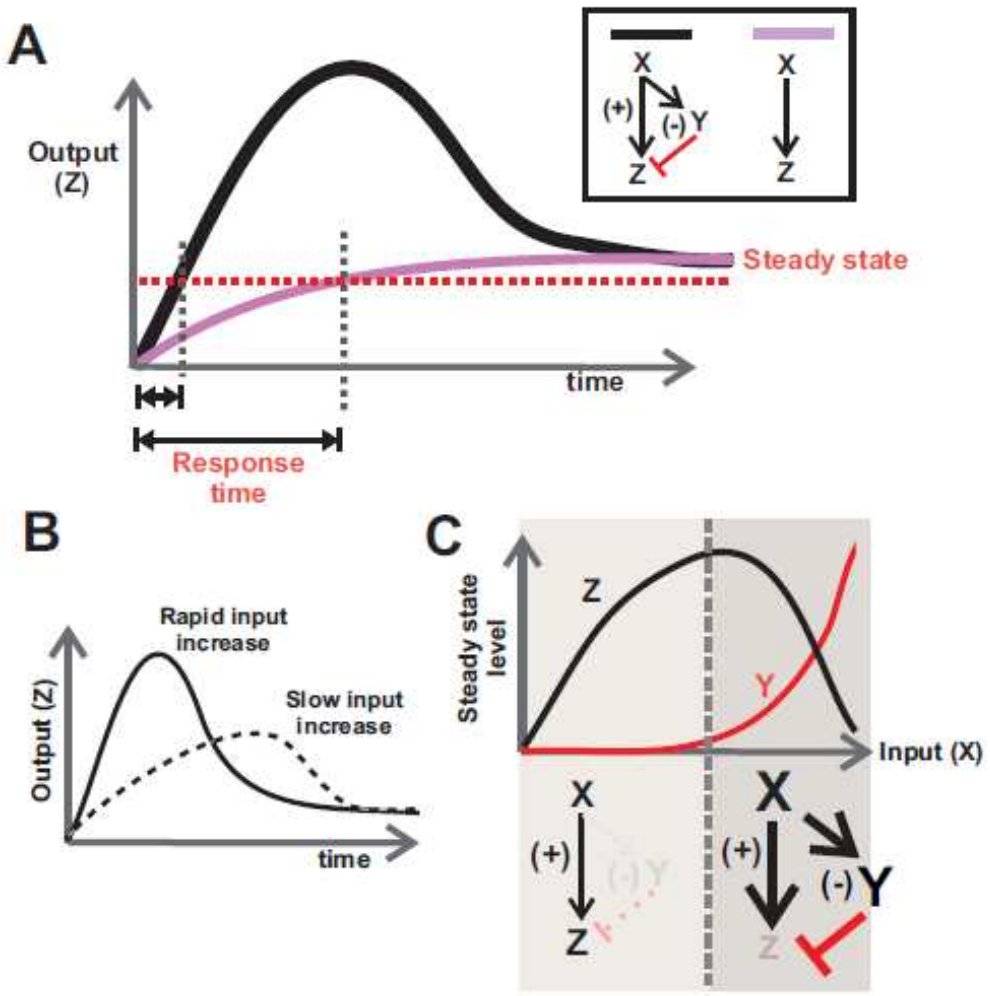

Figure 3.12. Representative graphs illustrating the output characteristics which can potentially be produced by the I-FFL motif. (A) Accelerated response time of induced I-FFL (black line) in contrast to a simple regulatory pathway (lilac line) which both produce an identical magnitude steady state of output (Z). 'Response time' correlates to the time taken for each response curve to reach a threshold level (red dashed line). (B) Differential pulse kinetics produced by an I-FFL in response to varied increase rates of the input signal and (C) non-monotonic steady state response of output (Z) to varied constant input (X) values due to the reduced sensitivity of inhibitor (Y) to low input levels.

Such studies show that the relative induction dynamics of the positive and negative pathways constituting an I-FFL can produce differential behaviour with regards to output dynamics. Notably, the relative sensitivity of the two antagonistic pathways has been shown to produce input increase rate sensitive responses (iii) and a non-monotonic response (iv). However, a notable omission from these studies is a consideration of the relative timings of interactions and the potential such timings could have on output dynamics.

3.3.2. Interaction timings in the *TNFA*/*BCL3* I-FFL

While a catalogue of interactions, as defined in this chapter for *TNFA* and *BCL3* transcription, is important; the static arrow diagram produced (fig 3.11.A) assumes the positive and negative pathway legs occur simultaneously and instantaneously. However, closer examination of data concerning *TNFA* and *BCL3* transcript increases indicates that this is not the case. Notably, in figures 3.2.B and C, the rates of increase in *TNFA* and *BCL3* transcript levels following TNFα stimulation is not uniform: with *TNFA* rates of change reaching maximal levels at an earlier time period than *BCL3* transcripts (which display dramatic increases only after 60 minutes of TNFα stimulation). The rate of BCL-3 production, and consequently the time taken to reach a level sufficient to inhibit *TNFA* transcription, will clearly have an effect on the magnitude of *TNFA* transcriptional response. Notably, BCL-3 protein induction kinetics [3.2.5.1.2.] plus the binding of BCL-3 at the TNFA promoter [3.2.7.] correlate well with decreases in *TNFA* transcript levels.

Intriguingly in this genetic circuit, NF-κB mediates both *TNFA* transcription and also a mechanism for limiting this effect via BCL-3 up-regulation. The relative speeds of these positive and negative legs (with respect to their effect on *TNFA* transcription) will determine the magnitude of *TNFA* transcription response and is an understudied aspect of general considerations of the I-FFL motif. The differential response of two genes to the same inductive stimuli (TNFα), the effects of which are mediated by a common molecular pathway (NF-κB), is further defined and studied in Chapter 4.

Chapter 4

Investigating NF-κB mediated induction of *BCL3* transcription

4.1. Introduction

4.1.1. Mechanisms of NF-κB induced transcription

NF-κB acts as a transcription activator via recruitment of histone acetyltransferase (HAT) enzymes to NF-κB responsive genes (i.e. those containing a κB binding site), with consequent acetylation of histones in the vicinity (Sharma et al., 2007). Such signalling dependent histone acetylation acts to recruit further bromodomain containing proteins which can act to initiate transcription in two predominant ways:

- Acetylation of lysine residues 5,8 and 12 in histone 4 can bind bromodomain containing factor Brd4 which subsequently recruits p-TEFb – a factor required to phosphorylate previously bound and stalled RNAP molecules and facilitate transition to an elongating form of the enzyme [1.6.5.3.] (Hargreaves et al., 2009).
- Bromodomain dependent recruitment of chromatin remodelling complexes to promoters facilitating transition to an open chromatin structure and allowing binding of further transcription co-activators or RNA pol. II [1.5.4.].

4.1.2. NF-κB acts at different points in the Transcription Cycle

The binding of RNAP to a gene's promoter, subsequent promoter clearance and transition to an actively elongating form of the enzyme occurs over a series of stages known as the Transcription Cycle [1.6.5.]. In genes which are not constitutively active, progression of RNAP can be restricted at diverse points in the Transcription Cycle – with successful completion of the cycle dependent on the activity of an activating factor. The points of action of such activators can be broadly assigned to two main points: being required for initial RNAP binding at the promoter or for the activation of previously bound and 'paused' RNAP [1.6.5.2.]. As outlined in [4.1.1.], NF-κB is able to act at either of these points, dependent on context.

The occurrence of promoter bound and stalled RNAP is becoming increasingly apparent as a wide spread occurrence across genomes and has been suggested as a mechanism to mediate rapid transcriptional response [1.6.6.]. Such binding avoids potentially rate-limiting steps in PIC assembly and RNAP loading which can instead occur prior to an activating stimulus and has been observed, although based on a relatively limited number of studies, as occurring in greatest frequency at genes which respond to environmental or developmental cues (Wu and Snyder, 2008).

4.1.3. Chapter aims

Work in the previous chapter showed that NF-κB was a causative factor in TNFα induction of both the *TNFA* and *BCL3* genes – however, while activation of the genes was by a common factor, *BCL3* transcript levels appeared to increase at a relatively delayed time point. In this chapter, the response rates of the two genes are further defined and mechanisms investigated to account for the delayed response of the *BCL3* gene.

4.2. Results

4.2.1. TNFα induces *BCL3* transcript increases in a delayed manner relative to *TNFA* transcript levels

The size of an induced *TNFA* transcriptional pulse will be determined by both the speed at which *TNFA* transcription initiates following cell stimulation and the time taken for BCL-3 to accumulate to sufficient levels to inhibit transcription. As seen in fig 3.2.A, *TNFA* transcript levels peak at an earlier time point than *BCL3* (90 and 180 minutes respectively) and appears to initiate increases in transcript levels at earlier time points (compare fig 3.2.B with 3.2.C). Transcript levels were further analysed using greater resolution of early time points following TNFα induction (ten minute increments from 30-70 minutes). This showed that while *TNFA* transcript levels were significantly induced above basal, unstimulated levels (i.e. at t=0) at 30 minutes post-stimulation, *BCL3* transcript levels were not significantly induced at this time (fig 4.1); in fact, significant inductions in *BCL3* transcript levels were only seen after 60 minutes of TNFα stimulation

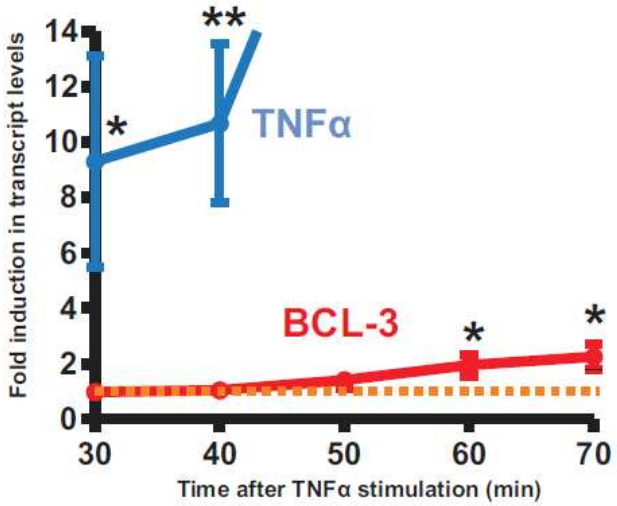

Figure 4.1. Delayed induction of *BCL3* transcript increases, relative to *TNFA* transcript increases, in HT1080 cells following TNFα stimulation. Fold inductions of *TNFA* and *BCL3* transcripts relative to levels in unstimulated cells (i.e. at t=0) at times after TNFα stimulation of HT1080 cell populations. The basal level of transcript levels (value of 1 corresponding to unstimulated cells) is shown as a horizontal red dashed line. Three independent samples measured per data point. Significance is relative to unstimulated cells for each gene's transcript. *P<0.05; **P<0.01. Error bars show standard deviation.

4.2.2. RNAP dynamics at the *TNFA* and *BCL3* genes

To investigate the differential response rate of *TNFA* and *BCL3* genes to the same NF-κB transcription inducing signal, the binding of RNAP at each gene in resting, pre-stimulation cells was investigated using ChIP. Primers were used to detect DNA sequence proximal to the TSS and also within the coding sequence of each gene (fig 4.2.A). A sufficient distance – i.e. greater than the size of DNA fragments produced by sonication as in [3.2.7.1.] - was left in between each primer set to ensure that RNAP bound at the TSS would not be detected by coding sequence primers and vice versa. These primers were used in PCRs conducted using template DNA fragments precipitated by anti-RNA pol. II antibodies, anti-mouse IgG antibodies (negative control) and initial Input chromatin (positive control) – with PCR outputs resolved and visualised on a 1% agarose gel by electrophoresis [2.8.4.] (fig 4.2.B).

4.2.2.1. RNAP is bound in a paused state at the *TNFA* gene promoter in unstimulated cells - in contrast to no observed binding at the *BCL3* gene

RNAP binding was observed at the TSS of the *TNFA* gene but not within the coding sequence of this gene or at all at the *BCL3* gene (fig 4.2.B). This suggests that while conditions are permissive for RNAP binding at the *TNFA* gene's core promoter, progression to fully elongating activity of the enzyme is inhibited until stimulated by TNFα induced signalling. NF-κB has a previously documented role as relieving paused polymerase (Ainbinder et al., 2002; Hargreaves et al., 2009) and is a strong candidate for this function at the *TNFA* gene. Preloading of RNAP at genes has previously been linked to a rapid

induction of gene transcription [1.6.5.2.] and would account for the rapid increase in *TNFA* transcript levels. In contrast, the *BCL3* gene shows no pre-stimulus RNAP binding. The two genes can therefore be seen to be restricted at different points in the transcription cycle [1.6.5.]: with a required stimulus to either activate bound RNAP (*TNFA* gene) or allow the polymerase enzyme to bind (*BCL3* gene). Binding of RNAP requires a multi-step assembly of a Pre-Initiation Complex (Dennis et al., 2003) – the requirement at the *BCL3* gene for this to occur would account for the delay in transcript induction levels. *TNFA*, alternatively, requires an activation signal which can be as simple as a post-transcriptional modification to an already bound complex – a far more rapid process allowing for a quick transcriptional response.

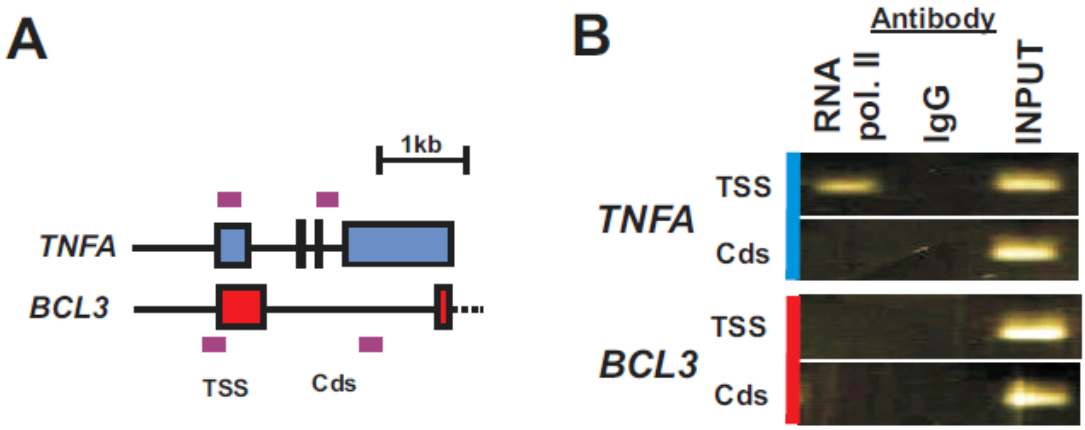

Figure 4.2. RNA polymerase II is bound at the *TNFA* gene promoter prior to TNFα stimulation but is not detected within the *TNFA* coding sequence. (A) Position of primer amplified sequence in both the *TNFA* and *BCL3* genes. Primers were designed to amplify sequence proximal to the transcription start site and within the coding sequence (Cds) of each gene. Sequences amplified by PCR are shown as purple bars. (B) PCR reactions performed on DNA precipitated by ChIP using chromatin from unstimulated HT1080 cells and precipitated with an anti-RNAP antibody (lane 1; #05-623, Millipore), an anti-mouse IgG antibody (lane 2; #12-371; Millipore) and also using 1% initial total chromatin (lane 3; Input) as template. Primers used are as shown in 4.2.A for both *TNFA* and *BCL3* genes.

4.2.3. RNAP exhibits TNFα induced binding at the *BCL3* promoter in a manner correlated with enhanced histone 3 acetylation

No RNA pol. II was observed bound at the *BCL3* TSS in unstimulated HT1080 cells [4.2.2.1.]; therefore binding of the enzyme over time following TNFα was measured using ChIP with anti-RNAP antibodies and primers (fig 4.3.A) as in [4.2.2.]. As before (fig 4.2.B), negligible RNAP binding was observed at the *BCL3* TSS in cell unstimulated with TNFα (t=0; fig 4.3.B). Delayed increases in RNAP binding were observed at this site up to 90 minutes post-TNFα stimulation – with increases in levels initially low until 45 minutes, after which time binding levels increased dramatically (fig 4.3.B).

Binding of RNAP is often reliant upon induced epigenetic changes in the vicinity of TSSs, including acetylation of histones (Nightingale et al., 1998) [1.6.4.4.]. It was hypothesised that binding of RNAP to the *BCL3* TSS was reliant upon stimulus dependent acetylation of histones at this site. ChIP conducted using an anti-acetylated histone 3 (H3ac) antibody at the *BCL3* TSS (using primers as before) at the same time points as the RNAP ChIP showed a gradual increase in acetylated histone 3 levels up to 90 minutes (fig 4.3.B). Induced acetylation of histones is a phenomenon closely linked to remodelling of chromatin and the enhanced accessibility of RNAP and transcription factors to the DNA. The time taken for histones to become acetylated at this site is correlated with, and potentially causative of, the delayed RNAP binding observed (fig 4.3.B) and the appearance of *BCL3* transcripts (as previously shown in fig 3.2.A).

4.2.4. Transcription initiation at the *BCL3* promoter is induced by the NF-κB mediated acetylation of histones

To confirm a functional link between histone acetylation and *BCL3* transcription initiation, the effect of enhanced histone acetylation on early post-TNFα induction of *BCL3* transcript levels was investigated. Acetylated histone levels were globally enhanced within the cell's genome by pre-treatment of cells with Trichostatin A (TSA) – an inhibitor of histone deacetylase (HDAC) enzymes [1.4.]. Cells were pre-treated with 0, 200 and 400nM concentrations of TSA for 12 hours prior to stimulation with TNFα for 30 minutes and the fold induction of *BCL3* transcript levels measured by qRT-PCR [2.2.]. No effect on viability was seen in cells treated with TSA in such a way with any concentration of TSA used ($P>0.05$). In TSA untreated cells, no significant increases in *BCL3* transcript levels are seen at this post-TNFα treatment time point (see fig 4.3.C); however, pre-treatment of cells with 400nM TSA resulted in significant increases in *BCL3* transcript levels relative to non-TSA treated cells (fig 4.3.C). The greater responsiveness of cells to induced *BCL3* transcripts suggest that the time taken for increased acetylation of histones at the *BCL3* gene promoter as a result of TNFα stimulation (as shown in fig 4.3.B) causes the delayed RNAP binding at this site and consequent delayed transcript increases observed.

To investigate whether NF-κB was involved in acetylation at the *BCL3* gene TSS, ChIP was again used to determine the relative level of histone 3 acetylation at this site - using the same primer set (as in fig 4.3.A) – after 90 minutes of TNFα stimulation in cells with and without pre-treatment with the NF-κB inhibitor SN50 [3.2.2.]. A final concentration of 30ng/ml of SN50 was used, as previously determined [3.2.2.]. A significant decrease in histone 3 acetylation was observed in cells pre-treated with SN50, showing a role for NF-κB in mediating this change in histone status. The occurrence of NF-κB (or more specifically, p65) dependent acetylation has previously been demonstrated (Boekhoudt et al.,

2003) and occurs via recruitment of co-activator complexes possessing histone acetylating activity, for example CBP/p300 (Gerritsen et al., 1997).

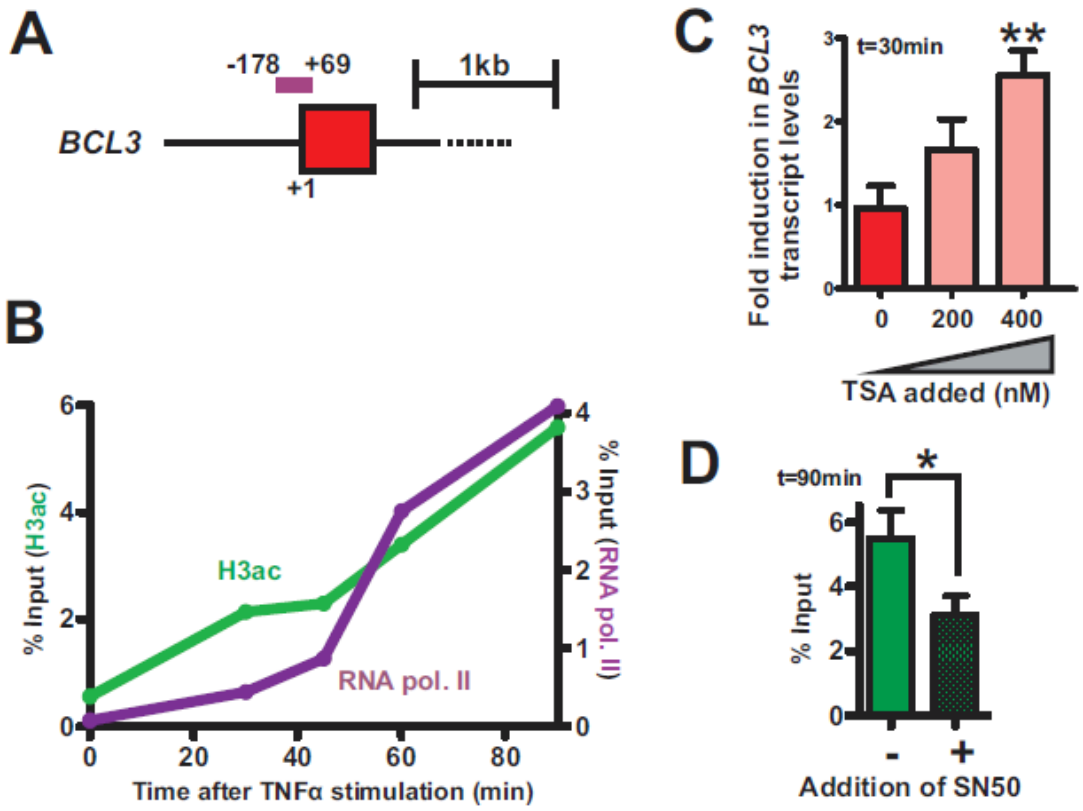

Figure 4.3. Binding of RNA polymerase II at the *BCL3* gene occurs in a delayed manner and correlates with the acetylation state of histone 3 at this site. (A) Location of sequence amplified by primers proximal to the *BCL3* gene TSS (+1) and used in (B) a ChIP assay performed on HT1080 cells stimulated with TNFα for varying lengths of time and with chromatin immunoprecipitated with anti-RNAP (#05-623; Millipore) and anti-acetylated histone 3 (#06-599; Millipore) antibodies. Precipitated DNA levels were measured by qPCR and expressed as a percentage of signal obtained from initial total Input chromatin. (C) Pre-treatment of HT1080 cells with 0, 200 and 400nM TSA prior to induction with TNFα for 30 minutes (n=3). Significance relates to comparison with induction levels of non-TSA treated cells. (D) Inhibition of NF-κB nuclear movement by pre-incubation with 30ng/ml peptide SN50 causes a significant decrease in histone 3 acetylation at the *BCL3* TSS after 90 minutes of TNFα stimulation. ChIP performed using anti-histone 3 acetylated antibody as before and primer as shown in A (n=3). In all ChIP experiments chromatin was also precipitated with a negative control anti-mouse IgG antibody (#12-371; Millipore) which did not exhibit %Input values above 0.25%. *P<0.05; **P<0.01. Error bars show standard deviation.

4.2.5. Differential binding timing of NF-κB sub-unit p65 at the *BCL3* and *TNFA* promoters

Induction of both *TNFA* and *BCL3* transcription by NF-κB/p65 has been previously shown to be predominantly reliant on promoter proximal κB sites (Yao et al., 1997; Brasier et al., 2001). Binding of

p65 at such TSS proximal locations was assayed by ChIP over several post TNFα treatment time points.

Primers were used which either amplified the gene's proximal κB site (*BCL3*) or nearby sequence which was close enough such that DNA fragments produced by sonication would include both the amplified sequence and the κB site (*TNFA*) (fig 4.4.A). Chromatin precipitated by anti-p65 antibodies was analysed with these primers using qPCR to compare relative levels of binding of p65 at the two promoter sites at times following TNFα stimulation. Binding levels initially increased at a greater rate at the *TNFA* gene and were significantly higher than at the *BCL3* site after 30 and 45 minutes of TNFα stimulation (fig 4.4.B). Binding at the *BCL3* gene occurs in a more delayed fashion, with binding levels between the two genes narrowing over time and are indistinguishable by 60 minutes (fig 4.4.B). Again, the dynamics of p65 at the two gene's promoters is qualitatively similar to the relative appearance of transcripts in response to TNFα.

Delays in binding at the *BCL3* gene cannot be attributed to a lack of p65 presence in the nucleus as the rate at which the protein binds at the *TNFA* gene occurs at a higher rate in earlier time intervals and nuclear localisation of p65 in response to TNFα treatment has previously been shown to be rapid [3.2.4.1.2.]. Delayed binding of p65, and previously demonstrated RNAP [4.2.4.], suggest chromatin remodelling may be required for DNA access of factors at the *BCL3* promoter – a mechanism which would account for the differential response of *TNFA* and *BCL3* genes to same NF-κB stimulation. The acetylation of histones – previously shown to be linked to transcription initiation at the *BCL3* promoter (fig 4.3.) – is closely linked to the remodelling of chromatin either via counteracting electrostatic interactions between DNA and histones or by recruiting remodelling enzymes via bromodomains [1.5.4.].

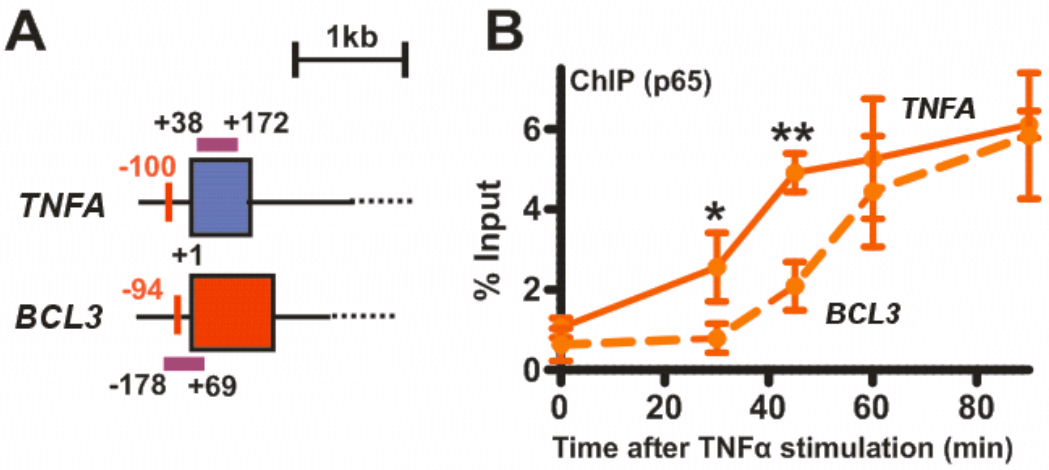

Figure 4.4. The binding of p65 occurs at a delayed rate at a proximal region to the *BCL3* gene TSS relative to the *TNFA* gene TSS proximal region. (A) Location of primer amplified sequences proximal to the TSSs of *TNFA* and *BCL3* genes used to detect this sequence in pools of DNA precipitated by anti-p65 antibodies (#3034; Cell Signalling Technology) in a ChIP assay. Vertical red lines and red text denote position of proximal κB site at each gene. (B) Time course of p65 binding at TSSs of the *TNFA* and *BCL3* genes in HT1080 cell populations stimulated with TNFα for varying lengths of time as measured by ChIP and qPCR, with values expressed as a percentage of signal obtained from total initial Input chromatin samples. Chromatin was also precipitated with a negative control anti-mouse IgG antibody (#12-371; Millipore) which did not exhibit %Input values above 0.15%. (n=3). Significance relates to comparisons of the binding level at each gene per time point. *P<0.05; **P<0.01. Error bars show standard deviation.

4.2.6. Assaying chromatin accessibility at a proximal κB site in the *BCL3* promoter

4.2.6.1. XcmI chromatin accessibility assay design and optimisation

Previous work outlined in this chapter led to the hypothesis that delayed binding of p65 and RNAP at sites proximal to the *BCL3* gene TSS occurs as a result of the need for chromatin remodelling to make DNA accessible for binding by non-nucleosome factors. The accessibility of chromatin in extracted nuclei to DNA binding proteins can be assayed by the relative access of restriction enzymes to DNA and resultant cutting. The *BCL3* proximal κB site occurs within an XcmI restriction endonuclease cutting site (see fig 4.5.A) allowing a direct assay of the DNA binding by the enzyme at this site. The XcmI sites proximity to the TSS (-94) will also give an indication as the accessibility of RNAP to binding at the TSS, although highly localised differences in chromatin state cannot be definitively excluded. The relative amount of binding, and consequent cutting, of XcmI at this site in native chromatin was assayed by PCR using primers which amplified across this site (purple bar in fig 4.5.A). Greater XcmI cleavage at this site would reduce template DNA available for the PCR; a reduction in PCR output will therefore occur proportional to the accessibility of chromatin to DNA binding at this site.

To determine an appropriate quantity of genomic DNA template to be used per reaction, PCRs were conducted using the XcmI site primer set (as in fig 4.5.A) and a varied quantities of extracted genomic DNA (from 100 to 0.01 ng per reaction) [2.8.3.2.]. Reactions were run for 25 PCR cycles and 10µl of each reaction resolved by gel electrophoresis (fig 4.5.B). No difference in band intensity is observed when between 5 and 100ng of genomic DNA were used per reaction – the reaction is saturated with template – however decreases below 5ng showed a linear decrease in band intensity (fig 4.5.B). The quantity of 5ng of genomic DNA was therefore chosen as most appropriate for this assay – as it gives a highly visible PCR product output in uncut genomic DNA but at a level of template DNA at which the PCR is sensitive to deceases in template quantity below this amount (as would assumed to occur if genomic DNA is cut with XcmI).

A further step in the protocol optimised was the quantity of XcmI enzymes added to extracted nuclei. Nuclei were extracted from untreated HT1080 cells [2.1.1.2.] and treated with 10, 5, 2.5 and 0.5 Units of XcmI enzyme for 30 minutes at 37℃ [2.10.1.]. T he reaction was subsequently stopped, genomic DNA extracted [2.10.2.] and 5ng used in a PCR (as before), of which 10µl was resolved by gel electrophoresis (fig 4.5.C). The highest quantity of XcmI enzyme which left enough template DNA to remain for a visual PCR reaction output was 2.5U. This value was therefore selected for use in the assay – which aimed to detect relative decreases in template DNA concentration, from such a reference untreated population of cells, as a result of TNFα treatment.

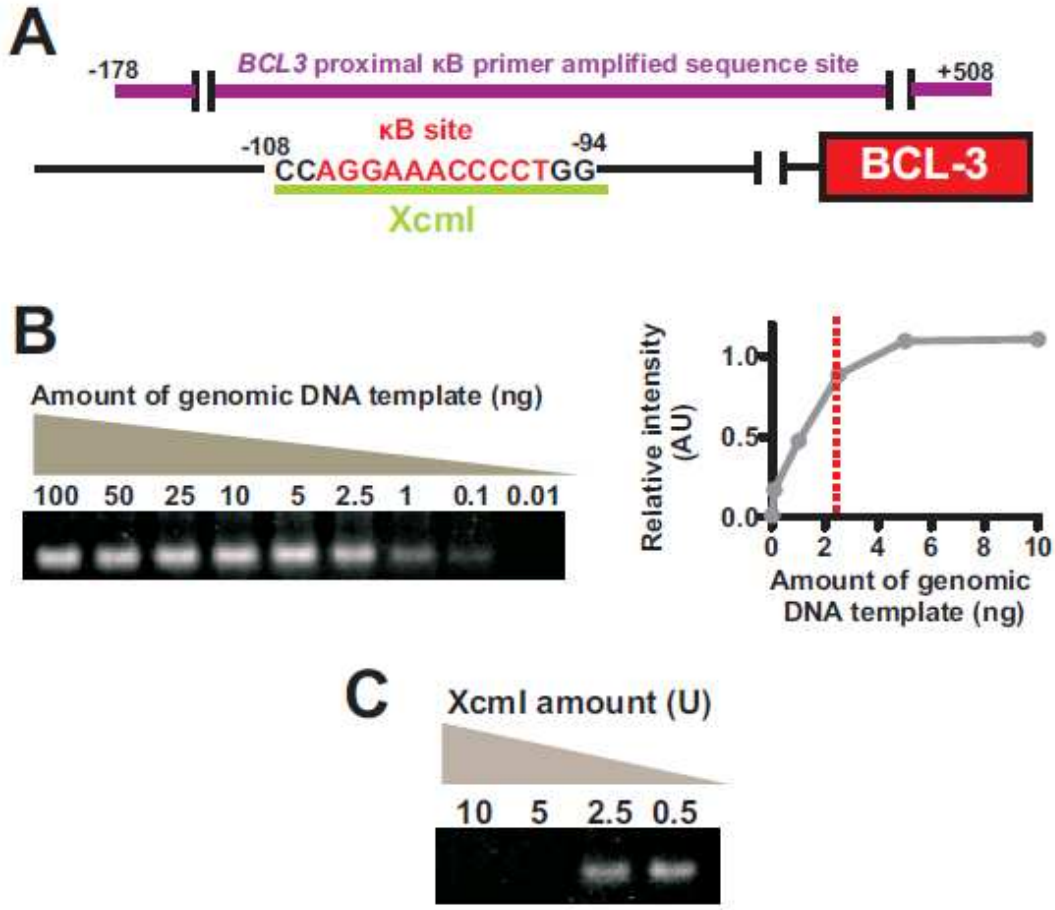

Figure 4.5. Design and optimisation of an assay to detect changes in chromatin accessibility at a proximal κB site in the *BCL3* gene promoter utilising an XcmI cleavage site at the same location. (A) Location of sequence amplified by primers (purple bar) either side of a proximal κB site (-108 to -94) in the *BCL3* gene promoter. Sequence of the κB site is shown as well as its location within an XcmI enzyme cutting site (green bar). (B) Gel electrophoresis resolved PCR outputs produced using primers shown in 4.5.A on varying quantities of extracted genomic DNA used per PCR reaction and densitometry of these bands produced with DNA template quantities below 10ng. (C) PCR outputs, as in 4.5.B, produced from nuclei extracted from untreated HT1080 cell populations and treated with varying amounts of XcmI enzymes for 30 minutes at 37℃; with 5ng subsequently extracted genomic DNA used per PCR reaction [2.8.3.]. 10µl of a 20µl PCR were run in each gel lane. PCR performed with 25 cycles, with a 58℃ annealing temperature used.

4.2.6.2. TNFα treatment of HT1080 cells induces chromatin remodelling at a proximal κB site in the *BCL3* gene promoter

HT1080 cell populations treated with and without 90 minutes of TNFα were compared using the chromatin assay outlined in [2.10.] and [4.2.6.1.]. Exposure to TNFα clearly caused a decrease in PCR product output (fig 4.6.A – compare lanes 1 and 2) – consistent with increased digestion of genomic DNA at this site resulting from enhanced chromatin accessibility. In addition to using spectroscopic methods to ensure that equal amounts of template genomic DNA were used per PCR, a positive

control *CYPA* primer pair was also used (which had previously been confirmed to amplify sequence lacking an XcmI cleavage site).

To determine the influence of histone acetylation on chromatin accessibility, cells were also treated with and without 400nM of TSA for 12 hours (with no TNFα addition) and assayed in the same manner (fig 4.6.A; compare lanes 1 and 3). Cell treated with TSA (therefore possessing enhanced acetylated histone levels) showed a slight but consistent and significant decrease in band intensity as measured by densitometry on independent triple replications of the experiment – with bands produced from TSA treated cells being 54.01±13.90% (mean±SD; n=3) of the intensity of bands produced from TSA untreated cell populations ($P<0.05$). This link between histone acetylation states and chromatin accessibility to DNA binding proteins is consistent with the hypothesis that TNFα acts to increase chromatin accessibility, and consequently transcription of the *BCL3* gene, by inducing acetylation of histones situated proximal to the *BCL3* gene's TSS.

To determine the rate at which chromatin remodelling occurs in response to TNFα treatment, chromatin was assayed in the same manner from cells stimulated with TNFα for 0, 30, 45, 60 and 90 minutes. The relative quantity of intact genomic DNA template following XcmI treatment was assayed using qPCR to determine the fold change in viable genomic DNA template in comparison with TNFα unstimulated cells (i.e. t=0). Plotting this data as a time course (fig 4.6.B) shows a decrease in intact κB/XcmI site sequence over an increasing length of TNFα exposure, after an initial delay of 30 minutes. To plot the data as an increase in chromatin accessibility to DNA binding at this site (which is considered proportional to decreased PCR output), the absolute difference between basal qPCR at t=0 and at subsequent time points was plotted. Output points fitted with a line of best fit again show chromatin accessibility increasing over time following an initial delay.

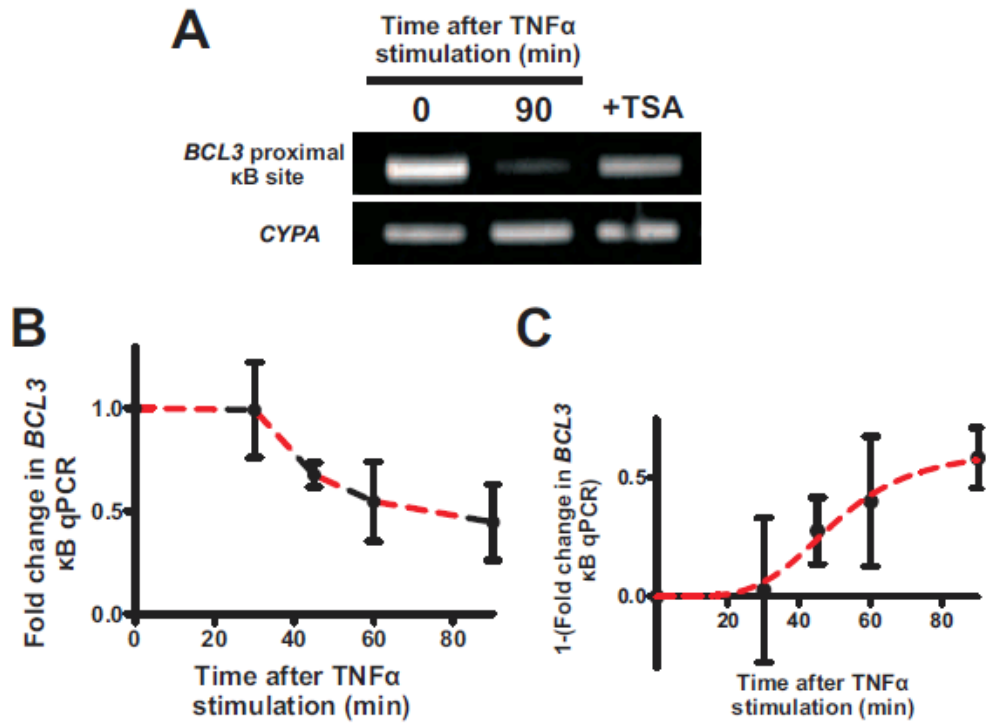

Figure 4.6. A proximal κB site in the *BCL3* gene promoter exhibits TNFα induced increases in accessibility to the XcmI restriction endonuclease. (A) Incubation of cells with TNFα and TSA increases the accessibility of the proximal κB site in the *BCL3* gene promoter to XcmI digestion as assayed by consequent decreases in PCR output amplifying from sequence across this region. Bands shown are PCR products produced after 25 cycle reactions with 58℃ annealing temperature and 5ng genomic DNA used per reaction, with 10µl from a 20µl reaction run per lane. Primers amplifying from the *CYPA* gene act as a positive control. (B) Fold change in signal produced from genomic DNA extracted from HT1080 cell populations treated with TNFα for varying lengths of time as measured in comparison to signal from unstimulated cells (t=0) using qPCR and primers as shown in fig 4.5.A. (n=3) (C) Same data as in 4.6.B but changes in signal expressed as an absolute difference from values obtained at t=0 to show increases in chromatin accessibility as a result of TNFα treatment. Red dashed line denotes a fitted Hill equation (K_d=49.81; h=4.35; R^2=0.638). Error bars show standard deviation.

Increased chromatin accessibility at this XcmI site has direct implications for NF-κB binding – the κB site falls within the XcmI cleavage site – however implications for RNAP binding are less clear, particularly as no obvious binding site for RNAP is the *BCL3* promoter exists (a TATA box, for example). Nucleosome remodelling can occur either at a very localised level with <50bp changes in DNA accessibility resulting from partial unwinding of DNA wound around a nucleosomes core (Métivier et al., 2003) or through total dissociation of nucleosome-DNA binding which makes a far larger amount of sequence accessible (Boeger et al., 2003). From this work, focused on a single DNA sequence site, wider assertions made about the binding accessibility of surrounding sequence must be made with

caution. However, ChIP work in this chapter shows RNAP does bind proximal to the *BCL3* TSS in a delayed manner similar to p65 following TNFα stimulation (compare fig 4.3.A and 4.4.B) and the proximity of the XcmI cleavage site (-108 to -94) to the TSS (+1) suggests that chromatin remodelling in this area, even if very localised, will influence RNAP binding. Alternatively, the RNAP binding site may be constitutively accessible but delayed binding of p65 at the proximal site is required to mediate RNAP binding.

4.3. Discussion

4.3.1. TNFα induced transcription of the *BCL3* gene occurs via a sequence of events culminating in chromatin remodelling

Work in this chapter has confirmed a delayed transcriptional induction of the *BCL3* gene, relative to the *TNFA* gene, following stimulation of HT1080 cells with TNFα [4.2.1.]. Furthermore, this work has outlined mechanisms to explain this difference: while the *TNFA* gene possesses a constitutive, pre-stimulation bound RNAP poised to rapidly initiate transcription; the *BCL3* gene requires stimulus dependent RNAP binding [4.2.2.]. Furthermore, delayed binding of p65 at a TSS proximal site in the *BCL3* gene promoter [4.2.4.][4.2.5.] has been shown to be closely linked to, and likely dependent on, chromatin remodelling at a proximal κB site previously shown to mediate NF-κB mediated up-regulation of *BCL3* transcription [4.2.6.]. The proximity of this site to the gene's TSS also suggests chromatin remodelling may also be required for RNAP binding. Levels of acetylation of histone 3 at this *BCL3* TSS site have also been shown to be induced by TNFα in an NF-κB dependent manner [4.2.4.][4.2.6.]. Histone acetylation at this site has also been shown to cause chromatin remodelling [4.2.6.].

The chain of events leading to *BCL3* transcription following TNFα stimulation of HT1080 cells is summarised in fig 4.7. Work in this chapter has addressed the previously identified NF-κB→*BCL3* mRNA relationship outlined in Chapter 3 in greater detail to include underlying mechanism within the interaction.

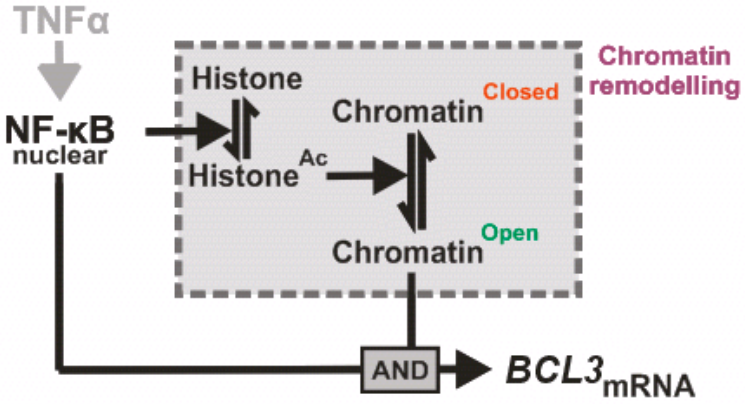

Figure 4.7. Schematic view of events constituting the induction of *BCL3* transcription following HT1080 cell stimulation with TNFα. Two parallel NF-κB mediated pathways are shown as necessary for *BCL3* transcription: NF-κB mediated histone acetylation and subsequent chromatin remodelling which in turn allows further NF-κB and RNAP binding.

4.3.2. A dual role for NF-κB in inducing *BCL3* transcription

An apparent contradiction is raised by this work regarding the role of NF-κB in inducing *BCL3* transcription: while NF-κB has been shown to be required for histone acetylation, histone acetylation is also required for the chromatin remodelling necessary to create a permissive environment for NF-κB binding.

One potential explanation for this apparent paradox is that the NF-κB binding, as determined by ChIP [4.2.5.], and chromatin accessibility were both measured at a proximal (-94) κB site in the *BCL3* promoter. While this proximal κB site has previously been identified as sufficient for NF-κB mediated induction of *BCL3* transcription, other κB sites also exist – at a more distal site in the gene's promoter (-861) and also within intronic sequence (Brasier et al., 2001; Ge et al., 2003). It is possible that NF-κB can bind at one or more of these sites and induce histone acetylation which subsequently allows binding at the more proximal κB site. It is notable that studies identifying the sufficiency of this proximal κB site in NF-κB induced *BCL3* transcription were conducted using sequence introduced in a plasmid vector. Such exogenous sequence may not have adopted the same chromatin status as the native *BCL3* promoter sequence – potentially allowing a constitutively accessible state and obscuring the importance of other κB sites with chromatin remodelling roles required for *BCL3* transcription. Unfortunately, suitable primers for amplification of proximal sequence to these additional κB sites could not be designed (primers designed either amplified non-specifically or not at all), consequently ChIP could not be used to investigate p65 binding at these sites. Furthermore, the possibility of long-range interactions from even more distal, and potentially undiscovered, κB sites means that even if binding

was not observed at κB sites in the immediate vicinity of the *BCL3* gene, histone acetylation activity could still be provided by NF-κB binding at more distal κB sites.

A further possibility also exists: that NF-κB is autonomously responsible for re-modelling its own binding site. Such a scenario has been shown for a proximal binding site for the nuclear factor 1 (NF1) transcription factor in GR mediated induction of the mouse mammary tumour virus (MMTV) promoter (Hebbar and Archer, 2003). Here, NF1 binding site at the proximal site had previously been shown to require GR mediated chromatin remodelling for measurable binding; however, mutagenesis of the NF1 binding site prevented this chromatin remodelling occurring in response to GR signalling (mutagenesis of the NF1 binding site has no effect on the well characterised positioning of nucleosomes in this region). The authors went on to confirm NF1 dependent recruitment of chromatin remodelling component BRG1 to the promoter and concluded that NF1 was a vital component in the GR-mediated chromatin remodelling of a region of the MMTV promoter which contained its own binding site (Hebbar and Archer, 2003).

Explanations for such behaviour rely on binding of NF1 at this supposed inaccessible site, potentially at a level too low to be detected by experimental techniques. Binding of transcription factors to nucleosome associated DNA is permitted at low levels, reliant on factors such as rotational positioning of the binding site and nucleosome breathing allowing transient periods of accessible DNA [1.5.]. Such hypothesises lead to changes in thinking in chromatin accessibility; relying on probabilities of a factor binding rather than absolute can or cannot bind certainties. Lower accessibilities of binding sites could in theory be compensated for by increased levels of the binding factors; particularly if low level binding can effect a change in local chromatin structure which makes the site subsequently more accessible to further biding – as, for example, NF1 has been shown to do by recruiting chromatin remodelling complexes. Such work raises the possibility that NF-κB may be able to bind at the proximal site in the *BCL3* promoter, despite an apparent non-permissive chromatin state, and cause remodelling which enhances subsequent binding to levels detectable by ChIP.

4.3.3. Chromatin states as a determinant of the response rate of NF-κB responsive genes

Work in this chapter has emphasised the effect that chromatin states can have on the timing of transcriptional responses. Chromatin in the region of the *BCL3* gene TSS has been shown to require remodelling for binding; and, while a constitutively permissive chromatin state has not directly been shown at the *TNFA* gene, the pre-stimulus binding of RNAP at the gene's TSS [4.2.2.] suggests this is the case. Such differential chromatin state between TSS adjacent regions of *TNFA* and *BCL3* gene promoters is proposed to account for the different relative binding timings of p65 at the two genes – rapidly in the case of *TNFA* and in a significantly delayed manner at the *BCL3* gene [4.2.5.].

Such differential NF-κB binding has previously been described for diverse NF-κB responsive genes, with NF-κB binding described as occurring in temporal 'waves' dependent on the accessibility of promoter sites (Saccani et al., 2001; Ramirez-Carrozzi et al., 2006). However, such work offers no suggestions as to the functionality of the differential response timings. Having observed and characterised the delayed binding of NF-κB at the *BCL3* gene, a developed aim of this study was to investigate any functionality of this delayed binding with respect to BCL-3's inhibition of *TNFA* gene transcription.

As stated in Chapter 3, the interactions of these genes and their products forms an incoherent feed forward loop (I-FFL) – a motif which has been previously studied with a focus on the occurrence and sensitivities of interactions but without consideration of interaction timings [3.3.2.]. The identified difference in *TNFA* and *BCL3* genes responses to NF-κB offers an opportunity to study the effects of differential induction on the two legs of the I-FFL motif. Measurement of not just the output of the motif (*TNFA*/*BCL3* transcript outputs) but also the characterisation of processes and mechanisms involved in their production (histone acetylation, chromatin accessibility) allows the construction of a mathematical model. Such a model created to faithfully recreate observed behaviour can be used to investigate potential functions of delayed BCL-3 production with regard to its effect on *TNFA* production dynamics. Chapter 5 concerns the production of such a model; using data accumulated in Chapters 3 and 4 plus additional experimental measurements as required.

Chapter 5

Modelling the temporal effects of BCL-3 on *TNFA* gene transcription

5.1. Introduction

Work in previous chapters has outlined the interactions and events constituting NF-κB mediated induction of *TNFA* and *BCL3* gene expression in HT1080 cells and the subsequent inhibition of *TNFA* transcription by BCL-3 – as outlined in figure 5.1. In this chapter, an ODE (ordinary differential equation) mathematical model is developed, using parameters and equations to describe the rates of these interactions and recreate experimentally observed changes in *TNFA* and *BCL3* transcript levels. The measurements or logic used to create such equations is outlined in the Results section [5.2.] along with subsequent experiments conducted to both verify the model and test model generated hypothesises concerning the functionality of delayed *BCL3* transcription induction in regulating *TNFA* transcription.

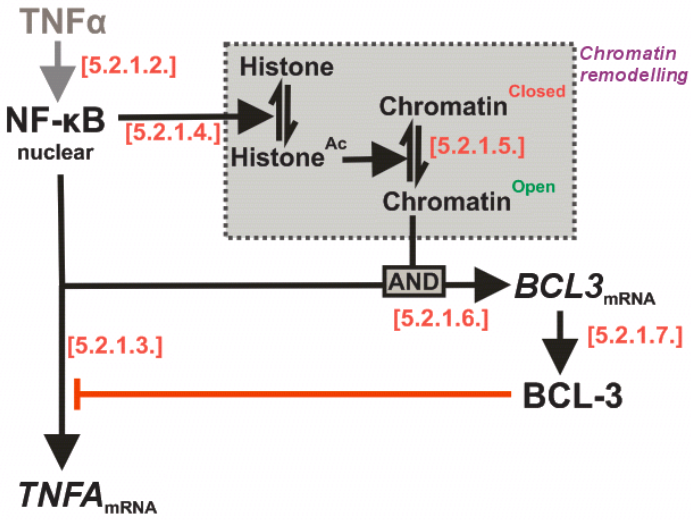

Figure 5.1. Overview of NF-κB mediated induction of both *TNFA* and *BCL3* gene expression and subsequent inhibition of *TNFA* transcription by BCL-3. Individual steps described by equations in the Results section [5.2.2.] are shown as red text: [5.2.1.2.] TNFα induced nuclear localisation of NF-

κB; [5.2.1.3.] NF-κB induction of *TNFA* transcription; [5.2.1.4.] NF-κB mediated acetylation of histones at the *BCL3* promoter; [5.2.1.5.] Acetylated histone dependent changes in the chromatin state at the *BCL3* promoter; [5.2.1.6.] Induction of *BCL3* transcription and [5.2.1.7.] translation of the *BCL3* transcript.

5.2. Results

Modelling of the mutual induction of *TNFA* and *BCL3* transcription, incorporating chromatin remodelling at the *BCL3* gene promoter, was performed using ODE modelling following the scheme outlined in figure 5.1. The equations and parameters used are outlined below. The MATLAB code comprising this model is provided in Appendix 8 (A.8.1.).

5.2.1. Equations

5.2.1.1. Volume of a fibroblast cell

The average volume of human fibroblast was considered to be 2,000 μm^3 with a 5:1 volume ratio of cytoplasm:nucleus (Lipniacki et al., 2004). Consequently, cytoplasmic and nuclear volumes used were 1,667 and 333 μm^3 respectively.

5.2.1.2. Nuclear translocation of NF-κB

The induced nuclear localisation of NF-κB following TNFα stimulation had previously been measured using single cell fluorescence microscopy of cells expressing p65-dsRed [3.2.4.1.2.]. Data from the 15 cells analysed was averaged; with the average nuclear/total cell fluorescence at t=0 taken as basal level (i.e. equal to 0) and increases above this value expressed as a fraction of the largest average increase seen for all cells (fig 5.2.). A Two Phase exponential association curve was fitted to the data (R^2=0.9857) and used to define an equation which plots levels of nuclear p65 as a function of time. Maximal nuclear NF-κB concentration is assumed to be 260nM, as in (Ashall et al., 2009).

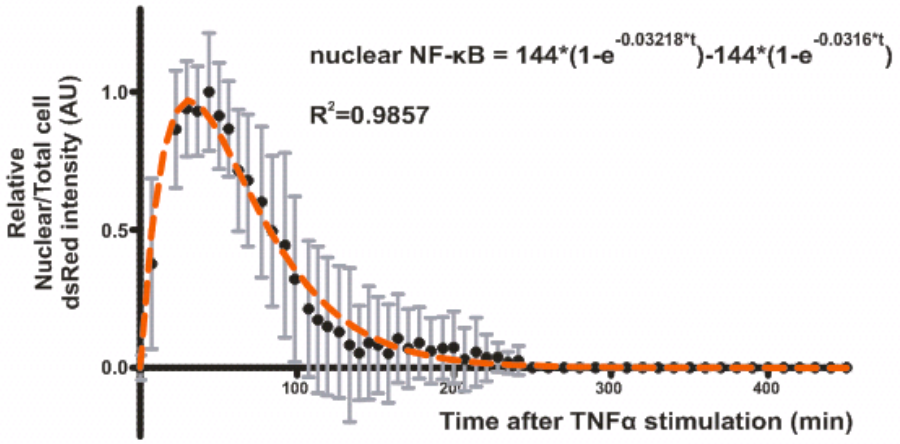

Figure 5.2. Population levels of induced nuclear p65-dsRed localisation in HT1080 cells. Relative increase above basal levels (at t=0) of the nuclear levels of p65-dsRed in 15 HT1080 cells stimulated with TNFα (as in fig 3.5.D/[3.2.4.1.2.]), with increases expressed as a fraction of maximal fluorescence level increase (1.0). A Two Phase exponential association line is fitted to the data with an equation shown which expresses nuclear p65 as a function of time. Error bars relate to standard deviation.

In the produced model, nuclear NF-κB levels over time is input using this derived equation – with time the only variable determining NF-κB levels. The omission of other variables which will be likely to determine nuclear NF-κB levels – such as activated TNFα receptors, IKK etc – reflects a lack of data on such components in HT1080 cells. Given the difference in oscillatory NF-κB behaviour observed between HT1080 cells (this study – [3.2.4.1.2.]) and SK-N-AS cells previously used to construct models (Nelson et al., 2004), use of the same code was not considered appropriate.

Equation: Nuclear NF-κB levels

```
nNFκB=260*(144*(1-exp(-0.03218*t))-144*(1-exp(-0.03160*t)));
      t = time
      nNFκB = Concentration of nuclear NF-κB
```

5.2.1.3. NF-κB induction of *TNFA* mRNA

Changes in transcript levels were expressed as ODE equations with production rate taken as the maximal possible rate of transcript production from the gene's promoter (amount of mRNA produced per minute) multiplied by the percentage activity of the promoter - which has been shown to be dependent on the concentration of NF-κB in the nucleus [3.2.2.]. Degradation rate constants were measured from the transcript's half life.

Two independent κB sites have been shown to influence *TNFA* transcription – a proximal site which binds NF-κB [4.2.5.] and a distal site binding BCL-3 [3.2.7.3.]. The occurrence of transcription is dependent on the probability of NF-κB being bound at the proximal site and BCL-3 not being bound at the distal site; i.e. P(*TNFA* transcription)=P(NF-κB bound at proximal κB site)*(1-P(BCL-3 bound at distal κB site)). Probabilities of binding are dependent on concentrations of the binding factors and dissociation constants for DNA binding. BCL-3 binding has been assumed to occur independently, i.e. without p50 or p52 homodimers - which are not considered in this model.

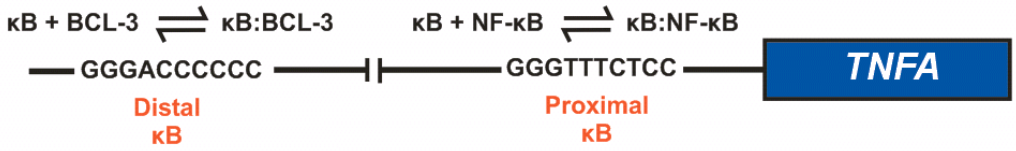

Figure 5.3. Schematic diagram of the binding reactions of NF-κB and BCL-3 to proximal and distal κB sites respectively in the *TNFA* gene promoter.

Equation : Rate of change in *TNFA* mRNA levels

dydt(1) = d[*TNFA*mRNA]/dt

```
dydt(1)=k101*((nNFκB./(nNFκB+k102))*(1-(BCL3./(BCL3+k103))))-TNFmRNA*k104;
      nNFκB = Concentration of nuclear NF-κB
      BCL-3 = Concentration of nuclear BCL-3
      TNFmRNA = Concentration of TNFA mRNA
```

Table 5.1. Parameter values for an ODE representing NF-κB induction and BCL-3 inhibition of transcription at the *TNFA* gene.

Parameter name	Description	Value	Rationale
k101	Maximal rate of *TNFA* transcription (mRNA molecules produced per minute)	6.6 x10^{-2} μM.min^{-1}	Calculated*
k102	K_D value for NF-κB binding at a proximal κB site in the *TNFA* promoter	69nM	Calculated**
k103	K_D value for BCL-3 binding at a distal κB site in the *TNFA* promoter	53nM	Calculated**
k104	Degradation rate for *TNFA* mRNA	3.45 x10^{-2} min^{-1}	Measured***

* The maximum rate of RNAP initiation is assumed to be 33 min^{-1} - based on transcription speed of 55nt/s and minimal spacing between transcribing polymerases of 100nt (Cheong et al., 2006) or 66 min^{-1} when both copies of a gene are considered. Transcripts are transported to the cytoplasm (assumed to be instantaneous in relation to the timescale of other processes in this model) where 66 mRNA molecules produced per minute corresponds to 6.6 x10^{-2} nM.s^{-1} (assuming a cytoplasmic volume of 1.67x10^{-12} l – [5.2.1.1.]).

** The binding of transcription factors such as NF-κB to DNA is dependent on not only the DNA sequence bound but also physiological factors, such as NaCl concentration (Phelps et al., 2000). NaCl concentrations within nuclei in experiments are considered to be ~100mM based on similar concentrations in cell culture media. The dissociation constant for p50/p65 binding at a proximal κB site in the *TNFA* promoter is consequently considered to be 69nM (Phelps et al., 2000). The distal κB site within the *TNFA* promoter is, in contrast to the proximal site, a strong palindrome (GGGACCCCCC) – a feature strongly associated with enhanced p50 homodimer (and therefore BCL-3) binding [1.2.6.1.]. Relative values for the affinity of classic NF-κB dimers (p50/p65) and BCL-3/p50 homodimer affinity for κB sites are taken from (Fujita et al., 1992). Here an endogenous IFN-β κB site (GGGxxxxTCC) and palindrome induced mutant version (GGGxxxxCCC) are compared for affinity to p50/p65 heterodimers and p50 homodimers. Relative affinities for the two dimer combinations for the two κB site types from this paper were used to calculate the relative dissociation constant values for BCL-3 (assumed with p50 homodimer) binding a palindromic κB site (such as the distal *TNFA* promoter κB site) and a classic NF-κB dimer binding at a non-palindromic κB site (such as the proximal *TNFA* promoter κB site). This ratio was calculated to be 1:1.3 (values measured in molarity); consequently, k103 is valued at 53nm.

*** From an experimentally determined half life at 20 minutes. HT1080 cells were stimulated with TNFα for 90 minutes followed by inhibition of further transcription by addition of inhibitor actinomycin D [2.1.4.], with qRT-PCR used to detect decreases in the mRNA level of *TNFA* and *BCL3* transcripts at increasing times following transcription inhibition (at t=0) [2.2.]. One phase decay equations were fitted to the data and used to calculate each transcript's half live and subsequently constant of degradation.

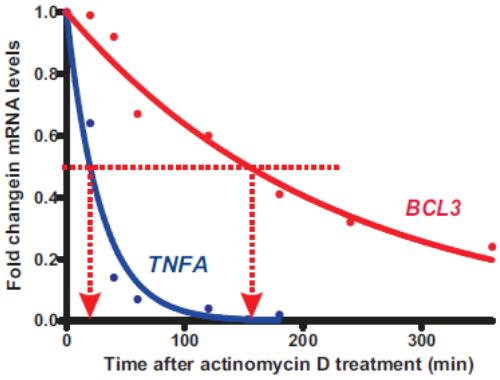

Figure 5.4. Calculation of the half life of *TNFA* and *BCL3* transcripts. HT1080 cells were induced with TNFα for 90 minutes then treated with actinomycin D and decreases in transcript level (relative to levels when actinomycin D was added at t=0) measured by qRT-PCR. One phase decay equation lines are fitted (*TNFA* R^2 = 0.9570; *BCL3* R^2=0.9609).

5.2.1.4. NF-κB induced histone 3 acetylation at the *BCL3* promoter

Acetylation of histone 3 at the *BCL3* promoter has been shown to occur in an NF-κB dependent manner [4.2.4.], therefore acetylation of histones at the *BCL3* promoter was expressed as a function of nuclear NF-κB levels. The rate of histone deacetylation was assumed to be a constant value.

Equation: Rate of change in histone 3 acetylation state

dydt(2) = d[Histone^{acetylated}]/dt

```
dydt(2)=k105*(nNFκB^2./(nNFκB^2+k106^2))-k107*HisAc;
      nNFκB = Concentration of nuclear NF-κB
      HisAc =Concentration of acetylated histone 3 at the BCL3 promoter
```

Table 5.2. Parameter values for an ODE representing changes in histone acetylation at the *BCL3* promoter

Parameter name	Description	Value	Rationale
k105	Rate of histone 3 acetylation	0.00055 min^{-1}	Fitted*
k106	Value of nNFκB at which half max acetylation rate is induced	260nM	Fitted*
k107	Rate of histone 3 deacetylation	0.00055 min^{-1}	Fitted*

* The concentration of nuclear NF-κB at which half maximum acetylation rate is reached, the rates of acetylation and deacetylation plus the Hill coefficient determining the rate of acetylation increase with respect to NF-κB concentration are fitted to the experimentally observed rate of histone 3 acetylation observed (fig 4.3.). Values are used to recreate the relative timing and rate of acetylation increase. With regard to the magnitude of response, total concentration of histone acetylated is assumed to be less than or equal to the maximum concentration of histone 3 in the cell. This value is assumed to be ~$2x10^{-2}$nM - based on four histone 3 molecules (two H3 per nucleosome remodeled in the *BCL3* promoter, with two gene copies) in a nuclear volume of $3.33x10^{-13}$ liters. This, admittedly, greatly simplifies the potentially complex profile of histone acetylation - with potential multiple acetylated sites - however due to a lack of resolution in this work regarding specific acetylated sites, histones are considered as either acetylated or not.

5.2.1.5. Induced chromatin accessibility at the *BCL3* promoter

'Chromatin accessibility' refers to the relative ability of transcription factors (NF-κB in this case) or RNAP to bind DNA. In this model, chromatin state is exclusively determined by the level of histone acetylation 3 (HisAc) – based on the close observed relationship between the rate of histone 3

acetylation level increase and chromatin accessibility state [4.2.6.2.]. The increase in chromatin accessibility is considered to be directly causative of the binding of NF-κB and RNAP.

Equation : Rate of change in chromatin accessibility at the *BCL3* gene promoter

dydt(3) = d[accessible chromatin]/dt

```
dydt(3)=k108*(HisAc^3./(HisAc^3+k109^3))-Chr*k110;
      HisAc =Concentration of acetylated histone 3 at the BCL3 promoter
      Chr = Concentration of accessible chromatin at the BCL3 promoter
```

Table 5.3. Parameter values for an ODE representing changes in chromatin accessibility at the *BCL3* promoter

Parameter name	Description	Value	Rationale
k108	Rate of chromatin opening	$0.4min^{-1}$	Fitted*
k109	Value of HisAc at which half max rate of chromatin opening is induced	0.08nM	Fitted*
k110	Rate of chromatin re-condensation	$0.4min^{-1}$	Fitted*

* Values fitted to obtain observed changes in chromatin accessibility at a promoter proximal site in the *BCL3* gene following TNFα treatment – as shown in figure 4.6.C. Values were used such that the magnitude of remodeled chromatin concentration response did not exceed ~$1x10^{-2}$nM (based on two chromatin molecules – two copies of gene per cell – in a nuclear volume of $3.33x10^{-13}$ liters).

5.2.1.6. NF-κB/chromatin remodelling induced *BCL3* mRNA levels

The equation form for *BCL3* transcript levels is as for *TNFA* transcripts [5.2.1.3.].

5.2.1.6.1. BCL-3 inhibits *BCL3* transcript levels in HT1080 cells

BCL-3 has a previously identified auto inhibitory effect on transcription of its own gene through binding at κB sites in the gene's promoter or second intron (Brocke-Heidrich et al., 2006). To confirm this activity in HT1080 cells, expression of endogenous *BCL3* transcripts was observed in cells which over express *BCL3* under the control of the CMV promoter introduced in a plasmid vector [2.3.1.] (as previously described in [3.2.6.]). Endogenous and plasmid derived *BCL3* transcripts were distinguished using primers which amplified from *BCL3* gene coding sequence (detecting transcripts from both origins) and a further primer set amplifying from 3'UTR sequence – which was not included in the *BCL3* plasmid sequence (start codon to stop codon cDNA sequence) (Brasier et al., 2001) (fig 5.5.A). Specificity was confirmed by using each primer set to amplify from plasmid and cDNA templates; with the coding sequence primer set amplifying from both templates but the 3'UTR primer set failing to amplify from plasmid DNA (fig 5.5.B). PCRs were conducted on cDNA extracted from

HT1080 cells transfected with the CMV overexpressing *BCL3* plasmid [3.2.6.] and also untransfected cells. Coding sequence *BCL3* primers amplified from both cell population cDNA; however, the 3'UTR primer set failed to amplify from cells containing the *BCL3* overexpression plasmid (fig 5.5.C). This occurred despite observed increases in the amount of total *BCL3* transcript as amplified by the coding sequence primer set – which rules out decreased expression due to gene silencing resulting from overexpression of the *BCL3* transcript. Therefore, a negative interaction between BCL-3 protein and *BCL3* gene transcription has been confirmed in HT1080 cells (fig 5.5.D) and has been incorporated into the model coding (Appendix 8; A.8.1.).

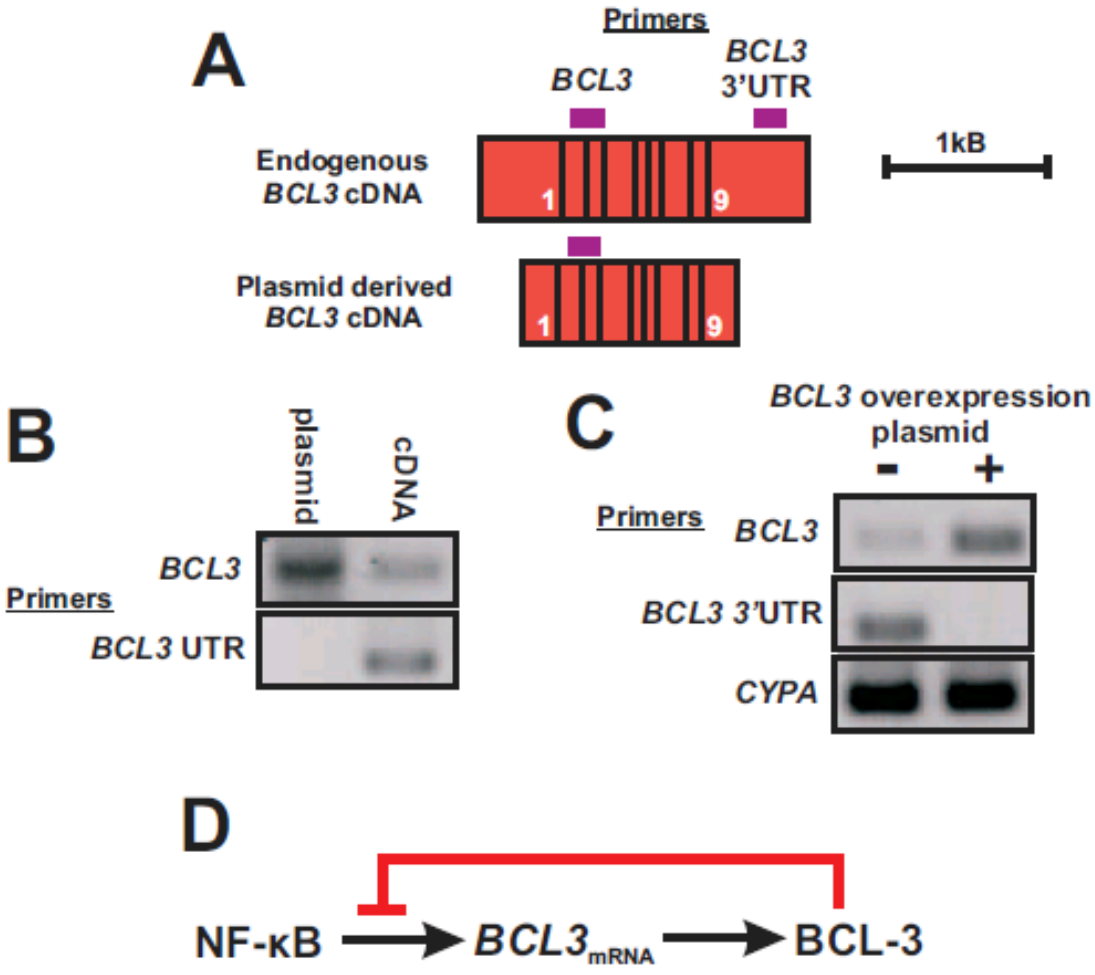

Figure 5.5. BCL-3 negatively regulates transcription of its own gene. (A) Location of primers amplifying from endogenous *BCL3* cDNA and cDNA derived from transcripts produced from plasmid expressed *BCL3*. Two primer sets are shown: amplifying from *BCL3* coding sequence ('BCL3') and the gene's 3'UTR region ('BCL3 3'UTR'; FOR CCTACCCATACACCCCCTCT, REV CACCTCTCCCCTCCTCAGTT). (B) Amplification using both primer sets in PCRs amplifying from the *BCL3* overexpression plasmid ([3.2.6.]; 'plasmid') and also cDNA derived from HT1080 cells stimulated with TNFα for 3 hours ('cDNA'). (C) PCRs performed on HT1080 cells (stimulated with TNFα for 3

hours) with and without transfection of a *BCL3* ovexpression plasmid [3.2.6.]. Primers used are as in 5.10.A with the additional use of control primer sets amplifying from the cyclophilin A gene.

Equation: Rate of change in *BCL3* mRNA level

dydt(4) = d[*BCL3*mRNA]/dt

```
dydt(4)=(Chr^3./(Chr^3+k111^3))*k112*((nNFκB./(nNFκB+k113)*(1-
(BCL3./(BCL3+k114)))))-BCL3mRNA*k115;
      nNFκB = Concentration of nuclear NF-κB
      Chr = Concentration of accessible chromatin at the BCL3 promoter
      BCL3mRNA = Concentration of BCL3 mRNA
```

Table 5.4. Parameter values for an ODE representing changes in *BCL3* transcript levels

Parameter name	Description	Value	Rationale
k111	Level of chromatin accessibility ('Chr') at which half maximal activation at the *BCL3* promoter occurs.	0.005nM	Fitted*
k112	Maximal rate of *BCL3* transcription.	6.6 $x10^{-2}$ $\mu M.min^{-1}$	As for k101
k113	K_D value for NF-κB binding at κB site in *BCL3* promoter	69nM	As for k102
k114	K_D value for *BCL3* binding at the *BCL3* gene to mediate BCL-3 self inhibition**	53nM	As for k103
k115	Degradation rate of *BCL3* mRNA	$4.5x10^{-3}$ min^{-1}	Measured***

* Fitted to replicate timing of *BCL3* transcript induction (as in fig 3.2.A).

** BCL-3 protein has been shown to inhibit transcription of its own transcript [5.2.1.6.1.]. Dissociation constant is as used for BCL-3 binding at the *TNFA* promoter (k103).

**** From an experimentally determined half life of 154 minutes (fig 5.4.).

5.2.1.7. *BCL3* mRNA translation

BCL-3 protein is assumed to be instantaneously (upon production by translation) available for DNA binding. BCL-3 protein has been widely shown to be a predominantly nuclear localised factor in various cell lines (Nolan et al., 1993; Zhang et al., 1994) and confirmed in HT1080 cells in this study [3.2.5.2.].

Equation: Rate of change in BCL-3 protein level

dydt(5) = d[BCL-3]/dt

```
dydt(5)=k116*BCL3mRNA-k117*BCL3;
      BCL3mRNA = Concentration of BCL3 mRNA
      BCL3 = Concentration of BCL-3 protein
```

Table 5.5. Parameter values for an ODE representing changes in BCL-3 protein level

Parameter name	Description	Value	Rationale
k116	Rate of BCL-3 protein synthesis	3.6nM/nm of *BCL3* mRNA/min	Calculated*
k117	Rate of BCL-3 protein degradation	$2.4x10^{-3}$ min^{-1}	Calculated**

* Maximal rate of translation (3.6 nm/nm of *BCL3* mRNA/min) calculated after (Lipniacki et al., 2004) based on a translation rate of 180 amino acids per minute (Siller et al., 2010) with 9 ribosomes acting simultaneously - ribosome spacing of 150 nt (Cataldo et al., 1999) - acting on the ~1400 nt *BCL3* transcript to produce 3.6 peptides per minute per *BCL3* mRNA molecule in a cytoplasm of volume 1,667μm^3.

** Relative rate of BCL-3 protein degradation estimated from (Keutgens et al., 2010); Western blots of relative BCL-3 occurrence at varying lengths of time after cells (Human Embryonic Kidney 293 and Karpas cell lines) had been treated with cyclohexamide. The protein half-life value was calculated at 280 minutes.

5.2.2. Model outputs

5.2.2.1. A linear chain of sequential and dependent events recreates chromatin modification behaviour at the *BCL3* promoter and transcript induction dynamics for the *TNFA* and *BCL3* genes

A key design criterion for the model was that it should be able to accurately recreate events at the *BCL3* promoter which lead to TNFα induced transcription of this gene – including histone acetylation, chromatin accessibility and mRNA levels as measured in Chapters 3 and 4. A summary of the induction timings of such events (previously determined in this study), measured over 90 minutes following TNFα stimulation, is shown in figure 5.6.A. A comparison of the relative rates of processes measured using different techniques (qRT-PCR, ChIP/qPCR) was performed by calculating relative rates of events through expressing occurrence on a scale between 0 and 1; with 0 taken as the value

at t=0 and all other values expressed as a fraction of the maximal increase above basal levels (1) achieved in this 90 minute time frame (fig 5.6.A).

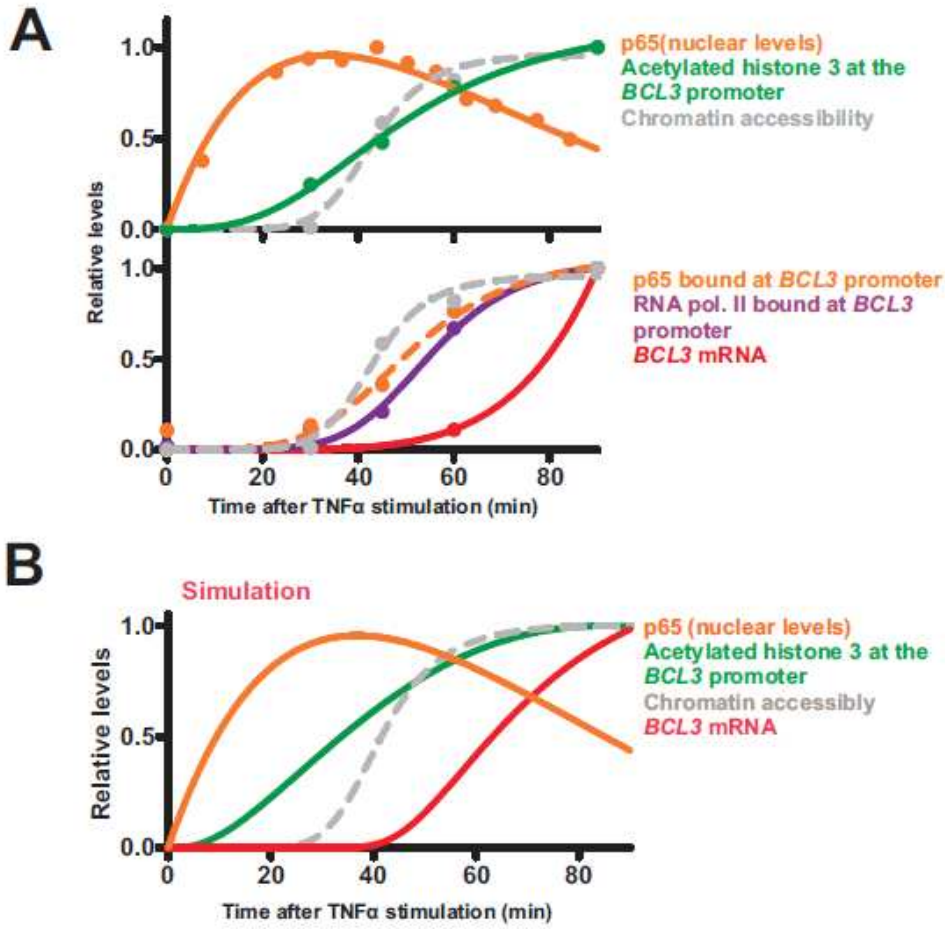

Figure 5.6. The timing of TNFα induced transcription enabling events at the *BCL3* gene promoter in HT1080 cells. (A) Relative levels of previously measured events at the *BCL3* promoter: p65 nuclear levels (orange line) [5.2.1.2.]; histone 3 acetylation (green line) [4.2.4.]; chromatin accessibility (grey dashed line) [4.2.6.2.]; bound p65 (orange dashed line) [4.2.5.]; bound RNAP (purple line) [4.2.4.] and *BCL3* mRNA levels (red line) [3.2.1.3.]. The equations and parameters of lines fitted to the data points are given in Appendix 7. (B) Simulation of such events using an ODE model developed in section [5.2.1.].

In addition to measuring the rates of reaction, previous work had also determined interactions between these model components – as summarised in figure 5.1. A linear chain of interactions was proposed to represent interactions at the *BCL3* promoter; i.e. that NF-κB induces histone acetylation, histone acetylation causes increased chromatin accessibility and increased chromatin accessibility allows further NF-κB binding and *BCL3* transcription. Construction of a model on these principles [5.2.1.] faithfully recreated observed behaviour - compare figure 5.6.B (the simulation) with figure 5.6.A (the

experimental data). Notably, the sequential induction timing of histone acetylation, chromatin accessibility and *BCL3* mRNA appearance is remarkably similar - therefore, despite the use of equations which clearly over-simplify the processes they represent, the model is able to generate induction kinetics which represents experimental observations.

Furthermore, simulated levels of both *TNFA* and *BCL3* transcription by the model are qualitatively comparable to observed levels from initial qRT-PCR experiments over a 900 minute time course (compare fig 5.7. with fig 3.2A).

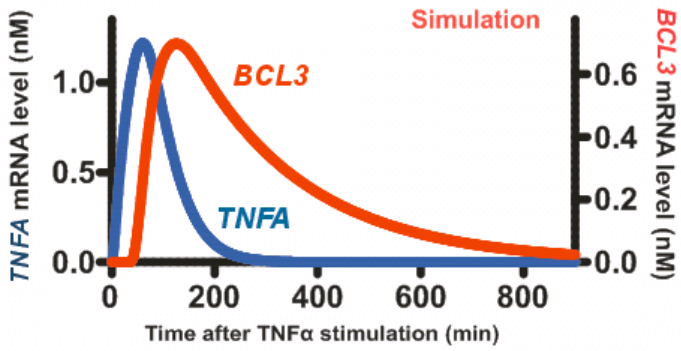

Figure 5.7. ODE simulated induction of *TNFA* and *BCL3* transcript levels following TNFα stimulation.

Further verification of the model's ability to replicate actual cell responses to TNFα was assessed by varying the dynamics of TNFα stimulation - in reality and in the model – and comparing the produced outcomes.

5.2.3. Secondary TNFα stimulation

Previous work was conducted using cells stimulated with a single, continuous introduction of TNFα cytokine. However, cells in an inflamed tissue are perhaps more likely to receive not only this initial stimulus but also subsequent pulses of cytokine signalling (Ashall et al., 2009). Having shown BCL-3 as an attenuating factor for the initial TNFα stimulation, effects on subsequent TNFα stimuli were also determined. To investigate, cells were first stimulated with TNFα for 180 minutes (a time at which an initial *TNFA* transcript pulse response has been attenuated – see fig 3.2.A), washed twice with PBS and subsequently left for 180, 360 and 720 minutes, at which point BCL-3 binding at the *TNFA* promoter (as in [3.2.7.3.]) was measured using ChIP/qPCR. To measure induction of *TNFA* transcript levels by secondary TNFα stimulation, further cell populations underwent identical treatment but were ultimately stimulated with a further 60 minutes of TNFα and induced *TNFA* transcript levels measured by qRT-PCR. This experimental process is summarised in fig 5.8.A.

5.2.3.1. BCL-3 mediates a diminished *TNFA* transcriptional response to subsequent TNFα stimuli

The fold induction of *TNFA* transcript levels increased as the time which elapsed prior to the secondary stimulation also increased (left axis; fig 5.8.B). Such increases cannot be attributed to differences in NF-κB nuclear translocation following secondary TNFα stimulation; as nuclear NF-κB levels of cells re-stimulated after 180, 360 and 720 minute delays, as measured by immunocytochemistry [2.6.] [3.2.5.2.], are not significantly different relative to each other (fig 5.8.C; $P>0.05$). Rather, in keeping with the role previously shown for BCL-3 in inhibiting *TNFA* transcription, an increase in *TNFA* transcript response levels was negatively correlated with the level of BCL-3 bound at the *TNFA* promoter (right axis; fig 5.8.B). Therefore levels of BCL-3 appear to control the responsiveness of HT1080 cells to subsequent TNFα induction, at least with respect to *TNFA* transcriptional response. The decrease in BCL-3 bound as time after the initial TNFα stimulation increases is presumably due to degradation of the BCL-3 that mediated the initial inhibition of *TNFA* transcription.

To test the developed model [5.2.1.], secondary pulses of nuclear NF-κB at 180, 360 and 720 minutes following removal of an initial 180 minute nuclear NF-κB stimulus were used as model input (fig 5.8.D) and levels of *TNFA* transcripts observed (fig 5.8.E) for each of these nuclear NF-κB input profiles. As previously described for the experimental system, induction magnitudes of *TNFA* transcripts increased as the time elapsed prior to the secondary nuclear NF-κB stimulus increased. This increase was again negatively correlated with BCL-3 levels present in the cell at the time of secondary TNFα stimulation (fig 5.8.F). The ability of the model to respond to secondary TNFα signalling perturbation in a comparable manner to behaviour observed experimentally - compare fig 5.8.F (simulation) with 5.8.B (experimental) - is further verification of its suitability in representing the cellular system.

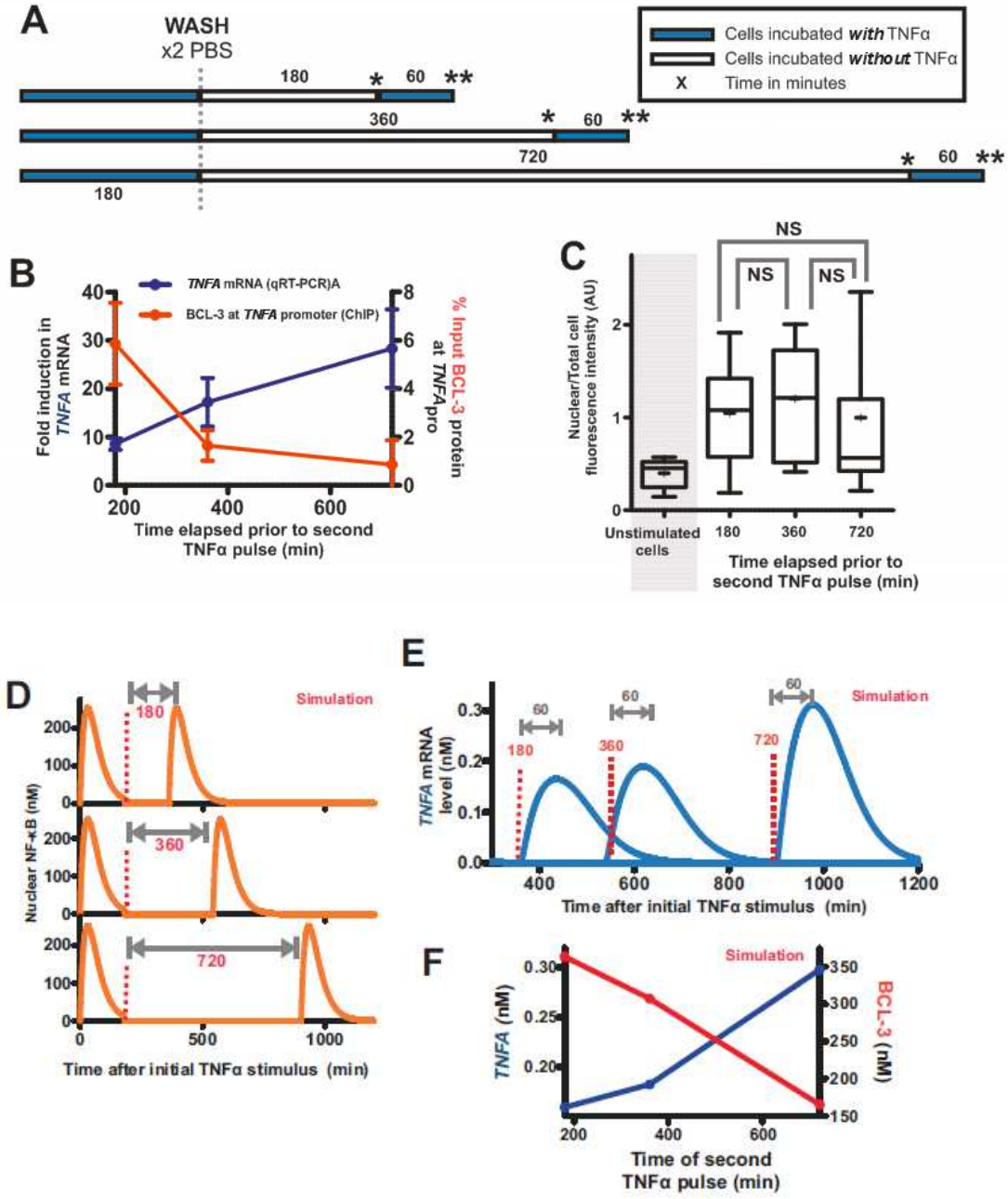

Figure 5.8. Secondary stimulation of HT1080 cells with TNFα. (A) Schematic of experimental design for secondary stimulation of cells with TNFα. Cells were stimulated with TNFα for 180 minutes, signal was washed off and cells left for varying periods of time (180, 360 or 720 minutes) and re-stimulated for 60 minutes with TNFα. (B) Negative correlation of BCL-3 bound at the *TNFA* promoter at time of re-stimulation (right axis) – assayed with ChIP performed as in [3.2.7.3.] at times marked * in fig 5.8.A – and the fold induction of *TNFA* transcript levels induced by the secondary TNFα stimulation (left axis) – measured by qRT-PCR across the time points * and ** in fig 5.8.A – with secondary TNFα stimulations performed with varying lengths of recovery following an initial stimulus: 180, 360 or 720 minutes as in fig 5.8.A. (C) Nuclear levels of p65 in cells stimulated with 60 minutes of secondary TNFα pulse following varied recovery times after an initial TNFα stimulus (180 minutes) - ** time points

in fig 5.7.A – as measured by immunocytochemistry with an anti-p65 antibody (*#3034;* Cell Signalling Technology). Significance tests performed using one-way ANOVA between secondary stimulated cell populations as indicated. NS: Not Significant. Twenty cells were analysed per time point. Secondary stimulations were also simulated using the model outlined in [5.2.1]. Nuclear NF-κB levels were used to simulate secondary TNFα stimuli after varied post-initial stimuli delays (180, 360 and 720 minutes as before) (D) and *TNFA* transcript levels measured after 60 minutes of secondary stimuli occurring (E and also F; left axis). Amounts of BCL-3 protein in simulated cells measured at time of secondary TNFα stimulation (F; right axis).

5.2.4. Delayed *BCL3* transcription allows an initially large magnitude of *TNFA* transcription response but with robust later inhibition

A way to assess the impact of the delayed *BCL3* transcription is to use the model to examine behaviour in the same system in which no such delay is present, i.e. where *BCL3* and *TNFA* transcription initiate simultaneously in response to nuclear NF-κB. A schematic of such a model – hereafter referred to as the 'non-delay model' - is shown in figure 5.9.A (in contrast to the original model in fig 5.1.).

The more rapid induction of *BCL3* transcript levels, and consequently BCL-3 protein levels, in this non-delay model causes a quicker inhibition of induced *TNFA* transcript levels, resulting in a smaller pulse size (solid blue line; fig 5.9.B) when compared to a *TNFA* pulse generated in the original model containing the delayed *BCL3* transcription (blue dashed line; fig 5.9.B).

Attempts were then made to recreate the *TNFA* transcript dynamics produced by the original, BCL-3 delayed, model in the non-delay model by slowing the rate of *BCL3* transcription – therefore increasing the time taken for BCL-3 to accumulate to a level able to inhibit *TNFA* transcription. Decreasing the maximal rate of *BCL3* gene transcription (parameter k112; [5.2.1.6.]) can increase the size of the initial *TNFA* transcript pulse in the non-delay model (figure 5.9.C); with a maximal *BCL3* transcription rate decreased to 1/100th original value producing comparable *TNFA* transcript dynamics to those produced by the *BCL3* chromatin remodelling model (blue dashed line; fig 5.9.C). However, while decreased *BCL3* transcription rate produces a comparable simulated *TNFA* transcript response to a primary (1°) NF-κB translocation, response to a secondary (2°) NF- κB nuclear translocation induced 360 minutes after the first (nuclear NF-κB input dynamics shown in fig 5.9.D) occur at a far greater magnitude (fig 5.9.D). Delayed transcription of the inhibitory *BCL3* gene, relative to *TNFA*, can therefore be seen to have potentially beneficially response kinetics in comparison to simultaneous transcription of the genes: allowing an initially large pulse of *TNFA* transcript but coupled to a strong latter inhibition of *TNFA* gene expression. Such a genetic circuit allows HT1080 cells to amplify an initial perception of inflammatory TNFα cytokine levels to propagate potentially small or transitory signal; but, crucially, restricts later production of the signalling molecule to prevent an excessive inflammatory response.

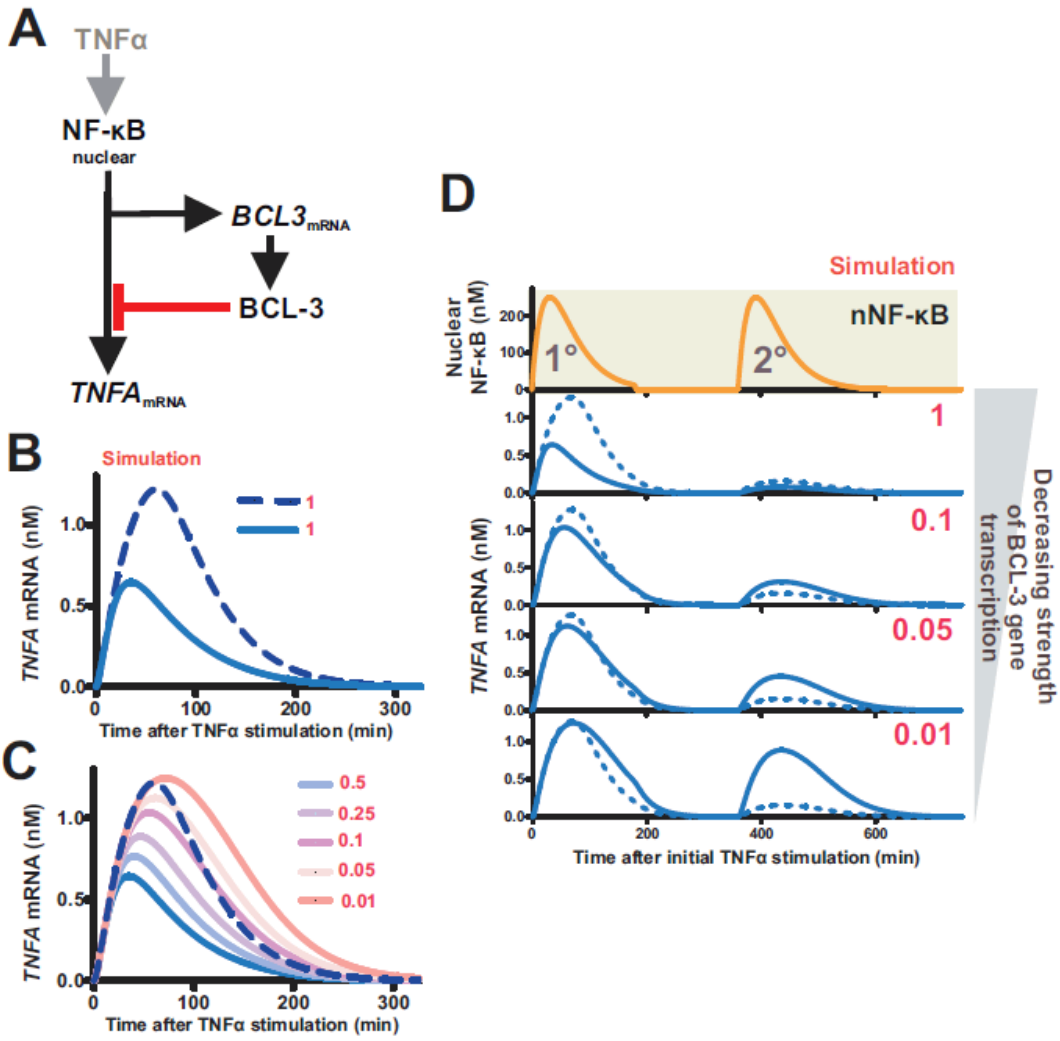

Figure 5.9. Simulated modelling of simultaneous *TNFA* and *BCL3* transcription in response to nuclear NF-κB induction. (A) Schematic showing a model lacking the chromatin remodelling component of *BCL3* transcription induction (in contrast to fig 5.1.). (B) *TNFA* transcript induction in two models: original chromatin containing model (as in fig 5.1) – blue dashed line – or non-delay model (as in fig 5.9.A) – blue solid line. (C) Effect of decreasing parameter k112 on *TNFA* transcript outputs. Fractional k112 values (in comparison to the original value) are used - with red numbers denoting the fractional value of k112 used in non-delay model simulations. (D) Effect of secondary nuclear NF-κB stimulation on *TNFA* mRNA output in a model containing chromatin (fig 5.1) – blue dashed line (constant in all graphs) – and non-delay models (solid blue lines) run with varied fractional levels of parameter k112 (red numbers). Nuclear NF-κB levels used as stimuli (1° and 2°) in all simulat ions shown as an orange line (top graph).

5.2.4.1. A delayed inhibitory leg of an I-FFL uncouples inhibitory response speed and magnitude

As previously stated [3.3.1.], induction by a single activating factor of both positive and negative influences on the same output event forms an incoherent feed forward loop (I-FFL). In this study, the issue of relative timing in the two legs of such an I-FFL (- and +; relating to their effect on the production of output) have been addressed; having described a motif in which the positive leg of the feed forward loop (NF-κB→*TNFA* transcription) responds more rapidly than the inhibitory leg (NF-κB→BCL-3 which inhibits *TNFA* transcription) which, due to a requirement for chromatin remodelling events for *BCL3* transcription, experiences a delay before acting.

A simplified model of BCL-3/*TNFA* interactions in which nuclear NF-κB levels are constant (200nM), rather than transitory, allows induced model components to reach stable steady state conditions (other than zero). The transcriptional induction of *BCL3*, again, occurs either via a chromatin mediated delay or immediately but with varied levels of transcription magnitude (parameter k112; from 1 to 0.01; fig 5.10.A). Reducing the *BCL3* maximal transcription rates clearly causes an increase in the initial *TNFA* peak but also occurs with an associated higher stable steady state (fig 5.10.B). This behaviour is explained by the BCL-3 protein levels produced in the same simulations. Lower *BCL3* transcription rates decreases BCL-3 protein production rate but also reduces the final steady state of protein accumulation (fig 5.10.C); consequently, inhibition of *TNFA* transcription also occurs to a lower extent and transcripts persist at higher levels. In contrast, delayed production of BCL-3 (dashed line; fig 5.10.C) produces a large magnitude response but inhibition at a later time point. These kinetics produce a distinctive 'shark's fin' *TNFA* transcript kinetics (dashed line; fig 5.10.B); with low levels of transcript ultimately achieved after an initial high magnitude pulse. The characteristic pulse-like response outputs of an I-FFL can, therefore, be seen to be determined by the induction kinetics of the inhibitory leg of the motif. Use of a discrete delay in inhibitor production effectively uncouples the response rate and final magnitude of the inhibitory response.

This work emphasises the importance in timing of interactions between components, or nodes, in a genetic circuitry motif. Discrete delays produced by chromatin remodelling contrast favorably, in this instance, with a continuous but slower accumulation of inhibitory factor BCL-3. Chromatin remodelling is therefore important in defining not just which genes can and cannot respond to cell stimuli events, but also, by altering the rate of response, providing an additional tool for cells to employ in regulating responses of potentially harmful genes.

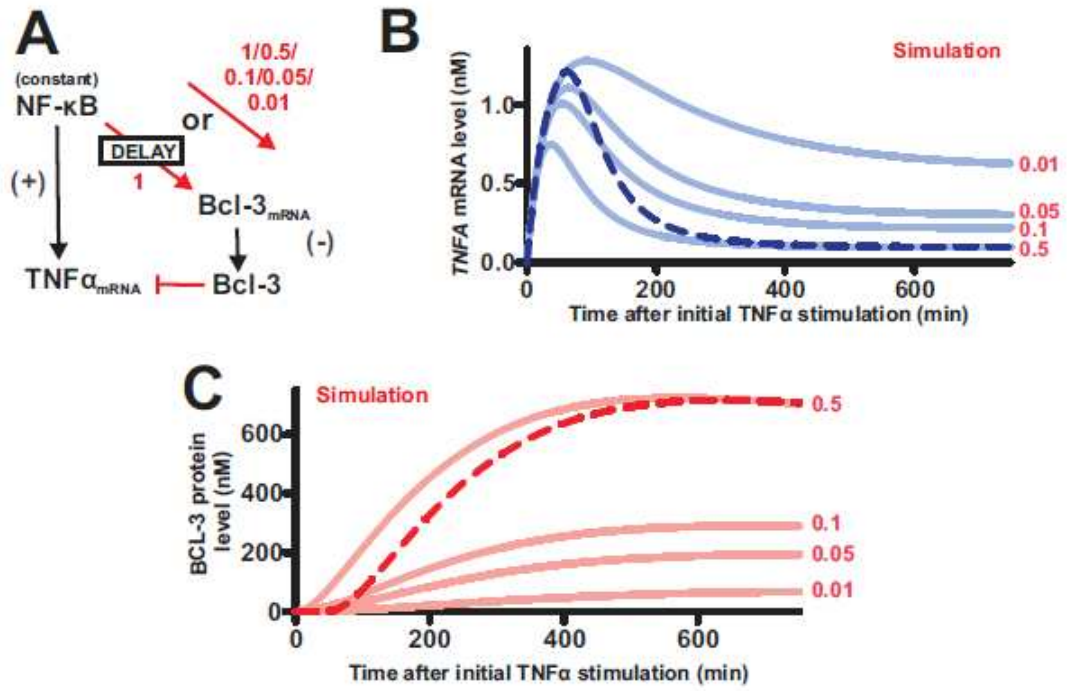

Figure 5.10. Simulation of BCL-3 inhibition of *TNFA* utilising a constant nuclear NF-κB level input. (A) Schematic overview of the two contrasting model forms used – containing delayed *BCL3* transcription or instantaneous *BCL3* production but with varied transcription rates of the gene (red numbers – relating to parameter k112). A constant concentration of nuclear NF-κB is used in this model (200nM) in contrast to previous model simulations. (B) *TNFA* transcript and (C) BCL-3 protein outputs produced from model with chromatin delay (dashed lines) and non-delay models (pale solid lines) with varied relative k112 parameter vales (red numbers).

5.2.5. An I-FFL containing a delayed inhibitory leg exhibits non-linear output responses to pulsed inputs

5.2.5.1. The propensity for pulsed cytokine signalling

As previously mentioned [5.2.3.], cells in physiological conditions are often exposed to pulses of inflammatory stimulation rather than a continuous signal. Consideration of a pulse-like production of cytokines - from neighbouring cells or localised professional immune cells in the vicinity - is increasingly relevant given growing evidence that transcription is itself intrinsically pulsatile. Notably, a recent study demonstrated stochastic bursts of transcription occurring from a constitutive promoter with a minimum, but otherwise variable, refractory period between bursts (Harper et al., 2011). Furthermore, a seminal study by Metivier et al. characterising the presence of transcription promoting complexes at an ERα inducible promoter showed that the binding of such complexes occurs in a cyclical manner (Métivier et al., 2003). Sequential binding of transcription promoting complexes, culminating in RNAP binding, is followed by clearance of such complexes and removal of permissive

chromatin marks at the promoter site – re-establishing a non-permissive chromatin state. Continued presence of active ERα ligand later restores further transcription events; as such, a constitutive transcription response to the continuous presence of an inducing signal (ERα ligand) is actually comprised of sequential pulses of RNAP binding and transcription (Métivier et al., 2003). In addition to the intrinsic pulsatile nature of transcription, as shown in this study [Chapter 3], induction of *TNFA* mRNA occurs in a pulsed manner due to the activity of BCL-3 in an incoherent feed forward loop (I-FFL). Therefore, when considering the TNFα cells are exposed to – as predominantly produced by transcription from cells within its vicinity – a pulsatile input into the model would have potential physiological relevance.

5.2.5.2. Shorter pulses of nuclear NF-κB induce prolonged *TNFA* transcript induction

In light of the potential pulsatile nature of cytokine signalling, it was considered of interest to investigate the response of the described model [5.2.1.] to pulses of input inflammatory stimuli (nuclear NF-κB induced by such pulsatile cytokine stimulation). Pulsed profiles of nuclear NF-κB levels were used; pulses, of magnitude 260nM nuclear NF-κB, began at t=0 and lasted for varied periods of time - with a fixed 60 minute interval between pulses (fig 5.11.A). Simulations were run with 10, 20, 30 and 60 minute nuclear NF-κB pulse sizes over 800 minutes and the resulting *TNFA* mRNA levels observed (fig 5.11.B). Notably, while the initial magnitude of *TNFA* mRNA peaks increased with longer pulse times, such peaks appear to be inhibited at earlier time points in simulations using longer pulse times - contrast the consistent *TNFA* mRNA peaks obtained from 10 minutes pulses with the clearly diminishing *TNFA* mRNA peaks obtained from 60 minute pulses (fig 5.11.B).

A quantitative comparison of *TNFA* mRNA produced by varied pulse sizes of nuclear NF-κB was conducted by comparing the magnitude of *TNFA* mRNA peaks produced by the 2nd, 5th and 8th pulses of nuclear NF-κB across a range of pulse lengths (2.5 to 90mins) (fig 5.11.C). While *TNFA* mRNA output initially increased as pulse lengths increased, further increases resulted in less *TNFA* mRNA produced per pulse. The threshold at which increases in pulse length went from causing an upward trend in *TNFA* mRNA output to a decrease reduced as the pulse number observed increased – in keeping with figure 5.11.B in which decreases in *TNFA* mRNA peak outputs are apparent at earlier times as nuclear NF-κB pulse sizes increase.

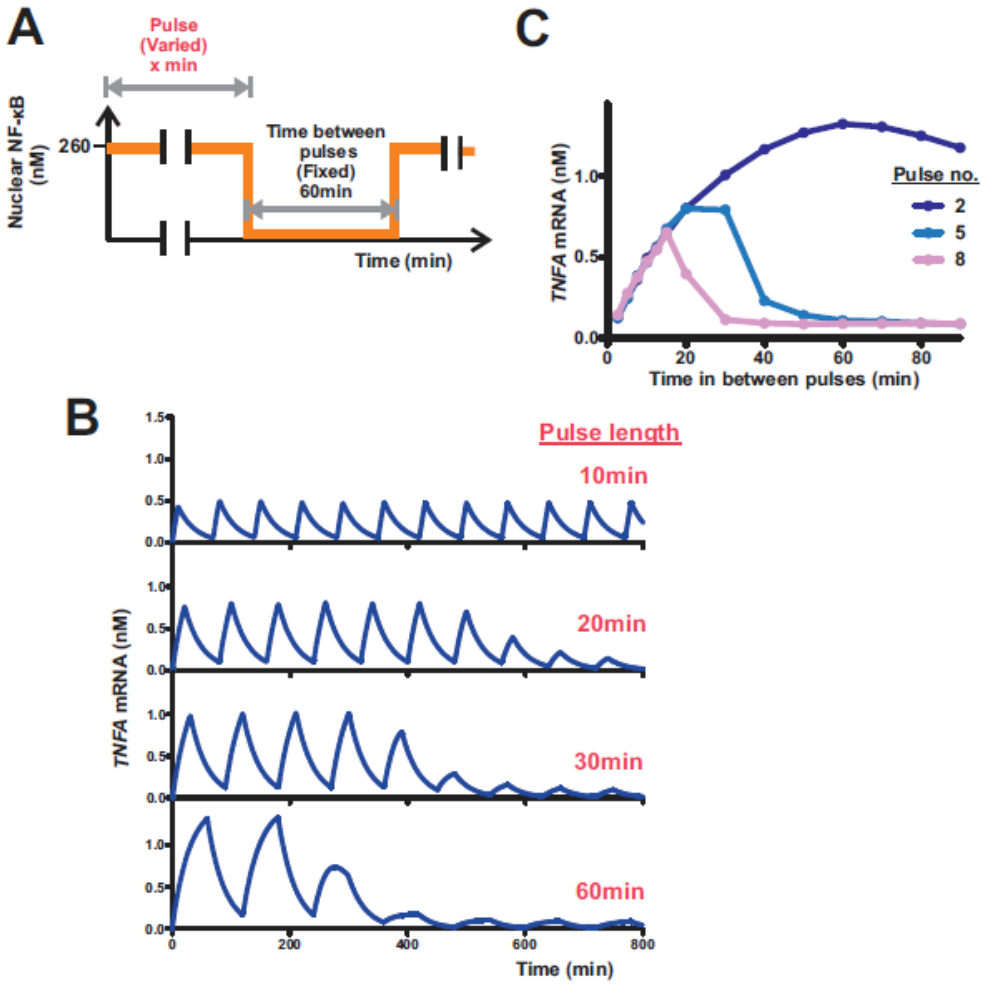

Figure 5.11. Simulated responses of *TNFA* mRNA levels produced by a model (outlined in [5.2.1.]) stimulated with varied length pulses of nuclear NF-κB levels at 60 minute intervals. **(**A) Schematic representation of nuclear NF-κB input used in simulations. Pulses – of magnitude 260nM - start at t=0 and persist for a varied (but constant per simulation) length of time, with an interval of 60 minutes between pulses. (B) *TNFA* mRNA simulated outputs to varied size pulses of nuclear NF-κB at 60 minute intervals. Size of pulse used is indicated in red text. (C) Size of *TNFA* mRNA output peak achieved after 2, 5 and 8 pulses of nuclear NF-κB – varied size pulses of nuclear NF-κB used (x-axis) with a 60min interval between pulses (as before). Size of peak corresponds to maximal amount of *TNFA* mRNA resulting from the designated nuclear NF-κB pulse.

5.2.5.3. Non-monotonic output of an I-FFL generated by a delayed inhibitory leg rather than differential response sensitivities

The output profile of *TNFA* mRNA described in [5.2.5.1.] is similar to a previously described non-monotonic response profile generated by an I-FFL as outlined in [3.3.1.] – non-monotonic responses being those in which outputs do not follow a consistent trend (increasing or deceasing) as inputs increase. Briefly, in a previous study (Kaplan et al., 2008), the positive and negative legs of the studied

I-FFL had different sensitivities to a common input signal; with the positive leg exhibiting greater activity at lower input levels. Functionally, that meant that lower input levels predominantly induced the positive leg of the I-FFL (resulting in high output levels) whereas higher input levels not only induced the positive but also the negative component of the I-FFL (resulting in decreased output levels). Therefore, output of this motif initially increased at low input levels, but exhibited a sharp decrease in output levels as input levels rose – illustrated in fig 3.12.C.

5.2.5.3.1. The *TNFA* and *BCL3* genes exhibit equal sensitivity to transcript upregulation by TNFα

To measure the sensitivity of both *TNFA* and *BCL3* gene transcription to TNFα stimulatory levels, cells were exposed to varied levels of TNFα and the relative level of transcript produced measured. As the *TNFA* and *BCL3* genes respond to TNFα at differing times, initial analysis aimed to determine a time point at which each gene is being actively induced by a range of TNFα concentrations to use for comparative analysis. HT1080 cells were exposed to 0.5 and 2.5ng/ml of TNFα and transcript levels (relative to initial basal levels at t=0) measured with qRT-PCR at different times following stimulation [2.2.]. Times at which each gene were induced by both levels of TNFα stimulation used (low: 0.25ng/ml and mid: 2.5ng/ml) were identified as 45 minutes for the *TNFA* gene (fig 5.12.A) and 90 minutes for the *BCL3* gene (fig 5.12.B). Cell populations were subsequently induced with a range of TNFα concentrations (from 0.25 to 10ng/ml) and fold inductions above basal levels measured at 45 minutes (for *TNFA*) and 90 minutes (for *BCL3*) and expressed as a fraction of the induction caused by stimulation with 10ng/ml (assumed to be maximal induction) (fig 5.12.C). A Hill equation was fitted to these points and used to calculate the value of TNFα at which half maximum induction of the two genes was achieved (red dashed line in fig 5.12.C). No significant difference was seen in the half maximum values of *TNFA* and *BCL3* transcript levels (fig 5.12.D) – each gene was therefore considered to have equal sensitivity to TNFα stimulation in HT1080 cells.

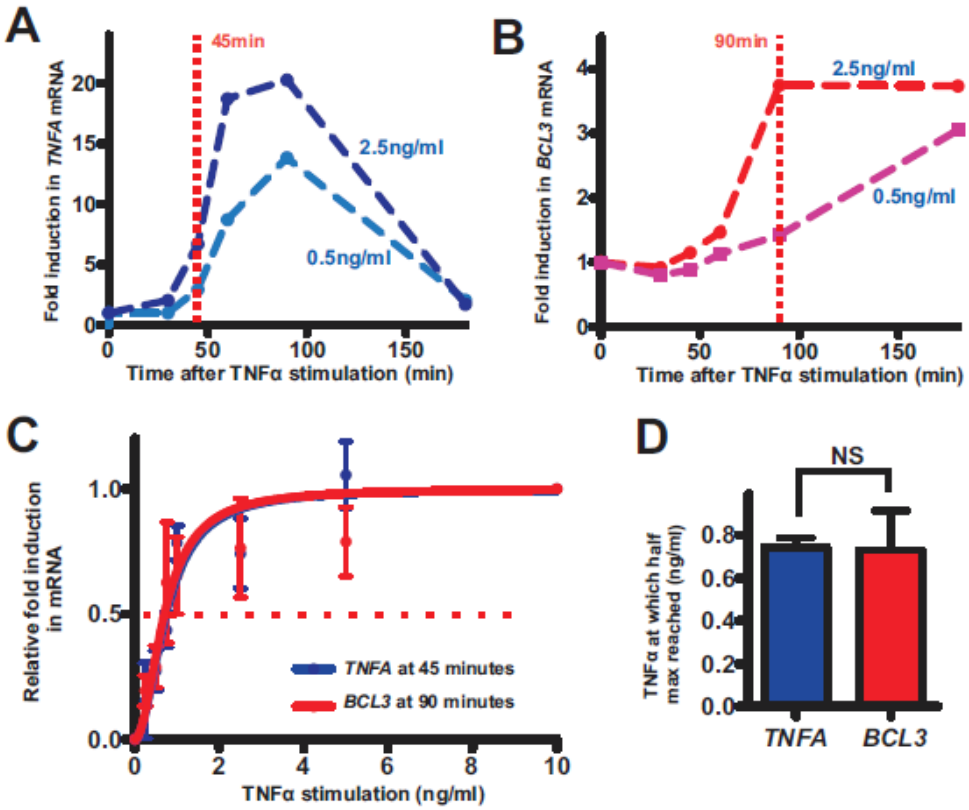

Figure 5.12. TNFα dose-dependent transcription responses of the *TNFA* and *BCL3* genes in HT1080 cells. Time course of the induction of *TNFA* (A) and *BCL3* (B) transcript levels following induction with 0.5 and 2.5ng/ml TNFα. Fold induction is given relative to levels at t=0 (i.e. unstimulated cells). (C) Relative transcript level response of the *TNFA* gene (at 45 minutes) and *BCL3* gene (at 90 minutes) to a range of TNFα stimulation doses. Points expressed as a fraction of the average values obtained from cells stimulated with 10ng/ml of TNFα and are fitted with Hill equation lines; constrained so that Vmax value is at 1 and the Hill coefficient is 2. R^2 values are 0.8986 (*TNFA*) and 0.8027 (*BCL3*). n=3 for each data point. (D) Comparison of the half max values of *BCL3* and *TNFA* gene transcript level induction obtained by fitting a Hill equation, as described in C, to three independent replicates of cells stimulated with varied levels of TNFα, again as in C. NS: Not Significant.

In this study, non-monotonic outputs of *TNFA* mRNA output have been demonstrated in response to increasing sized pulses of nuclear NF-κB stimuli: counter intuitively, increasing pulse sizes (i.e. more input signal for *TNFA* transcription) causes decreases in *TNFA* mRNA output, at least at later time points [5.2.5.1.]. The generation of such behaviour in a system in which the output (*TNFA* mRNA) and inhibitor (*BCL3* mRNA) have equal sensitivity to input stimuli (TNFα) suggests an alternative mechanism of generating such behaviour; due to delayed induction of the inhibitor rather than as a result of lower sensitivity to inductive signal.

5.2.5.4. *BCL3* transcription shows a limited response to pulsed inductive signals

The mechanism by which delayed production of the inhibitor BCL-3 can cause such behaviour is illustrated by comparisons of *TNFA* mRNA output generated by the model simulated with continuous nuclear NF-κB (260nM) or 7.5 minute pulses of nuclear NF-κB (to the same 260nM magnitude) at 60 minute intervals (fig 5.12.A). While the continuous input produced a large initial *TNFA* mRNA output, this was subsequently inhibited to low levels at the latter stages of the time course. In contrast, pulse stimulated *TNFA* mRNA levels were induced to relatively low levels but notably peaks of *TNFA* mRNA output were sustained across the 1,000 minute simulation (fig 5.13.A).

Sustained *TNFA* mRNA response in the pulse-induced model can be explained by the limited induction of BCL-3 which occurs under this stimulus (fig 5.13.B). Small nuclear NF-κB pulses, while able to stimulate *TNFA* transcription (which occurs instantaneously), are insufficient to allow the successful completion of the chain of events (histone acetylation – consequent chromatin accessibility – consequent *BCL3* transcription) necessary for *BCL3* transcript production – therefore BCL-3 does not accumulate to a level able to inhibit *TNFA* transcription (fig 5.13.B). In this instance, it is the slower response time for *BCL3* transcription rather than differential sensitivity which causes its lower expression (and consequent lower inhibition of *TNFA* transcription) to a smaller magnitude (pulsed) inductive signal in comparison to a larger inductive stimulus (continuous). Pulsed nuclear NF-κB is consequently able to induce *TNFA* transcription over a sustained period of time, in contrast to levels of *TNFA* transcription induced by a larger, continuous stimulus,

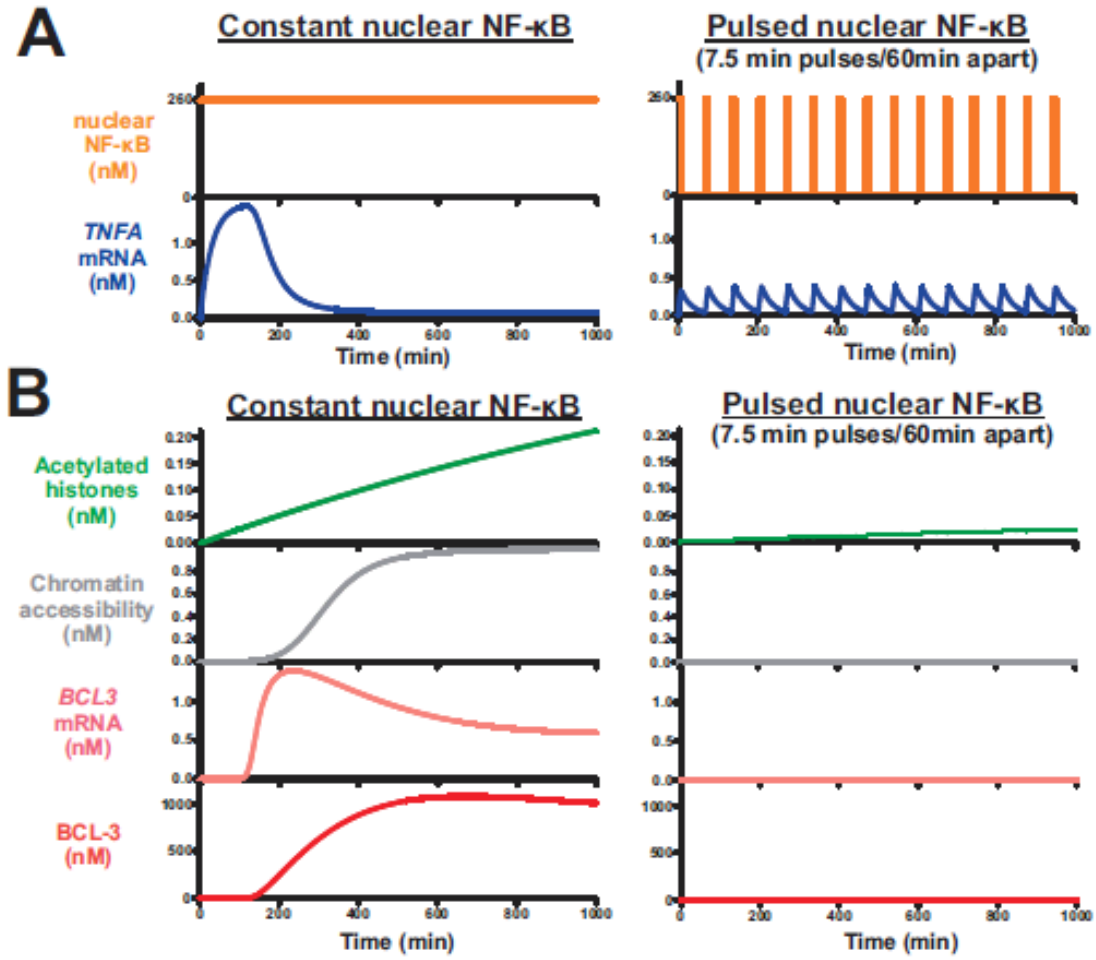

Figure 5.13. An I-FFL motif with a delayed inhibitory leg can exhibit differential responses to continuous and pulsed input stimuli – demonstrated using an ODE model [5.2.1.]. (A) Comparison of simulated *TNFA* mRNA profiles produced by stimulating an ODE model [5.2.1.] with continuous nuclear NF-κB (260nM) input or 7.5min pulses of nuclear NF-κB at 60min intervals (pulsed nuclear NF-κB also of 260nM magnitude). (B) Levels produced, in the same two model simulations, of acetylated histones, chromatin accessibility, *BCL3* mRNA and BCL-3 protein.

5.2.5.5. Desensitisation of cells to continued high magnitude TNFα signalling

A particularly salient point arising from this theoretical work is the ability of cells to respond, in terms of *TNFA* transcription response, to a nuclear NF-κB movement in light of previously experienced NF-κB signalling. Cells which have experienced sizeable previous NF-κB stimulation pulses lose the ability to induce *TNFA* expression, whereas cells previously exposed to relatively small NF-κB pulses are able to continue responding over a longer time period. Such an ability can be viewed as a kind of 'inflammatory memory'; limiting inflammatory cytokine production in a tissue area which has already undergone significant inflammation.

The potential ability of short pulsed NF-κB signalling to induce prolonged *TNFA* expression, in contrast to continuous NF-κB signalling, is an intriguing ability [5.2.5.4.] – although the functionality can only be speculated. This issue is further discussed in a following section [5.3.2.3.].

5.2.5.6. *BCL3* transcription exhibits reduced sensitivity to low frequency NF-κB stimulation

Work in previous sections [5.2.5.2.] [5.2.5.4.] concerned varied nuclear NF-κB pulse sizes at constant intervals (pulse frequency); however, a further consideration is the effect of pulse frequency (i.e. varied time in between pulses) on *TNFA* transcription produced by the model.

Ten pulses of 15 minutes nuclear NF-κB stimuli were input into the model and the produced output of BCL-3 protein observed. Frequencies varied from 2 pulses per hour (i.e. 15 min intervals between pulses) to 0.25 pulses per hour (i.e. 225 min interval between pulses). While the same magnitude of nuclear NF-κB signal was used in each model (each model receives ten 15 minutes nuclear NF-κB pulses), reduced amounts of BCL-3 protein are produced as the frequency of pulses decreases (fig 5.14.A). Notably, when pulse frequency decreases to 0.25 h^{-1}, no BCL-3 protein is produced – a behaviour which, in the context of this model, equates to no inhibition of *TNFA* transcription.

The lack of BCL-3 induction at low frequency NF-κB stimulation can again be attributed to the chain of events required for transcription of its gene. A comparison of the rate of H3 acetylation which occurs in models stimulated with nuclear NF-κB pulses (again 15 min duration) at 0.25 and $2h^{-1}$ frequency shows a far slower rate of increase occurring at the lower frequency NF-κB stimulation (fig 5.14.B); longer intervals of time in between stimulatory pulses allows greater decreases in acetylated histone levels in between pulses. Effectively the system partially resets in between pulses – consequently a reduced magnitude of acetylated histone 3 is achieved. This reduced histone acetylation translates into far more drastic decreases in open chromatin level, and consequent *BCL3* mRNA levels, due to acetylated histone 3 levels not reaching threshold levels necessary to induce open chromatin within the time frame of this stimulation (fig 5.14.B).

5.2.5.7. Cells are predicted to remain able to induce *TNFA* transcription over extended periods of low frequency NF-κB stimulation due to low BCL-3 responses to such stimulation

This insensitivity of *BCL3* transcription to low frequency nuclear NF-κB pulses is manifest as a continued ability of cells (as predicted by this model) to induce *TNFA* transcription over an extended period of time (3,500 mins; fig 5.14.C). It is again noticeable from this simulation that the lack of BCL-3 induction when stimulated with $0.25h^{-1}$ NF-κB pulses across this time course allows cells to respond to each inductive event with an undiminished *TNFA* transcript level response.

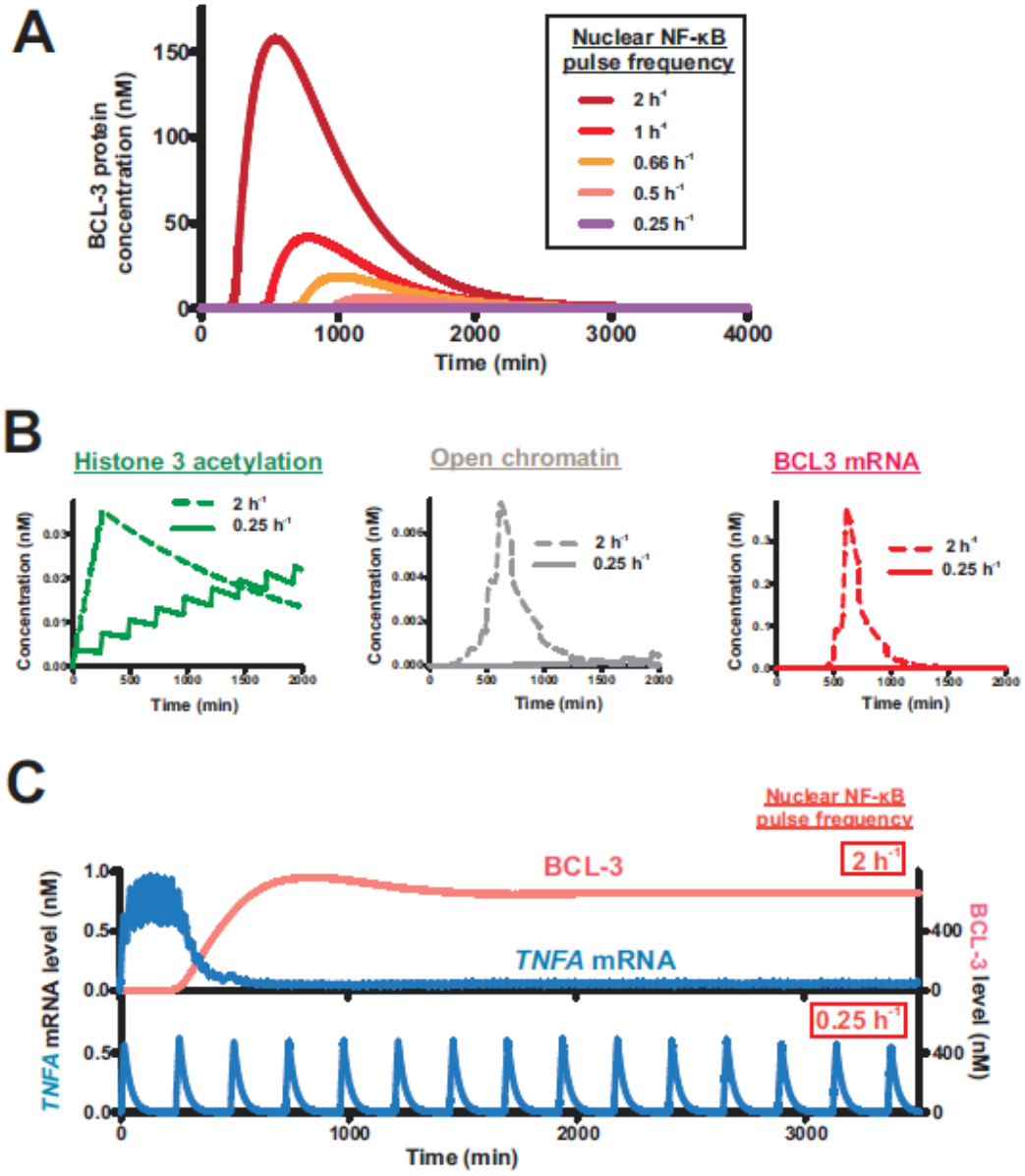

Figure 5.14. *BCL3* transcription shows sensitivity to the frequency of nuclear NF-κB stimulation. (A) Simulation using the model described in [5.2.1.] of BCL-3 protein levels produced by ten 15 minutes pulses of nuclear NF-κB at varying pulse frequencies (indicated in the figure key). (B) Histone 3 acetylation, open chromatin and *BCL3* mRNA levels produced by ten 0.25 and $2h^{-1}$ frequency pulses of 15 minutes nuclear NF-κB, as in fig 5.14.A. (C) Extended time course (3,500 mins) of *TNFA* mRNA and BCL-3 protein levels produced by 15 minute nuclear NF-κB pulses again at 0.25 and $2h^{-1}$ frequencies.

5.3. Discussion

Work in this chapter has involved creating a mathematical model that accurately recreates NF-κB induced transcription of the *TNFA* and *BCL3* genes and a subsequent inhibition of *TNFA* transcription by the induced BCL-3 protein. Experimental work described in previous chapters [Chapters 3 and 4] had shown that induced transcription of *BCL3*, in contrast to *TNFA*, required histone acetylation and consequent chromatin remodelling for transcription to occur – effectively defining an incoherent feed forward loop (I-FFL) in which the inhibitory leg of the motif occurred with a significant delay relative to the positive leg (fig 5.15). A key aim for the constructed model was to investigate the potential effect of this delayed timing on outputs from the motif (*TNFA* transcription) – particularly with the aim to relate such behaviour to physiological TNFα signalling.

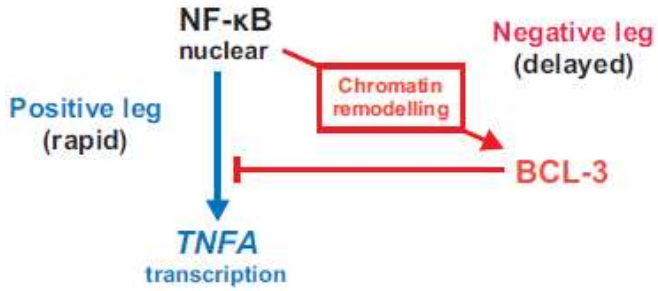

Figure 5.15. Summary of the two legs comprising the I-FFL comprising NF-κB induction of both *TNFA* transcription and an inhibitor of this process: BCL-3.

Two potential benefits of delayed *BCL3* transcription in the context of this motif were identified using the model:

1. An initial strong pulse of *TNFA* transcription was permitted by delayed production of the inhibitory BCL-3; but, crucially, the delay allowed a later strong and stimulus-sensitive production of *BCL3* transcription, which subsequently mediated a strong repression of *TNFA* transcription - [5.3.1.].

2. A non-monotonic production characteristic of *TNFA* transcription in response to pulsatile nuclear NF-κB induction - [5.3.2.].

5.3.1. Regulating the size of cytokine transcriptional pulse responses

Work regarding the regulation of cytokine expression following an initial inflammatory stimulus has generally focussed on the need for repression; particularly in light of the medical issues caused by

cytokine overexpression [1.4.2.] [6.1.1.]. However, the role of cytokines such as TNFα in inducing transcription of their own gene is clearly required to perpetuate an initial stimulus: premature or excessive inhibition of such expression would therefore limit the innate immune response in terms of size or longevity. Therefore a refined control mechanism of such cytokine expression is required: permitting enough TNFα production to successfully initiate, and maintain, an inflammatory response but also to robustly limit the length of this transcription if cytokine signalling persists.

Theoretical work in this chapter illustrates the benefits that chromatin delayed production of an inhibitory factor (BCL-3) can have on cytokine production (*TNFA* transcription). Delayed inhibition essentially creates a window of time in which *TNFA* transcription can proceed at high levels before being strongly inhibited by eventual BCL-3 induction. Use of a slower rate of BCL-3 production (via reduced rates of transcription) fails to recreate *TNFA* transcript dynamics; as the slower rate of BCL-3 production also results in a smaller magnitude of response [5.2.4.]. Consequently, *TNFA* transcription levels persist in response to subsequent TNFα stimuli – a scenario which would potential cause hyper-inflammation [5.2.4.]. As such, in addition to defining interactions that occur in a genetic network, it is also important to take into account the relative timings of such interactions: delayed interactions can produce behaviour unobtainable with simultaneous interaction occurrence.

Furthermore, the work shows the importance of chromatin state in transcription: not just in regard to whether gene transcription can or cannot be induced, but in terms of defining the timing of its response rate. While traditionally genes have been classified as in 'open' or 'closed' chromatin, a changing view of the field allows for a more dynamic nature of chromatin in which genes can be induced to a transcription amenable state [1.5.]. In parallel, an appreciation has grown of the prevalence of RNAP binding and pausing at promoters in the absence of inductive stimuli; essentially being poised to start transcription upon receiving an inductive signal [1.6.5.2.]. Therefore, two classes of gene can broadly be defined with regard to their ability to respond to transcription inductive signals: rapidly responding genes (with RNAP pre-bound) and slower responsive genes (with chromatin remodelling required for transcription). Work in this chapter has shown a potential functionality for such differential gene responsiveness; in which a rapidly responding gene (*TNFA*) is negatively regulated by a slower responding gene (*BCL3*) in a manner which provides functional response kinetics which are not possible if both genes are induced simultaneously.

5.3.2. *TNFA* transcription shows a non-monotonic response to enhanced magnitude and frequency NF-κB signalling

Modelled outcomes conducted in this chapter suggest that *TNFA* transcription would remain sensitive to small duration pulses of nuclear NF-κB over an extended period of time; in contrast, stimulation with

longer duration (or continuous) NF-κB pulses would result in a more rapid desensitisation of the gene [5.2.5.1.]. In addition, lower frequency NF-κB pulses also induce *TNFA* transcription over an extended time span; in contrast higher frequency NF-κB pulses result in enhanced inhibition of *TNFA* transcription over time [5.2.5.7.]. This behaviour is mediated by delayed *BCL3* transcription – which fails to occur under either short or low frequency stimuli; consequently, *TNFA* transcription is not inhibited under these circumstances.

An output response which initially increases as input levels (NF-κB pulse size or frequency) increase but later decreases as input levels climb higher is defined an a non-monotonic response. While such responses have been previously shown to be produced by incoherent feed forward loop (I-FFL) motifs, these instances were caused by lower sensitivity to induction by the negative leg of the motif, rather than, as in this case, slower response timing of the negative motif leg [5.2.5.2.]. It is notable that previous theoretical modelling work investigating the potential outputs of I-FFLs have tended to work by purely varying parameter rates/sizes rather than timing (Entus et al., 2007; Rodrigo and Elena, 2011). An appreciation that a model 'interaction' (such as an induced transcription event) may in fact comprise of numerous sub-events will assist in the analysis of naturally occurring or synthetically developed I-FFL motifs - particularly as the timing arsing from such events may, as illustrated by this work, be a rich source of variation in motif output dynamics.

5.3.2.1. Potential functionality of such a non-monotonic response in induced *TNFA* transcription dynamics

The functionality of this non-monotonic *TNFA* transcription response to nuclear NF-κB pulse sizes in a physiological scenario can only be speculated at. Essentially, the behaviour ensures that cells exposed to either small magnitude or infrequent NF-κB stimulation are able to respond with the production of their own TNFα over extended periods of time – in contrast to larger magnitude or frequency NF-κB stimuli which invoke BCL-3 expression and consequent down regulate the cells subsequent *TNFA* transcription ability.

The cause of such NF-κB stimuli (i.e. induced NF-κB nuclear movement) in a physiological setting is likely to be TNFα signal produced by transcriptionally induced *TNFA* genes in neighbouring cells or localised professional immune cells. As previously outlined, *TNFA* transcription in such cells is likely to be produced in a pulsatile manner with varying refractory periods between each pulse [5.2.5.1.].

The determination of a physiologically feasible pulse frequency is a complex manner. While the production of transcription from 'constitutively' active promoters is increasingly seen to be in reality a sustained pulsatile phenomena [5.2.5.1.], the frequency of such observed pulses is varied; from 50 to

180 minutes delays between transcriptional bursts (Métivier et al., 2003; Harper et al., 2011). In addition, consideration needs to be given to the number of cells in the vicinity of signal and the range of TNFα produced by such cells to determine the actual nature of TNFα input a cell is exposed to due to signalling from neighbouring cells. Further observations of *in situ* inflammatory events are required to provide clarification on such issues; however, this remains a technologically challenging issue – as defined in following sections.

5.3.2.2. Defining the nature of localised TNFα transcriptional pulses

Currently, such speculation over the nature of TNFα – and subsequent nuclear NF-κB localisation – is predominantly based on extrapolating observations of cytokine production in cell cultures and the intrinsically pulsatile nature of transcription [5.2.5.4.]. However, to confirm and refine such assumptions for the better design of experiments, a greater characterisation of cell signalling at inflammatory sites is required. Such characterisation would involve defining not just which professional immune cells are recruited to inflammation sites, but in what numbers plus the cytokine output dynamics and levels of all cells in the inflamed region.

Histology of such inflamed sites in experimental organisms may provide static snapshots of cell compositions, with cytokine levels also being detected from sampled blood and interstitial fluid. However, for dynamic analysis of cytokine production it will be necessary to produce experimental systems with tagged cytokine protein or promoter-reporter constructs. Use of co-cultures including immune cells along with cells from various tissues in quantities informed by histological studies of inflamed sites (as outlined before) will assist in the design of such experiments - regarding, for example, relative numbers of cell types to use (Miki et al., 2012). Increased experimental resemblance to *in situ* inflammatory scenarios will increase the application and value of data obtained form such experiments.

5.3.2.3. Pulse frequency as an indication of the extent of local TNFα signalling

While theoretical in nature and requiring experimental work for validity, modelled outcomes in this chapter present an intriguing mechanism to regulate a cell's ability to transcribe *TNFA* in regards to its signalling environment. It is hypothesised that limited *TNFA* transcription which results from induction by lengthy or frequent pulses of TNFα signal/NF-κB stimuli is a mechanism to limit TNFα production in an environment in which many local cells are already producing TNFα.

The nature of TNFα signal produced by multiple cells will depend on the coordination of induced *TNFA* transcription. High frequency TNFα signalling, and consequent NF-κB induction, may result not from highly pulsile TNFα production from a single cell but rather by asynchronous production from numerous

neighbouring cells. Notably, NF-κB induced transcription has been shown to occur in such a manner: with the stochastic induction of negative NF-κB feedback loops causing varied NF-κB nuclear localisation dynamics – and consequent transcription response – resulting in a highly heterogeneous response across a cell population to a common inductive signal (Paszek et al., 2010). Such a scenario would result in varied time outputs of TNFα; perceived as high frequency signalling by a recipient cell.

As such, the nature of TNFα signal to which a cell is exposed – pulse frequency – could conceivably therefore be due to the number of cells in its vicinity engaged in TNFα production. Circumstances in which large numbers of local cells are producing TNFα pulses would produce a limited *TNFA* transcriptional response in an induced cell; in contrast, small numbers of cells producing TNFα in the vicinity of an induced cell will induce a prolonged ability to respond with TNFα pulses of its own. As shown in this chapter, such behaviour is due to the induction mechanism of *BCL3*: a mechanism which rather than operating due to reduced sensitivity to inductive signal (as compared to *TNFA*), operates with equal sensitivity but with a delayed rate of inhibitory factor production.

5.3.2.4. A consideration of secreted TNFα dynamics

While potentially instructive, work in this chapter lacks consideration of a vital component: that the TNFα produced by cells will also be able to act in stimulating further *TNFA* transcription – i.e. autocrine signalling forming a positive feedback loop. For simplicity, input levels (levels of NF-κB induced to be nuclear localised by TNFα signalling) has been considered to be a fixed characteristic (i.e. set level or set pulse frequency) without a consideration of the effect further secreted TNFα would have on NF-κB activation levels. This issue is addressed in the next chapter.

Chapter 6

Modelling the TNFα positive feedback loop

6.1. Introduction

6.1.1. Problems with cytokine self amplification: cytokine storms and cancer

As shown in current literature [1.4.1.] and also in this study, TNFα cell stimulation is able to induce transcription of its own gene product; effectively forming a self amplification, or positive feedback, loop. The amplification of inflammatory signalling molecules such as TNFα can have severe consequences if occurring to excess [1.4.2.]. 'Cytokine storms' (hypercytokinemia) occur when overproduction of cytokine results in the recruitment of excessive numbers of active immune cells to an area; cells which further produce more cytokines and exacerbate the problem. A generalised inflammatory overexpression – in which an acute initial stimuli induces a disproportionate response in terms of both magnitude and longevity – is closely linked to tissue damage and can, in the event of elevated cytokine and hyper-induced immune cells leaking into the bloodstream, spread to cause multiple organ failure (Wang and Ma, 2008).

Furthermore, chronic inflammation is increasingly seen to increase susceptibility to the development of cancer, with ~20% cancers linked to infection and chronic inflammation (Grivennikov and Karin, 2011). Mechanistic explanations of inflammation induced cancers have shown a protumourogenic role for inflammatory cytokines such as TNFα and IL-6 though their role in inducing potentially oncogenic transcription factors NF-κB, STAT3 and AP-1 in endothelial cells (Karin, 2006). Notably, an observed development of hepatocellular carcinoma in mice with chronically inflamed livers occurred due to overstimulation of NF-κB in hepatocyte cells caused by paracrine TNFα signalling from nearby endothelial and immune cells with abnormally high *TNFA* transcript levels. Crucially, anti-TNFα treatment in such mice reduces the progression to hepatocellular carcinoma (Pikarsky et al., 2004).

6.1.2. Chapter aims

The augmentation of an initial stimuli with further cytokine production is clearly therefore a mechanism which needs regulating. A schematic overview of the TNFα positive feedback loop is shown in figure

6.1. and the construction of a simple mathematical model representing the process is outlined in the following sections. Using this model, work in this chapter aims to characterise the TNFα positive feedback loop; determining the effect that varying the quantitative value of several steps in the process have on long term *TNFA* gene transcription and discussing the implications for such behaviours in the context of the inflammatory response and possible therapeutics.

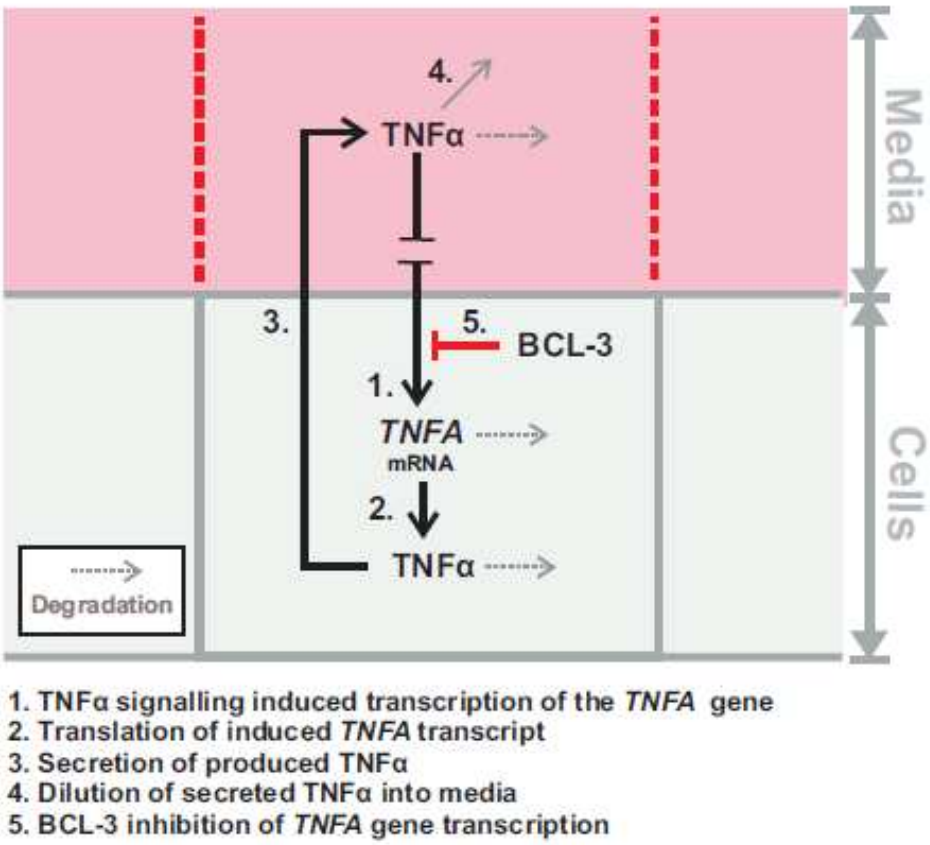

Figure 6.1. Overview of simplified TNFα self-amplification, as modeled in [6.2.1.].

6.2. Results

6.2.1. Modelling the TNFα positive feedback loop

MATLAB code for the model equations outlined in the following sections is given in Appendix 8 [A.8.3].

6.2.1.1. TNFα induction of *TNFA* transcription

Previous work has shown that TNFα induces *TNFA* transcription via the NF-κB pathway [3.2.2.]. In the previously constructed model [5.2.1.3.], levels of induced NF-κB nuclear localisation in response to

10ng/ml TNFα stimulation were measured and used as the input for *TNFA* transcription [5.2.1.2.]; however, a key requirement for the model developed in this chapter is a consideration of the relative occurrence of *TNFA* transcription as levels of TNFα vary (potentially in response to altered TNFα levels resulting from this very transcriptional event). Measurement of the sensitivity of *TNFA* transcript responses as a function of TNFα concentration has already been conducted – [5.2.5.3.1.] – allowing the fitting of a Hill equation determining the fractional level of *TNFA* transcription as a function of TNFα concentration. The maximum magnitude of *TNFA* transcription is again theoretically calculated – as in [5.2.1.3.].

```
Equation: Rate of change in TNFA mRNA
dydt(1)= d[TNFAmRNA]/dt
dydt(1)=k1*((TNFαEX.^2./(TNFαEX.^2+k2.^2) - TNFAmRNA*k3;
      TNFαEX = Concentration of cell external TNFα
      TNFAmRNA = Concentration of TNFA mRNA
```

For the purpose of this model, TNFα protein is categorised as cell 'internal' (TNFαIN) or 'external' (i.e. secreted; TNFαEX).

Table 6.1. Parameter values for an ODE representing TNFα induced transcription of the *TNFA* gene.

Parameter name	Description	Value	Rationale
k1	Maximal rate of *TNFA* transcription (mRNA molecules produced per minute)	6.6 x10^{-2} μM.min^{-1}	As before [5.2.1.3.]
k2	Half max value of TNFα induced *TNFA* transcription	0.7438 ng/ml	Measured*
k3	Degradation rate of *TNFA* mRNA	3.45 x 10^{-2} min^{-1}	Measured (fig 5.4.)

* This value was determined from the relative responsiveness of *TNFA* transcript levels to varied TNFα stimulation levels – as shown in fig 5.12.

A notable omission from this model is the lack of NF-κB signalling. The relationship between lower dose TNFα cell stimulation and NF-κB levels is a potentially complex one – contrarily described as an approximately linear relationship even down to very low TNFα doses (Cheong et al., 2006) or a highly heterogeneous response by cells across a population in which a response depends on the crossing of a stochastic threshold value and with response times varying across observed cells (Turner et al., 2010). Consequently, the construction of an equation calculating nuclear NF-κB levels as a function of TNFα in the surrounding cell media was not considered possible in this study.

6.2.1.2. *TNFA* transcript translation

Cell internal TNFα (TNFαIN) is produced by translation of *TNFA* transcript – with the rate theoretically calculated as before [5.2.1.7.]. Decreases in protein level occur through degradation and also through efflux from the cell.

```
Equation: Rate of change in cell internal TNFα protein
dydt(2) = d[TNFαINT]/dt
dydt(2)=k4*TNFAmRNA-k5*TNFαINT- k6*TNFαINT;
      TNFαIN = Concentration of cell internal TNFα
      TNFAmRNA = Concentration of TNFA mRNA
```

Table 6.2. Parameter values for an ODE representing *TNFA* translation.

Parameter name	Description	Value	Rationale
k4	Rate of TNFα protein synthesis	5nM/nm of *TNFA* mRNA/min	Calculated*
k5	Degradation rate of TNFα	0.0115 min^{-1}	Literature value**

* Logic used as described in [5.2.1.7.] assuming a *TNFA* transcript of ~1700bp and a protein of 233 amino acids.

** While cytokine half lives are frequently described as 'short', quantitative analysis or even the experimental data from which such assertions are made is lacking. A half life of 60 minutes has been used in this model as measured by Mueller et al. in murine blood serum (Mueller et al., 2010). It must, however, be stated that this value is not necessarily true for TNFα stability within cells (either prior to secretion or in an invaginated vesicle) or in the media solution used experimentally – but, in the absence of more applicable data, this value is used as a theoretical starting point.

6.2.1.3. TNFα secretion and stability in solution

Production of external TNFα (TNFαEX) occurs due to the secretion of protein produced by translation - in addition, a starting amount of external TNFα is provided as an initial stimulus for the system (corresponding to 10ng/ml unless otherwise stated). Changes in the level of external TNFα is considered to be due to numerous factors: not only due to basal degradation of the protein but also dilution when it is secreted from the cell and also potentially active degradation mechanisms. Values for such parameters are severely lacking from the literature (see below); therefore, in this theoretical study a range of values for these parameters are used in order to investigate the potential implications that parameter values can have on system behaviour.

Equation: Rate of change in cell TNFα concentration

dydt(3) = d[TNFαEX]/dt

```
dydt(3)=k6*TNFαINT-k7*TNFαEX;
      TNFαEX = Concentration of cell external TNFα
      TNFαIN = Concentration of cell internal TNFα
```

Table 6.3. Parameter values for an ODE representing secreted TNFα levels.

Parameter name	Description	Value	Rationale
k6	Secretion rate of TNFα	Varied	Calculated*
K7	Stability of external TNFα	Varied	Calculated**

* Quantitative data on the secretion rates of molecules per cell is lacking from the literature, therefore a range of values were used in model simulations: from 0 (i.e. no secretion) to the maximal possible amount (i.e. that every molecule of TNFα produced by translation is instantly secreted). Fibroblasts are assumed to have a diameter of ~10μm (Uhal et al., 1998; Green et al., 2009) with a surface area (assuming an approximately circular shape) of 7.85×10^{-11} m^2. Experiments were conducted in a 100mm plate with cells grown to confluence – with cells assumed to be two dimensional with only the top surface exposed to media (and consequently also TNFα). A 10ml (or 1×10^{-5} m^3) volume of media was used experimentally, forming a volume of liquid of height 0.0013m high. Therefore the volume of liquid immediately above each cell is 1×10^{-13} m^3 (or 1×10^{-10} liters) – each cell is assumed to secrete TNFα into this volume. As this external volume is 60 times the cell's internal volume, the concentration of TNFα produced is diluted 60 fold upon secretion – assuming that secretion is instantaneous. Therefore, a production value of 0.0167 $nM.min^{-1}$ (i.e. 1/60) is considered the maximal secretion rate of TNFα.

** TNFα stability in media (or even more generally in any solution) is another poorly defined parameter. As such, a range of values is used to represent the rate of decrease of secreted TNFα.

6.2.2. Effects of parameters k6 and k7 on *TNFA* mRNA steady states

TNFA mRNA levels was taken as an output for system behaviour. To determine the effect of parameter values for k6 and k7 on *TNFA* mRNA steady states, the rate of change in *TNFA* mRNA (d[*TNFA*mRNA]/dt) was expressed as a function of external TNFα levels ([TNFαEX]) using the constant equation parameters outlined in [6.2.1.]. Derivation of the equation (1) (shown below) is outlined in Appendix 8 (A.8.4.).

$$d[\textit{TNFA}\text{mRNA}]/dt = k1*([TNF\alpha EX]^2/([TNF\alpha EX]^2+k2^2) - Q*[TNF\alpha EX] \qquad (1)$$

where $Q = (k3*(k5+k6)*k7)/(k4*k6)$

TNFA mRNA steady states will be achieved when there is no change in the concentration of *TNFA* mRNA (i.e. when d[*TNFA*mRNA]/dt =0):

At steady state:

$$d[TNFAmRNA]/dt = 0 = k1*([TNF\alpha EX]^2/([TNF\alpha EX]^2+k2^2) - Q*[TNF\alpha EX]$$

$$[TNF\alpha EX] = x;$$

$$\rightarrow \quad 0 = x * (Q*x^2 - k1*x + k2^2*Q) \qquad \textbf{(2)}$$

A steady state is clearly attained when x=0 (i.e. no TNFα stimulating the cell); however, can non-zero values of stimulatory TNFα also attain a steady state? Such a scenario is only possible when values of x in the equation $Q*x^2 – k1*x +k2^2*Q$ allow it to equal zero.

$$0 = x * (Q*x^2 - k1*x + k2^2*Q)$$

$$x=0 \qquad Q*x^2 - k1*x + k2^2*Q = 0 \qquad \textbf{(3)}$$

Equation (3) is a quadratic equation of general form $ax^2+bx+c=0$. The number of roots of such equations (i.e. values of x at which the equation is true) is determined by the values of a, b and c and can be assessed using the Discriminant (D) value which equals $b^2 - 4ac$. When the Discriminant is greater than zero, one or more values of x are possible to make the equation work (i.e. in this case, steady states are possible).

$$ax^2 + bx + c = 0 ; \qquad \text{Discriminant (D)} = b^2 - 4ac$$

$$\text{Discriminant} = (-k1)^2 - 4*Q^2*k2^2 \qquad \textbf{(4)}$$

where $Q = (k3*(k5+k6)*k7)/(k4*k6)$

Parameters k1-k5 are fixed values – as outlined in [6.2.1.] – therefore variation in the number of potential roots, or steady states, possible is determined by the values of the varied parameters: k6 and k7 [6.2.1.3.]. More specifically, *TNFA* mRNA steady states are possible when values for k6 and k7 produce a Discriminant value (equation (4)) greater than zero. Figure 6.2.A shows the output level of the Discriminant when k6 (x axis) and k7 (y axis) are varied, with non-zero steady states possible when the Discriminant is greater than zero (non-white in fig 6.2.A). Parameters k6 and k7 exert opposite influence on the attainment of a non-zero *TNFA* mRNA steady state; with increasing k7 values (i.e. increasing instability of external TNFα) decreasing the occurrence of stable *TNFA* mRNA production and increasing k6 (i.e. increasing rate of TNFα secretion) making attainment of such a steady state more likely (fig 6.2.A).

The effect on *TNFA* mRNA levels over time following stimulation with 10ng/ml TNFα are shown for three combinations of k6 and k7 parameter values (I, II and III; fig 6.2.A) in fig 6.2.B. As expected, k6/k7 values at I. lead to *TNFA* mRNA returning to zero values after a transient induction; however, k6/k7 values at II. and III. lead to the attainment of a stable, non-zero *TNFA* mRNA state (fig 6.2.B).

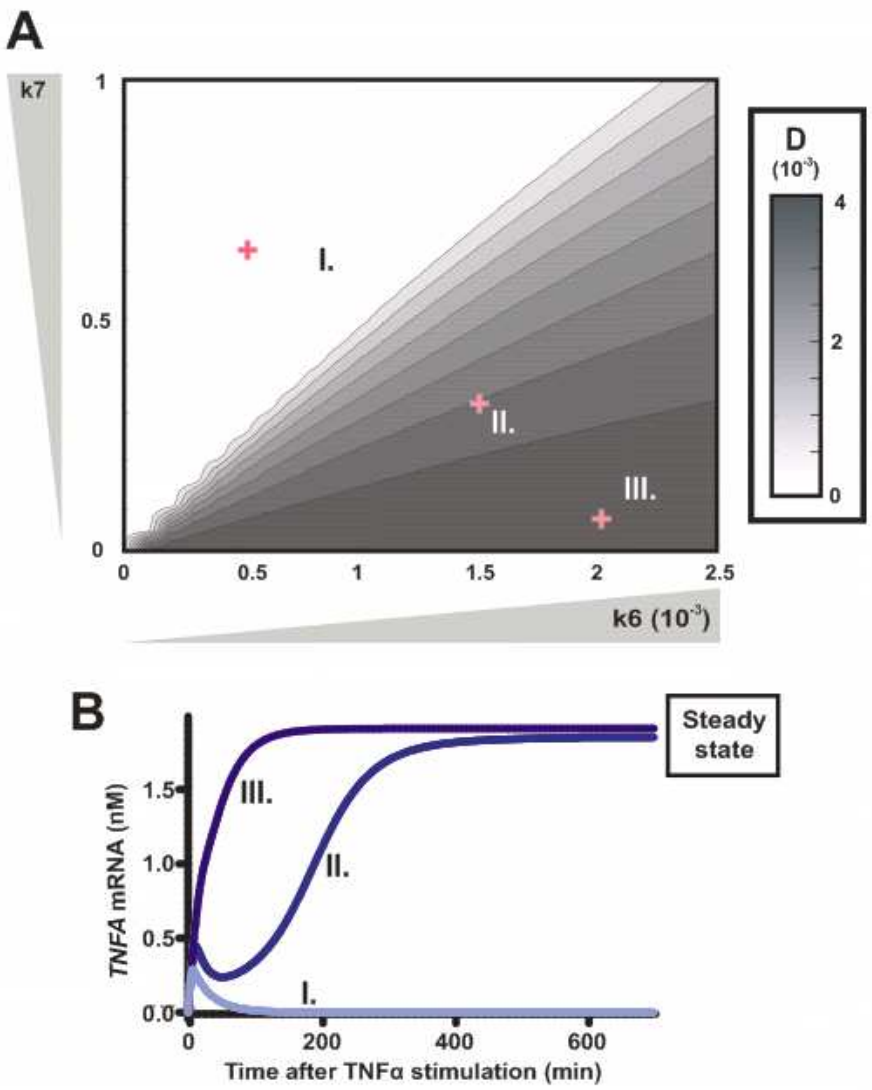

Figure 6.2. Effect of varying parameters k6 and k7 on the steady states which can be achieved by *TNFA* mRNA. (A) Discriminant ('D'; b^2 -4ac from $ax^2+bx+c=0$) relating to the occurrence of non-zero *TNFA* mRNA steady states. Three marked points (+) correspond to the following {k6,k7} coordinates: I. {0.0005, 0.6}; II. {0.0015, 0.4} and III. {0.002, 0.1}. (B) Simulated time course of *TNFA* mRNA levels following stimulation with 10ng/ml TNFα, run with three sets of k6/k7 parameters values (I, II and III) denoted in fig A.

6.2.3. The rate of decrease in secreted TNFα (parameter k7) defines the number and nature of *TNFA* mRNA steady states the system can attain

While previous analysis [6.2.2.] shows that certain values of parameter k7 allow *TNFA* mRNA steady states to be reached, no indication is given by this analysis as to the number or nature of such steady states or any indication as to any link between the level of stimulatory TNFα used to stimulate the system and the resulting *TNFA* mRNA steady state.

These issues were addressed by plotting of the rate in *TNFA* mRNA change as a function of external TNFα concentration ([TNFαEX]; equation (1) [6.2.2.]). At TNFα input levels at which such a plotted line cross the x-axis (i.e. at a point where d[TNFAmRNA]/dt = 0), no change in *TNFA* mRNA occurs; a steady state has been reached. The nature of this steady state – stable or unstable – depends on the gradient of the line at the point at which it transects the x axis: with positive gradients denoting an unstable steady state and, conversely, negative gradients denoting a stable steady state.

Three such graphs have been plotted with different values of k7 (0.1, 0.6 and 0.9) – with values k1-k5 as before [5.2.6.1.] and k6 set at 0.0015 (fig 6.3.A). The effect of varied k7 has a clear effect on the potential steady states the system can achieve. A k7 of 0.1 ensures that stimulation with any TNFα concentration above 0 leads to a tendency for the system to further increase to a stable steady state (fig 6.3.A; k7=0.1). In contrast, use of a k7=0.9 creates a system in which no non-zero steady state exists; the system in effect, regardless of what concentration of TNFα it is initially stimulated with, decays to zero (fig 6.3.A; k7=0.9). A k7 value of 0.6 creates a further scenario: a bi-stable system in which two stable steady states occur either side of an unstable steady state (fig 6.3.A; k7=0.6). In this system, the stable outcome of *TNFA* mRNA depends on the concentration of TNFα with which the system is initially stimulated. Stimulation with a level of TNFα below the unstable steady state (red arrow 1. in fig 6.3.A k7=0.6) will result in *TNFA* mRNA levels eventually reverting to zero concentration – as illustrated in fig 5.16.B. In contrast, stimulation with TNFα levels above the unstable steady state (red arrows 2. and 3. in fig 6.3.A) cause the system to attain a non-zero steady state of *TNFA* mRNA – as illustrated in fig 6.4.B. In effect, the unstable steady state acts as a bifurcation point in the system.

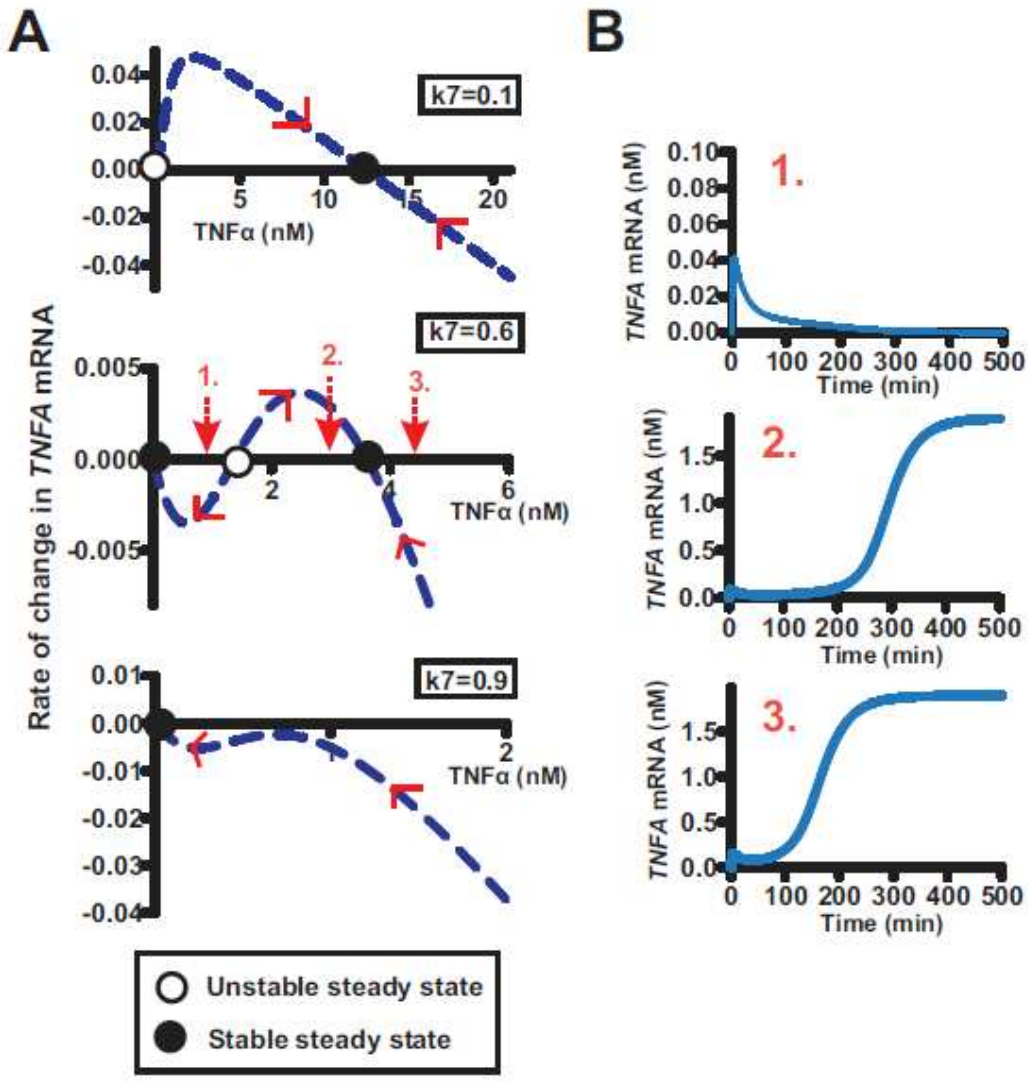

Figure 6.3. Rate of change in *TNFA* mRNA levels as a function of the external TNFα concentration. (A) Rate of change in *TNFA* mRNA = k1*([TNFα]^2/[TNFα]^2+k2^2) – Q*[TNFα]; where Q = (k3*(k5+k6)*k7)/(k4*k6); parameters k1 to k5 are as in [5.2.6.1.], k6 = 0.0015 and k7 is 0.1, 0.6 or 0.9 as denoted on the graphs in the figure. TNFα values producing *TNFA* mRNA steady states occur where the line crosses the x-axis, with the type of steady state (stable or unstable) denoted as shown in the figure key. (B) Time course of *TNFA* mRNA levels stimulated with varying levels of initial TNFα - 1., 2. and 3. as denoted with red arrows in fig 6.3.A – in a system with k7=0.6.

The magnitude of the k7 parameter can therefore be seen to be a key determinant in the responsiveness of systems to TNFα; allowing systems to either always or never attain a (non-zero) stable steady state *TNFA* mRNA level, or to set a threshold of TNFα stimulation level at which changes in system behaviour occur. That the stability of secreted TNFα can have such profound effects on expression of its own gene is perhaps intuitive; however, that the system can behave in such a varied

manner dependent on the numerical value of TNFα stability is more surprising – particularly as factors determining the stability of TNFα in the vicinity of cells, such as the rate of flow in solution surrounding cells, will vary across physiological locations. A scenario in which cells located in a relative flow 'back water' in an tissue bathed in solutions experiencing limited flow will tend to accumulate localised TNFα concentrations to a greater degree than cells in which are situated in a rapid flow environment. In such a scenario, cell which are bathed in a sluggish aqueous environment and which can accumulate TNFα secreted by local cells are more likely to continue transcribing the gene – causing further localised buildup and a potentially harmful scenario. Mechanisms which actively prevent such unlimited *TNFA* transcription, such as BCL-3, can therefore be seen to be vital.

6.2.4. BCL-3 acts to limit the number of steady states which *TNFA* mRNA can attain

As previously shown, BCL-3 acts to inhibit *TNFA* transcription [3.2.6.]. To determine the effects of BCL-3 on the attainment of *TNFA* mRNA steady states, the model previously outlined [6.2.1.] was again run but in the presence of constant levels of BCL-3 set at 0, 10, 20 and 30nM (fig 6.4.A). While systems with lower levels of BCL-3 (0, 10 and 20nM) were still able to attain a *TNFA* mRNA stable steady state, a further increase to 30nM led to the system being unable to sustain *TNFA* mRNA levels despite an initial increase in transcript levels (fig 6.4.A; Close up). This occurred in a system (with k7=0.1) in which previously stimulation with any quantity of TNFα led to the attainment of a (non-zero) steady stable state (fig 6.4.B; BCL-3=0nM). Introduction of BCL-3 can be seen to alter the number of possible *TNFA* mRNA steady states in the system (fig 6.4.B). In the absence of BCL-3, the system once stimulated with any concentration of TNFα tends to move to a stable steady state at a non-zero TNFα concentration; however, introduction of BCL-3 (50nM) leads to a system in which this steady state is abolished and TNFα=0 is the only possible steady state (fig 6.4.B). Such altering of system behaviour illustrates the value of the BCL-3 inhibitory mechanism: ensuring that even in the presence of high levels of stable TNFα cell stimuli, *TNFA* transcription can be effectively reduced to zero.

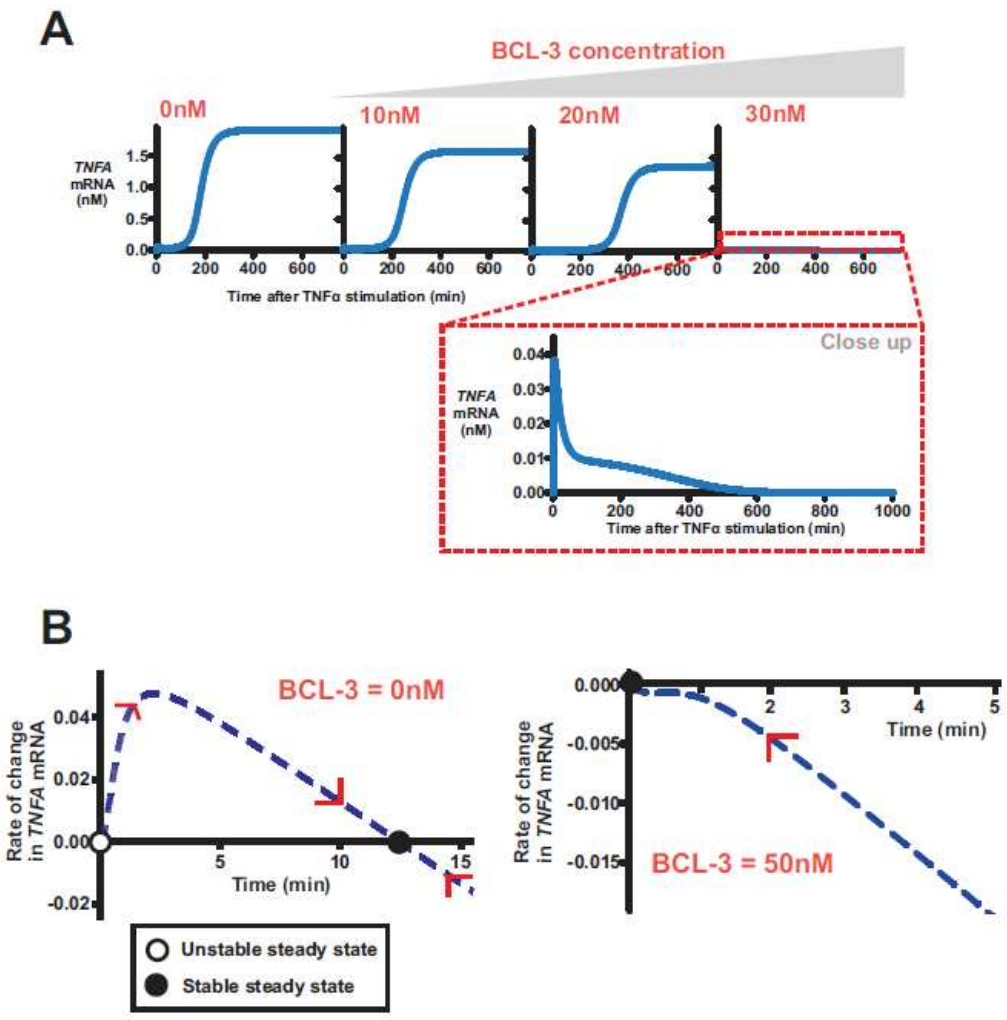

Figure 6.4. Effect of BCL-3 on *TNFA* mRNA steady state attainment. (A) Cells initially stimulated with 10ng/ml TNFα with varied levels of BCL-3 (denoted by red numbers). *TNFA* mRNA is able to achieve a stable, non-zero, steady state when incubated with 0, 10 and 20nM BCL-3 but not in the presence of 30nM BCL-3. k7=0.1, k6=0.0015. (B) The rate of change in *TNFA* mRNA (equation (1) [6.2.2.]) plotted against external TNFα stimuli levels, with (50nM) and without (0nM) BCL-3.

6.3. Discussion

6.3.1. The stability of secreted TNFα can potentially have a profound effect on long term *TNFA* transcription

The potential drawback for a positive feedback loop involving TNFα is that a mechanism which causes a modest amplification of an initial TNFα stimuli can come at the potential cost of prolonged, even theoretically infinitive, expression of the *TNFA* gene. However, as shown in this chapter, the relative

longevity – or stability – of components forming the TNFα positive feedback loop can dramatically alter the characteristic output of *TNFA* transcription: notably the stability of secreted, or cell external, TNFα. The rate of degradation of external TNFα in this case effectively encompasses process including degradation of the protein, decreases in concentration due to secretion into a large volume and, in a physiological setting, removal of protein due to flow rate surrounding the secreting cells.

As shown, high rates of secreted TNFα removal result in systems in which *TNFA* transcription cannot attain a steady state other than zero (i.e. where all components of the system have degraded) (fig 6.3.). Conversely, stable secreted TNFα results in a system in which even small initial TNFα stimuli results in high steady state *TNFA* transcription being achieved (fig 6.3.). Intermediate secreted TNFα stability results in bistable systems in which a threshold of TNFα exists; above which *TNFA* transcription is induced to a stable level but below which induced *TNFA* levels eventually degrade to zero (fig 6.3.). Such positive feedback loop created bistable systems have previously been described as 'decision making' genetic circuitry – in which cells are insensitive to low level signalling but produce a robust response once a threshold magnitude of signalling is achieved (Xiong and Ferrell, 2003). The extracellular stability of TNFα may therefore set the sensitivity of cell responses; creating systems in which levels of TNFα are able to set an all or nothing *TNFA* transcriptional responses or make such a response conditional on the level of TNFα stimulating the cell – effectively moderating cell sensitivity.

6.3.2. Further potential experimental work on secreted TNFα dynamics

Further work is clearly needed to define TNFα dynamics once the protein has been secreted from cells – introducing quantitative data to the theoretical values used in this study. However, such measurements are far from trivial to obtain due to two reasons: (a.) the difficulty in observing proteins once secreted from cells and (b.) a lack of information on conditions which should be used to replicate physiological locations in experimental scenarios.

TNFα protein levels can be measured in experimental media using an ELISA assay. Traditional criticisms of ELISA – that it is non-dynamic process and conducted on populations of cells – are potentially answered by techniques developed to isolate single or small groups of cells in nanowells and draw off small volumes of media at multiple sequential time points for cytokine assaying using ELISA (Han et al., 2011). In contrast, the utilisation of fluorescent protein tagged TNFα protein is potentially problematic once the protein fusion has left the cell. While dynamic 3D measurement of fluorescent molecules in solution (for example a potential TNFα-GFP fusion protein) is increasingly feasible, such studies are still restricted to relatively small volumes to a depth of ~10μm (Kubitscheck et al., 2000; Pucadyil and Chattopadhyay, 2006).

6.3.3. Further considerations for secreted TNFα stability

The demonstrated importance of secreted TNFα accumulation rate also has implications for conducting experiments in a Petri dish with cultured cells bathed in a stationary volume of media. A potential technique to better recreate physiological conditions experimentally is microfluidics. This technique involves the use of small fluid volumes which can be manipulated to replicate flow rates, used in conjunction with live fluorescence microscopy to dynamically image fluorescent protein levels in cells. The use of dynamic fluid behaviour plus secretion of cytokines into small volumes – in which fluids are subject to small scale forces not apparent at the macrofluidic level – will give a greater relevance to experimental data. However, a greater appreciation of the localised signalling environment that cell secrete cytokines into will be vital in replicating such conditions experimentally.

Signalling at the localised level (rather than through the blood) occurs through an interstitial space consisting of a fluid and extracellular matrix (ECM) component. Fluid and signalling molecules enter and leave the interstitial fluid through connections to capillary blood vessels – consequently the magnitude of fluid dynamics in the interstitial fluid plus the loss of cytokines to the bloodstream will be determined by the proximity of tissue to the local blood vessels. Furthermore, the volume of interstitial fluid immediately surrounding cells will be determined by the density of cells and potentially the size of the ECM - a meshed network of glycosaminoglycans and fibrous proteins – surrounding cells. Information on such parameters will be vital in ensuring experimental conditions edge closer to the physiological scenarios they aim to emulate. While a complete body-wide consensus of such measurements is perhaps ambitious, work which set upper and lower limits or perhaps even physiologically feasible values would be extremely useful.

In addition, formation of tumourous tissue causes alternations in interstitial space in terms of composition, size and density of blood vessels. Such alterations in a tumour's microenvironment will have a potential impact on the effect of localised cytokine signalling – such changes are particularly of note given the growing link between inflammatory signalling and cancer [6.1.1.] (Wiig et al., 2010). The field would also benefits from a greater appreciation of the role of the ECM in cytokine signalling: ECM constituent component proteoglycans have the potential to interact with cytokines and either moderate their activity or cause storage in the ECM (Sch et al., 2000).

6.3.4. Active removal of secreted TNFα: natural and therapeutic methods

In addition to passive loss of TNFα – through diffusion, loss to nearby blood vessels or basal degradation – further work on TNFα signalling should also consider mechanisms which actively target the protein for degradation. For example, the human myelomonocytic cell line U937 possesses cell membrane surface serine peptidases (DDP IV-like and tripeptidyl endopeptidase) capable of cleaving

TNFα into small, non-functional fragments (Bauvois et al., 1992). Furthermore, under conditions of hypoxia, LPS induced TNFα secretion is decreased in primary mouse peritoneal macrophages through inhibition of secretory lysosomes and enhanced protein degradation while in such lysosomes (Lahat et al., 2008). Consequently, the expression – basal or induced – of such peptidase enzymes or the localised oxygen conditions in tissue – which may vary under different environmental or health factors – are potentially moderators of the longevity of TNFα signalling and areas which warrant further characterisation; particularly as the modification of TNFα stability is a growing therapeutic target.

It may also be beneficial to conduct further work at more physiologically appropriate values of TNFα concentration. Values in the range of ~1-3pg/ml TNFα have been observed in human blood plasma (Nilsson et al., 1998; Nakai et al., 1999); however, patients suffering sepsis exhibit 100-5,000pg/ml TNFα in blood serum, with higher levels being associated with severe cases of sepsis and mortality (Damas et al., 1989). Typical levels of TNFα used experimentally (10ng/ml or 10,000pg/ml) therefore resemble conditions of severe inflammation. However, a further point of note is that the measurement of TNFα comes from blood plasma samples, rather than at the level of fluid surrounding inflamed tissues – as such there may be a potentially unappreciated higher cytokine level at such localised sites. Further clarification of TNFα concentration at such precise sites, admittedly a considerable technical challenge, would again greatly inform the design of physiologically appropriate experiments.

6.3.5. The role of BCL-3 in moderating *TNFA* mRNA steady states

Stability of TNFα is a feature largely beyond cellular control - being determined predominantly by local microenvironment conditions. As such, it is possible that environments exist in which secreted TNFα can accumulate to levels able to achieve stable steady state *TNFA* transcription and consequently perpetuate an initial TNFα stimulus over long, and potentially harmful, time periods. As previously shown [3.2.6.], BCL-3 can counteract such a tendency by actively inhibiting *TNFA* transcription.

Work in this chapter has shown that a gradual increase in BCL-3 concentration, rather than decreasing *TNFA* mRNA in a commensurate manner, causes a collapse in the occurrence of a *TNFA* mRNA steady state once a threshold of inhibitory BCL-3 level is exceeded [6.2.4.] (fig 6.4.B). This occurs as increased levels of BCL-3 inhibit, or 'slows', the TNFα feedback loop to a level at which *TNFA* mRNA is not produced at a sufficient rate to replenish the TNFα signal population; consequently, both protein and mRNA levels will decrease until decaying to zero. BCL-3 therefore plays an active role in inhibiting the TNFα positive feedback loop through altering the number of possible steady states to which *TNFA* mRNA can attain – a characteristic particularly relevant in locations in which TNFα exhibits relative stability once secreted from a cell (fig 6.5).

Chapter 7

Developing tools to visualise BCL-3 dynamics in live cells using a BAC expression system

7.1. Introduction

7.1.1. Live visualisation of single cell protein dynamics

While use of cell population based assays has provided considerable data on protein expression, such assays measure homogenous, or average, protein levels and behaviour in all cells in the population. Consequently, heterogeneous cell behaviour can be lost. Such behaviour can include different sub-populations of protein expressing cells; caused, for example, by bi-stable expression states in which cells adopt either a high or low stable level of protein expression (Chang et al., 2006). In addition, protein localisation behaviour, such as nuclear-cytoplasm oscillations, if occurring in a non-synchronised manner between cells may not be discernable from whole cell population assays (Nelson et al., 2004; Spiller et al., 2010).

Furthermore, when using techniques which involve cell destruction (such as Western blots) for assays performed over a time course, measurements at different times are performed out of necessity on different cell populations rather than following a single population over time. In addition, samples are taken at discrete, experimentally determined, time points. Dynamic processes, particularly changes in protein localisation in response to cell signalling processes, can occur over a very short time frame – requiring short intervals between sample measurements which makes destructive cell assay techniques very labour intensive. In contrast, use of endogenous proteins fused to fluorescent tags has allowed the continuous imaging of protein dynamics in live cells over extended periods of time.

7.1.1.1. Fluorescent protein tagging

Diverse fluorescence tools have been developed using mutagenesis of the original green florescent protein (GFP) derived from *Aequorea victoria* jellyfish to alter protein properties, including emission and excitation peaks (to, for example, YFP variants) and also maturation dynamics. Slow maturation time of fluorescent protein delays the appearance observable signal from newly synthesised endogenous protein fused to the fluorescent protein, with the multi-step oxidation of the protein's chromophore a particularly lengthy process (Tsien, 1998). In this study, a mutagenesis derived rapid maturation

variant of YFP (called 'Venus') is used; the protein having previously shown to have significantly faster maturation responses than conventional YFP (Nagai et al., 2002). This reporter molecule also exhibits high quantum yield. Recombinant DNA molecules containing sequences coding for such fluorescent proteins fused in frame to an endogenous protein coding sequence can be introduced and expressed in human cells through the use of several potential expression vectors.

7.1.2. Expression vectors

7.1.2.1. Distal enhancer elements

In addition to protein coding sequence, in order to recreate an endogenous expression profile expression vectors must also contain all sequence elements which drive expression of the gene. Sequences required for expression include not only a minimal or core promoter sequence contiguous with the transcription start site (Wu et al., 2010) but also *cis* elements (enhancers) which assist in recruitment of RNAP to a gene's promoter, often under specific spatiotemporal cues. Functional metazoan enhancers and insulators have been observed to be present in excess of 50kb from gene coding sequences (Yang et al., 1997) – a size of sequence which plasmids and lentiviral vectors will be unable to accommodate (with a limit of approximately 10kb for these vectors). In addition to requiring the use of smaller regulatory sequences, plasmid and lentiviral methods also often use cDNA for gene coding sequence – removing regulatory sequence contained within introns.

The focus of past research in using short upstream promoter sequences as a representation of regulatory sequence has biased identification of important *cis* sequences to these regions. Identification of extremely distal sites is more problematic given their lack of spatial linkage to the gene upon which they operate – functional enhancers have even been identified within the introns of neighbouring genes (Yang et al., 1997; Lettice et al., 2002). Despite the difficulty in their identification, the importance of considering distal enhancer sites in research is highlighted by genetic diseases which, rather than being caused by mutations within or proximal to the affected gene, are linked to chromosome aberrations at sites up to 100kb away (Crolla and van Heyningen, 2002; Kleinjan and van Heyningen, 2005).

7.1.3. Bacterial Artificial Chromosomes (BACs)

The need for greater sequence flanking genes of interest has led to development of methods to facilitate the introduction of large fragments of human genomic sequence, such as yeast artificial chromosomes (YACs) and the shorter but more stable bacterial artificial chromosomes (BACs). BACs are able to contain up to 350kb fragments of human genomic DNA along with a short sequence cassette contain sequence necessary for selection (antibiotic resistance) and replication in bacterial cells (Shizuya et al., 1992). An example of the value of BACs in allowing inclusion of distal gene

flanking sequence has been shown by studies on the murine zinc-finger gene *RU49.* Expression of a reporter gene driven by a 10kb promoter fragment from the *RU49* gene failed to recreate previously observed endogenous tissue localisation of the gene's transcript in the murine brain. However, expression of the same reporter gene introduced from *RU49* adjacent sequence contained within a 131kb BAC was able to accurately recreate the endogenous observed gene expression pattern (Yang et al., 1997).

However, despite the advantages of using BACs, their size and low copy number make extraction, manipulation and transfection into human cells problematic. In addition, the lack of unique restriction endonuclease sites prevents the use of conventional techniques to, for example, introduce fluorescent protein coding sequence. Instead, homologous recombination techniques are utilised.

7.1.3.1. Modifying BACs by Recombineering

Induction of a fluorescent reporter gene to a BAC by recombinant mediated engineering (Recombineering) requires addition of lengths of sequence homologous to the desired site of integration ('homology arms') either side of the sequence to be introduced. This DNA 'cassette' (amplified by PCR) can subsequently be transformed into bacteria containing the BAC of interest for homologous recombination to occur.

7.1.3.2. Recombination system: GalK selection method strain *Escherichia coli* strain SW102

An existing double-strand break repair pathway in *E. coli* cells (the RecBCD pathway) is used to facilitate homologous recombination. However, while the RecBCD protein complex can catalyse reactions essential for homologous recombination, it also contains nuclease activity which degrades any single strand DNA introduced to the cell – such as the recombination cassettes. As strains mutant for RecBCD have severely defective growth, an alternative strategy for subverting the activity of the protein has been developed; using an *E. coli* strain (SW102) which has Recombinant Defective λ phage (the 'Red system') integrated into its genome. This sequence encodes a suite of genes including Gam – which inhibits RecBCD and allows introduction of ssDNA; Exo – which degrades DNA at the 5' end to generate single strand 3' ends and Beta – which binds and protects these exposed 3' ends and allows recombination to occur. Constitutive RecBCD inhibition is detrimental to bacteria – therefore the Red suite of genes is expressed under the negative control of the heat sensitive cI857 protein (also encoded in the phage DNA) which can be briefly down regulated by exposing the bacteria to 42 ℃ condition - providing a short window for introduction of the desired cassette and recombineering (Yu et al., 2000; Copeland et al., 2001).

7.1.3.2.1. GalK selection

Successful integration of exogenous sequence to BACs is screened using a positive/negative selection strategy using the galK gene. This gene encodes the galactokinase enzyme which is essential in phosphorylating galactose into a form which can be metabolised as a carbon source. Homology arms flanking the galk gene sequence are initially used to introduce the gene into the BAC – with selection through growth of transformed bacteria on media in which galactose is the sole carbon source (SW102 *E. coli* are deficient in the galK gene and unable to metabolise galactose). Once a colony containing such a modified BAC is identified, secondary targeting introduces the sequence of interest – which is also introduced with the same flanking homology arms. Successful replacement of the galK sequence with the sequence of interest is confirmed by growth of transformed cells on media containing 2-dexy-galactose (DOG); a galactose analog which when phosphorylated by galK accumulates as a toxic product in cells – therefore selecting cells which have lost the galK sequence through replacement with the sequence of interest (Warming et al., 2005).

7.1.4. Chapter aims

Building on work carried out in previous chapters, the aim of this chapter's work was to develop a vector capable of using endogenous sequence elements to drive expression of BCL-3 protein fused to a fluorescent protein tag - allowing monitoring of BCL-3 protein dynamics in live, single cells over extended periods of times. A particular aim of the work was to determine a tool which had potential for future applications in the field - such as interaction dynamics of the protein and possibly *in vivo* studies - and which expressed protein under the same influences and controls as experienced by endogenous protein. The chapter also aims to provide considerations of the limits of current research and outline possible future research directions to increase the relevance of experimental work to physiological conditions.

7.2. Results

An outline of the cloning strategy used to introduce Venus YFP coding sequence into a BAC containing *BCL3* sequence to produce a C-terminal fusion of Venus to the BCL-3 protein is outlined in figure 7.1. Relevant details relating to cloning and Recombineering steps are outlined below.

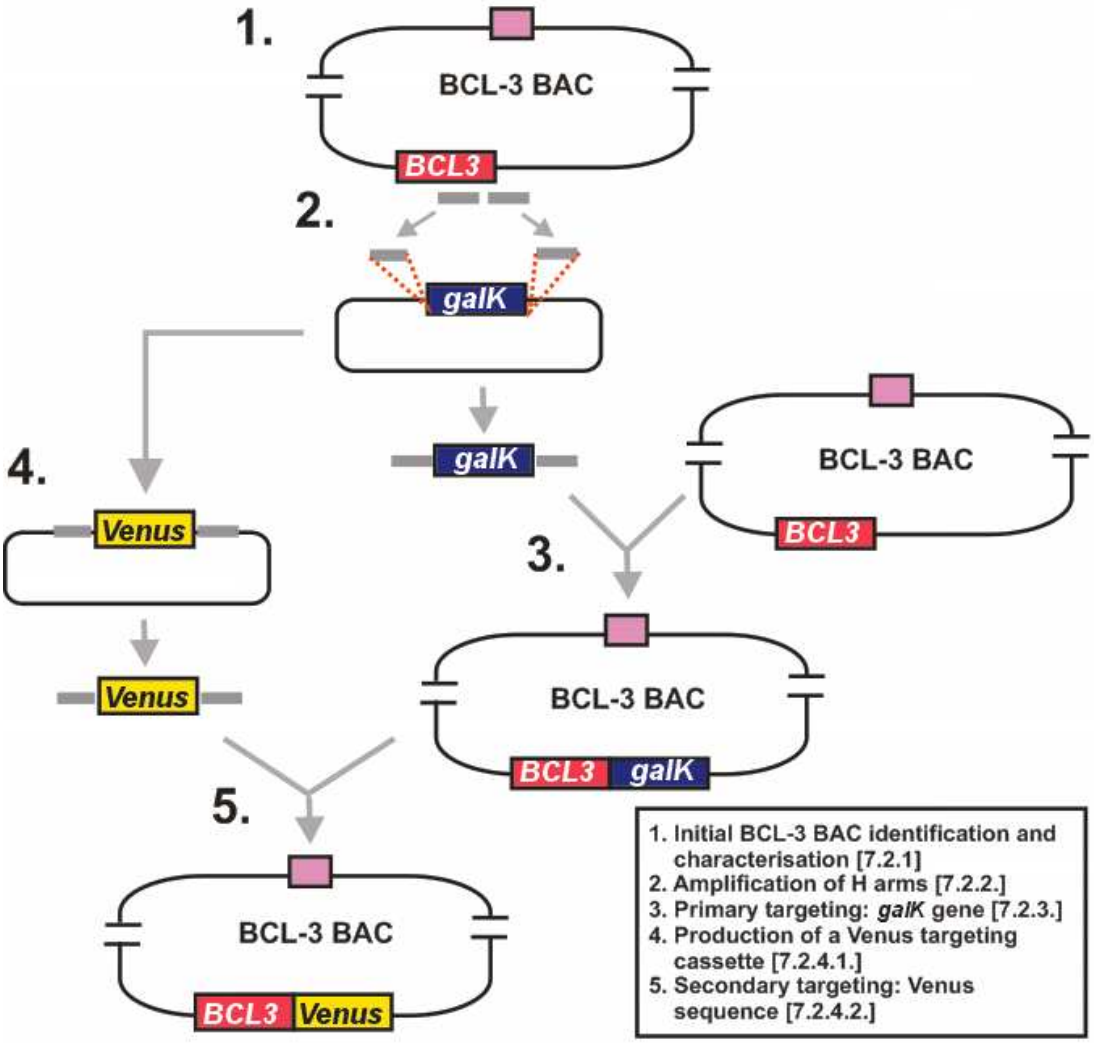

Figure 7.1. Schematic outline of steps involved in the introduction of Venus fluorescent protein coding sequence into a *BCL3* gene containing BAC using a Recombineering strategy. Cloning steps and Recombineering are described in the text, with the relevant chapter sections corresponding to steps in the diagram shown.

7.2.1. Identification and characterisation of a BCL-3 BAC

7.2.1.1. Identification of a BAC containing *BCL3* gene sequence

The genomic location of *BCL3* gene sequence was determined using the Ensembl database (www.ensembl.org; chromosome 19: 45,250,962-45,263,301) and used to identify potential BACs containing sequence spanning this region in the UCSC Genome Browser (http://genome.ucsc.edu/) [2.9.1.]. Several potential BACs contain the BCL3 gene; the chosen BAC (CTD-2608C5) contains 141,941bp sequence with the *BCL3* gene sequence in a relatively central position – with 79,721bp upstream sequence and 50,724bp downstream sequence (fig 7.2.A).

7.2.1.2. Characterisation of the CTD-02608C5 BAC

7.2.1.2.1. Restriction endonuclease digestion profile

The CTD-2608C5 BAC (hereafter referred to as the 'BCL-3 BAC') was obtained as DNA and transformed into the SW102 *E. coli* strain [2.9.2.]. BAC DNA was subsequently extracted from cultures of transformed SW102 [2.9.3.] and characterised to ensure that the human genomic DNA contained was as described in the database. Expected DNA fragment sizes produced by digestion with the SalI and NotI restriction endonuclease enzymes are shown in figure 7.2.B. Extracted (putative) BCL-3 BAC DNA was digested with both enzymes independently [2.9.4.1.] and resolved using PFGE [2.9.4.2.]. Observed digestion profiles matched expectations – with the exception of an approximately 7kb band observed, but not expected, in the NotI digested sample (marked with an * in fig 7.2.B). Given the long length of digestion time (overnight) this is unlikely to be a partially digested fragment – the fragment was observed from multiple, independent, digestions – and presumably results from sequence variations between sequence used to obtain the database sequence and sequence contained within the BAC (a SNP, for example). Smaller fragments sizes (for example the NotI produced 379 and 630bp or SalI produced 280bp) run off the end of the gel under the conditions required for resolution for the larger fragments and are therefore not seen in the gel.

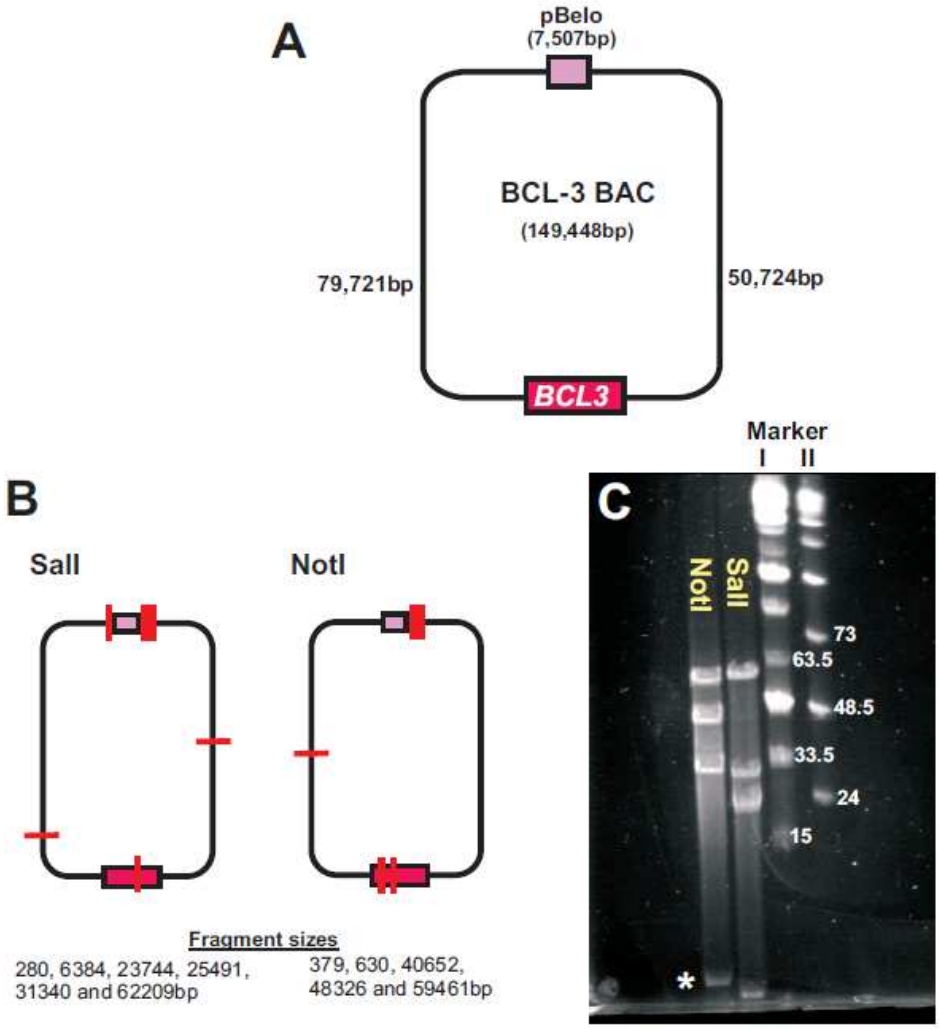

Figure 7.2. Characterisation of the *BCL3* gene sequence containing BAC CTD-2608C5. (A) Schematic image showing the location of *BCL3* gene sequence in the CTD-2608C5 BAC. Image is representative and not to scale. pBelo cassette contains a chloramphenicol resistance conferring gene plus sequences allowing replication of the BAC in bacterial cells. (B) Schematic diagrams showing the location of cleavage site for SalI and NotI restriction endonucleases within the CTD-2608C5 BAC along with lists of expected fragment sizes. Images are representative and not to scale. (C) Digestion profiles of CTD-2608C5 BAC cut with NotI and SalI high fidelity restriction endonculases (both New England Biolabs) as resolved using PGFE. Mid Range PFG marker I and Mid Range PFG marker II (both New England Biolabs) are also shown. Numbers relate to adjacent band sizes in Marker lanes (in kilobases).

7.2.1.2.2. Southern blot

A further confirmation that the correct region of interest is present with the putative BCL-3 BAC was obtained using Southern blotting with three probes complementary to regions proximal to the *BCL3* gene and at more distal sites (both up- and downstream) [2.9.5.1.]. Sites of designed Southern probes

in the CTD-2608C5 BAC are shown in fig 6.3.A. Detection across the entire span of the expected genomic sequence tests for any random recombination events which may have altered the genomic sequence. BAC DNA was extracted [2.9.3.] and cut with EcoRI restriction endonuclease – an enzyme chosen to fragment the BAC into multiple fragments which were subsequently separated using PFGE [2.9.4.2.] (fig 6.3.B). Probes were expected to anneal to bands of size 19, 8.5 and 7.1kb (fig 6.3.A); however, while probes were observed binding fragments of approximately 10 and 8kb, the third probe bound at a smaller than expected fragment size – at approximately 5kb (fig 6.3.C). The smaller than expected fragment size is likely to result from point mutation variation between the expected and actual sequence which creates an additional EcoRI site within one of the fragments complementary to a Southern probe. The binding of all three probes confirms the presence of expected sequence within the BAC, albeit with minor sequence variation, and further confirms the suitability of this BAC to represent *BCL3* genomic sequence.

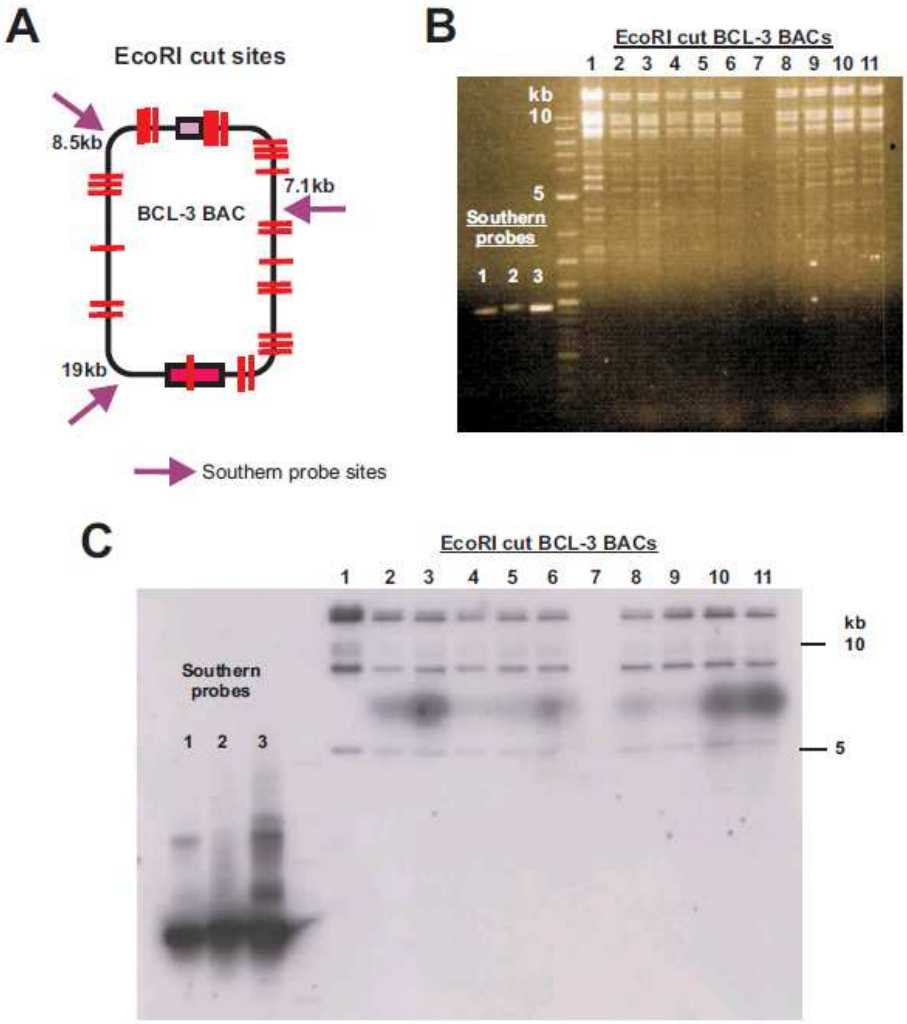

Figure 7.3. Southern blot of EcoRI digested BCL-3 BAC DNA. (A) Schematic map of expected EcoRI sites in the BCL-3 BAC. Sites at which Southern blot probes were designed to anneal to are indicated by purple arrows with corresponding BAC fragment sizes given (in kilobases). Image is representative and not to scale. (B) PFGE resovled 1% agaorse gel showing amplified Southern blot probes (lanes 1-3), ladder (lane 4) and EcoRI cut BCL-3 BAC DNA extracted from 11 transformed SW102 *E. coli* colonies (lanes 5-15). (C) Southern blot performed on DNA fragments resolved on gel as shown in fig 6.3.B using probes SP1,2, and 3. Approximate fragment sizes (in κB) was determined by overlaying images of the original gel (fig 6.3.B) containing a DNA ladder with the produced Southern blot film.

7.2.2. Amplification of homology arms to introduce galK sequence to the BCL-3 BAC by homologous recombination

To introduce galK sequence into the BCL-3 BAC by homologous recombination, short lengths of ~300bp sequence (homology arms/H arms) were introduced either side of the galK gene contained within the pBlueGalK plasmid [2.9.6.1.]. The sequences to be used for H arms were located at the 3'

end of the gene (corresponding to the C-terminus end of the peptide) and were amplified using primers and high fidelity taq polymerase [2.8.3.]. The primers were designed to amplify sequence either side of the *BCL3* gene stop codon (TGA; see fig 6.4.A) – ensuring that homologous recombination would introduce sequence contained within these H arms at this site and remove the stop codon – ensuring continuous translation of the *BCL3* gene and introduced fluorescence protein sequence and creation of a fusion protein.

Primers used to amplify the H arms also introduced restriction endonuclease sites [2.8.3.1.], allowing the sequential introduction of H arms to site either side of galK gene sequence contained within a pBlueGalK plasmid cut with the same restriction endonucleases [2.8.5.] (fig 7.4.B/7.4.C). A linear DNA cassette containing the H arms and *galK* sequence (H-galK-H) was produced by PCR using primers amplifying across this region in the plasmid (primer sites shown as purple bars in fig 7.4.B).

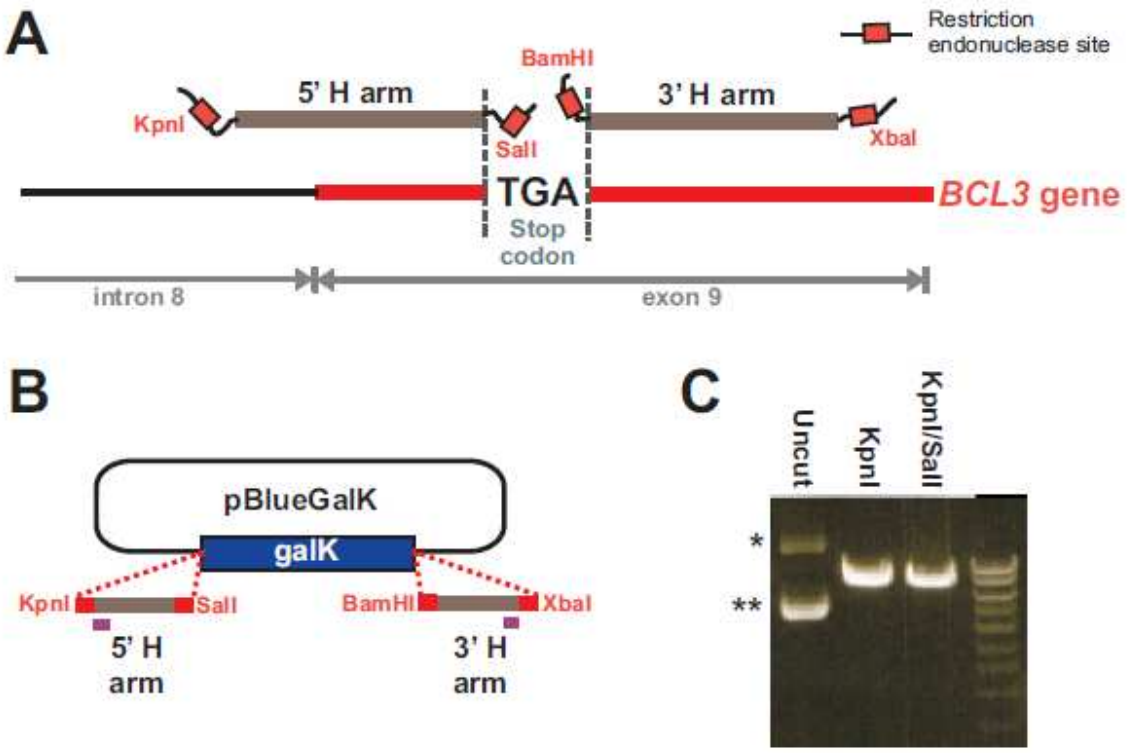

Figure 7.4. Design and production of H arms to introduce *galK* sequence into the BCL-3 BAC. (A) Schematic diagram showing the site of sequence used to amplify H arms at sites either side of the *BCL3* gene's stop codon (TGA) with introduction of restriction endonuclease sites at flanking sites of each H arm. (B) Schematic of the introduction of 5' and 3' homology arms to flanking sites of the *galK* gene contained within the pBlueGalK plasmid. Location of primers to subsequently amplify a linear cassette containing H arms and galK gene are shown as purple bars. (C) Agarose gel showing Uncut, KpnI cut and KpnI plus SalI cut pBlueGalK plasmid as resolved by gel electrophoresis. Uncut plasmid runs as two bands depending on whether the plasmid is supercoiled (**) or not (*).

7.2.3. Introduction of galK sequence into BCL-3 BACs contained within SW102 *E. coli* cells

Produced H-galK-H cassettes were introduced into SW102 cultures which had been induced into a recombination amenable state [2.9.2.] [7.1.3.2.]. Cells in which positive recombination events had occurred were selected by growing transformed bacteria on plates containing galactose as a sole carbon source [7.1.3.2.1.]. A further selection criteria was applied by streaking colonies identified in this way onto MacConkey media plates [Appendix 1] – with colonies in which galactose metabolism is occurring (due to the presence of galK gene) turning bright pink. Such colonies were subsequently grown, stored as glycerol stocks [2.8.2.1.] and BAC DNA extracted for further analysis. Extracted BAC DNA was digested with NotI and SalI high fidelity restriction enzymes and compared to digestion profiles produced from BCL-3 BAC DNA prior to galK homologous recombination (as in fig 7.2.C). Only BACs that retained the original digestion profile were selected.

7.2.4. Secondary targeting: introduction of Venus coding sequence into the BCL-3 BAC

7.2.4.1. Production of a targeting cassette containing Venus flanked with *BCL3* gene H arms

The secondary targeting stage involved the introduction of Venus sequence to replace the previously introduced galK sequence within the BCL-3 BAC. For this, the same H arms as previously used to introduce galK [7.2.3.] were again used. A H-Venus-H cassette was created by initially replacing galK sequence in the pBlueGalK plasmid containing *BCL3* H arms (as previously produced – [7.2.2.]). GalK sequence was excised by cutting the plasmid with SalI and BamHI enzymes and gel extracting the resulting plasmid backbone sequence (which still contains the *BCL3* H arms) (fig 7.5.A and B). Venus sequence was amplified by PCR using primers which introduced flanking SalI and BamHI cleavage sites at the 5' and 3' ends of the Venus sequence respectively. This fragment was cut with these enzymes and subsequently ligated with the SalI/BamHI cut pBlueGalk plasmid – creating a plasmid which contained Venus sequence flanked with 5' and 3' BCL3 H arms (fig 7.5.A). A linear H-Venus-H cassette was produced by amplification, from this plasmid, using flanking primers as before for production of the H-galK-H cassette (fig 7.5.A and C).

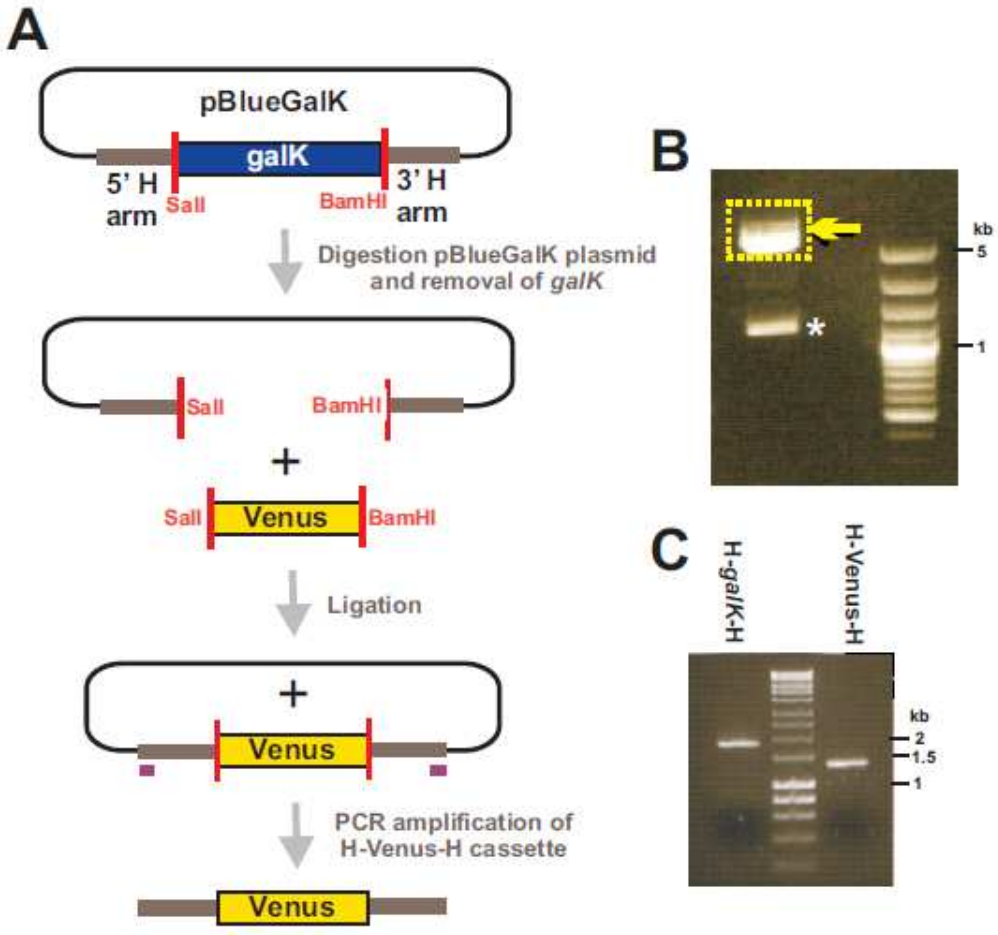

Figure 7.5. Cloning strategy for the production of BCL-3 H arms flanking Venus fluorescent protein coding sequence. (A) Schematic diagram showing the removal of galK sequence in the pBlueGalK plasmid through SalI/BamHI digestion and subsequent ligation into the plasmid of Venus sequence amplified by PCR with the addition of SalI and BamHI restriction cleavage sites. Plasmid contained Venus is subsequently amplified by primers (shown as purple bars) to produce the H-Venus-H cassette. (B) pBlueGalK plasmid digested with SalI and BamHI showing the excised galK sequence (*) and plasmid backbone (yellow box) which was subsequently removed by gel extraction. (C) PCR amplified cassettes of both H-galK-H (~1.8κB) and H-Venus-H (~1.2κB).

7.2.4.2. Secondary recombination introduction of Venus sequence into the BCL-3 BAC

The H-Venus-H cassette produced [7.2.4.1.] was introduced to SW102 cells containing the BCL-3 BAC previously modified to contain the galK sequence [7.2.3.] [2.9.6.1.]. Successful introduction of the Venus sequence was selected for by growing transformed bacteria on media containing deoxy-galactose (DOG) – a galactose analog which accumulates as a toxic compound in cells expressing the *galK* gene. A successful Venus sequence recombination event would result in the removal of galK sequence (the same H arms were used for each recombination) - therefore previously galK+ cells will

be galK- if Venus is incorporated and will be able to grow on DOG media [Appendix 1] [7.1.3.2.1.]. As a secondary screening step, colonies which grew on DOG media plates were streaked onto MacConkey plates to confirm loss of galactose metabolising activity (i.e. cells are galK-). However, cells which have lost the galK gene will not necessarily have done so due to secondary recombination of the Venus sequence; BACs within the cells may simply have lost the galK sequence containing region by a non-homologous recombination. Therefore, colonies which had passed previous selection criteria were assayed for the presence of the Venus sequence – using colony PCR with primers specific to Venus sequence (which had been previously confirmed not to amplify from the galK containing BCL-3 BAC). An example of such a screen performed on 10 potential SW102 colonies is shown in figure 6.6.A. The success rate for the presence of Venus sequence is seen as relatively low – just 30% of these colonies identified as lacking the galK gene also contain the Venus sequence.

Colonies which have confirmed presence of Venus were grown, glycerol stocks made and BAC DNA extracted [2.8.2.1.][2.9.3.]. BAC DNA was then digested with SalI enzyme (as before - [7.2.1.2.1.][2.9.4.1.]) to confirm the BCL-3 BAC had retained its sequence integrity. One difference is expected between the original BCL-3 BAC and sequence into which Venus has been introduced: an additional SalI site is contained within one of the H arms – consequently a former 25.5kb fragment should now consist of 18 and 8.2kb fragments (the introduction of ~700bp Venus sequence accounts for 18+8.2 not equalling 25.5κB) (fig 6.6B). Seven Venus+ BCL-3 BAC containing SW102 colonies were analysed in this manner and resolved using PFGE [2.9.4.2.], with an original BCL-3 BAC sequence also digested with SalI and fragment size markers (fig 7.6.C). The striking difference in digestion profiles obtained from Venus+ BACs (when compared with the original BCL-3 BAC digest) suggests that a considerable level of non-specific recombination is occurring. In all colonies analysed the 6kb band corresponding to the pBelo sequence containing fragment is present (** in fig 7.6.C). This sequence contains the chloramphenicol resistance gene required for colony survival (growth plates and media contain the antibiotic), however considerable recombination has usually occurred at other sites within the BAC sequence.

Such recombination will occur in the brief period of time in which the expression of a recombination amenable suite of genes (the 'Red System' – [7.1.3.2.] is induced in the SW102 cells by heat shock to facilitate homologous recombination of the H-Venus-H cassette. No experimental techniques have as yet been discovered to minimise this non-specific recombination – large numbers of colonies consequently have to be screened. Figure 7.6.C shows an example of 7 colonies screened (out of a total of 54) in which one colony contains a BAC with the required digestion profile (number 6; fig 7.6.C).

This BAC DNA was further checked with PCR; using primers which amplified the recombination cassettes used to introduced first galK then Venus sequence (location of primers is shown as purple

bars in fig 7.7.A). An expected band size of ~1.2kb was produced from this putative BCL-3/Venus BAC – the same size band as produced from the initial plasmid from which the H-Venus-H cassette was amplified and smaller than the band produced from BCL-3/galK BAC template (~1.8kb; fig 7.7.A). PCR was also repeated with the previously described primers used in colony PCR to detect Venus sequence (fig 7.6.A). This assay further confirmed the presence of the Venus sequence – producing the same size bands amplified from the BCL-3/Venus BAC and Venus containing plasmid, with no product observed from PCRs using BCL-3/galK BAC sequence as template (fig 7.7.B).

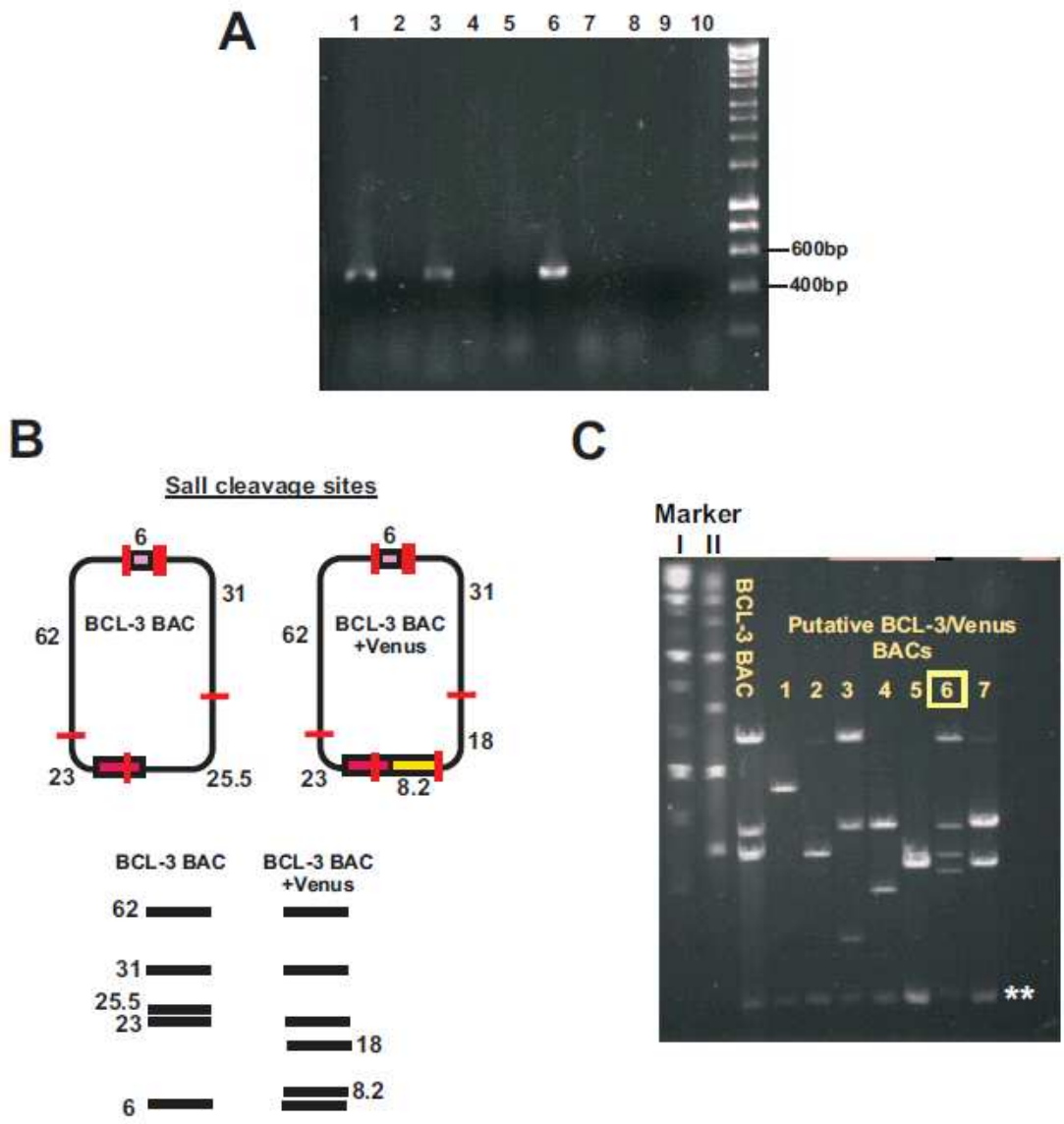

Figure 7.6. Identification and subsequent screening of Venus$^+$ BCL-3 BAC containing SW102 cells. (A) Colony PCR screening of previously galK$^+$ cells which have lost galK gene activity following transfection with a H-Venus-H recombination cassette. PCR performed using a primer within the Venus sequence. Numbers relate to colony number. (B) Schematic map of SalI cleavage sites in an original BCL-3 BAC and the same BAC into which H-Venus-H has been integrated. Expected digestion profiles are also shown for each BAC. Numbers correspond to fragment sizes (in kilobases). (C) SalI digestion profile of 7 Venus$^+$ BCL-3 BAC SW102 colonies resolved by PFGE. 'BCL-3 BAC' refers to an original, i.e. no galK or Venus introduced, form of the BAC. Numbers refer to colony numbers. Mid Range PFG marker I and Mid Range PFG marker II (both New England Biolabs) are also shown. ** refers to 6kb fragment containing the pBelo sequence (see fig 6.2.A).

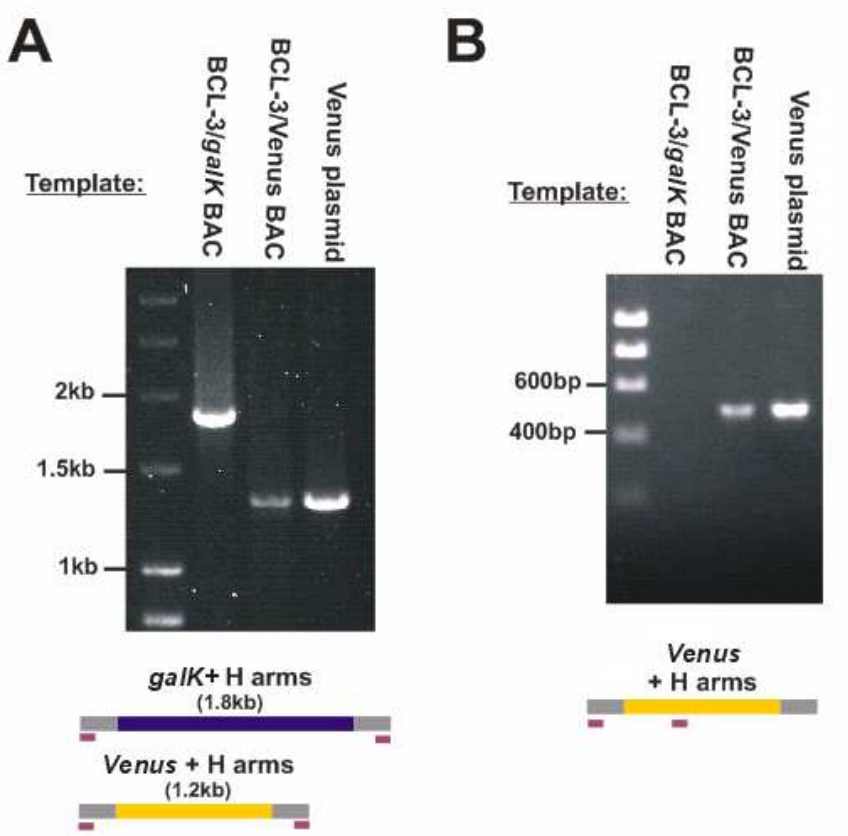

Figure 7.7. PCR confirmation of the presence of Venus sequence in a putatively identified BCL-3/Venus BAC. (A) PCR performed with primers amplifying across the recombination cassette used for both galK and Venus, showing the BCL-3/Venus BAC (lane 3) produced the required size of band (as confirmed by comparison with product amplified from a H-Venus-H containing plasmid – lane 4) and confirming that the BAC had lost the galK sequence (which produces a larger 1.8kb band – lane 2). (B) Confirmation of Venus sequence in the BCL-3/Venus BAC (lane 3) using a Venus specific primer – as comparable with sequence produced from the H-Venus-H containing plasmid and in contrast to no product from the BCL-3/galK BAC.

7.2.4.3. Sequencing of the Venus gene sequence and fusion boundary with the *BCL3* gene

Venus sequence in the BAC, plus the linker sequence between *BCL3* gene and Venus, was confirmed through sequencing from a primer situated within the Venus sequence plus a primer used to produce the 3' H arm (as in figure 7.7.A.). Fidelity of the Venus sequence was retained, the *BCL3* stop codon had been removed plus the linker sequence maintained the correct frame of the Venus sequence (being 33bp in length) [Appendix 9]. Comparison of sequences was conducted using alignment program ClustalW2 (http://www.ebi.ac.uk/Tools/msa/clustalw2/).

7.2.5. Transfection of BCL-3:Venus BACs into human cell lines

7.2.5.1. BAC transfection of HT1080 cells

Initially, HT1080 cells were transfected with 1µg BCL-3:Venus BAC DNA per 35mm culture dish with the ExGen500 transfection reagent [2.3.1.1.] and visualised 48 hours later [2.4.]. Due to the relatively low basal level of BCL-3 present in unstimulated HT1080 cells – as previously observed by Western blotting [3.2.5.1.] – identification of transfected HT1080 cells prior to TNFα stimulation was expected to be problematic. Therefore, wide field images (with a 20x lens) were used to observe multiple cells per frame and to maximise the chance of including a transfected cell. However, following stimulation with TNFα, Venus signal was not observed in any of the ~100 cells analysed over a 12 hour time course – a length of time in which endogenous BCL-3 protein levels had been shown to be induced [3.2.5.1.].

As such, screening of greater numbers of cells putatively transfected with BCL-3:Venus BAC was undertaken using Flow Cytometry; allowing measurement of transfection efficiency (HT1080 cell line not having previously been successfully transfected with BACs in this laboratory). Cells (again grown in 35mm dishes) were transfected with varied quantities of BCL-3:Venus BAC DNA – 0, 0.5 or 1µg per dish – and induced with TNFα for 6 hours in an attempt to increase BCL-3:Venus levels. Flow Cytometry was subsequently used to analyse Venus expression in 10,000 cells [2.11.]. Single viable cells were selected, or gated, for analysis on the basis of their Side and Forward Scatter (SSC and FSC) profiles; allowing removal of dead cells and contaminant particles which display distinct scatter profiles (fig 7.8.A).

No Venus expressing populations of cells were observed in transfected cell populations (when compared to fluorescence levels in untransfected cell populations) (fig 7.8.B). The introduction of BAC DNA – a large and inefficient trnasfection vector – into HT1080 cells was therefore considered to be too problematic to pursue in the time course of this investigation. Attention was instead switched to transfecting the human neuroblastoma cell line SK-N-AS [2.1.1.1.]; a cell line which is amenable to BAC transfection (personal communication: Dr Antony Adamson, University of Manchester).

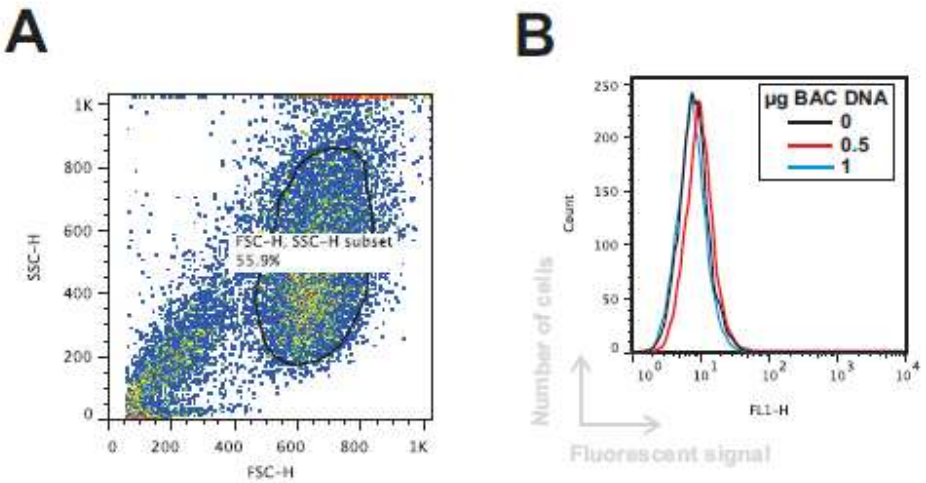

Figure 7.8. Transfection efficiency of HT1080 cells with BCL-3:Venus BAC as assayed by Flow Cytometry. (A) Forward and Side Scatter (SSC-H/FSC-H) profile of cells used to identify live HT-1080 cells (shown enclosed); 10,000 of such cells were analysed for Venus expression (FL-1). (B) Venus expression profiles (FL1) of 10,000 HT1080 cells transfected with 0, 0.5 and 1µg BCL-3:Venus BAC DNA per 35mm dish 48 hours prior to induction with TNFα for 6 hours.

7.2.5.2. BAC transfection of SK-N-AS cells

Populations of SK-N-AS cells grown to 30-50% confluence in 35mm dishes [2.1.] were transfected (ExGen500 [2.3.1.1.]) with 0, 0.5, 1 or 2µg BCL-3:Venus BAC DNA 48 hours prior to analysis, again by Flow Cytometry [2.11.]. In addition, to confirm transfection events, cells were co-transfected with a plasmid constitutively expressing p65-dsRed fusion protein (as previously described [3.2.4.1]; 0.5µg plasmid used per transfection). However, despite showing clear populations of cells expressing the dsRed protein (red arrow; fig 7.9.A), no Venus expressing cell populations was observed in any of the three transfection events (fig 7.9.B).

Co-transfection of vectors is assumed to be equally efficient – i.e. if a cell has taken up one vector it is assumed to also have taken up the other. To confirm that BAC DNA had been introduced to the cells, a PCR based screen was conducted to assay for the BCL-3:Venus transcript in cDNA obtained from populations of SK-N-AS cells transfected with BCL-3:Venus BAC, as before, and induced with TNFα for 6 hours [2.1.3.]. Primers were used which bound the Venus sequence – as before [7.2.4.2.] (fig 7.7.) – allowing detection of transcript derived purely from the exogenous BCL-3:Venus sequence. Such transcripts were detected in two independent populations of SK-N-AS cells transfected with BCL-3:Venus BAC , in contrast to untransfected cell populations (fig 7.9.C).

Therefore, while transcripts of the BCL-3:Venus recombinant gene are observed, the protein appears not to be expressed to detectable levels. Potential reasons for this are discussed in [7.3.1.].

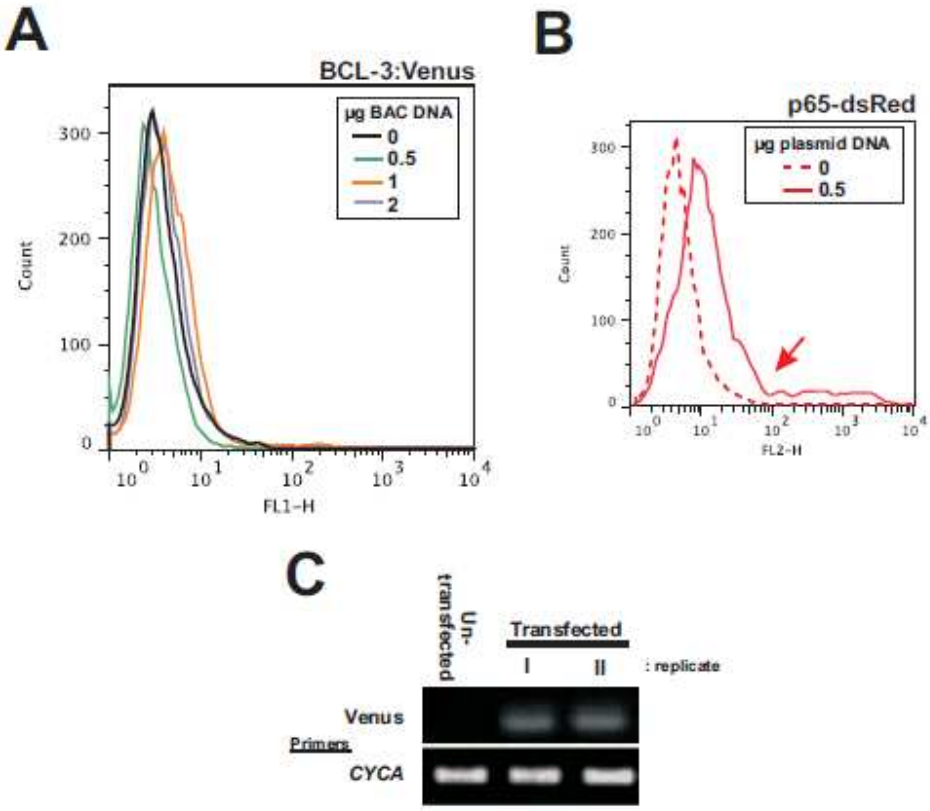

Figure 7.9. Analysis of SK-N-AS cells co-transfected with BCL-3:Venus BACs and p65 expressing plasmids. All SK-N-AS cell populations transfected with p65-dsRed expressing plasmid show dsRed expressing populations – an example is shown in (A) of enhanced dsRed levels (FL2) in cells transfected with 0.5µg plasmid DNA in comparison to plasmid untransfected cells (both cell populations were also transfected with 0.5µg BCL-3:Venus BAC DNA). However, no noticeable populations of Venus expressing cells (FL1) are seen in cells transfected with 0.5, 1 or 2 µg of BCL-3:Venus BAC DNA when compared with untransfected cells (all cells were also transfected with 0.5µg p65-dsRed plasmid) (B). (C) Detection of BCL-3:Venus transcripts in SK-N-AS cells transfected with 0.5µg BCL-3:Venus BAC DNA (replicated twice: I and II) using Venus amplifying primers (as in fig 7.7.B). *CYCA* primers used as positive control.

7.3. Discussion

In this study, a BAC engineered to express a BCL-3:Venus protein fusion has been produced and shown to successfully transfect into SK-N-AS cells. However, despite transcribing the introduced *BCL3*:Venus gene, a fluorescent protein signal was not observed [7.2.5.2.]. As such, it is considered that the BCL-3:Venus protein was either unstable or unable to form the folded conformation necessary for the attached Venus protein to fluoresce.

7.3.1. Problems with the expression of recombinant protein fusions

The occurrence of such misfolded protein fusions is likely to be underappreciated – due to the disinclination to publish negative results. However, given the size of fluorescent tags (typically ~25-30kDa), effects on folding of attached endogenous proteins is perhaps not surprising. In terms of a mechanistic explanation, overexpression of recombinant protein (the BCL-3:Venus is expressed in addition to the endogenous protein) can cause aggregation of BCL-3 protein which in turn prevents the correct folding of the fluorescent protein tag – affecting its ability to form a flurophore (Wang and Chong, 2003). Such protein aggregation can be caused by coalescence of misfolded endogenous protein and exposure of hydrophobic regions which would normally be sequestered within the protein (Rajan et al., 2001). It is possible that a more stable protein would be produced with an N-terminal Venus fusion to BCL-3; however, the extensive work required to produce such a vector was unfortunately outside the time scale of this project.

7.3.2. The importance of non-coding sequence in gene expression tools

Despite the extensive amount of work involved in the production of a BCL-3:Venus expressing BAC – and the lack of a successful product in this particular case - the value of the approach in terms of greater incorporation of genomic sequence must again be emphasised. This feature of the BAC expression system is particularly relevant in light of the demonstrated negative feedback BCL-3 effects on transcription of its own gene [5.2.1.6.1.]; a function which has previously been shown to occur via a site within the *BCL3* gene's second intron (Brocke-Heidrich et al., 2006). Incorporation of *BCL3* intronic sequence would require a length of genomic DNA of approximately 12kb (start of the 5'UTR to end of the 3'UTR) plus promoter and required enhancer sequence – a length of sequence which plasmid and lentiviral systems could not accommodate. Inclusion of the endogenous negative regulation is considered to be an essential aspect of BCL-3 regulation necessary to represent endogenous expression of the protein.

7.3.3. BCL-3 in single cell expression systems

The development of a tool to accurately monitor BCL-3 protein dynamics in single cells will enhance understanding of the protein and prevent population dynamics from obscuring characteristics at the single cell level [7.1.]; however, the vast majority of work concerning BCL-3 activity, including work in this thesis, has been conducted at the population level. For meaningful interpretation of BCL-3 single cell dynamics, therefore, single cell resolution work must also be conducted in tandem on factors which induce BCL-3 and upon which BCL-3 acts. In relation to this study, such work would involve the monitoring of *TNFA* and *BCL3* mRNA plus TNFα protein dynamics. Measurement of gene transcript dynamics can utilise marker gene expression driven by endogenous promoter sequence or, at a greater resolution, using systems such as MS2 to measure the production of single transcripts (Yunger

et al., 2010). Such systems not only retain the endogenous gene transcript sequence rather than reporter gene – retaining sequence elements which can influence transcript stability – but also give information on the number of transcripts produced rather than a relative level of reporter gene encoded protein signal. As previously noted [6.3.2.], measurement of TNFα protein dynamics is a technically challenging problem.

7.3.4. From cells to tissue: future applications of BAC expression tools

While a generalised trend in the field of gene/protein expression has been a move from population to the single cell level; increasingly studies are attempting to reconstruct population behaviour as a result of aggregated single cell behaviours. Integral to such work is the visualisation of protein dynamics at single cell resolution within the context of a tissue, or perhaps even an organ, system. Constructed BAC expression tools have potential value in observing protein expression beyond the cell culture level; BAC vectors have been successfully used to create BAC transgenic mice expressing GFP tagged proteins (Gong et al., 2003). While such transgenic techniques are not applicable to reconstitute transgenic humans, *ex vivo* reconstruction of human tissue and organs (so-called synthetic human tissue models or 'organoids') from pluripotent stem cells raise the possibility of using BACs to visualise proteins in such applications. Notably, studies in recent years have refined the production of human intestinal epithelium structures using 3D cell culture techniques in gel matrices infused with growth factors – particularly of note given that this is the site of several poorly understand inflammatory conditions such as inflammatory bowel and Crohn's disease (Sato et al., 2009; Spence et al., 2010). Regeneration of human tissue in immune deficient mice is a further potential application for BCL-3 BAC containing human cells (Khavari, 2006).

Chapter 8
Conclusions

8.1. Summary of conclusions derived from this work

Work in this study has confirmed, in the human fibrosarcoma HT1080 cell line, that the *TNFA* and *BCL3* genes are induced by TNFα through the NF-κB signalling pathway and that this *TNFA* induction is subsequently inhibited by BCL-3 – forming an Incoherent Feed Forward Loop (I-FFL) (Chapter 3). A noted delay in *BCL3* transcript increases, relative to *TNFA* transcripts, was shown to occur due to (i.) poised RNAP binding at the *TNFA* promoter and (ii.) the requirement for chromatin remodelling at the *BCL3* gene promoter to allow NF-κB and RNAP to bind at this region (Chapter 4). The implications of the differential response speeds of *TNFA* and *BCL3* genes was investigated through the construction of a mathematical model. This model was able to demonstrate benefits of a delayed BCL-3 inhibition of *TNFA* transcription: permitting highly efficient synthesis of *TNFA* mRNA but in short bursts plus continued sensitivity to low pulsed TNFα stimuli but a decreasing responsiveness to continued larger TNFα pulses. Such kinetic responses were considered to be physiologically beneficial [5.2.4.][5.2.5.5.] and were unobtainable without the delayed transcription of *BCL3* (Chapter 5). Furthermore, a model constructed which considers TNFα secretion and consequent feedback on cells demonstrated the effect that differential molecule stability, once secreted, can have in such systems and illustrated the need for greater data in this area [6.3.2.]. Finally, the development of tools for the analysis of live cell BCL-3 protein dynamics was discussed and preliminary efforts in this area outlined (Chapter 7).

8.2. Timing in genetic circuits

A key outcome of this study has been the observation that the output of a genetic motif can depend not just on the occurrence and rate of interactions constituting the motif but also their timing. Notably, genetic circuits are often represented as a web of linked interactions (‘arrow’ or ‘wiring’ diagrams) in which interactions are dependent purely on the concentration of constituent molecules. However, when considering transcription events such interactions are often extremely simplified; for example, the presence of transcription factor X induces instantaneous mRNA production of gene Y; $X \rightarrow Y_{mRNA}$. In reality, such interactions (or ‘arrows’) incorporate numerous sub-reactions, as shown for the NF-κB → $BCL3_{mRNA}$ interaction which includes histone acetylation and chromatin remodelling (Chapter 4); interactions which delay the rate of *BCL3* mRNA production and create distinct output dynamics of the I-FFL within which the interaction resides. Inclusion of such events is vital in maintaining accurate

transcription timing, with oversimplification potentially missing model elements capable of significantly altering motif output.

This point is of particular relevance given that Systems Biology models show an increasing tendency to expand in constituent component number in order to cover wider networks of genes and proteins. Given the potential errors in reaction timing, which could result from omission of reaction details, care must be taken to ensure that such expansion does not come at the expense of detailed analysis of individual interactions; rather, such networks should be built up of such detailed studies. Notably, techniques are being developed to incorporate both instantaneous and time-delayed interactions into Bayesian genetic networks, however substantial further work is required to base such large scale networks on (Morshed et al., 2012).

Such requirements raise a dilemma: focusing on a single or limited number of cell lines will create comprehensive data sets necessary for model construction but potentially limits the model's applications to just a few cell types. Notably, the variation in nucleosome positioning observed between cell types mean transcriptional responses to common stimuli may vary in occurrence or rate of occurrence (John et al., 2010) – particularly given that small changes in nucleosome position can have substantial effects on the ability of proteins to bind [1.5.2.]. Such issues are widespread in molecular biology; analogies can be made to the use of model species such as *Arabidopsis thaliana* to represent all plant species. Broadening studies to further cell types will benefit the creation of multiple cell type models for use in simulation of tissues niches – an essential goal for emulating physiological scenarios.

8.3. RNA polymerase II dynamics

In addition to delays in transcript initiation caused by chromatin remodelling, the process of transcript elongation is also a potentially neglected source of variation in transcript production timing. Notably, in a study in which the elongation time required to produce a gene was increased (through experimental variation in intron size), such behaviour was able to significantly alter the output dynamics of an autoinhibitory motif in which the gene was present (Swinburne et al., 2008).

Despite its importance, available data on RNAP dynamics is relatively low resolution; predominately based on the extrapolation of fixed point gels into a series of dynamic events. Current modelling (including this study) uses theoretically derived parameters for the rate of RNAP elongation and transcription timing. For models to gain enhanced ability to describe RNAP dynamics, further data will be required; both more accurate descriptions of the events constituting RNAP promoter escape and quantitative measurements of such processes. Single molecule studies on RNAP are showing this to be a complex process, with considerable variation in the time taken to produce different RNA

molecules. Such variation in elongation rates can be due to sequence elements – for example secondary RNA structures – or processes such as splicing, in which considerable variation is observed in the time taken to splice different introns (Schafer et al., 1991; Audibert et al., 2002). Even more striking is variation in the time to produce different RNA molecule of the same sequence. The occurrence of elongation, far from being a continuous processive event, is increasingly shown to occur in a series of short bursts through nucleosome associated regions of DNA. Such bursts are proposed to occur when thermal fluctuations in DNA-histone interactions within a nucleosome barring the RNAP progression cause a partial unwinding of DNA from the histone core, permitting RNAP to move into this previously occluded sequence, destabilising the entire nucleosome (possibly via recruitment of remodelling enzymes) and permitting passage of the enzyme (Hodges et al., 2009). Such a method of motion suggests a highly stochastic elongation process. In addition, the binding and initiation of subsequent RNAP molecules following a successful transcription event is a highly stochastic process, with varied refractory periods between RNAP binding events – potentially due to the induced remodelling of promoter region chromatin into a non-permissive state by successful completion of promoter escape by RNAP (Métivier et al., 2003; Harper et al., 2011). Not surprisingly, mammalian mRNA outputs have been seen occurring stochastically in single cell studies, with production occurring at varied times after introduction of an initial stimuli (Raj et al., 2006; Larson et al., 2009). Further modelling work incorporating stochastic elements into transcription would be informative as to any effects such variation can have on motif outputs.

8.4. Measuring chromatin remodelling dynamics

A further area in which enhanced characterisation would benefit models is the post transcriptional modification of histones and subsequent binding of chromatin remodelling complexes. Histone acetylation, far from being a bulk quantity issue, is increasingly linked to modification of specific lysine residues and the enabling of further binding of these sites by specific proteins [1.5.4.]. Identification of the specific lysine residues modified, and downstream effects of these events, will assist in the measurement of temporal occurrence and the construction of models representing this process.

Highly admirable studies such as Metivier et al. have considered specific histone residue acetylation (and methylation) in time course experiments. However, this work was informed by substantial earlier studies of a well characterised signalling molecule (ERα) binding at a highly studied promoter (pS2) – at which the species of protein binding and nucleosome sites had been identified (Métivier et al., 2003). Broader analysis of differential promoter sites will allow identification of general principles of chromatin modification and remodelling; however, it is difficult to assess how applicable data derived from such model promoters can be applied to other sites without considerable studies confirming that the promoters act in a comparable manner.

Work conduced in this thesis, in concert with wider work in the field, shows chromatin state across the genome is important in not just determining whether genes are able to respond to transcriptional stimuli but also in affecting the timing of response (Natoli et al., 2011). Genome wide profiling of nucleosome positioning is increasingly showing variation in nucleosome occupancy between different cell lines derived from the same species (John et al., 2010); potentially acting as a mechanism for cell types to respond differently to the same inductive stimuli. Notably, NF-κB binding at the *IL6* gene promoter is observed rapidly – following LPS stimulation – in fibroblast cell lines but only after several hours at the same location in macrophage cells (Natoli et al., 2011). Chromatin state should not, however, be considered a static property but a dynamic and changeable one; furthermore, chromatin remodelling at a site can potentially persist over long periods of time – notably, an induced nucleosome depleted region in the promoter of the *S. cerevisiae PHO5* gene has been observed to be inherited through DNA replication in the absence of active transcription or the presence of continued activator presence (Ohsawa et al., 2009).

8.4.1. Measuring chromatin modifications and states: Population and single cell studies

The occurrence over time of histone modifications, protein binding at promoters and chromatin state is measured in general, and in this study, using ChIP or restriction endonuclease assays conducted at population level at discrete time points. However, research on transcription is increasingly carried out at the single cell level in real time - to measure mRNA and protein levels/localisation – raising potential discrepancies regarding the comparison of data raised in these two distinct manners.

Several techniques have been developed to measure protein-DNA interactions in real time, including:

(i.) Fluorescent loss in photo bleaching (FLIP): utilising multiple concatenated DNA binding sites in a cell line expressing fluorescent tagged binding proteins to create a visual foci of binding, the recovery or loss of which can be assayed following denaturation of fluorescent protein by photo bleaching (Bosisio et al., 2006).

(ii.) Fluorescence correlation spectroscopy (FCS): measuring the alteration of a fluorescently tagged molecule's diffusion time through a small intracellular volume as a result of binding DNA (Michelman-Ribeiro et al., 2009).

In addition, *in vitro* techniques can also be utilised. Surface plasmon resonance (SPR) measures the change in resonance of a surface bound with immobilised DNA molecules resulting from binding of additional molecules provided by purified protein solutions. Cell lysates can also be used but in this case the identity of binding protein is not necessarily apparent (Stockley and Persson, 2009). FRET has also been used to dynamically measure the association between fluorophore tagged DNA and histone molecules in real time (Li et al., 2005).

While offering benefits in terms of measurement time points and observations based on single cell, or small numbers of molecules, such techniques do also have several disadvantages. These include the use of modified (fluorescent protein tagged) rather than endogenous proteins often expressed at high levels, the use of altered DNA binding sites (large numbers are required to produce a visible foci), performance in an *in vitro* environment, which may not include all endogenous factors related to DNA binding, and the use of relatively small lengths of DNA which may not accurately recreate endogenous chromatin structure.

While ChIP and endonuclease cutting assays may have low temporal resolution, they do offer several advantages over current microscopy based techniques. The techniques are unobtrusive - requiring no introduction of exogenous DNA sequence or proteins - and observe chromatin in its natural *in situ* conformation. ChIP is also able to distinguish between particular post transcriptionally modified forms of proteins (assuming specific antibodies are available) – something fluorescently labeled protein assays cannot do.

Performance of higher temporal resolution ChIP studies have been performed – at one minute intervals – following transcription stimulation (Métivier et al., 2003); however such studies are both time and financially expensive. In addition, to get synchronised populations of cells, such studies use inhibitors of RNAP such as α-amanitin – an inhibitor of RNAP translocation – to ensure no basal transcription; however, the effects of such factors on paused RNAP is unclear. Also, stochastic responses have been hypothesised to have a function in tissue level responses (Paszek et al., 2010), coordinating cell populations will destroy such behaviours and further distance experimental work from physiological conditions.

As such, measurement of the binding of proteins to promoters and resulting chromatin state changes remains an exercise in pragmatism; utilising techniques but being aware of their limitations. The difficulty in measuring PTM of histones is part of a wider technological bottleneck regarding this area, for example phosphorylation events in signalling cascades. Regarding the measurement of changes in chromatin state, an immediate methodology could perhaps conceivable involve the reconstruction *in vitro* of a region of chromatin which is shown to exist in a native conformation – as for the extensively studied mouse MMTV promoter (Deroo and Archer, 2001) – to which various cellular components can be introduced and techniques such as FRET used for real time visualisation.

8.5. Regulating cytokine expression levels

Previous studies regarding cytokine production have often focussed on the problems of too much production (e.g. cytokine storms) but often neglect to consider the problems of too little cytokine response. Cytokine signals are transient molecules which need to induce a lengthy process;

consequently, in the absence of signal amplification, long processes such as wound healing are unlikely to be carried out to completion. Mechanisms controlling the size of cytokine responses are essential but need to be considered in the light of producing an optimum amount of response commensurate with the inductive signal.

An important point made in this study is the ability of the described I-FFL to not only robustly inhibit *TNFA* transcription, but for this inhibition to occur only after a sizeable initial *TNFA* mRNA pulse. A delayed inhibition of *TNFA* transcription is shown to be beneficial in this regard by uncoupling the final amount of protein produced (i.e. magnitude of inhibition) from its response time [5.2.2.]. Furthermore, as inflammatory responses are long processes, consideration was also given to subsequent (i.e. beyond the first) TNFα stimuli of cells, with regard to their *TNFA* transcriptional response. Here, BCL-3 induction was insensitive to infrequent or small pulse NF-κB stimuli [5.2.5.], effectively acting as a kind of memory of previous inflammatory stimulation in which the inhibitory mechanism was only triggered if sufficient previous stimulation has been incurred. Such desensitisation mechanisms have been previously outlined, such as receptor desensitisation, i.e. removal or inactivation of signal perceiving receptor. However, mechanisms which focus on inhibition at specific gene targets allow signal (TNFα in this case) to still be perceived in general by the cell, but selective responses, *TNFA* transcription, are altered dependent on previous recent stimulatory environment.

As previously remarked [6.3.2.], far greater physiological data is required on cytokine expression dynamics, quantities, persistence and 3D arrangements of cells which act in an inflamed location. Without such observations there is a risk that experimental work, if not conducted in light of good physiological observations and input, will drift to increasingly theoretical status.

8.6. Further mediators of *TNFA* transcription

BCL-3 cannot directly bind DNA but acts within a complex with p50 or p52 homodimers [1.3.2.]. While BCL-3 levels have been considered in this study, for simplicity p50 or p52 levels have not. Details regarding levels and localisation of such homodimers are relatively poorly characterised and subject to change upon cell stimulation: transcription of the p50 encoding gene can be induced by NF-κB (Ten et al., 1992) plus induced processing of p50/p52 bound to their unprocessed precursor forms into p50/p52 homodimers allows nuclear translocation [1.2.2.]. Defining the dynamics of such induction will further refine our understanding of BCL-3 activity.

While BCL-3 is an important factor in attenuating TNFα self induction, the existence of other factors must be acknowledged. Additional down regulation of inflammatory signalling can also occur by desensitising cells to continued cytokine signalling though secretion of soluble forms of cytokine receptors (i.e. dissociated from intracellular signalling pathway) – which reduce the concentration of

free cytokine able to bind cell surface receptors – for example sequestration of free LPS by high-density lipoproteins (HDL) (Kitchens et al., 2000). Alternatively, prolonged cytokine signalling can also down regulate expression of inflammatory signal detecting receptors; for example, the TLR4 receptor in response to LPS signalling (Hadley et al., 2007). Signalling pathways can also be targeted; for example, the suppressor of cytokine signalling (SOCS) protein family member SOCS1 has a documented role in targeting nuclear p65 for degradation in prolonged cytokine signalling (Strebovsky et al., 2011).

Inflammatory cytokine induction of anti-inflammatory cytokine expression can also attenuate signalling; notably IL-10 which can increase the stability of IκBa proteins and consequently reduce the ability of NF-κB to enter the nucleus in the presence of inflammatory cytokines (Shames et al., 1998) or induce, via the STAT3 signalling pathway, an inhibitory factor which targets inflammatory cytokine genes (including *TNFA*) (Murray, 2005). However, it must be further noted that a strong candidate for the IL-10 induced negative factor is BCL-3 itself [1.3.9.]; furthermore, no IL-10 expression was detected in HT1080 cells in this study [3.2.3.]. However, the integration of fibroblasts into a fully physiological context may require further work considering signals not only derived from the fibroblasts themselves (monoculture) but also signalling factors derived from various additional cell types. The value of fibroblast inclusion in such experimental systems or models is emphasised by this study; with fibroblasts shown as able to respond to and produce cytokine signal integral to the inflammatory response. Signalling motifs such as outlined here regulate the magnitude of such responses; further studies will be needed to integrate this TNFα regulating mechanism with other signalling pathways, cytokine signals and, furthermore, within multi-cell type enviroments.

8.7. Additional considerations for the work

8.7.1. Further κB sites potentially relevant to *TNFA* transcription

As previously noted [1.4.5.1.], there are considerably more κB sites in the region of the *TNFR* gene than analysed in this study – which has purely concerned four sites within 1 kb of the gene's TSS. This is a reflection of the current state of knowledge concerning the functionality of κB sites and *TNFR* transcription – for which little, or nothing, is known regarding more distal sites. Furthermore, the close proximity of genes either side of the *TNFR* gene sequence (see figure 1.3) means that κB sites close to this gene cannot be assumed to have a functional role in its transcription; they are also close to additional genes, or alternatively – as discussed in [1.6.1.]- they may only act on gene promoters at a far more distal location. Further studies will be required to assess whether any of the additional κB sites in this region of the genome have a role in regulating *TNFR* transcription. A recent example of such work was performed by Smallie et al., who deonstarted that a κB site downsltream of the *TNFR* gene's 3'UTR was required for LPS stimulated transcription of the gene through p65 mediated

recruitment of cyclin-dependent kinase (CDK) 9 whih was required for transcription elongation (Smallie et al., 2010).

8.7.2. Further mechanisms negatively regulating *TNFA* transcription

Work in this thesis has not considered additional, i.e. non-BCL-3, mechanisms for preventing prolonged NF-κB induction of *TNFA.* Such mechanisms include removal of NF-κB by IκBα [1.4.3.1.] and insensitivity to prolonged TNFα signalling through A20 [1.4.3.2.], which both act to inhibit NF-κB action by preventing its nuclear localisation. While further work considering these elements would be beneficial, it is considered that the BCL-3 mechanism has prominence in terms of longer term inhibition of NF-κB induction of *TNFA* transcription. To support this assertion, data in Ashall et al., showed that a 200 minute gap in between TNFα pulses in SK-N-AS cells led to no change in NF-κB nuclear localisation (Ashall et al., 2009). Furthermore, in this study no difference was observed in the nuclear presence of p65 (as assayed by immunocytochemistry; fig. 5.8./[5.2.3.1.]) induced by secondary TNFα stimulation administered at varying times after an initial 180 minute stimulation. Therefore, no mechanism acting to inhibit the nuclear movement of NF-κB was active; however, *TNFA* transcription was still restricted in a manner correlating to time since the previous TNFα stimulation due to BCL-3. BCL-3 is therefore considered a mechanism for longer term moderation of *TNFA* transcription in response to cell stimulation with TNFα – a fact which may be important in moderating inflammation which, as previously stated, is a process which occurs over a long time period. Such a gene specific mechanism may be beneficial, as it can limit inhibition to specific gene targets rather than all NF-κB target genes (as a mechanism which inhibits NF-κB entry to the nucleus does).

In addition, a study performed by Rao et al. has shown that IκBβ is able to bind p65:c-Rel heterodimers bound to proximal sites in the *TNFA* gene promoter and make such complexes resistant to removal by IκBα (Rao et al., 2010). Therefore, even in nuclei in which p65 levels appear low in the nucleus in general, such complexes may still be stably bound at DNA sites, such as in the *TNFA* promoter, prolonging transcription. In such a scenario, mechanisms which prevent more p65 entering the nucleus will not be able to prevent prolonged binding by existing nuclear p65 complexes. However, the BCL-3 mechanism outlined in this thesis can: by directly binding at promoter sites and causing a negative transcription effect which could override the prolonged p65 complex binding.

APPENDICES

Appendix 1: Methods

50x TAE buffer
121g Tris base
28.6ml acetic acid
50ml 0.5M EDTA (pH 8.0)
Make up to 500ml with dH_2O.

10x TBE buffer
108g Tris base
55g Boric acid
9.3g EDTA
Made up to 1l with dH_2O.

6x DNA Loading buffer
3ml glycerol
7ml dH_2O
0.2% (w/v) bromophenol blue

Bacterial culture plates
All plate were prepared under aseptic conditions and stored/cultured in an inverted orientation. Unless otherwise stated, all antibiotics were used at concentrations given in table A.1.

Table A.1. Antibiotics used in culture plates

Antibiotic	Dissolved in	Concentration (µg/ml)
Ampicillin	Water	50
Chloramphenicol	Ethanol	15
Kanamycin	Water	30
Tetracycline	Ethanol	12.5

i. LB plates
LB Agar (Sigma-Aldrich) was dissolved in dH_2O (37.5g/l), briefly boiled to fully dissolve and autoclaved at 121 ℃ for 15 minutes. Media was cooled to 50℃ prior to addition of relevant antibiotics and pouring in to Petri dishes to set.

ii. McConkey plates
McConkey agar media powder (BD Difco) was dissolved in dH_2O (40g/l). The media was briefly boiled, then autoclaved at 121 ℃ for 15 minutes. The media solution was cooled to 50℃, then 1% galactose (autoclaved), chloramphenicol and tetracycline were added and the media poured into Petri dishes and left to cool.

iii. M63 minimal media plates
5x M63 minimal media
10g $(NH_4)_2SO_4$
68g KH_2PO_4

2.5mg $FeSO_4.7H_2O$
Adjust to pH7.0 with KOH (10M) and autoclave.

A 15g quantity of agar (Sigma-Alrich) was dissolved in 800ml dH_2O, autoclaved and cooled to 50℃. Once cooled, 200ml of 5x M63 media and 1ml of 1M $MgSO_4.7H_2O$ (autoclaved) was added and total volume made up to 1 litre with dH_2O. Volumes of 5ml of d-biotin (0.2mg/ml; sterile filtered), 4.5ml L-leucine (10mg/ml; sterile filtered) and Chloramphenicol to a final concentration of 12.5µg/ml were then added.

Finally, a carbohydrate source was added to the solution, using either:

- 10ml of 20% galactose (autoclaved), or
- 5ml 20% 2-deoxy-galactose plus 5ml 20% glycerol (both autoclaved).

Media was then poured into Petri dishes and left to cool.

LB Broth
LB Broth (Sigma-Aldrich) was dissolved in dH_2O (20g/l), boiled and autoclaved at 121 ℃ for 15 minutes and cooled to room temperature. Relevant antibiotics were added to the media as required immediately prior to use.

M9 media
6g Na_2HPO_4
3g KH_2PO_4
1g NH_4Cl
0.5g NaCl
Make to 1 litre with dH_2O and autoclave.

SOC
20g Bacto Tryptone
5g Bacto Yeast Extract
2ml 5M NaCl
2.5ml 1M KCl
10ml 1M $MgCl_2$
10ml 1M $MgSO_4$
20ml 1M glucose
Made up to 1l with dH_2O.
Autoclaved.

Appendix 2: Equipment suppliers

Table A.2. Cell culture equipment/reagents

Item	Catalogue number	Supplier
T75 flask	3290	Corning Inc., distributor in UK – Appleton Woods Ltd., Birmingham
6 well plate	3335	Corning Inc., distributor in UK – Appleton Woods Ltd., Birmingham
150 mm Tissue Culture Dish	12-556-003	Fisher Scientific Ltd., Loughborough, UK
22x50 mm No 1 SLS Cover Slip	MIC3316	Scientific Laboratory Supplies Ltd., Wilford, UK
Cryogenic vial	73.379	Sarstedt Ltd., Leicester, UK
Dimethylsulfoxide (DMSO)	D8418	Sigma-Aldrich Company Ltd., Dorset, UK
Dulbecco's Modified Eagle's Medium	56469C	Sigma-Aldrich Company Ltd., Dorset, UK

Dulbecco's Phosphate Buffered Saline without Ca&Mg	D5652	Sigma-Aldrich Company Ltd., Dorset, UK
Foetal Bovine Serum Heat Inactivated	F4135	Sigma-Aldrich Company Ltd., Dorset, UK
Iwacki cell culture microscopy dishes	3931-035	Iwacki
Microscope Slide SuperFrost®	A00008032E	Menzel-Glaser, Charnock Richard, UK

Table A.3. Plasticware

Item	Catalogue number	Supplier
15ml tube	SS-4001	Sarstedt Ltd., Leicester, UK
50ml tube	SS-8004	Sarstedt Ltd., Leicester, UK
96 well PCR plates	E1403-8200	StarLab, Milton Keynes, UK
Advanced Polyolefin StarSeal 96-well Plate Sealant	E2796-9792	StarLab, Milton Keynes, UK
Eppendorf Tube (0.5ml)	0030 121 023	Eppendorf Ltd., Cambridge, UK
Eppendorf Tube (1.5ml)	0030 120 086	Eppendorf Ltd., Cambridge, UK
Syringe Filter 0.45 µm	17598Q	Sartorius Stedim Ltd., Surrey, UK

Restriction endonuclease enzymes and buffers
New England Biolabs Ltd (Hitchin, UK): NotI, SalI.
Roche Diagnostics Ltd (Burgess Hill, UK): BamHI, EcoRI, PstI, XbaI.
Enzymes were used with buffers recommended and supplied at 37℃ (unless otherwise stated).

Table A.3. Reagents

Reagent	Catalogue number	Supplier
2-Deoxy-D-galactose	D4407	Sigma-Aldrich Company Ltd., Dorset, UK
2-Propanol (isopropanol)	#190762	Sigma-Aldrich Company Ltd., Dorset, UK
Acetic Acid	A35-500	Fisher Scientific Ltd., Loughborough, UK
Acrylamide/Bis-acrylamide	A3574	Sigma-Aldrich Company Ltd., Dorset, UK
Actinomycin D	A1410	Sigma-Aldrich Company Ltd., Dorset, UK
Agar	05039	Sigma-Aldrich Company Ltd., Dorset, UK
Agarose, molecular biology grade (SeaKem® LE Agarsoe)	#50004	Lonza Biologics plc, Cambridge UK
Ammonium Persulphate (APS))	A3678	Sigma-Aldrich Company Ltd., Dorset, UK
Ampicillin Sodium	AMP25	ForMedium, Hunstanton, UK
β-mercaptoethanol	M7154	Sigma-Aldrich Company Ltd., Dorset, UK
Bio-Rad Protein Assay Reagent	#500-0002	Bio-Rad Laboratories Ltd., Hemel Hempstead, UK
Bromophenol Blue (3',3",5',5"-tetrabromophenolsulfonphthalein)	B0126	Sigma-Aldrich Company Ltd., Dorset, UK
ColorPlus Prestained Protein Marker	#4090	New England BioLabs Ltd., Hitchin, UK
cOmplete, EDTA Protease inhibitor cocktail tablets	11873580001	Roche Diagnostics Ltd., Burgess Hill, UK
Chloramphenicol	C0378	Sigma-Aldrich Company Ltd., Dorset, UK
Deoxyribonuclease I (DNase I)	M0303L	New England BioLabs Ltd., Hitchin, UK
Electroporation Cuvettes, Sterile, Individually Wrapped, 1mm, Red Cap	E6-0050	Geneflow Ltd., Fradley, Staffordshire UK
Ethanol, molecular biology grade	E7023	Sigma-Aldrich Company Ltd., Dorset, UK

Ethylenediaminetetraacetic Acid Disodium Salt	20296.260	VWR International Ltd., Lutterworthor, UK
Fugene 6	05061377001	Roche Diagnostics Ltd., Burgess Hill, UK
Extra Thick Blot Paper	170-3966	Bio-Rad Laboratories Ltd., Hemel Hempstead, UK
E.Z.N.A. mRNA extraction	R6834-01	Omega Biotek, Leicestershire, UK
formaldehyde	F8775	Sigma-Aldrich Company Ltd., Dorset, UK
Gene Pulser® II Elecroporation System	165-2105	Bio-Rad Laboratories Ltd., Hemel Hempstead, UK
D-Galactose	G0750	Sigma-Aldrich Company Ltd., Dorset, UK
Glycerol, molecular biology grade	G5516	Sigma-Aldrich Company Ltd., Dorset, UK
Glycine	BP381	Fisher Scientific Ltd., Loughborough, UK
High Capacity cDNA Reverse Transcipriton kit	4368814	Applied Biosystems Ltd., Warrington, UK
HS HRP WB Substrate.	98490B	UptiLight™ Cheshire Sciences Ltd., Aldford, UK
Immersion Oil	N1518	Applied Precision LLC, Marlborough, UK
Kanamycin sulfate	K4378	Sigma-Aldrich Company Ltd., Dorset, UK
Kodak® Biomax® XAR	Z358487,	Sigma Aldrich
LB Agar	L2897	Sigma-Aldrich Company Ltd., Dorset, UK
LB Broth	L3022	Sigma-Aldrich Company Ltd., Dorset, UK
Lipofectamine™ 2000	11668019	Life Technologies Ltd, Paisley UK
McConkey Agar	212123	BD Difco, Oxford UK
Methanol, molecular biology grade	A452-1	Fisher Scientific Ltd., Loughborough, UK
Mini-PROTEAN 3 Multi-Casting Chamber (0.75mm spacer plate)	#165-4111,	Bio-Rad Laboratories Ltd., Hemel Hempstead, UK
NaCl	7647-14-5	Fisher Scientific Ltd., Loughborough, UK
NEBlot Phototope Kit	#N7550S	New England BioLabs Ltd., Hitchin, UK
Nonidet P-40 (Octyl Phenoxylpolyethoxylethanol)	11332473001	Roche Diagnostics Ltd., Burgess Hill, UK
Opti-MEM®	11058-021	Invitrogen Gibco™ Ltd., Paisley, UK
Paraformaldehyde	15713-S	Electron Microscopy Sciences, Hatfield, UK
Ponceau S	P3504	Sigma-Aldrich Company Ltd., Dorset, UK
Power SYBR® Green PCR Master mix	4368577	Applied Biosystems Ltd., Warrington, UK
Protein G Agarose/Salmon Sperm DNA beads	#16-201	Millipore (UK) Ltd, Watford UK
Proteinase k	P6556	Sigma-Aldrich Company Ltd., Dorset, UK
MEM medis	M4655	Sigma-Aldrich Company Ltd., Dorset, UK
Mid Range PFG marker I	#N3551S	New England BioLabs Ltd., Hitchin, UK
Mid Range PFG marker II	#N3552S	New England BioLabs Ltd., Hitchin, UK
Nitrocellulose membrane	N8017	Sigma-Aldrich Company Ltd., Dorset, UK
Ponceau S	P3504	Sigma-Aldrich Company Ltd., Dorset, UK
Pulse Field Certified agarose	#162-0137	Bio-Rad Laboratories Ltd., Hemel Hempstead, UK
QIAshredder spin column kits	79654	Qiagen Ltd., Crawley, UK
Ribonuclease A (RNAse A)	12091-039	Sigma-Aldrich Company Ltd., Dorset, UK
RNeasy Mini kit	74104	Qiagen Ltd., Crawley, UK
Skim Milk powder	#70166	Sigma-Aldrich Company Ltd., Dorset, UK
SN50 NF-κB Cell-Permeable Inhibitor Peptide	481480	Merck Chemicals Ltd, Nottingham UK

Stealth RNAi™ siRNA Negative Control Med GC Duplex #2	# 12935112	Life Technologies Ltd, Paisley UK
Stealth RNAi™ siRNA Negative Control Hi GC Duplex #2	# 12935114	Life Technologies Ltd, Paisley UK
SYBR® Green MasterMix	4309155	Applied Biosystems Ltd., Warrington, UK
TEMED (N,N,N',N'-tetrametyloetylenodiamina)	T9281	Sigma-Aldrich Company Ltd., Dorset, UK
Tetracycline	87128	Sigma-Aldrich Company Ltd., Dorset, UK
TNF-α, Human, Recombinant, *E. coli*	654205	Merck Chemicals Ltd, Nottingham UK
Tris Base Ultra Pure (Tris(hydroxymethyl)aminomethane)	TRIS01	ForMedium, Hunstanton, UK
Triton X-100	X100	Sigma-Aldrich Company Ltd., Dorset, UK
Trypan Blue Solution 0.4%	T8154	Sigma-Aldrich Company Ltd., Dorset, UK
Trypsin-EDTA	T3924	Sigma-Aldrich Company Ltd., Dorset, UK
Trichostatin A (TSA)	T8552	Sigma-Aldrich Company Ltd., Dorset, UK
TWEEN® 20 (Polyoxyethylenesorbitan Monolaurate)	P1379	Sigma-Aldrich Company Ltd., Dorset, UK
VECTORSHIELD Mounting Medium with DAPI	H-1200	Vector Laboratories Ltd., Peterborough, UK

Table A.5. Equipment and Software

Item	Supplier
7300 Real Time PCR Thermocycler	Applied Biosystems Ltd., Warrington, UK
ABI 7300 System Software	Applied Biosystems Ltd., Warrington, UK
ELx800 Plate Reader	BIO-TEK, Potton, UK
KCjunior Software	BIO-TEK, Potton, UK
Trans-Blot Semi-Dry Transfer Cell	Bio-Rad Laboratories Ltd., Hemel Hempstead, UK

Appendix 3: Location of BCL3 qRT-PCR primers

(Exon 2) GAGCCTTACTGCCTTTGTACCCCACTCGGGCCATGGGCTCCCCGTTTCCTCTGGTGAACC
TGCCTACACCCCTATACCCCATGATGTGCCCCATGGAACACCCCCTTTCTGCTGACATCG
CCATGGCCACCCGTGCAGATGAGGACGGAGACAC
(intron 2)
(**Exon 3)** GCCTCTCCATATTGCTGTGGTGCAGGGTAACCTGCCAGCTGTGCACCGGCTGGTCAACCT
CTTCCAGCAGGGGGGCCGGGAGCTCGACATCTACAACAACCTACGGCAG

Appendix 4: Localisation of primers amplifying proximal to TSSs of *BCL3* and *TNFA* genes

AGCTACGT Exon 1
ACGT 5'UTR
ACGT Primer sequence

***BCL3* gene**

GGGGTTGCGGAGAGAAACACCTACTCAGACAGGAGAACCAGAGAGACAGTTACAGACTCA
GAGATAGAGATGTTGAGAGATAGGGCCAGAAAGACAAAAACAGAGGCAGAGAGAGCGGCC
CTTGGCAGCAGGGGTGGGGACACCCCCCCACCCCCCGACCCCGCCTCCTCTCCCCCCACC
CCTCCTTTCCTCTCCCTCCCCCGCCGAGGCCTGGCTGCCCCAGGCGCCGCGGGCCGGGAG
GGGGCAAGCGGGGCGCGGCGCGGGCGGGGCGCAGGGCAGGCTGCACCTCAGAGCGGCGGG
AGCAGCGGCGGGTCCAGGAAACCCCTGGGGCGTACGGGTGGCCCCGGGGGGGCCGGGGGC
GGGGAGGCGGGCGGCCGGCACCGCCCCGGCCGACAAAAGTCCCTTCAGTTCAGCCGGCTG
CAGGGGAAGTCCCGGCGCCCGGCGAAACCACCCTCCCGTGCAGCCGAGCCCAGCCGCTCT
CCGGCCGCCGTCCCCGGCGGCCCCATGCCCCGATGCCCCGCGGGGGCCATGGACGAGGGG
CCCGTGGACCTGCGCACCCGGCCCAAGGCCGCCGGACTCCCGGGCGCCGCGCTGCCGCTC

***TNFA* gene**

TGCAGGGCCCACTACCGCTTCCTCCAGATGAGCTCATGGGTTTCTCCACCAAGGAAGTTT
TCCGCTGGTTGAATGATTCTTTCCCCGCCCTCCTCTCGCCCCAGGGACATATAAAGGCAG
TTGTTGGCACACCCAGCCAGCAGACGCTCCCTCAGCAAGGACAGCAGAGGACCAGCTAAG
AGGGAGAGAAGCAACTACAGACCCCCCCTGAAAACAACCCTCAGACGCCACATCCCCTGA
CAAGCTGCCAGGCAGGTTCTCTTCCTCTCACATACTGACCCACGGCTCCACCCTCTCTCC
CCTGGAAAGGACACCATGAGCACTGAAAGCATGATCCGGGACGTGGAGCTGGCCGAGGAG
GCGCTCCCCAAGAAGACAGGGGGGCCCCAGGGCTCCAGGCGGTGCTTGTTCCTCAGCCTC

Appendix 5: Primers to amplify distal (-869) κB site in the *TNFA* promoter for ChIP assay

ACGT	Distal (-869) κB site
AGCTACGT	Exon 1
ACGT	5'UTR
ACGT	Primer sequence

ACCAGGTGAGGCCGCCAGACTGCTGCAGGGGAAGCAAAGGAGAAGCTGAGAAGATGAAGG
AAAAGTCAGGGTCTGGAGGGGCGGGGGTCAGGGAGCTCCTGGGAGATATGGCCACATGTA
GCGGCTCTGAGGAATGGGTTACAGGAGACCTCTGGGGAGATGTGACCACAGCAATGGGTA
GGAGAATGTCCAGGGCTATGGAAGTCGAGTATGGGGACCCCCCCTTAACGAAGACAGGGC
CATGTAGAGGGCCCCAGGGAGTGAAAGAGCCTCCAGGACCTCCAGGTATGGAATACAGGG
GACGTTTAAGAAGATATGGCCACACACTGGGGCCCTGAGAAGTGAGAGCTTCATGAAAAA
AATCAGGGACCCCAGAGTTCCTTGGAAGCCAAGACTGAAACCAGCATTATGAGTCTCCGG
GTCAGAATGAAAGAAGAAGGCCTGCCCCAGTGGGGTCTGTGAATTCCCGGGGGTGATTTC
ACTCCCCGGGGCTGTCCCAGGCTTGTCCCTGCTACCCCCACCCAGCCTTTCCTGAGGCCT
CAAGCCTGCCACCAAGCCCCCAGCTCCTTCTCCCCGCAGGGACCCAAACACAGGCCTCAG
GACTCAACACAGCTTTTCCCTCCAACCCCGTTTTCTCTCCCTCAAGGACTCAGCTTTCTG
AAGCCCCTCCCAGTTCTAGTTCTATCTTTTTCCTGCATCCTGTCTGGAAGTTAGAAGGAA
ACAGACCACAGACCTGGTCCCCAAAAGAAATGGAGGCAATAGGTTTTGAGGGGCATGAGG
ACGGGGTTCAGCCTCCAGGGTCCTACACACAAATCAGTCAGTGGCCCAGAAGACCCCCCT
CGGAATCGGAGCAGGGAGGATGGGGAGTGTGAGGGGTATCCTTGATGCTTGTGTGTCCCC
AACTTTCCAAATCCCCGCCCCCGCGATGGAGAAGAAACCGAGACAGAAGGTGCAGGGCCC
ACTACCGCTTCCTCCAGATGAGCTCATGGGTTTCTCCACCAAGGAAGTTTTCCGCTGGTT
GAATGATTCTTTCCCCGCCCTCCTCTCGCCCCAGGGACATATAAAGGCAGTTGTTGGCAC
ACCCAGCCAGCAGACGCTCCCTCAGCAAGGACAGCAGAGGACCAGCTAAGAGGGAGAGAA
GCAACTACAGACCCCCCCTGAAAACAACCCTCAGACGCCACATCCCCTGACAAGCTGCCA
GGCAGGTTCTCTTCCTCTCACATACTGACCCACGGCTCCACCCTCTCTCCCCTGGAAAGG
ACACCATGAGCACTGAAAGCATGATCCGGGACGTGGAGCTGGCCGAGGAGGCGCTCCCCA
AGAAGACAGGGGGGCCCCAGGGCTCCAGGCGGTGCTTGTTCCTCAGCCTCTTCTCCTTCC
TGATCGTGGCAGGCGCCACCACGCTCTTCTGCCTGCTGCACTTTGGAGTGATCGGCCCCC
AGAGGGAAGAGGTGAGTGCCTGGCCAGCCTTCATCCACTCTCCCACCCAAGGGGAAATGG

Appendix 6: Site of primers amplifying across XcmI/proximal κB site in the *BCL3* gene promoter

ACGT	Proximal κB site
ACGTACGT	Exon 1
ACGT	5'UTR
ACGT	Primer sequence

GAGATGGTGACAGACACAAAGAGACAAAAGAGAGAGACAGAGACGGAACAGAGCACACAG
AGACAAACGCGGGGTTGCGGAGAGAAACACCTACTCAGACAGGAGAACCAGAGAGACAGT
TACAGACTCAGAGATAGAGATGTTGAGAGATAGGGCCAGAAAGACAAAAACAGAGGCAGA
GAGAGCGGCCCTTGGCAGCAGGGGTGGGGACACCCCCCCACCCCCCGACCCCGCCTCCTC
TCCCCCCACCCCTCCTTTCCTCTCCCTCCCCCGCCGAGGCCTGGCTGCCCCAGGCGCCGC
GGGCCGGGAGGGGGCAAGCGGGGCGCGGCGCGGGCGGGGCGCAGGGCAGGCTGCACCTCA
GAGCGGCGGGAGCAGCGGCGGGTCCAGGAAACCCCTGGGGCGTACGGGTGGCCCCGGGGG
GGCCGGGGGCGGGGAGGCGGGCGGCCGGCACCGCCCCGGCCGACAAAAGTCCCTTCAGTT
CAGCCGGCTGCAGGGGAAGTCCCGGCGCCCGGCGAAACCACCCTCCCGTGCAGCCGAGCC
CAGCCGCTCTCCGGCCGCCGTCCCCGGCGGCCCCATGCCCCGATGCCCCGCGGGGGCCAT
GGACGAGGGGCCCGTGGACCTGCGCACCCGGCCCAAGGCCGCCGGACTCCCGGGCGCCGC
GCTGCCGCTCCGCAAGCGCCCGCTGCGCGCGCCCTCCCCGGAGCCCGCCGCTCCCCGCGG
CGCTGCGGGCCTTGTCGTCCCCCTGGACCCTCTGCGCGGCGGCTGCGACCTGCCGGCGGT
CCCCGGGCCCCCCCACGGCCTGGCCCGGCCGGAGGCGCTTTACTACCCCGGTGAGTGGCC
CCCGAGGGTCCGGGCCGGGTGGGATCCACACAGAGCATAGGGTCACCAGAGCCAGGAGGC

Appendix 7: Lines fitted to relative experimental time courses (fig 5A)

Equations used (t=time);

Two phase exponential association: $Y=Y_{MAX1}(1-e^{(-k1*t)})+Y_{MAX2}(1-e^{(-k2*t)})$;

Plateau followed by one phase association: $Y=Y_0$ when $t<t_x$;

$Y= Y_0+(P- Y_0)*(1-e^{(-k*(t-tx))})$ when $t>t_x$.

One site – specific binding with Hill slope: $Y=Y_{MAX}*t^H/(K_d{}^H+t^H)$

Nuclear levels of p65/NF-κB (orange line)
Two phase exponential association, R^2=0.986
Y_{MAX1}=-103.5; k1=0.02696; Y_{MAX2}=103.3; k2=0.02773;

Histone 3 acetyaltion levels (green line)
One site – specific binding with Hill slope, R^2=0.996
Y_{MAX}=1.19; H= 2.872; K_d=49.64.

Chromatin accessibility (grey dashed line)
One site – specific binding with Hill slope, R^2=0.989
Y_{MAX}=0.9608; H= 7.347; K_d=43.16.

P65 binding at BCL-3 TSS
One site – specific binding with Hill slope, R^2=0.975
Y_{MAX}=1.089; H= 4.473; K_d=50.99.

RNA pol. II binding at the BCL-3 TSS
One site – specific binding with Hill slope, R^2=0.988
Y_{MAX}=1.061; H= 5.938; K_d=55.33.

***BCL3* mRNA levels**
One site – specific binding with Hill slope, R^2=0.999
Y_{MAX}=1189; H= 5.406; K_d=333.4.

Appendix 8: Model code

A.8.1: Model as described in [5.2]

```
function ModelName
       [t,y] = ode45(@BCL3network,[0 900],[0,0,0,0,0]);

    xlswrite('FileName',[t,y])
    function dydt=BCL3network(t,y)
        k101=6.6*10^-2;
        k102=69;
        k103=53;
        k104=3.45*10^-2;
        k105=0.001;
        k106=260;
        k107=0.009;

        k108=0.005;
        k109=0.0125;
        k110=0.5;
        k111=0.01;
        k112=6.6*10^-2;
        k113=69;
        k114=53;
        k115=4.5*10^-3;
        k116=3.6;
        k117=2.4*10^-3;
        nNFκB=260*(144*(1-exp(-0.03218*t))-144*(1-exp(-0.03160*t)));

TNFmRNA=y(1);
HisAc=y(2);
Chr=y(3);
BCL3mRNA=y(4);
BCL3=y(5);

dydt(1)=k101*((nNFκB./(nNFκB+k102))*(1-(BCL3./(BCL3+k103))))-TNFmRNA*k104;
dydt(2)=k105*(nNFκB^2./(nNFκB^2+k106^2))-k107*HisAc;
dydt(3)=k108*(HisAc^6./(HisAc^6+k109^6))-Chr*k110;
dydt(4)=(Chr^3./(Chr^3+k111^3))*k112*((nNFκB./(nNFκB+k113)*(1-
(BCL3./(BCL3+k114)))))-BCL3mRNA*k115;
dydt(5)=k116*BCL3mRNA-k117*BCL3;

        dydt=dydt';
    end
end
```

Models performed without chromatin remodelling at the *BCL3* promoter [5.2.4.] use the above code with the dydt(4) equation modified as below:

```
dydt(4)=k112*((nNFκB./(nNFκB+k113)*(1-(BCL3./(BCL3+k114)))))-BCL3mRNA*k115;
```

A.8.2. Nuclear NF-κB pulse generating code

Code shown is for generating the varied nuclear NF-κB levels ('nNFκB') as used in chapter 5 [5.2.5]. Pulse duration and frequency were varied, as outlined in the relevant results sections. Other model components were as in A.8.1.

```
        if (t<=z);
        nNFκB=260;
```

```
        elseif(t>z);
         nNFκB=0;
        end

        if (t>=(x+z));
        nNFκB=260;
        end

        if(t>(2*z+x));
       nNFκB=0;
        end

                  [..this repetitive code is repeated to achieve the
                  required number of pulses]
```

```
z= pulse size (min)7.5;
x= time between pulses (min).
Magnitude of pulse is 260nM.
```

A.8.3. TNFα self amplification model code (Chapter 6)

Model based on equations outlined in [6.2.1.].

```
function TNFselfamp
       [t,y] = ode45(@BCL3network,[0 15000],[0,0,10]);

   plot(t,y(:,1)),axis([0 15000 0 15]);
  %xlswrite('may11BCL3i',[t,y])
    function dydt=BCL3network(t,y)

        k1=6.6*10^-2;
        k2=0.7438;
        k3=3.45*10^-2;
        k4=5;
        k5=0.0115;
        k6=0.0015;
        k7=0.4;

        k8=53;
        BCL3=<VARIED>;

TNFAmRNA=y(1);
TNFαINT=y(2);
TNFαEX=y(3);

dydt(1)=k1*((TNFαEX.^2./(TNFαEX.^2+k2.^2))*(1-(BCL3./(BCL3+k8))))-
TNFAmRNA*k3;
dydt(2)=k4*TNFAmRNA-k5*TNFαINT-k6*TNFαINT;
dydt(3)=k6*TNFαINT-k7*TNFαEX;

        dydt=dydt';
    end
end
```

A.8.4. Derivation of equations outlined in [6.2.2.].

$$d[TNFA\text{mRNA}]/dt = k1*([TNF\alpha Ex]^2/([TNF\alpha Ex]^2+k2^2) - k3*[TNFA\text{mRNA}] \quad (A)$$

$$d[TNF\alpha IN]/dt = k4*[TNFA\text{mRNA}] - k5*[TNF\alpha IN] - k6*[TNF\alpha IN] \quad (B)$$

$$d[TNF\alpha EX]/dt = k6*[TNF\alpha IN] - k7*[TNF\alpha EX] \quad (C)$$

Assuming steady states is reached - i.e. that the change in all model components is zero - then:

$$[TNFA\text{mRNA}]= ((k5+k6)/k4)*[TNF\alpha IN] \quad (D)$$

$$[TNF\alpha IN] = (k7/k6)*[TNF\alpha EX] \quad (E)$$

Combine (D) and (E):

$$[TNFA\text{mRNA}] = ((k5+k6)*k7*[TNF\alpha EX])/(k4*k6) \quad (F)$$

Combine (A) and (F):

$$d[TNFA\text{mRNA}]/dt = k1*([TNF\alpha EX]^2/([TNF\alpha EX]^2+k2^2) - Q*[TNF\alpha EX] \quad (1)$$

where $Q = (k3*(k5+k6)*k7)/(k4*k6)$

Appendix 9: Sequencing of the Venus gene in a BCL-3:Venus BAC [7.2.4.3.]

ACGT BCL3 sequence
ACGT Linker sequence
ACGT Venus sequence
ACGT 3' H arm

GCGCAACTGTTGGGAAGGGCGATCGGTGCGGGCCTCTTCGCTATTACGCCAGCTGGCGAAAGGGGGATGTGCTGC
AAGGCGATTAAGTTGGGTAACGCCAGGGTTTTCCCAGTCACGACGTTGTAAAACGACGGCCAGTGAATTGTAATA
CGACTCACTATAGGGCGAATTGGGTACCACCCGAGTCCAGACCCCCAGCCCCTCCTCCCTCAGACCCAGATCTCA
GGCCCCAGCCCCTGCTCTCTGGGTCTAGCCTCTCACCACCCACCCCTCTGTCTCTCTTCCTTCCTCAGGTCTTCT
CTCCGCATCACCATCCTCCTCACCCTCCCAGTCTCCCCCCAGGGACCCCCCTGGATTCCCCATGGCTCCTCCCAA
TTTCTTCCTTCCTTCCCCATCTCCACCCGCCTTCCTGCCCTTTGCTGGGGTCCTCCGAGGCCCTGGCCGGCCGGT
GCCCCCCTCCCCAGCTCCAGGAGGCAGCGTCGACGGTATCGATAAGCTTGATATCGAATTCATGGTGAGCAAGGG
CGAGGAGCTGTTCACCGGGGTGGTGCCCATCCTGGTCGAGCTGGACGGCGACGTAAACGGCCACAAGTCAGCGTG
TCCGGCGAGGGCGAGGGCGATGCCACCTACGGCAAGCGACCCTGAAGCTGATCTGCACCACCGGCAAGCTGCCCG
TGCCCTGGCCCACCCTCGTGACCACCCTGGGCTACGGCCTGCAGTGCTTCGCCCGCTACCCCGACCACATGAAGC
AGCACGACTTCTTCAAGTCCGCCAGCCCGAAGGCTACGTCCAGGAGCGCACCATCTTCTTCAAGGACGACGGCAA
CTACAAGACCCGCGCCGAGGTGAAGTTCGAGGGCGACACCCTGGTGAACCGCATCGAGCTGAAGGGCATCGACTT
CAAGGAGGACGCAACATCCTGGGGCACAAGCTGGAGTACAACTACAACAGCCACAACGTCTATATCACCGCCGAC
AAGCAGAAGAACGGCATCAAGGCCAACTTCAAGATCCGCCACAACATCGAGGACGGCGGCGTGCAGCTCGCCGCC
ACTACCAGCAGAACACCCCCATCGGCGACGGCCCCGTGCTGCTGCCCGACAACCACTACCTGAGCTACCAGTCCG
CCCTGAGCAAAGACCCCAACGAGAAGCGCGATCACATGGTCCTGCTGGAGTTCGTGACCGCGCCGGGATCACTCT
CGGCATGGACGAGCTGTACAAGTAAGGGGGATGGGGGGGCAGATCTTGGACTCATGAGGAGGGGCCCCCCTGCCC
TGTGGGGTCAACCCTTCTGGAAACTGTGAAGATCTCACTCTGCCCCCCCCCCCATCTTCGGGACCAGGATTTGC
ACAGAAGCACATGCACCTACCCATACACCCCCTCTTCTGAGCACAGATGTTCCCCCATCTCGCTCCCTCCCAGGA
CTCTGACCCCAGCATTCTCAGGCACCAGTCCCTGTCCGGAATGCCACCCACATCTTCCATTTCCATGTCCCCT

References

Abu-Amer, Y.,Ross, F. P.,McHugh, K. P.,Livolsi, A.,Peyron, J.-F. and Teitelbaum, S. L. (1998) Tumor Necrosis Factor-α Activation of Nuclear Transcription Factor-ÎκB in Marrow Macrophages Is Mediated by c-Src Tyrosine Phosphorylation of IkappaBalpha. **Journal of Biological Chemistry** *273*, 29417-29423

Aggarwal, B. B. (2003) Signalling pathways of the TNF superfamily: a double-edged sword. **Nat Rev Immunol** *3*, 745-756

Ahn, S. H.,Kim, M. and Buratowski, S. (2004) Phosphorylation of Serine 2 within the RNA Polymerase II C-Terminal Domain Couples Transcription and 3' End Processing. **Molecular Cell** *13*, 67-76

Aida, M.,Chen, Y.,Nakajima, K.,Yamaguchi, Y.,Wada, T. and Handa, H. (2006) Transcriptional Pausing Caused by NELF Plays a Dual Role in Regulating Immediate-Early Expression of the junB Gene. **Mol. Cell. Biol.** *26*, 6094-6104

Ainbinder, E.,Revach, M.,Wolstein, O.,Moshonov, S.,Diamant, N. and Dikstein, R. (2002) Mechanism of Rapid Transcriptional Induction of Tumor Necrosis Factor Alpha-Responsive Genes by NF-κB. **Mol. Cell. Biol.** *22*, 6354-6362

Al-Lamki, R. S.,Wang, J.,Skepper, J. N.,Thiru, S.,Pober, J. S. and Bradley, J. R. (2008) Expression of Tumor Necrosis Factor Receptors in Normal Kidney and Rejecting Renal Transplants. **Lab Invest** *81*, 1503-1515

Albert, I.,Mavrich, T. N.,Tomsho, L. P.,Qi, J.,Zanton, S. J.,Schuster, S. C. and Pugh, B. F. (2007) Translational and rotational settings of H2A.Z nucleosomes across the Saccharomycescerevisiae genome. **Nature** *446*, 572-576

Allan, J.,Hartman, P. G.,Crane-Robinson, C. and Aviles, F. X. (1980) The structure of histone H1 and its location in chromatin. **Nature** *288*, 675-679

Alland, L.,Muhle, R.,Hou, H.,Potes, J.,Chin, L.,Schreiber-Agus, N. and DePinho, R. A. (1997) Role for N-CoR and histone deacetylase in Sin3-mediated transcriptional repression. **Nature** *387*, 49-55

Amir, R. E.,Haeker, H.,Karin, M. and Ciechanover, A. (2004) Mechanism of processing of the NF-k B2 p100 precursor: Identification of the specific polyubiquitin chainanchoring lysine residue and analysis of the role of NEDD8-modification on the SCF(b-TrCP) ubiquitin ligase. **Oncogene** *23*, 2540-2547

Anderson, J. D. and Widom, J. (2001) Poly(dA-dT) Promoter Elements Increase the Equilibrium Accessibility of Nucleosomal DNA Target Sites. **Mol. Cell. Biol.** *21*, 3830-3839

Andreu-Vieyra, C.,Lai, J.,Berman, B. P.,Frenkel, B.,Jia, L.,Jones, P. A. and Coetzee, G. A. (2011) Dynamic Nucleosome-Depleted Regions at Androgen Receptor Enhancers in the Absence of Ligand in Prostate Cancer Cells **Mol Cell Biol** *31*, 4648-4662

Andrulis, E. D.Guzman, E.Daering, P.,Werner, J. and Lis, J. T. (2000) High-resolution localisation of Drosophila Spt5 and Spt6 at heat shock genes in vivo: roles in promoter proximal pausing and transcription elongation. **Genes & Development** *14*, 2635-2649

Angelov, D.,Lenouvel, F. Hans, F.,Muller, C. W.,Bouvet, P.,Bednar, J.,Moudrianakis, E. N.,Cadet, J. and Dimitrov, S. (2004) The Histone Octamer Is Invisible When NF-κB Binds to the Nucleosome. **Journal of Biological Chemistry** *279*, 42374-42382

Arch, R. H.,Gedrich, R. W. and Thompson, C. B. (1998) Tumor necrosis factor receptor-associated factors (TRAFs) are a family of adapter proteins that regulates life and death. **Genes & Development** *12*, 2821-2830

Archer, T. K.,Cordingley, M. G.,Wolford, R. G. and Hager, G. L. (1991) Transcription factor access is mediated by accurately positioned nucleosomes on the mouse mammary tumor virus promoter. **Mol Cell Biol** *11*, 688-698

Ardehali, M. B.,Mei, A.,Zobeck, K. L.,Caron, M.,Lis, J. T. and Kusch, T. (2011) Drosophila Set1 is the major histone H3 lysine 4 trimethyltransferase with role in transcription. **EMBO J** *30*, 2817-2828

Arenzana-Seisdedos, F.,Thompson, J.,Rodriguez, M. S.,Bachelerie, F.,Thomas, D. and Hay, R. T. (1995) Inducible nuclear expression of newly synthesized I kappa B alpha negatively regulates DNA-binding and transcriptional activities of NF-kappa B. **Molecular and Cellular Biology** *15*, 2689-2696

Asea, A.,Rehli, M.,Kabingu, E.,Boch, J. A.,Barac, O.,Auron, P. E.,Stevenson, M. A. and Calderwood, S. K. (2002) Novel Signal Transduction Pathway Utilized by Extracellular HSP70. **Journal of Biological Chemistry** *277*, 15028-15034

Ashall, L.,Horton, C. A.,Nelson, D. E.,Paszek, P.,Harper, C. V.,Sillitoe, K.,Ryan, S.,Spiller, D. G.,Unitt, J. F.,Broomhead, D. S.,Kell, D. B.,Rand, D. A.,See, V. and White, M. R. H. (2009) Pulsatile Stimulation Determines Timing and Specificity of NF-{kappa}B-Dependent Transcription. **Science** *324*, 242-246

Audibert, A.,Weil, D. and Dautry, F. (2002) In Vivo Kinetics of mRNA Splicing and Transport in Mammalian Cells. **Molecular and Cellular Biology** *22*, 6706-6718

Awad, S. and Hassan, A. H. (2008) The Swi2/Snf2 Bromodomain Is Important for the Full Binding and Remodelling Activity of the SWI/SNF Complex on H3- and H4-acetylated Nucleosomes. **Annals of the New York Academy of Sciences** *1138*, 366-375

Badi and Barberis (2001) Proteins that genetically interact with the Saccharomyces cerevisiae transcription factor Gal11p emphasize its role in the initiation-elongation transition. **Molecular Genetics and Genomics** *265*, 1076-1086

Baer, M.,Dillner, A.,Schwartz, R. C.,Sedon, C.,Nedospasov, S. and Johnson, P. F. (1998) Tumor Necrosis Factor Alpha Transcription in Macrophages Is Attenuated by an Autocrine Factor That Preferentially Induces NF-kappa B p50. **Mol. Cell. Biol.** *18*, 5678-5689

Baldwin, A. S. (1996) THE NF-κB AND IκB PROTEINS: New Discoveries and Insights. **Annual Review of Immunology** *14*, 649-681

Barboric, M.,Nissen, R. M.,Kanazawa, S.,Jabrane-Ferrat, N. and Peterlin, B. M. (2001) NF-κB Binds P-TEFb to Stimulate Transcriptional Elongation by RNA Polymerase II. **Molecular Cell** *8*, 327-337

Barre, B. and Perkins, N. D. (2007) A cell cycle regulatory network controlling NF-kappaB subunit activity and function. **EMBO J** *26*, 4841-4855

Basu, S.,Mehreja, R.,Thiberge, S.,Chen, M.-T. and Weiss, R. (2004) Spatiotemporal control of gene expression with pulse-generating networks. **Proceedings of the National Academy of Sciences of the United States of America** *101*, 6355-6360

Bauvois, B.,Sancéau, J. and Wietzerbin, J. (1992) Human U937 cell surface peptidase activities: characterisation and degradative effect on tumor necrosis factor-α. **European Journal of Immunology** *22*, 923-930

Beato, M. and Eisfeld, K. (1997) Transcription factor access to chromatin. **Nucleic Acids Research** *25*, 3559-3563

Beg, A. A.,Ruben, S. M.,Scheinman, R. I.,Haskill, S.,Rosen, C. A. and Baldwin, A. S. (1992) I kappa B interacts with the nuclear localisation sequences of the subunits of NF-kappa B: a mechanism for cytoplasmic retention. **Genes & Development** *6*, 1899-1913

Bell, S. D.,Kosa, P. L.,Sigler, P. B. and Jackson, S. P. (1999) Orientation of the transcription preinitiation complex in Archaea. **Proceedings of the National Academy of Sciences** *96*, 13662-13667

Benderdour, M.,Hess, K.,Dzondo-Gadet, M.,Nabet, P.,Belleville, F. and Dousset, B. (1998) Boron Modulates Extracellular Matrix and TNF Synthesis in Human Fibroblasts. **Biochemical and Biophysical Research Communications** *246*, 746-751

Benjamin, L. R. and Gilmour, D. S. (1998) Nucleosomes are not necessary for promoter-proximal pausing in vitro on the Drosophila hsp70 promoter. **Nucleic Acids Research** *26*, 1051-1055

Betts, J. C. and Nabel, G. J. (1996) Differential regulation of NF-kappaB2(p100) processing and control by amino-terminal sequences. **Molecular and Cellular Biology** *16*, 6363-6371

Black, R. A.,Rauch, C. T.,Kozlosky, C. J.,Peschon, J. J.,Slack, J. L.,Wolfson, M. F.,Castner, B. J.,Stocking, K. L.,Reddy, P.,Srinivasan, S.,Nelson, N.,Boiani, N.,Schooley, K. A.,Gerhart, M.,Davis, R.,Fitzner, J. N.,Johnson, R. S.,Paxton, R. J.,March, C. J. and Cerretti, D. P. (1997) A metalloproteinase disintegrin that releases tumour-necrosis factor-[alpha] from cells. **Nature** *385*, 729-733

Boeger, H.,Griesenbeck, J.,Strattan, J. S. and Kornberg, R. D. (2003) Nucleosomes Unfold Completely at a Transcriptionally Active Promoter. **Molecular Cell** *11*, 1587-1598

Boekhoudt, G. H.,Guo, Z.,Beresford, G. W. and Boss, J. M. (2003) Communication Between NF-κB and Sp1 Controls Histone Acetylation Within the Proximal Promoter of the Monocyte Chemoattractant Protein 1 Gene. **The Journal of Immunology** *170*, 4139-4147

Bondarenko, V. A.,Steele, L. M.,Ãšjvari, A.,Gaykalova, D. A.,Kulaeva, O. I.,Polikanov, Y. S.,Luse, D. S. and Studitsky, V. M. (2006) Nucleosomes Can Form a Polar Barrier to Transcript Elongation by RNA Polymerase II. **Molecular Cell** *24*, 469-479

Bonizzi, G. and Karin, M. (2004) The two NF-[kappa]B activation pathways and their role in innate and adaptive immunity. **Trends in Immunology** *25*, 280-288

Boothby, M. (2001) Specificity of SN50 for NF-kappaB? **Nat. Immunology** *2*, 471.

Bosisio, D.,Marazzi, I.,Agresti, A.,Shimizu, N.,Bianchi, M. E. and Natoli, G. (2006) A hyper-dynamic equilibrium between promoter-bound and nucleoplasmic dimers controls NF-kappaB-dependent gene activity. **EMBO J** *25*, 798-810

Bouazoune, K.,Miranda, T. B.,Jones, P. A. and Kingston, R. E. (2009) Analysis of individual remodeled nucleosomes reveals decreased histone DNA contacts created by hSWI/SNF. **Nucleic Acids Research** *37*, 5279-5294

Bours, V.,Franzoso, G.,Azarenko, V.,Park, S.,Kanno, T.,Brown, K. and Siebenlist, U. (1993) The oncoprotein Bcl-3 directly transactivates through κB motifs via association with DNA-binding p50B homodimers. **Cell** *72*, 729-739

Brasier, A. R.,Lu, M.,Hai, T.,Lu, Y. and Boldogh, I. (2001) NF-kappaB-inducible BCL-3 Expression Is an Autoregulatory Loop Controlling Nuclear p50/NF-kappaB1 Residence. **Journal of Biological Chemistry** *276*, 32080-32093

Brocke-Heidrich, K.,Ge, B.,Cvijic, H.,Pfeifer, G.,Loffler, D.,Henze, C.,McKeithan, T. W. and Horn, F. (2006) BCL3 is induced by IL-6 via Stat3 binding to intronic enhancer HS4 and represses its own transcription. **Oncogene** *25*, 7297-7304

Brown, C. R.,Mao, C.,Falkovskaia, E.,Law, J. K. and Boeger, H. (2011) In Vivo Role for the Chromatin-remodelling Enzyme SWI/SNF in the Removal of Promoter Nucleosomes by Disassembly Rather Than Sliding. **Journal of Biological Chemistry** *286*, 40556-40565

Brown, S. A.,Imbalzano, A. N. and Kingston, R. E. (1996) Activator-dependent regulation of transcriptional pausing on nucleosomal templates. **Genes & Development** *10*, 1479-1490

Buckley, C. D.,Pilling, D.,Lord, J. M.,Akbar, A. N.,Scheel-Toellner, D. and Salmon, M. (2001) Fibroblasts regulate the switch from acute resolving to chronic persistent inflammation. **Trends in Immunology** *22*, 199-204

Bulger, M. and Groudine, M. (2010) Enhancers: The abundance and f unction of regulatory sequences beyond promoters. **Dev. Biol.** 339, 250-257.

Bundy, D. L. and McKeithan, T. W. (1997) Diverse Effects of BCL3 Phosphorylation on Its Modulation of NF-kappaB p52 Homodimer Binding to DNA. **Journal of Biological Chemistry** *272*, 33132-33139

Buratowski, S.,Hahn, S.,Guarente, L. and Sharp, P. A. (1989) Five intermediate complexes in transcription initiation by RNA polymerase II. **Cell** *56*, 549-561

Burke, T. W. and Kadonaga, J. T. (1997) The downstream core promoter element, DPE, is conserved from Drosophila to humans and is recognized by TAF(II)60 of Drosophila. **Genes & Development** *11*, 3020-3031

Burley, S. K. and Roeder, R. G. (1996) Biochemistry and Structural Biology of Transcription Factor IID (TFIID). **Annual Review of Biochemistry** *65*, 769-799

Caamano, J. H.,Perez, P.,Lira, S. A. and Bravo, R. (1996) Constitutive expression of Bcl-3 in thymocytes increases the DNA binding of NF-kappa B1 (p50) homodimers in vivo. **Molecular and Cellular Biology** *16*, 1342-1348

Carey, M. F.,Peterson, C. L. and Smale, S. T. (2009) Chromatin Immunoprecipitation (ChIP). **Cold Spring Harbor Protocols** *2009*, pdb.prot5279

Carmody, R. J.,Ruan, Q. G.,Palmer, S.,Hilliard, B. and Chen, Y. H. H. (2007) Negative regulation of Toll-like receptor signalling by NF-kappa B p50 ubiquitination blockade. **Science** *317*, 675-678

Cataldo, L.,Mastrangelo, M.-A. and Kleene, K. C. (1999) A quantitative sucrose gradient analysis of the translational activity of 18 mRNA species in testes from adult mice. **Molecular Human Reproduction** *5*, 206-213

Chan, F. K.-M.,Chun, H. J.,Zheng, L.,Siegel, R. M.,Bui, K. L. and Lenardo, M. J. (2000) A Domain in TNF Receptors That Mediates Ligand-Independent Receptor Assembly and Signalling. **Science** *288*, 2351-2354

Chang, B.,Chen, Y.,Zhao, Y. and Bruick, R. K. (2007) JMJD6 Is a Histone Arginine Demethylase. **Science** *318*, 444-447

Chang, H.,Oh, P.,Ingber, D. and Huang, S. (2006) Multistable and multistep dynamics in neutrophil differentiation. **BMC Cell Biology** *7*, 11

Chatterjee, N.,Sinha, D.,Lemma-Dechassa, M.,Tan, S.,Shogren-Knaak, M. A. and Bartholomew, B. (2011) Histone H3 tail acetylation modulates ATP-dependent remodelling through multiple mechanisms. **Nucl. Acids Res.** *39*, 8378-8391

Chen-Park, F. E.,Huang, D.-B.,Noro, B.,Thanos, D. and Ghosh, G. (2002) The ÎkappaB DNA Sequence from the HIV Long Terminal Repeat Functions as an Allosteric Regulator of HIV Transcription. **Journal of Biological Chemistry** *277*, 24701-24708

Chen, G. and Goeddel, D. V. (2002) TNF-R1 Signalling: A Beautiful Pathway. **Science** *296*, 1634-1635

Chen, J.,Petrus, M.,Bryant, B. R.,Phuc Nguyen, V.,Stamer, M.,Goldman, C. K.,Bamford, R.,Morris, J. C.,Janik, J. E. and Waldmann, T. A. (2008) Induction of the IL-9 gene by HTLV-I Tax stimulates the spontaneous proliferation of primary adult T-cell leukemia cells by a paracrine mechanism. **Blood** *111*, 5163-5172

Chen, L.F.,Mu, Y. and Greene, W. C. (2002) Acetylation of RelA at discrete sites regulates distinct nuclear functions of NF-[kappa]B. **EMBO J** *21*, 6539-6548

Chen, P. C.-H.,DuBois, G. C. and Chen, M.-J. (1995) Mapping the Domain(s) Critical for the Binding of Human Tumor Necrosis Factor- to Its Two Receptors. **Journal of Biological Chemistry** *270*, 2874-2878

Chen, Z. J. (2005) Ubiquitin signalling in the NF-[kappa]B pathway. **Nat Cell Biol** *7*, 758-765

Cheng, J. D.,Ryseck, R.-P.,Attar, R. M.,Dambach, D. and Bravo, R. (1998) Functional Redundancy of the Nuclear Factor ÎkappaB Inhibitors IkappaBalpha and IkappaBbeta. **The Journal of Experimental Medicine** *188*, 1055-1062

Chen, Z.J. (2005). Ubiquitin signalling in the NF-kappaB pathway. **Nat. Cell Biol**. 7, 758–765.

Cheong, R.,Bergmann, A.,Werner, S. L.,Regal, J.,Hoffmann, A. and Levchenko, A. (2006) Transient IkappaB Kinase Activity Mediates Temporal NF-kappaB Dynamics in Response to a Wide Range of Tumor Necrosis Factor-alpha Doses. **Journal of Biological Chemistry** *281*, 2945-2950

Chi, T. and Carey, M. (1996) Assembly of the isomerized TFIIA--TFIID--TATA ternary complex is necessary and sufficient for gene activation. **Genes & Development** *10*, 2540-2550

Chinnaiyan, A. M.,O'Rourke, K.,Yu, G.-L.,Lyons, R. H.,Garg, M.,Duan, D. R.,Xing, L.,Gentz, R.,Ni, J. and Dixit, V. M. (1996) Signal Transduction by DR3, a Death Domain-Containing Receptor Related to TNFR-1 and CD95. **Science** *274*, 990-992

Cho, H.,Orphanides, G.,Sun, X.,Yang, X.-J.,Ogryzko, V.,Lees, E.,Nakatani, Y. and Reinberg, D. (1998) A Human RNA Polymerase II Complex Containing Factors That Modify Chromatin Structure. **Molecular and Cellular Biology** *18*, 5355-5363

Clapier, C. R. and Cairns, B. R. (2009) The Biology of Chromatin Remodelling Complexes. **Annual Review of Biochemistry** *78*, 273-304

Cohen, S.,Achbert-Weiner, H. and Ciechanover, A. (2004) Dual Effects of IkappaB Kinase alpha Mediated Phosphorylation on p105 Fate: SCFÎ²-TrCP-Dependent Degradation and SCF-TrCP-Independent Processing. **Molecular and Cellular Biology** *24*, 475-486

Coleman, J. W. (2001) Nitric oxide in immunity and inflammation. **International Immunopharmacology** *1*, 1397-1406

Collart, M. A.,Baeuerle, P. and Vassalli, P. (1990) Regulation of tumor necrosis factor alpha transcription in macrophages: involvement of four kappa B-like motifs and of constitutive and inducible forms of NF-kappa B. **Mol. Cell. Biol.** *10*, 1498-1506

Conaway, R. C. and Conaway, J. W. (1993) General Initiation Factors for RNA Polymerase II. **Annual Review of Biochemistry** *62*, 161-190

Copeland, N. G.,Jenkins, N. A. and Court, D. L. (2001) Recombineering: a powerful new tool for mouse functional genomics. **Nat Rev Genet** *2*, 769-779

Corey, L. L.,Weirich, C. S.,Benjamin, I. J. and Kingston, R. E. (2003) Localized recruitment of a chromatin-remodelling activity by an activator in vivo drives transcriptional elongation. **Genes & Development** *17*, 1392-1401

Cowles, C. R.,Hirschhorn, J. N.,Altshuler, D. and Lander, E. S. (2002) Detection of regulatory variation in mouse genes. **Nat Genet** *32*, 432-437

Croft, M. (2009) The role of TNF superfamily members in T-cell function and diseases. **Nat Rev Immunol** *9*, 271-285

Crolla, J. A. and van Heyningen, V. (2002) Frequent Chromosome Aberrations Revealed by Molecular Cytogenetic Studies in Patients with Aniridia. **The American Journal of Human Genetics** *71*, 1138-1149

Damas, P.,Resuter, A.,Gysen, P.,Demonty, J.,Lamy, M. and Franchimont, P. (1989) Tumor necrosis factor and interleukin-1 serum levels during severe sepsis in humans. **Crit Care Med.** *17*, 975-978

Davey, C. A.,Sargent, D. F.,Luger, K.,Maeder, A. W. and Richmond, T. J. (2002) Solvent Mediated Interactions in the Structure of the Nucleosome Core Particle at 1.9A Resolution. **Journal of Molecular Biology** *319*, 1097-1113

Davie, J. R. (1998) Covalent modifications of histones: expression from chromatin templates. **Current Opinion in Genetics & Development** *8*, 173-178

Dechend, R.,Hirano, F.,Heissmeyer, V.,Ansieau, S.,Gulba, D. C.,Scheidereit, C. and Leutz, A. (1999) The histone acetylase TIP60 forms higher ordered complexes with NF-κB-p50/Bcl3, which activate P-Selectin gene expression - a novel mechanism in the activation of adhesion factors. **Annals of Hematology** *78*, A20

Deleault, K. M.,Skinner, S. J. and Brooks, S. A. (2008) Tristetraprolin regulates TNF TNF-Î± mRNA stability via a proteasome dependent mechanism involving the combined action of the ERK and p38 pathways. **Molecular Immunology** *45*, 13-24

Demarchi, F.,Bertoli, C.,Sandy, P. and Schneider, C. (2003) Glycogen Synthase Kinase-3alpha Regulates NF-alphaB1/p105 Stability. **Journal of Biological Chemistry** *278*, 39583-39590

Deng, L., Wang, C., Spencer, E., Yang, L., Braun, A., You, J., Slaughter,C., Pickart, C., and Chen, Z.J. (2000). Activation of the IkappaB kinase complex by TRAF6 requires a dimeric ubiquitin-conjugating enzyme complex and a unique polyubiquitin chain. **Cell** 103, 351–361.

Dennis, G. J.,Sherman, B. T.,Hosack, D. A.,Yang, J.,Gao, W.,Lane, H. C. and Lempicki, R. A. (2003) DAVID: Database for Annotation, Visualisation, and Integrated Discovery. **Genome Biol** *4*, R60

Deroo, B. and Archer, T. K. (2001) Glucocorticoid receptor-mediated chromatin remodelling in vivo. **Oncogene** *20*, 3039-3046

Dhalluin, C.,Carlson, J. E.,Zeng, L.,He, C.,Aggarwal, A. K. and Zhou, M.-M. (1999) Structure and ligand of a histone acetyltransferase bromodomain. **Nature** *399*, 491-496

DiDonato, J. A.,Hayakawa, M.,Rothwarf, D. M.,Zandi, E. and Karin, M. (1997) A cytokine-responsive I[kappa]B kinase that activates the transcription factor NF-[kappa]B. **Nature** *388*, 548-554

Dobrzanski, P.,Ryseck, R. P. and Bravo, R. (1995) Specific inhibition of RelB/p52 transcriptional activity by the C-terminal domain of p100. **Oncogene** *10*, 1003-1007

Dokmanovic, M.,Clarke, C. and Marks, P. A. (2007) Histone Deacetylase Inhibitors: Overview and Perspectives. **Molecular Cancer Research** *5*, 981-989

Drouet, C.,Shakhov, A. N. and Jongeneel, C. V. (1991) Enhancers and transcription factors controlling the inducibility of the tumor necrosis factor-alpha promoter in primary macrophages. **J Immunol** *147*, 1694-1700

Duran, A.,Diaz-Meco, M. T. and Moscat, J. (2003) Essential role of RelA Ser311 phosphorylation by [zeta]PKC in NF-[kappa]B transcriptional activation. **EMBO J** *22*, 3910-3918

Ea. C., Deng, L., Xia, Z., Pineda,G.and Chen, Z. (2006) Activation of IKK by TNFa Requires Site-Specific Ubiquitination of RIP1 and Polyubiquitin Binding by NEMO**. Mol. Cell** 22, 245-257.

Eisfeld, K.,Candau, R.,Truss, M. and Beato, M. (1997) Binding of NF1 to the MMTV promoter in nucleosomes: influence of rotational phasing, translational positioning and histone H1. **Nucleic Acids Research** *25*, 3733-3742

Emami, K. H.,Jain, A. and Smale, S. T. (1997) Mechanism of synergy between TATA and initiator: synergistic binding of TFIID following a putative TFIIA-inducedâ€‰isomerisation. **Genes & Development** *11*, 3007-3019

Entus, R.,Aufderheide, B. and Sauro, H. (2007) Design and implementation of three incoherent feed-forward motif based biological concentration sensors. **Systems and Synthetic Biology** *1*, 119-128

Escalante, C. R.,Shen, L.,Thanos, D. and Aggarwal, A. K. (2002) Structure of NF-[kappa]B p50/p65 Heterodimer Bound to the PRDII DNA Element from the Interferon-[beta] Promoter. **Structure** *10*, 383-391

Fabrega, C.,Shen, V.,Shuman, S. and Lima, C. D. (2003) Structure of an mRNA Capping Enzyme Bound to the Phosphorylated Carboxy-Terminal Domain of RNA Polymerase II. **Molecular Cell** *11*, 1549-1561

Fischle, W.,Wang, Y. and Allis, C. D. (2003) Histone and chromatin cross-talk. **Current Opinion in Cell Biology** *15*, 172-183

Flanagan, J. F.,Mi, L.-Z.,Chruszcz, M.,Cymborowski, M.,Clines, K. L.,Kim, Y.,Minor, W.,Rastinejad, F. and Khorasanizadeh, S. (2005) Double chromodomains cooperate to recognize the methylated histone H3 tail. **Nature** *438*, 1181-1185

Fong, A. and Sun, S.-C. (2002) Genetic Evidence for the Essential Role of Î²-Transducin Repeat-containing Protein in the Inducible Processing of NF-kappaB2/p100. **Journal of Biological Chemistry** *277*, 22111-22114

Franzoso, G.,Bours, V.,Park, S.,Tomitayamaguchi, M.,Kelly, K. and Siebenlist, U. (1993) A NOVEL FUNCTION FOR THE CANDIDATE ONCOPROTEIN BCL-3 - AN ANTAGONIST OF P50/NF-KB-MEDIATED REPRESSION. **Journal of Acquired Immune Deficiency Syndromes and Human Retrovirology** *6*, 691-691

Franzoso G., Carlson L., Scharton-Kersten T., Shores E.W., Epstein S., Grinberg A., Tran T., Schacter E., Leonardi A., Anver M., Love P., Sher A., Siebenlist U. *(1997) Critical roles for the Bcl-3 oncoprotein in T cell-mediated immunity, splenic microarchitecture, and germinal center reactions.* ***Immunity*** *6:479–490.*

Friedrichsen, S. N.,Harper, C. V.,Semprini, S.,Wilding, M.,Adamson, A. D.,Spiller, D. G.,Nelson, G.,Mullins, J. J.,White, M. R. H. and Davis, J. R. E. (2006) Tumor Necrosis Factor-alpha Activates the Human Prolactin Gene Promoter via Nuclear Factor-kappaB Signalling. **Endocrinology** *147*, 773-781

Fuda, N. J.,Ardehali, M. B. and Lis, J. T. (2009) Defining mechanisms that regulate RNA polymerase II transcription in vivo. **Nature** *461*, 186-192

Fujinaga, K.,Irwin, D.,Huang, Y.,Taube, R.,Kurosu, T. and Peterlin, B. M. (2004) Dynamics of Human Immunodeficiency Virus Transcription: P-TEFb Phosphorylates RD and Dissociates Negative Effectors from the Transactivation Response Element. **Mol. Cell. Biol.** *24*, 787-795

Fujita, T.,Nolan, G. P.,Ghosh, S. and Baltimore, D. (1992) Independent modes of transcriptional activation by the p50 and p65 subunits of NF-kappa B. **Genes & Development** *6*, 775-787

Fujita, T.,Nolan, G. P.,Liou, H. C.,Scott, M. L. and Baltimore, D. (1993) The candidate proto-oncogene bcl-3 encodes a transcriptional coactivator that activates through NF-kappa B p50 homodimers. **Genes & Development** *7*, 1354-1363

Fuseler, J. W.,Merrill, D. M.,Rogers, J. A.,Grisham, M. B. and Wolf, R. E. (2006) Analysis and Quantitation of NF-[kappa]B Nuclear Translocation in Tumor Necrosis Factor Alpha (TNF-[alpha]) Activated Vascular Endothelial Cells. **Microscopy and Microanalysis** *12*, 269-276

Gallea-Robache, S.,Morand, V. R,Millet, S.,Bruneau, J.-M.,Bhatnagar, N.,Chouaib, S. and Roman-Roman, S. (1997) A METALLOPROTEINASE INHIBITOR BLOCKS THE SHEDDING OF SOLUBLE CYTOKINE RECEPTORS AND PROCESSING OF TRANSMEMBRANE CYTOKINE PRECURSORS IN HUMAN MONOCYTIC CELLS. **Cytokine** *9*, 340-346

Gao, N.,Asamitsu, K.,Hibi, Y.,Ueno, T. and Okamoto, T. (2008) AKIP1 Enhances NF-kappaB-dependent Gene Expression by Promoting the Nuclear Retention and Phosphorylation of p65. **Journal of Biological Chemistry** *283*, 7834-7843

Ge, B.,Li, O.,Wilder, P.,Rizzino, A. and McKeithan, T. W. (2003) NF-kappaB Regulates BCL3 Transcription in T Lymphocytes Through an Intronic Enhancer. **J Immunol** *171*, 4210-4218

Gerritsen, M. E.,Williams, A. J.,Neish, A. S.,Moore, S.,Shi, Y. and Collins, T. (1997) CREB-binding protein/p300 are transcriptional coactivators of p65. **Proceedings of the National Academy of Sciences** *94*, 2927-2932

Ghosh, A.,Shuman, S. and Lima, Christopher D. Structural Insights to How Mammalian Capping Enzyme Reads the CTD Code. **Molecular Cell** *43*, 299-310

Ghosh, S.,May, M. J. and Kopp, E. B. (1998) NF-kappa B and rel proteins: Evolutionarily conserved mediators of immune responses. **Annual Review of Immunology** *16*, 225-260

Gilchrist, D. A.,Fromm, G.,Dos Santos, G.,Pham, L. N.,McDaniel, I. E.,Burkholder, A.,fargo, D. C. and Adelman, K. (2012) Regulating the regulators: the pervasive effects of Pol II pausing on stimulus-responsive gene networks **Genes & Development** *26*, 933-944

Goldfeld, A. E.,Doyle, C. and Maniatis, T. (1990) Human tumor necrosis factor alpha gene regulation by virus and lipopolysaccharide. **Proceedings of the National Academy of Sciences** *87*, 9769-9773

Gomes, I.,Mathur, S. K.,Espenshade, B. M.,Mori, Y.,Varga, J. and Ackerman, S. J. (2005) Eosinophil-fibroblast interactions induce fibroblast IL-6 secretion and extracellular matrix gene expression: Implications in fibrogenesis. **Journal of Allergy and Clinical Immunology** *116*, 796-804

Gong, S.,Zheng, C.,Doughty, M. L.,Losos, K.,Didkovsky, N.,Schambra, U. B.,Nowak, N. J.,Joyner, A.,Leblanc, G.,Hatten, M. E. and Heintz, N. (2003) A gene expression atlas of the central nervous system based on bacterial artificial chromosomes. **Nature** *425*, 917-925

Green, J. V.,Radisic, M. and Murthy, S. K. (2009) Deterministic Lateral Displacement as a Means to Enrich Large Cells for Tissue Engineering. **Analytical Chemistry** *81*, 9178-9182

Grell, M.,Douni, E.,Wajant, H.,Laehden, M.,Clauss, M.,Maxeiner, B.,Georgopoulos, S.,Lesslauer, W.,Kollias, G.,Pfizenmaier, K. and Scheurich, P. (1995) The transmembrane form of tumor necrosis factor is the prime activating ligand of the 80 kDa tumor necrosis factor receptor. **Cell** *83*, 793-802

Grivennikov, S. I. and Karin, M. (2011) Inflammatory cytokines in cancer: tumour necrosis factor and interleukin 6 take the stage. **Annals of the Rheumatic Diseases** *70*, i104-i108

Guenther, M. G.,Levine, S. S.,Boyer, L. A.,Jaenisch, R. and Young, R. A. (2007) A Chromatin Landmark and Transcription Initiation at Most Promoters in Human Cells. **Cell** *130*, 77-88

Guermah, M.,Malik, S. and Roeder, R. G. (1998) Involvement of TFIID and USA Components in Transcriptional Activation of the Human Immunodeficiency Virus Promoter by NF-kappa B and Sp1. **Mol. Cell. Biol.** *18*, 3234-3244

Guttridge, D. C.,Albanese, C.,Reuther, J. Y.,Pestell, R. G. and Baldwin, A. S., Jr. (1999) NF-kappa B Controls Cell Growth and Differentiation through Transcriptional Regulation of Cyclin D1. **Mol. Cell. Biol.** *19*, 5785-5799

Guyon, J. R.,Narlikar, G. J.,Sullivan, E. K. and Kingston, R. E. (2001) Stability of a Human SWI-SNF Remodeled Nucleosomal Array. **Molecular and Cellular Biology** *21*, 1132-1144

Ha, I.,Roberts, S.,Maldonado, E.,Sun, X.,Kim, L. U.,Green, M. and Reinberg, D. (1993) Multiple functional domains of human transcription factor IIB: distinct interactions with two general transcription factors and RNA polymerase II. **Genes & Development** *7*, 1021-1032

Hadley, J. S.,Wang, J. E.,Michaels, L. C.,Dempsey, C. M.,Foster, S. J.,Thiemermann, C. and Hinds, C. J. (2007) Alterations in Inflammatory Capacity and Tlr Expression on Monocytes and Neutrophils After Cardiopulmonary Bypass. **Shock** *27*, 466-473

Hager, G. L.,Fletcher, T. M.,Xiao, N.,Baumann, C. T.,Mueller, W. G. and McNally, J. G. (2000) Dynamics of gene targeting and chromatin remodelling by nuclear receptors. **Biochem. Soc. Transactions** *28*, 405-410

Han, Q.,Bagheri, N.,Bradshaw, E. M.,Hafler, D. A.,Lauffenburger, D. A. and Love, J. C. (2011) Polyfunctional responses by human T cells result from sequential release of cytokines. **Proceedings of the National Academy of Sciences** *109*, 1607-1612

Han, Y. P.,Tuan, T. L.,Wu, H.,Hughes, M. and Garner, W. L. (2001) TNF-alpha stimulates activation of pro-MMP2 in human skin through NF-(kappa)B mediated induction of MT1-MMP. **Journal of Cell Science** *114*, 131-139

Hargreaves, D. C.,Horng, T. and Medzhitov, R. (2009) Control of Inducible Gene Expression by Signal-Dependent Transcriptional Elongation. **Cell** *138*, 129-145

Harper, C. V.,Finkenstadt, B. R.,Woodcock, D. J.,Friedrichsen, S. N.,Semprini, S.,Ashall, L.,Spiller, D. G.,Mullins, J. J.,Rand, D. A.,Davis, J. R. E. and White, M. R. H. (2011) Dynamic Analysis of Stochastic Transcription Cycles. **PLoS Biol** *9*, e1000607

Hassan, A. H.,Prochasson, P.,Neely, K. E.,Galasinski, S. C.,Chandy, M.,Carrozza, M. J. and Workman, J. L. (2002) Function and Selectivity of Bromodomains in Anchoring Chromatin-Modifying Complexes to Promoter Nucleosomes. **Cell** *111*, 369-379

Hayden, M. S. and Ghosh, S. (2004) Signalling to NF-kappaB. **Genes & Development** *18*, 2195-2224

Hebbar, P. B. and Archer, T. K. (2003) Nuclear Factor 1 Is Required for Both Hormone-Dependent Chromatin Remodelling and Transcriptional Activation of the Mouse Mammary Tumor Virus Promoter. **Molecular and Cellular Biology** *23*, 887-898

Helenius, K.,Yang, Y.,Tselykh, T. V.,Pessa, H. K. J.,Frilander, M. J. and Merkel, T. P. (2011) Requirement of TFIIH kinase subunit Mat1 for RNA Pol II C-terminal domain Ser5 phosphorylation, transcription and mRNA turnover. **Nucleic Acids Research** *39*, 5025-5035

Hengartner, C. J.,Thompson, C. M.,Zhang, J.,Chao, D. M.,Liao, S. M.,Koleske, A. J.,Okamura, S. and Young, R. A. (1995) Association of an activator with an RNA polymerase II holoenzyme. **Genes & Development** *9*, 897-910

Hirose, Y.,Tacke, R. and Manley, J. L. (1999) Phosphorylated RNA polymerase II stimulates pre-mRNA splicing. **Genes & Development** *13*, 1234-1239

Hodges, C.,Bintu, L.,Lubkowska, L.,Kashlev, M. and Bustamante, C. (2009) Nucleosomal Fluctuations Govern the Transcription Dynamics of RNA Polymerase II. **Science** *325*, 626-628

Hoffmann, A.,Levchenko, A.,Scott, M. L. and Baltimore, D. (2002) The Ikappa B-NF-kappa B Signalling Module: Temporal Control and Selective Gene Activation. **Science** *298*, 1241-1245

Hoffmann, A.,Levchenko, A.,Scott, M. L. and Baltimore, D. (2002) The Ikappa B-NF-kappa B Signalling Module: Temporal Control and Selective Gene Activation. **Science** *298*, 1241 - 1245

Hotamisligil, G. S.,Murray, D. L.,Choy, L. N. and Spiegelman, B. M. (1994) Tumor necrosis factor alpha inhibits signalling from the insulin receptor. **Proceedings of the National Academy of Sciences** *91*, 4854-4858

Hsu, H.,Huang, J.,Shu, H.-B.,Baichwal, V. and Goeddel, D. V. (1996) TNF-Dependent Recruitment of the Protein Kinase RIP to the TNF Receptor-1 Signalling Complex. **Immunity** *4*, 387-396

Hsu, H.,Shu, H.-B.,Pan, M.-G. and Goeddel, D. V. (1996) TRADD TRAF2 and TRADD FADD Interactions Define Two Distinct TNF Receptor 1 Signal Transduction Pathways. **Cell** *84*, 299-308

Hsu, H.,Xiong, J. and Goeddel, D. V. (1995) The TNF receptor 1-associated protein TRADD signals cell death and NF-ÎºB activation. **Cell** *81*, 495-504

Hutti, J. E.,Turk, B. E.,Asara, J. M.,Ma, A.,Cantley, L. C. and Abbott, D. W. (2007) IkappaB Kinase {beta} Phosphorylates the K63 Deubiquitinase A20 To Cause Feedback Inhibition of the NF-kappaB Pathway. **Mol. Cell. Biol.** *27*, 7451-7461

Imbalzano, A. N.,Kwon, H.,Green, M. R. and Kingston, R. E. (1994) Facilitated binding of TATA-binding protein to nucleosomal DNA. **Nature** *370*,

Ioshikhes, I.,Bolshoy, A.,Derenshteyn, K.,Borodovsky, M. and Trifonov, E. N. (1996) Nucleosome DNA Sequence Pattern Revealed by Multiple Alignment of Experimentally Mapped Sequences. **Journal of Molecular Biology** *262*, 129-139

Ioshikhes, I. P.,Albert, I.,Zanton, S. J. and Pugh, B. F. (2006) Nucleosome positions predicted through comparative genomics. **Nat Genet** *38*, 1210-1215

Ishikawa, H.,Claudio, E.,Dambach, D.,Raventas-Suarez, C.,Ryan, C. and Bravo, R. (1998) Chronic Inflammation and Susceptibility to Bacterial Infections in Mice Lacking the Polypeptide (p)105 Precursor (NF-kappaB1) but Expressing p50. **The Journal of Experimental Medicine** *187*, 985-996

Ito, T.,Bulger, M.,Pazin, M. J.,Kobayashi, R. and Kadonaga, J. T. (1997) ACF, an ISWI-Containing and ATP-Utilizing Chromatin Assembly and Remodelling Factor. **Cell** *90*, 145-155

Izban, M. G. and Luse, D. S. (1992) The RNA polymerase II ternary complex cleaves the nascent transcript in a 3'----5' direction in the presence of elongation factor SII. **Genes & Development** *6*, 1342-1356

Jacobs, M. D. and Harrison, S. C. (1998) Structure of an IkappaB/NF-kappaB Complex. **Cell** *95*, 749-758

Jamaluddin, M.,Choudhary, S.,Wang, S.,Casola, A.,Huda, R.,Garofalo, R. P.,Ray, S. and Brasier, A. R. (2005) Respiratory Syncytial Virus-Inducible BCL-3 Expression Antagonizes the STAT/IRF and NF-{kappa}B Signalling Pathways by Inducing Histone Deacetylase 1 Recruitment to the Interleukin-8 Promoter. **J. Virol.** *79*, 15302-15313

Jang, M. K.,Mochizuki, K.,Zhou, M.,Jeong, H.-S.,Brady, J. N. and Ozato, K. (2005) The Bromodomain Protein Brd4 Is a Positive Regulatory Component of P-TEFb and Stimulates RNA Polymerase II-Dependent Transcription. **Molecular Cell** *19*, 523-534

Jin, C.,Zang, C.,Wei, G.,Cui, K.,Peng, W.,Zhao, K. and Felsenfeld, G. (2009) H3.3/H2A.Z double variant-containing nucleosomes mark 'nucleosome-free regions' of active promoters and other regulatory regions. **Nat Genet** *41*, 941-945

John, S.,Sabo, P. J.,Thurman, R. E.,Sung, M.-H.,Biddie, S. C.,Johnson, T. A.,Hager, G. L. and Stamatoyannopoulos, J. A. (2010) Chromatin accessibility pre-determines glucocorticoid receptor binding patterns. **Nat Genet** *43*, 264-268

Kadonaga, J. T. (2004) Regulation of RNA Polymerase II Transcription by Sequence-Specific DNA Binding Factors. **Cell** *116*, 247-257

Kagan, J. C.,Su, T.,Horng, T.,Chow, A.,Akira, S. and Medzhitov, R. (2008) TRAM couples endocytosis of Toll-like receptor 4 to the induction of interferon-[beta]. **Nat Immunol** *9*, 361-368

Kagey, M., Newman, J.J., Bilodeau, S., Zhan, Y., Orlando, D.A., van Berkum, N.L., Ebmeier, C.C., Goossens, G., Rahl, P.B., Levine, S.S., Taatjes, D.J., Dekker, J. and Young, R.A. (2010) Mediator and cohesin connect gene expression and chromatin architecture. **Nature** 467, 430-435.

Kaneko, S.,Chu, C.,Shatkin, A. J. and Manley, J. L. (2007) Human capping enzyme promotes formation of transcriptional R loops in vitro. **Proceedings of the National Academy of Sciences** *104*, 17620-17625

Kang, S. M.,Tran, A. C.,Grilli, M. and Lenardo, M. J. (1992) NF-kappa B subunit regulation in nontransformed CD4+ T lymphocytes. **Science** *256*, 1452-1456

Kanayama, A., Seth, R.B., Sun, L., Ea, C.K., Hong, M., Shaito, A., Chiu, Y.H., Deng, L., and Chen, Z.J. (2004). TAB2 and TAB3 activate the NF-kappaB pathway through binding to polyubiquitin chains. **Mol. Cell** 15, 535–548.

Kaplan, S.,Bren, A.,Dekel, E. and Alon, U. (2008) The incoherent feed-forward loop can generate non-monotonic input functions for genes. **Mol Syst Biol** *4*,

Karin, M. (2006) Nuclear factor-kappaB in cancer development and progression. **Nature** *441*, 431-436

Karin, M. and Ben-Neriah, Y. (2000) Phosphorylation Meets Ubiquitination: The Control of NF-kappaB Activity. **Annual Review of Immunology** *18*, 621-663

Kasten, M.,Szerlong, H.,Erdjument-Bromage, H.,Tempst, P.,Werner, M. and Cairns, B. R. (2004) Tandem bromodomains in the chromatin remodeler RSC recognize acetylated histone H3 Lys14. **EMBO J** *23*, 1348-1359

Kaushansky, K.,Lin, N. and Adamson, J. W. (1988) Interleukin 1 stimulates fibroblasts to synthesize granulocyte-macrophage and granulocyte colony-stimulating factors. Mechanism for the hematopoietic response to inflammation. **The Journal of Clinical Investigation** *81*, 92-97

Kearns, J. D.,Basak, S.,Werner, S. L.,Huang, C. S. and Hoffmann, A. (2006) IkappaB µ provides negative feedback to control NF-kappaB oscillations, signalling dynamics, and inflammatory gene expression. **The Journal of Cell Biology** *173*, 659-664

Kerr, L. D.,Duckett, C. S.,Wamsley, P.,Zhang, Q.,Chiao, P.,Nabel, G.,McKeithan, T. W.,Baeuerle, P. A. and Verma, I. M. (1992) The proto-oncogene bcl-3 encodes an I kappa B protein. **Genes & Development** *6*, 2352-2363

Keutgens, A.,Shostak, K.,Close, P.,Zhang, X.,Hennuy, B. t.,Aussems, M.,Chapelle, J.-P.,Viatour, P.,Gothot, A.,Fillet, M. and Chariot, A. (2010) The Repressing Function of the Oncoprotein BCL-3 Requires CtBP, while Its Polyubiquitination and Degradation Involve the E3 Ligase TBLR1. **Molecular and Cellular Biology** *30*, 4006-4021

Khavari, P. A. (2006) Modelling cancer in human skin tissue. **Nat Rev Cancer** *6*, 270-280

Kiernan, R.,Braes, V.,Ng, R. W. M.,Coudart, M.-P.,El Messaoudi, S.,Sardet, C.,Jin, D.-Y.,Emiliani, S. and Benkirane, M. (2003) Post-activation Turn-off of NF-kappaB-dependent Transcription Is Regulated by Acetylation of p65. **Journal of Biological Chemistry** *278*, 2758-2766

Kim, D.,Kolch, W. and Cho, K.-H. (2009) Multiple roles of the NF-kappaB signalling pathway regulated by coupled negative feedback circuits. **The FASEB Journal** *23*, 2796-2802

Kim, J.-Y.,Moon, S.-M.,Ryu, H.-J.,Kim, J.-J.,Kim, H.-T.,Park, C.,Kimm, K.,Oh, B. and Lee, J.-K. (2005) Identification of regulatory polymorphisms in the TNF–TNF receptor superfamily. **Immunogenetics** *57*, 297-303

Kim, J. L.,Nikolov, D. B. and Burley, S. K. (1993) Co-crystal structure of TBP recognizing the minor groove of a TATA element. **Nature** *365*,

Kim, T. H.,Barrera, L. O.,Zheng, M.,Qu, C.,Singer, M. A.,Richmond, T. A.,Wu, Y.,Green, R. D. and Ren, B. (2005) A high-resolution map of active promoters in the human genome. **Nature** *436*, 876-880

Kim, Y.,Geiger, J. H.,Hahn, S. and Sigler, P. B. (1993) Crystal structure of a yeast TBP/TATA-box complex. **Nature** *365*, 312-320

Kitchens, R. L.,Thompson, P. A.,O'Keefe, G. E. and Munford, R. S. (2000) Plasma constituents regulate LPS binding to, and release from, the monocyte cell surface. **Journal of Endotoxin Research** *6*, 477-482

Kleinjan, D. A. and van Heyningen, V. (2005) Long-Range Control of Gene Expression: Emerging Mechanisms and Disruption in Disease. **The American Journal of Human Genetics** *76*, 8-32

Koch, C. M.,Andrews, R. M.,Flicek, P.,Dillon, S. C.,Karaz, U.,Clelland, G. K.,Wilcox, S.,Beare, D. M.,Fowler, J. C.,Couttet, P.,James, K. D.,Lefebvre, G. C.,Bruce, A. W.,Dovey, O. M.,Ellis, P. D.,Dhami, P.,Langford, C. F.,Weng, Z.,Birney, E.,Carter, N. P.,Vetrie, D. and Dunham, I. (2007) The landscape of histone modifications across 1% of the human genome in five human cell lines. **Genome Research** *17*, 691-707

Komissarova, N. and Kashlev, M. (1997) RNA Polymerase Switches between Inactivated and Activated States By Translocating Back and Forth along the DNA and the RNA. **Journal of Biological Chemistry** *272*, 15329-15338

Komissarova, N. and Kashlev, M. (1997) Transcriptional arrest: Escherichia coli RNA polymerase translocates backward, leaving the 3' end of the RNA intact and extruded. **Proceedings of the National Academy of Sciences** *94*, 1755-1760

Komuro, T. (1990) Re-evaluation of fibroblasts and fibroblast-like cells. **Anatomy and Embryology** *182*, 103-112

Konev, A. Y.,Tribus, M.,Park, S. Y.,Podhraski, V.,Lim, C. Y.,Emelyanov, A. V.,Vershilova, E.,Pirrotta, V.,Kadonaga, J. T.,Lusser, A. and Fyodorov, D. V. (2007) CHD1 Motor Protein Is Required for Deposition of Histone Variant H3.3 into Chromatin in Vivo. **Science** *317*, 1087-1090

Kovalenko, A.,Chable-Bessia, C.,Cantarella, G.,Israel, A.,Wallach, D. and Courtois, G. (2003) The tumour suppressor CYLD negatively regulates NF-[kappa]B signalling by deubiquitination. **Nature** *424*, 801-805

Krappmann, D. and Scheidereit, C. (2005) A pervasive role of ubiquitin conjugation in activation and termination of I[kappa]B kinase pathways. **EMBO Rep** *6*, 321-326

Kratochvill, F.,Machacek, C.,Vogl, C.,Ebner, F.,Sedlyarov, V.,Gruber, A. R.,Hartweger, H.,Vielnascher, R.,Karaghiosoff, M.,Rulicke, T.,Muller, M.,Hofacker, I.,Lang, R. and Kovarik, P. (2011) Tristetraprolin-driven regulatory circuit controls quality and timing of mRNA decay in inflammation. **Mol Syst Biol** *7*,

Krikos, A.,Laherty, C. D. and Dixit, V. M. (1992) Transcriptional activation of the tumor necrosis factor alpha-inducible zinc finger protein, A20, is mediated by kappa B elements. **Journal of Biological Chemistry** *267*, 17971-17976

Kruppa, G.,Thoma, B.,Machleidt, T.,Wiegmann, K. and Kroenke, M. (1992) Inhibition of tumor necrosis factor (TNF)-mediated NF-kappaB activation by selective blockade of the human 55-kDa TNF receptor. **The Journal of Immunology** *148*, 3152-3157

Kubitscheck, U.,Kaeckmann, O.,Kues, T. and Peters, R. (2000) Imaging and Tracking of Single GFP Molecules in Solution. **Biophysical Journal** *78*, 2170-2179

Kumar, S.,Votta, B. J.,Rieman, D. J.,Badger, A. M.,Gowen, M. and Lee, J. C. (2001) IL-1- and TNF-induced bone resorption is mediated by p38 mitogen activated protein kinase*. **Journal of Cellular Physiology** *187*, 294-303

Kunsch, C. and Rosen, C. A. (1993) NF-kappa B subunit-specific regulation of the interleukin-8 promoter. **Mol. Cell. Biol.** *13*, 6137-6146

Kunsch, C.,Ruben, S. M. and Rosen, C. A. (1992) Selection of optimal kappa B/Rel DNA-binding motifs: interaction of both subunits of NF-kappa B with DNA is required for transcriptional activation. **Mol. Cell. Biol.** *12*, 4412-4421

Kuo, M. L.,Brownell, J. E.,Sobel, R. E.,Ranalli, T. A.,Cook, R. G.,Edmondson, D. G.,Roth, S. Y. and Allis, C. D. (1996) Transcription-linked acetylation by Gcn5p of histones H3 and H4 at specific lysines **Nature** *383*, 269-272

Kuwata, H.,Watanabe, Y.,Miyoshi, H.,Yamamoto, M.,Kaisho, T.,Takeda, K. and Akira, S. (2003) IL-10-inducible Bcl-3 negatively regulates LPS-induced TNF-alpha production in macrophages. **Blood** *102*, 4123-4129

Lagrange, T.,Kapanidis, A. N.,Tang, H.,Reinberg, D. and Ebright, R. H. (1998) New core promoter element in RNA polymerase II-dependent transcription: sequence-specific DNA binding by transcription factors. **Genes & Development** *12*, 34-44

Lahat, N.,Rahat, M. A.,Kinarty, A.,Weiss-Cerem, L.,Pinchevski, S. and Bitterman, H. (2008) Hypoxia enhances lysosomal TNF-alpha degradation in mouse peritoneal macrophages. **American Journal of Physiology - Cell Physiology** *295*, C2-C12

Lai, W. S.,Carballo, E.,Strum, J. R.,Kennington, E. A.,Phillips, R. S. and Blackshear, P. J. (1999) Evidence that Tristetraprolin Binds to AU-Rich Elements and Promotes the Deadenylation and Destabilisation of Tumor Necrosis Factor Alpha mRNA. **Molecular and Cellular Biology** *19*, 4311-4323

Laird, P. W.,Zijderveld, A.,Linders, K.,Rudnicki, M. A.,Jaenisch, R. and Berns, A. (1991) Simplified mammalian DNA isolation procedure. **Nucleic Acids Res** *19*, 4293-4293

Landick, R. (1997) RNA Polymerase Slides Home: Pause and Termination Site Recognition. **Cell** *88*, 741-744

Larson, D. R.,Singer, R. H. and Zenklusen, D. (2009) A single molecule view of gene expression. **Trends in cell biology** *19*, 630-637

Latimer, M.,Ernst, M. K.,Dunn, L. L.,Drutskaya, M. and Rice, N. R. (1998) The N-Terminal Domain of IkappaBalpha Masks the Nuclear Localisation Signal(s) of p50 and c-Rel Homodimers. **Molecular and Cellular Biology** *18*, 2640-2649

Ledebur, H.C. and Parks, T.P. (1995) Transcriptional Regulation of the Intercellular Adhesion Molecule-1 Gene by Inflammatory Cytokines in Human Endothelial Cells. **J. Biol. Chem**. 270, 933-943.

Lee, D. K.,Duan, H. O. and Chang, C. (2001) Androgen Receptor Interacts with the Positive Elongation Factor P-TEFb and Enhances the Efficiency of Transcriptional Elongation. **Journal of Biological Chemistry** *276*, 9978-9984

Lee, H.,Kraus, K. W.,Wolfner, M. F. and Lis, J. T. (1992) DNA sequence requirements for generating paused polymerase at the start of hsp70. **Genes & Development** *6*, 284-295

Lee, J. W.,Lee, Y. C.,Na, S. Y.,Jung, D. J. and Lee, S. K. (2001) Transcriptional coregulators of the nuclear receptor superfamily: coactivators and corepressors. **Cellular and Molecular Life Sciences** *58*, 289-297

Lettice, L. A.,Horikoshi, T.,Heaney, S. J. H.,van Baren, M. J.,van der Linde, H. C.,Breedveld, G. J.,Joosse, M.,Akarsu, N.,Oostra, B. A.,Endo, N.,Shibata, M.,Suzuki, M.,Takahashi, E.,Shinka, T.,Nakahori, Y.,Ayusawa, D.,Nakabayashi, K.,Scherer, S. W.,Heutink, P.,Hill, R. E. and Noji, S. (2002) Disruption of a long-range cis-acting regulator for Shh causes preaxial polydactyly. **Proceedings of the National Academy of Sciences** *99*, 7548-7553

Li, G.,Levitus, M.,Bustamante, C. and Widom, J. (2005) Rapid spontaneous accessibility of nucleosomal DNA. **Nat Struct Mol Biol** *12*, 46-53

Li, G. and Widom, J. (2004) Nucleosomes facilitate their own invasion. **Nat Struct Mol Biol** *11*, 763-769

Li, M.,Carpio, D. F.,Zheng, Y.,Bruzzo, P.,Singh, V.,Ouaaz, F.,Medzhitov, R. M. and Beg, A. A. (2001) An Essential Role of the NF-kappaB/Toll-Like Receptor Pathway in Induction of Inflammatory and Tissue-Repair Gene Expression by Necrotic Cells. **The Journal of Immunology** *166*, 7128-7135

Li, Q. and Verma, I. M. (2002) NF-kappaB regulation in the immune system. **Nat Rev Immunol** *2*, 725-734

Li, Q. and Wrange, O. (1995) The accessibility of a glucocorticoid response element dependent on its rotational positioning. **Mol Cell Biol** *15*, 4375-4384

Li, Z.-W.,Chu, W.,Hu, Y.,Delhase, M.,Deerinck, T.,Ellisman, M.,Johnson, R. and Karin, M. (1999) The IKKalpha Subunit of IkappaB Kinase (IKK) is Essential for Nuclear Factor kappaB Activation and Prevention of Apoptosis. **The Journal of Experimental Medicine** *189*, 1839-1845

Liang, G.,Lin, J. C. Y.,Wei, V.,Yoo, C.,Cheng, J. C.,Nguyen, C. T.,Weisenberger, D. J.,Egger, G.,Takai, D.,Gonzales, F. A. and Jones, P. A. (2004) Distinct localisation of histone H3 acetylation and H3-K4 methylation to the transcription start sites in the human genome. **Proceedings of the National Academy of Sciences of the United States of America** *101*, 7357-7362

Lickwar, C. R.,Mueller, F.,Hanlon, S. E.,McNally, J. G. and Lieb, J. D. (2012) Genome-wide protein-DNA binding dynamics suggest a molecular clutch for transcription factor function. **Nature** *484*, 251-255

Lin, L.,DeMartino, G. N. and Greene, W. C. (2000) Cotranslational dimerisation of the Rel homology domain of NF-[kappa]B1 generates p50-p105 heterodimers and is required for effective p50 production. **EMBO J** *19*, 4712-4722

Lin, Y.-Z.,Yao, S.,Veach, R. A.,Torgerson, T. R. and Hawiger, J. (1995) Inhibition of Nuclear Translocation of Transcription Factor NF-kappaB by a Synthetic Peptide Containing a Cell Membrane-permeable Motif and Nuclear Localisation Sequence. **Journal of Biological Chemistry** *270*, 14255-14258

Ling, L.,Cao, Z. and Goeddel, D. V. (1998) NF-kappaB-inducing kinase activates IKKalpha by phosphorylation of Ser-176. **Proceedings of the National Academy of Sciences** *95*, 3792-3797

Lipniacki, T.,Paszek, P.,Brasier, A. R.,Luxon, B. and Kimmel, M. (2004) Mathematical model of NF-kappaB regulatory module. **Journal Of Theoretical Biology** *228*, 195-215

Lis, J. T.,Mason, P.,Peng, J.,Price, D. H. and Werner, J. (2000) P-TEFb kinase recruitment and function at heat shock loci. **Genes & Development** *14*, 792-803

Liu, C. L.,Kaplan, T.,Kim, M.,Buratowski, S.,Schreiber, S. L.,Friedman, N. and Rando, O. J. (2005) Single-Nucleosome Mapping of Histone Modifications in S. cerevisiae. **PLoS Biol** *3*, e328

Liu, H.,Sidiropoulos, P.,Song, G.,Pagliari, L. J.,Birrer, M. J.,Stein, B.,Anrather, J. and Pope, R. M. (2000) TNF-alpha Gene Expression in Macrophages: Regulation by NF-kappaB Is Independent of c-Jun or C/EBP. **The Journal of Immunology** *164*, 4277-4285

Luebben, W. R.,Sharma, N. and Nyborg, J. K. (2010) Nucleosome eviction and activated transcription require p300 acetylation of histone H3 lysine 14. **Proceedings of the National Academy of Sciences**

Luisi, B. F.,Xu, W. X.,Otwinowski, Z.,Freedman, L. P.,Yamamoto, K. R. and Sigler, P. B. (1991) Crystallographic analysis of the interaction of the glucocorticoid receptor with DNA. **Nature** *352*, 497-505

MacNaul, K. L.,Hutchinson, N. I.,Parsons, J. N.,Bayne, E. K. and Tocci, M. J. (1990) Analysis of IL-1 and TNF-alpha gene expression in human rheumatoid synoviocytes and normal monocytes by in situ hybridisation. **The Journal of Immunology** *145*, 4154-4166

Malik, S. and Roeder, R. G. (2000) Transcriptional regulation through Mediator-like coactivators in yeast and metazoan cells. **Trends in Biochemical Sciences** *25*, 277-283

Malinin, N. L.,Boldin, M. P.,Kovalenko, A. V. and Wallach, D. (1997) MAP3K-related kinase involved in NF-KB induction by TNF, CD95 and IL-1. **Nature** *385*, 540-544

Manavalan, B.,Basith, S.,Choi, Y.-M.,Lee, G. and Choi, S. (2010) Structure-Function Relationship of Cytoplasmic and Nuclear IkappaB Proteins: An In Silico Analysis. **PLoS ONE** *5*, e15782

Mangan, S. and Alon, U. (2003) Structure and function of the feed-forward loop network motif. **Proceedings of the National Academy of Sciences of the United States of America** *100*, 11980-11985

Mangan, S.,Itzkovitz, S.,Zaslaver, A. and Alon, U. (2006) The Incoherent Feed-forward Loop Accelerates the Response-time of the gal System of Escherichia coli. **Journal of Molecular Biology** *356*, 1073-1081

Marc, F.,Fionula M, B.,Michael J, E.,Richard O, W. and Ravinder N, M. (1995) TNFalpha; Is an Effective Therapeutic Target for Rheumatoid Arthritis **Annals of the New York Academy of Sciences** *766*, 272-278

Mark, K. S.,Trickler, W. J. and Miller, D. W. (2001) Tumor Necrosis Factor-alpha Induces Cyclooxygenase-2 Expression and Prostaglandin Release in Brain Microvessel Endothelial Cells. **Journal of Pharmacology and Experimental Therapeutics** *297*, 1051-1058

Martinez, E.,Zhou, Q.,L'Etoile, N. D.,Oelgeschlaeger, T.,Berk, A. J. and Roeder, R. G. (1995) Core promoter-specific function of a mutant transcription factor TFIID defective in TATA-box binding. **Proceedings of the National Academy of Sciences** *92*, 11864-11868

Mason, P. B. and Lis, J. T. (1997) Cooperative and Competitive Protein Interactions at the Hsp70 Promoter. **Journal of Biological Chemistry** *272*, 33227-33233

Massoumi, R.,Chmielarska, K.,Hennecke, K.,Pfeifer, A. and Faessler, R. (2006) Cyld Inhibits Tumor Cell Proliferation by Blocking Bcl-3-Dependent NF-kappaB Signalling. **Cell** *125*, 665-677

Massoumi, R.,Kuphal, S.,Hellerbrand, C.,Haas, B.,Wild, P.,Spruss, T.,Pfeifer, A.,Fassler, R. and Bosserhoff, A. K. (2009) Down-regulation of CYLD expression by Snail promotes tumor progression in malignant melanoma. **The Journal of Experimental Medicine** *206*, 221-232

Mavrich, T. N.,Jiang, C.,Ioshikhes, I. P.,Li, X.,Venters, B. J.,Zanton, S. J.,Tomsho, L. P.,Qi, J.,Glaser, R. L.,Schuster, S. C.,Gilmour, D. S.,Albert, I. and Pugh, B. F. (2008) Nucleosome organisation in the Drosophila genome. **Nature** *453*, 358-362

McKeithan, T.W., Ohno, H., Dickstein, J. and Hume, E. (1995) Genomic Structure of the Candidate Proto-oncogene *BCL3*. **Genomics** 24, 120-126.

Meneghini, M. D.,Wu, M. and Madhani, H. D. (2003) Conserved Histone Variant H2A.Z Protects Euchromatin from the Ectopic Spread of Silent Heterochromatin. **Cell** *112*, 725-736

Mercurio, F.,Zhu, H.,Murray, B. W.,Shevchenko, A.,Bennett, B. L.,Li, J. w.,Young, D. B.,Barbosa, M.,Mann, M.,Manning, A. and Rao, A. (1997) IKK-1 and IKK-2: Cytokine-Activated IkappaB Kinases Essential for NF-kappaB Activation. **Science** *278*, 860-866

Métivier, R.,Penot, G.,Hübner, M. R.,Reid, G.,Brand, H.,Koa, M. and Gannon, F. (2003) Estrogen Receptor-alpha Directs Ordered, Cyclical, and Combinatorial Recruitment of Cofactors on a Natural Target Promoter. **Cell** *115*, 751-763

Micheau, O. and Tschopp, J. (2003) Induction of TNF Receptor I-Mediated Apoptosis via Two Sequential Signalling Complexes. **Cell** *114*, 181-190

Michelman-Ribeiro, A.,Mazza, D.,Rosales, T.,Stasevich, T. J.,Boukari, H.,Rishi, V.,Vinson, C.,Knutson, J. R. and McNally, J. G. (2009) Direct Measurement of Association and Dissociation Rates of DNA Binding in Live Cells by Fluorescence Correlation Spectroscopy. **Biophysical Journal** *97*, 337-346

Miki, Y.,Ono, K.,Hata, S.,Suzuki, T.,Kumamoto, H. and Sasano, H. (2012) The advantages of co-culture over mono cell culture in simulating in vivo environment. **The Journal of Steroid Biochemistry and Molecular Biology**

Mills, J. B. and Hagerman, P. J. (2004) Origin of the intrinsic rigidity of DNA. **Nucleic Acids Research** *32*, 4055-4059

Milo, R.,Shen-Orr, S.,Itzkovitz, S.,Kashtan, N.,Chklovskii, D. and Alon, U. (2002) Network Motifs: Simple Building Blocks of Complex Networks. **Science** *298*, 824-827

Min, I. M.,Waterfall, J. J.,Core, L. J.,Munroe, R. J.,Schimenti, J. and Lis, J. T. (2011) Regulating RNA polymerase pausing and transcription elongation in embryonic stem cells. **Genes & Development** *25*, 742-754

Missra, A. and Gilmour, D. S. (2010) Interactions between DSIF (DRB sensitivity inducing factor), NELF (negative elongation factor), and the Drosophila RNA polymerase II transcription elongation complex. **Proceedings of the National Academy of Sciences** *107*, 11301-11306

Mizuguchi, G.,Shen, X.,Landry, J.,Wu, W.-H.,Sen, S. and Wu, C. (2004) ATP-Driven Exchange of Histone H2AZ Variant Catalyzed by SWR1 Chromatin Remodelling Complex. **Science** *303*, 343-348

Moorthy, A. K.,Savinova, O. V.,Ho, J. Q.,Wang, V. Y.-F.,Vu, D. and Ghosh, G. (2006) The 20S proteasome processes NF-[kappa]B1 p105 into p50 in a translation-independent manner. **EMBO J** *25*, 1945-1956

Moreland, R. J.,Tirode, F.,Yan, Q.,Conaway, J. W.,Egly, J.-M. and Conaway, R. C. (1999) A Role for the TFIIH XPB DNA Helicase in Promoter Escape by RNA Polymerase II. **Journal of Biological Chemistry** *274*, 22127-22130

Morshed, N.,Chetty, M. and Nguyen, V. (2012) Simultaneous learning of instantaneous and time-delayed genetic interactions using novel information theoretic scoring technique. **BMC Systems Biology** *6*, 62-70

Mueller, N.,Schneider, B.,Pfizenmaier, K. and Wajant, H. (2010) Superior serum half life of albumin tagged TNF ligands. **Biochemical and Biophysical Research Communications** *396*, 793-799

Mukhopadhyay, A.,Suttles, J.,Stout, R. D. and Aggarwal, B. B. (2001) Genetic Deletion of the Tumor Necrosis Factor Receptor p60 or p80 Abrogates Ligand-mediated Activation of Nuclear Factor-kappaB and of Mitogen-activated Protein Kinases in Macrophages. **Journal of Biological Chemistry** *276*, 31906-31912

Mukhopadhyay, D.,Tsiokas, L. and Sukhatme, V. (1998) High cell density induces vascular endothelial growth factor expression via protein tyrosine phosphorylation. **Gene Expression** *7*, 53-60

Munro, J. M.,Pober, J. S. and Cotran, R. S. (1989) Tumor necrosis factor and interferon-gamma induce distinct patterns of endothelial activation and associated leukocyte accumulation in skin of Papio anubis. **Am J Pathol** *135*, 121-133

Murray, P. J. (2005) The primary mechanism of the IL-10-regulated antiinflammatory response is to selectively inhibit transcription. **Proceedings of the National Academy of Sciences of the United States of America** *102*, 8686-8691

Na, S.-Y.,Choi, H.-S.,Kim, J. W.,Na, D. S. and Lee, J. W. (1998) Bcl3, an IkappaB Protein, as a Novel Transcription Coactivator of the Retinoid X Receptor. **Journal of Biological Chemistry** *273*, 30933-30938

Na, S.-Y.,Choi, J.-E.,Kim, H.-J.,Jhun, B. H.,Lee, Y.-C. and Lee, J. W. (1999) Bcl3, an IkappaB Protein, Stimulates Activating Protein-1 Transactivation and Cellular Proliferation. **Journal of Biological Chemistry** *274*, 28491-28496

Nagai, T.,Ibata, K.,Park, E. S.,Kubota, M.,Mikoshiba, K. and Miyawaki, A. (2002) A variant of yellow fluorescent protein with fast and efficient maturation for cell-biological applications. **Nat Biotech** *20*, 87-90

Nakai, Y.,Hamagaki, S.,Takagi, R.,Taniguchi, A. and Kurimoto, F. (1999) Plasma Concentrations of Tumor Necrosis Factor-alpha (TNF-alpha) and Soluble TNF Receptors in Patients with Anorexia Nervosa. **Journal of Clinical Endocrinology & Metabolism** *84*, 1226-1228

Nakajima, T.,Uchida, C.,Anderson, S. F.,Lee, C.-G.,Hurwitz, J.,Parvin, J. D. and Montminy, M. (1997) RNA Helicase A Mediates Association of CBP with RNA Polymerase II. **Cell** *90*, 1107-1112

Narlikar, G. J.,Phelan, M. L. and Kingston, R. E. (2001) Generation and Interconversion of Multiple Distinct Nucleosomal States as a Mechanism for Catalyzing Chromatin Fluidity. **Molecular Cell** *8*, 1219-1230

Nativio R, Wendt KS, Ito Y, Huddleston JE, Uribe-Lewis S, et al. (2009) Cohesin Is Required for Higher-Order Chromatin Conformation at the Imprinted *IGF2-H19* Locus. **PLoS Genet** 5(11): e1000739. doi:10.1371/journal.pgen.1000739

Natoli, G.,Ghisletti, S. and Barozzi, I. (2011) The genomic landscapes of inflammation. **Genes & Development** *25*, 101-106

Naumann, M.,Wulczyn, F. G. and Scheidereit, C. (1993) The NF-kappa B precursor p105 and the proto-oncogene product Bcl-3 are I kappa B molecules and control nuclear translocation of NF-kappa B. **EMBO J** *12*, 213-222

Nechaev, S.,Fargo, D. C.,dos Santos, G.,Liu, L.,Gao, Y. and Adelman, K. (2010) Global Analysis of Short RNAs Reveals Widespread Promoter-Proximal Stalling and Arrest of Pol II in Drosophila. **Science** *327*, 335-338

Nelson, D. E.,Ihekwaba, A. E. C.,Elliott, M.,Johnson, J. R.,Gibney, C. A.,Foreman, B. E.,Nelson, G.,See, V.,Horton, C. A.,Spiller, D. G.,Edwards, S. W.,McDowell, H. P.,Unitt, J. F.,Sullivan, E.,Grimley, R.,Benson, N.,Broomhead, D.,Kell, D. B. and White, M. R. H. (2004) Oscillations in NF-kappaB Signalling Control the Dynamics of Gene Expression. **Science** *306*, 704-708

Nelson, G.,Paraoan, L.,Spiller, D. G.,Wilde, G. J. C.,Browne, M. A.,Djali, P. K.,Unitt, J. F.,Sullivan, E.,Floettmann, E. and White, M. R. H. (2002) Multi-parameter analysis of the kinetics of NF-kappaB signalling and transcription in single living cells. **Journal of Cell Science** *115*, 1137-1148

Neumann, H.,Hancock, S. M.,Buning, R.,Routh, A.,Chapman, L.,Somers, J.,Owen-Hughes, T.,van Noort, J.,Rhodes, D. and Chin, J. W. (2009) A Method for Genetically Installing Site-Specific Acetylation in Recombinant Histones Defines the Effects of H3 K56 Acetylation. **Molecular Cell** *36*, 153-163

Ni, Z.,Schwartz, B. E.,Werner, J.,Suarez, J.-R. and Lis, J. T. (2004) Coordination of Transcription, RNA Processing, and Surveillance by P-TEFb Kinase on Heat Shock Genes. **Molecular Cell** *13*, 55-65

Nightingale, K. P.,Wellinger, R. E.,Sogo, J. M. and Becker, P. B. (1998) Histone acetylation facilitates RNA polymerase II transcription of the Drosophila hsp26 gene in chromatin. **EMBO J** *17*, 2865-2876

Nilsson, J.,Jovinge, S.,Niemann, A.,Reneland, R. and Lithell, H. (1998) Relation Between Plasma Tumor Necrosis Factor-alpha and Insulin Sensitivity in Elderly Men With Non–Insulin-Dependent Diabetes Mellitus. **Arteriosclerosis, Thrombosis, and Vascular Biology** *18*, 1199-1202

Ninomiya-Tsuji, J., Kishimoto,K., Hiyama, A., Inou' J., Cao, Z. & Matsumoto, K. (1999) The kinase TAK1 can activate the NIK-IκB as well as the MAP kinase cascade in the IL-1 signalling pathway. **Nature** *398*, 252-256.

Nishitoh, H.,Saitoh, M.,Mochida, Y.,Takeda, K.,Nakano, H.,Rothe, M.,Miyazono, K. and Ichijo, H. (1998) ASK1 Is Essential for JNK/SAPK Activation by TRAF2. **Molecular Cell** *2*, 389-395

Nolan, G. P.,Fujita, T.,Bhatia, K.,Huppi, C.,Liou, H. C.,Scott, M. L. and Baltimore, D. (1993) The bcl-3 proto-oncogene encodes a nuclear I kappa B-like molecule that preferentially interacts with NF-kappa B p50 and p52 in a phosphorylation-dependent manner. **Mol. Cell. Biol.** *13*, 3557-3566

O'Dea, E. L.,Barken, D.,Peralta, R. Q.,Tran, K. T.,Werner, S. L.,Kearns, J. D.,Levchenko, A. and Hoffmann, A. (2007) A homeostatic model of IkappaB metabolism to control constitutive NF-kappaB activity. **Mol Syst Biol** *3*, 687-695

Oeth, P. A.,Parry, G. C.,Kunsch, C.,Nantermet, P.,Rosen, C. A. and Mackman, N. (1994) Lipopolysaccharide induction of tissue factor gene expression in monocytic cells is mediated by binding of c-Rel/p65 heterodimers to a kappa B-like site. **Mol. Cell. Biol.** *14*, 3772-3781

Ogryzko, V. V.,Schiltz, R. L.,Russanova, V.,Howard, B. H. and Nakatani, Y. (1996) The Transcriptional Coactivators p300 and CBP Are Histone Acetyltransferases. **Cell** *87*, 953-959

Ohkuma, Y.,Hashimoto, S.,Wang, C. K.,Horikoshi, M. and Roeder, R. G. (1995) Analysis of the role of TFIIE in basal transcription and TFIIH-mediated carboxy-terminal domain phosphorylation through structure-function studies of TFIIE-alpha. **Mol. Cell. Biol.** *15*, 4856-4866

Ohsawa, R.,Adkins, M. and Tyler, J. (2009) Epigenetic inheritance of an inducibly nucleosome-depleted promoter and its associated transcriptional state in the apparent absence of transcriptional activators. **Epigenetics & Chromatin** *2*, 11-22

Olave, I. A.,Reck-Peterson, S. L. and Crabtree, G. R. (2002) Nuclear actin and actin-related proteins in chromatin remodelling. **Annual Review of Biochemistry** *71*, 755-781

Opipari, A. W.,Boguski, M. S. and Dixit, V. M. (1990) The A20 cDNA induced by tumor necrosis factor alpha encodes a novel type of zinc finger protein. **Journal of Biological Chemistry** *265*, 14705-14708

Orange, J.S. and May, M.J. (2008) Cell penetrating peptide inhibitors of Nuclear Factor-kappa B. **Cell. Mol. Life Sci.** *65*, 3564-3591.

Orian, A.,Schwartz, A. L.,Israel, A.,Whiteside, S.,Kahana, C. and Ciechanover, A. (1999) Structural Motifs Involved in Ubiquitin-Mediated Processing of the NF-kappaB Precursor p105: Roles of the Glycine-Rich Region and a Downstream Ubiquitination Domain. **Molecular and Cellular Biology** *19*, 3664-3673

Orphanides, G.,LeRoy, G.,Chang, C.-H.,Luse, D. S. and Reinberg, D. (1998) FACT, a Factor that Facilitates Transcript Elongation through Nucleosomes. **Cell** *92*, 105-116

Orphanides, G.,Wu, W.-H.,Lane, W. S.,Hampsey, M. and Reinberg, D. (1999) The chromatin-specific transcription elongation factor FACT comprises human SPT16 and SSRP1 proteins. **Nature** *400*, 284-288

Ozsolak, F.,Song, J. S.,Liu, X. S. and Fisher, D. E. (2007) High-throughput mapping of the chromatin structure of human promoters. **Nat Biotech** *25*, 244-248

Palangat, M.,Renner, D. B.,Price, D. H. and Landick, R. (2005) A negative elongation factor for human RNA polymerase II inhibits the anti-arrest transcript-cleavage factor TFIIS. **Proceedings of the National Academy of Sciences of the United States of America** *102*, 15036-15041

Palmieri, C.,Roberts-Clark, D.,Assadi-Sabet, A.,Coope, R. C.,O'Hare, M.,Sunters, A.,Hanby, A.,Slade, M. J.,Gomm, J. J.,Lam, E. W. and Coombes, R. C. (2003) Fibroblast growth factor 7, secreted by breast fibroblasts, is an interleukin-1beta-induced paracrine growth factor for human breast cells. **Journal of Endocrinology** *177*, 65-81

Palombella, V. J.,Rando, O. J.,Goldberg, A. L. and Maniatis, T. (1994) The ubiquitinproteasome pathway is required for processing the NF-kappaB1 precursor protein and the activation of NF-kappaB. **Cell** *78*, 773-785

Pap, T.,Mueller-Ladner, U.,Gay, R. E. and Gay, S. (2000) Fibroblast biology: Role of synovial fibroblasts in the pathogenesis of rheumatoid arthritis. **Arthritis Res.** *2*, 361-367

Pardo, L.,Campillo, M.,Bosch, D.,Pastor, N. and Weinstein, H. (2000) Binding Mechanisms of TATA Box-Binding Proteins: DNA Kinking is Stabilized by Specific Hydrogen Bonds. **Biophysical Journal** *78*, 1988-1996

Paszek, P.,Ryan, S.,Ashall, L.,Sillitoe, K.,Harper, C. V.,Spiller, D. G.,Rand, D. A. and White, M. R. H. (2010) Population robustness arising from cellular heterogeneity. **Proceedings of the National Academy of Sciences** *107*, 11644-11649

Patterton, H. G. and Simpson, R. T. (1994) Nucleosomal location of the STE6 TATA box and Mat alpha 2p-mediated repression. **Mol. Cell. Biol.** *14*, 4002-4010

Pei, Y.,Hausmann, S. p.,Ho, C. K.,Schwer, B. and Shuman, S. (2001) The Length, Phosphorylation State, and Primary Structure of the RNA Polymerase II Carboxyl-terminal Domain Dictate Interactions with mRNA Capping Enzymes. **Journal of Biological Chemistry** *276*, 28075-28082

Perkins, N. D. (2006) Post-translational modifications regulating the activity and function of the nuclear factor kappa B pathway. **Oncogene** *25*, 6717-6730

Perkins, N. D.,Felzien, L. K.,Betts, J. C.,Leung, K.,Beach, D. H. and Nabel, G. J. (1997) Regulation of NF-kappaB by Cyclin-Dependent Kinases Associated with the p300 Coactivator. **Science** *275*, 523-527

Perkins, N. D.,Schmid, R. M.,Duckett, C. S.,Leung, K.,Rice, N. R. and Nabel, G. J. (1992) Distinct combinations of NF-kappa B subunits determine the specificity of transcriptional activation. **Proceedings of the National Academy of Sciences of the United States of America** *89*, 1529-1533

Perlmann, T. (1992) Glucocorticoid receptor DNA-binding specificity is increased by the organisation of DNA in nucleosomes. **Proceedings of the National Academy of Sciences** *89*, 3884-3888

Peterlin, B. M. and Price, D. H. (2006) Controlling the Elongation Phase of Transcription with P-TEFb. **Molecular Cell** *23*, 297-305

Phelps, C. B.,Sengchanthalangsy, L. L.,Malek, S. and Ghosh, G. (2000) Mechanism of IkappaB DNA binding by Rel/NF-kappaB dimers. **Journal of Biological Chemistry** *275*, 24392-24399

Pikarsky, E.,Porat, R. M.,Stein, I.,Abramovitch, R.,Amit, S.,Kasem, S.,Gutkovich-Pyest, E.,Urieli-Shoval, S.,Galun, E. and Ben-Neriah, Y. (2004) NF-kappaB functions as a tumour promoter in inflammation-associated cancer. **Nature** *431*, 461-466

Polach, K. J. and Widom, J. (1995) Mechanism of Protein Access to Specific DNA Sequences in Chromatin: A Dynamic Equilibrium Model for Gene Regulation. **Journal of Molecular Biology** *254*, 130-149

Polach, K. J. and Widom, J. (1996) A Model for the Cooperative Binding of Eukaryotic Regulatory Proteins to Nucleosomal Target Sites. **Journal of Molecular Biology** *258*, 800-812

Price, D. H. (2008) Poised Polymerases: On Your Mark...Get Set...Go! **Molecular Cell** *30*, 7-10

Pucadyil, T. and Chattopadhyay, A. (2006) Confocal Fluorescence Recovery After Photobleaching of Green Fluorescent Protein in Solution. **Journal of Fluorescence** *16*, 87-94

Rabut, G. and Ellenberg, J. (2004) Automatic real-time three-dimensional cell tracking by fluorescence microscopy. **Journal of Microscopy** *216*, 131-137

Radeff-Huang, J.,Seasholtz, T. M.,Chang, J. W.,Smith, J. M.,Walsh, C. T. and Brown, J. H. (2007) Tumor Necrosis Factor-Î±-stimulated Cell Proliferation Is Mediated through Sphingosine Kinase-dependent Akt Activation and Cyclin D Expression. **Journal of Biological Chemistry** *282*, 863-870

Rahl, P. B.,Lin, C. Y.,Seila, A. C.,Flynn, R. A.,McCuine, S.,Burge, C. B.,Sharp, P. A. and Young, R. A. (2010) c-Myc Regulates Transcriptional Pause Release. **Cell** *141*, 432-445

Raisner, R. M.,Hartley, P. D.,Meneghini, M. D.,Bao, M. Z.,Liu, C. L.,Schreiber, S. L.,Rando, O. J. and Madhani, H. D. (2005) Histone Variant H2A.Z Marks the 5' Ends of Both Active and Inactive Genes in Euchromatin. **Cell** *123*, 233-248

Raj, A.,Peskin, C. S.,Tranchina, D.,Vargas, D. Y. and Tyagi, S. (2006) Stochastic mRNA Synthesis in Mammalian Cells. **PLoS Biol** *4*, e309

Rajan, R. S.,Illing, M. E.,Bence, N. F. and Kopito, R. R. (2001) Specificity in intracellular protein aggregation and inclusion body formation. **Proceedings of the National Academy of Sciences** *98*, 13060-13065

Rajasingh, J.,Bord, E.,Luedemann, C.,Asai, J.,Hamada, H.,Thorne, T.,Qin, G.,Goukassian, D.,Zhu, Y.,Losordo, D. W. and Kishore, R. (2006) IL-10-induced TNF-alpha mRNA destabilisation is mediated via IL-10 suppression of p38 MAP kinase activation and inhibition of HuR expression. **The FASEB Journal** *20*, 2112-2114

Ramirez-Carrozzi, V. R.,Braas, D.,Bhatt, D. M.,Cheng, C. S.,Hong, C.,Doty, K. R.,Black, J. C.,Hoffmann, A.,Carey, M. and Smale, S. T. (2009) A Unifying Model for the Selective Regulation of Inducible Transcription by CpG Islands and Nucleosome Remodelling. **Cell** *138*, 114-128

Ramirez-Carrozzi, V. R.,Nazarian, A. A.,Li, C. C.,Gore, S. L.,Sridharan, R.,Imbalzano, A. N. and Smale, S. T. (2006) Selective and antagonistic functions of SWI/SNF and Mi-2 nucleosome remodelling complexes during an inflammatory response. **Genes & Development** *20*, 282-296

Rao, P. Hayden, M.S., Long, M., Scott, M.L. West, A.P., Zhang, D., Oeckinghaus, A., Lynch, C., Hoffmann, A., Baltimore, D. and Ghosh, S. (2010) IκBβ acts to inhibit and activate gene expression during the inflammatory response**. Nature** 466, 1115-1120.

Rasmussen, E. B. and Lis, J. T. (1995) Short Transcripts of the Ternary Complex Provide Insight into RNA Polymerase II Elongational Pausing. **Journal of Molecular Biology** *252*, 522-535

Ray, A. (2001) Response. **Nat. Immunology** *2*, 471-472.

Rebollo, A.,Dumoutier, L.,Renauld, J.-C.,Zaballos, A.,AyllÃ³n, V. n. and Martinez-A, C. (2000) Bcl-3 Expression Promotes Cell Survival following Interleukin-4 Deprivation and Is Controlled by AP1 and AP1-Like Transcription Factors. **Molecular and Cellular Biology** *20*, 3407-3416

Redon, C.,Pilch, D.,Rogakou, E.,Sedelnikova, O.,Newrock, K. and Bonner, W. (2002) Histone H2A variants H2AX and H2AZ. **Current Opinion in Genetics & Development** *12*, 162-169

Reines, D.,Ghanouni, P.,Li, Q. Q. and Mote, J. (1992) The RNA polymerase II elongation complex. Factor-dependent transcription elongation involves nascent RNA cleavage. **Journal of Biological Chemistry** *267*, 15516-15522

Richard, M.,Louahed, J.,Demoulin, J.-B. and Renauld, J.-C. (1999) Interleukin-9 Regulates NF-kappa B Activity Through BCL3 Gene Induction. **Blood** *93*, 4318-4327

Riemann, M.,Endres, R.,Liptay, S.,Pfeffer, K. and Schmid, R. M. (2005) The IkappaB Protein Bcl-3 Negatively Regulates Transcription of the IL-10 Gene in Macrophages. **J Immunol** *175*, 3560-3568

Rivas, M. n. A.,Carnevale, R. P.,Proietti, C. J.,Rosemblit, C.,Beguelin, W.,Salatino, M.,Charreau, E. H.,Frahm, I.,Sapia, S.,Brouckaert, P.,Elizalde, P. V. and Schillaci, R. (2008) TNFalpha acting on TNFR1 promotes breast cancer growth via p42/P44 MAPK, JNK, Akt and NF-kappaB-dependent pathways. **Experimental Cell Research** *314*, 509-529

Rodrigo, G. and Elena, S. F. (2011) Structural Discrimination of Robustness in Transcriptional Feedforward Loops for Pattern Formation. **PLoS ONE** *6*, e16904

Roeder, R. G. (2005) Transcriptional regulation and the role of diverse coactivators in animal cells. **FEBS Letters** *579*, 909-915

Roh, T.-Y.,Cuddapah, S.,Cui, K. and Zhao, K. (2006) The genomic landscape of histone modifications in human T cells. **Proceedings of the National Academy of Sciences** *103*, 15782-15787

Roh, T.-Y.,Cuddapah, S. and Zhao, K. (2005) Active chromatin domains are defined by acetylation islands revealed by genome-wide mapping. **Genes & Development** *19*, 542-552

Rougvie, A. E. and Lis, J. T. (1988) The RNA polymerase II molecule at the 52 end of the uninduced hsp70 gene of D. melanogaster is transcriptionally engaged. **Cell** *54*, 795-804

Roulis, M.,Armaka, M.,Manoloukos, M.,Apostolaki, M. and Kollias, G. (2011) Intestinal epithelial cells as producers but not targets of chronic TNF suffice to cause murine Crohn-like pathology. **Proceedings of the National Academy of Sciences** *108*, 5396-5401

Roy, A. L.,Du, H.,Gregor, P. D.,Novina, C. D.,Martinez, E. and Roeder, R. G. (1997) Cloning of an Inr- and E-box-binding protein, TFII-I, that interacts physically and functionally with USF1. **EMBO J** *16*, 7091-7104

Rundlett, S. E.,Carmen, A. A.,Kobayashi, R.,Bavykin, S.,Turner, B. M. and Grunstein, M. (1996) HDA1 and RPD3 are members of distinct yeast histone deacetylase complexes that regulate silencing and transcription. **Proceedings of the National Academy of Sciences** *93*, 14503-14508

Ryo, A.,Suizu, F.,Yoshida, Y.,Perrem, K.,Liou, Y.-C.,Wulf, G.,Rottapel, R.,Yamaoka, S. and Lu, K. P. (2003) Regulation of NF-Î°B Signalling by Pin1-Dependent Prolyl Isomerisation and Ubiquitin-Mediated Proteolysis of p65/RelA. **Molecular Cell** *12*, 1413-1426

Sabbah, M.,Kang, K. I.,Tora, L. and Redeuilh, G. (1998) Oestrogen receptor facilitates the formation of preinitiation complex assembly: involvement of the general transcription factor TFIIB. **Biochem. J.** *336*, 639-646

Saccani, S. and Natoli, G. (2002) Dynamic changes in histone H3 Lys 9 methylation occurring at tightly regulated inducible inflammatory genes. **Genes & Development** *16*, 2219-2224

Saccani, S.,Pantano, S. and Natoli, G. (2001) Two waves of nuclear factor κB recruitment to target promoters. **J Exp Med** *193*, 1351 - 1359

Saccani, S.,Pantano, S. and Natoli, G. (2003) Modulation of NF-kappaB Activity by Exchange of Dimers. *11*, 1563-1574

Sachdev, S.,Hoffmann, A. and Hannink, M. (1998) Nuclear Localisation of IkappaBalpha Is Mediated by the Second Ankyrin Repeat: the IkappaBalpha Ankyrin Repeats Define a Novel Class of cis-Acting Nuclear Import Sequences. **Molecular and Cellular Biology** *18*, 2524-2534

Saha, A.,Wittmeyer, J. and Cairns, B. R. (2005) Chromatin remodelling through directional DNA translocation from an internal nucleosomal site. **Nat Struct Mol Biol** *12*, 747-755

Saha, A.,Wittmeyer, J. and Cairns, B. R. (2006) Chromatin remodelling: the industrial revolution of DNA around histones. **Nat Rev Mol Cell Biol** *7*, 437-447

Sajan, S.A. and Hawkins, R.D. (2012) Methods for Identifying Higher-Order Chromatin Structure. **Annual Review of Genomics and Human Genetics** 13, 59-82.

Sakurai, H.,Chiba, H.,Miyoshi, H.,Sugita, T. and Toriumi, W. (1999) IkappaB Kinases Phosphorylate NF-kappaB p65 Subunit on Serine 536 in the Transactivation Domain. **Journal of Biological Chemistry** *274*, 30353-30356

Samkurashvili, I. and Luse, D. S. (1998) Structural Changes in the RNA Polymerase II Transcription Complex during Transition from Initiation to Elongation. **Mol. Cell. Biol.** *18*, 5343-5354

Sanjabi, S.,Hoffmann, A.,Liou, H.-C.,Baltimore, D. and Smale, S. T. (2000) Selective requirement for c-Rel during IL-12 P40 gene induction in macrophages. **Proceedings of the National Academy of Sciences** *97*, 12705-12710

Santee, S. M. and Owen-Schaub, L. B. (1996) Human Tumor Necrosis Factor Receptor p75/80 (CD120b) Gene Structure and Promoter Characterisation. **Journal of Biological Chemistry** *271*, 21151-21159

Sato, T.,Vries, R. G.,Snippert, H. J.,van de Wetering, M.,Barker, N.,Stange, D. E.,van Es, J. H.,Abo, A.,Kujala, P.,Peters, P. J. and Clevers, H. (2009) Single Lgr5 stem cells build crypt–villus structures in vitro without a mesenchymal niche. **Nature** *459*, 262-265

Savinova, O. V.,Hoffmann, A. and Ghosh, G. (2009) The NfκB1 and NfκB2 Proteins p105 and p100 Function as the Core of High-Molecular-Weight Heterogeneous Complexes. **Molecular Cell** *34*, 591-602

Sawarkar, R.,Sievers, C. and Paro, R. (2012) Hsp90 Globally Targets Paused RNA Polymerase to Regulate Gene Expression in Response to Environmental Stimuli. **Cell** *149*, 807-818

Saxonov, S.,Berg, P. and Brutlag, D. L. (2006) A genome-wide analysis of CpG dinucleotides in the human genome distinguishes two distinct classes of promoters. **Proceedings of the National Academy of Sciences of the United States of America** *103*, 1412-1417

Sch,nherr, E.,Hausser, H.-J. and Rgen (2000) Extracellular Matrix and Cytokines: A Functional Unit. **Developmental Immunology** *7*, 89-101

Schafer, D.,Gelles, J.,Sheetz, M. and Landick, R. (1991) Transcription by single molecules of RNA polymerase observed by light microscopy **Nature** *352*, 444-448

Schattner, A. (1994) Lymphokines in Autoimmunity--A Critical Review. **Clinical Immunology and Immunopathology** *70*, 177-189

Scheidereit, C. (2006) IkappaB kinase complexes: gateways to NF-kappaB activation and transcription. **Oncogene** *25*, 6685-6705

Schiraldi, M.,Raucci, A.,MuÃ±oz, L. M.,Livoti, E.,Celona, B.,Venereau, E.,Apuzzo, T.,De Marchis, F.,Pedotti, M.,Bachi, A.,Thelen, M.,Varani, L.,Mellado, M.,Proudfoot, A.,Bianchi, M. E. and Uguccioni, M. (2012) HMGB1 promotes recruitment of inflammatory cells to damaged tissues by forming a complex with CXCL12 and signalling via CXCR4. **The Journal of Experimental Medicine** *209*, 551-563

Schmittgen, T. D. and Livak, K. J. (2008) Analyzing real-time PCR data by the comparative CT method. **Nat. Protocols** *3*, 1101-1108

Schmitz, M. L.,Silva, M. A. d. S. and Baeuerle, P. A. (1995) Transactivation Domain 2 (TA) of p65 NF-B. **Journal of Biological Chemistry** *270*, 15576-15584

Schnitzler, G. (2008) Control of Nucleosome Positions by DNA Sequence and Remodelling Machines. **Cell Biochemistry and Biophysics** *51*, 67-80

Schnitzler, G. R.,Cheung, C. L.,Hafner, J. H.,Saurin, A. J.,Kingston, R. E. and Lieber, C. M. (2001) Direct Imaging of Human SWI/SNF-Remodeled Mono- and Polynucleosomes by Atomic Force Microscopy Employing Carbon Nanotube Tips. **Molecular and Cellular Biology** *21*, 8504-8511

Schones, D. E.,Cui, K.,Cuddapah, S.,Roh, T.-Y.,Barski, A.,Wang, Z.,Wei, G. and Zhao, K. (2008) Dynamic Regulation of Nucleosome Positioning in the Human Genome. **Cell** *132*, 887-898

Schwenger, P.,Skolnik, E. Y. and Vilcek, J. (1996) Inhibition of Tumor Necrosis Factor-induced p42/p44 Mitogen-Activated Protein Kinase Activation by Sodium Salicylate. **Journal of Biological Chemistry** *271*, 8089-8094

Scott, P. and Trinchieri, G. (1995) The role of natural killer cells in hostâ€"parasite interactions. **Current Opinion in Immunology** *7*, 34-40

Sedgwick, S. G. and Smerdon, S. J. (1999) The ankyrin repeat: a diversity of interactions on a common structural framework. **Trends in Biochemical Sciences** *24*, 311-316

Segal, E.,Fondufe-Mittendorf, Y.,Chen, L.,Thastrom, A.,Field, Y.,Moore, I. K.,Wang, J.-P. Z. and Widom, J. (2006) A genomic code for nucleosome positioning. **Nature** *442*, 772-778

Segil, N.,Guermah, M.,Hoffmann, A.,Roeder, R. G. and Heintz, N. (1996) Mitotic regulation of TFIID: inhibition of activator-dependent transcription and changes in subcellular localisation. **Genes & Development** *10*, 2389-2400

Sekinger, E. A.,Moqtaderi, Z. and Struhl, K. (2005) Intrinsic Histone-DNA Interactions and Low Nucleosome Density Are Important for Preferential Accessibility of Promoter Regions in Yeast. **Molecular Cell** *18*, 735-748

Sempowski, G. D.,Chess, P. R. and Phipps, R. P. (1997) CD40 is a functional activation antigen and B7-independent T cell costimulatory molecule on normal human lung fibroblasts. **The Journal of Immunology** *158*, 4670-4677

Sen, R. and Baltimore, D. (1986) Multiple nuclear factors interact with the immunoglobulin enhancer sequences. **Cell** *46*, 705-716

Serizawa, H.,Conaway, J. W. and Conaway, R. C. (1993) Phosphorylation of C-terminal domain of RNA polymerase II is not required in basal transcription **Nature** *363*, 543-550

Shahbazian, M. D. and Grunstein, M. (2007) Functions of Site-Specific Histone Acetylation and Deacetylation. **Annual Review of Biochemistry** *76*, 75-100

Shakhov, A. N.,Collart, M. A.,Vassalli, P.,Nedospasov, S. A. and Jongeneel, C. V. (1990) Kappa B-type enhancers are involved in lipopolysaccharide-mediated transcriptional activation of the tumor necrosis factor alpha gene in primary macrophages. **The Journal of Experimental Medicine** *171*, 35-47

Shames, B. D.,Selzman, C. H.,Meldrum, D. R.,Pulido, E. J.,Barton, H. A.,Meng, X.,Harken, A. H. and McLntyre, R. C., Jr. (1998) INTERLEUKIN-10 STABILIZES INHIBITORY κB-[alpha] IN HUMAN MONOCYTES. **Shock** *10*, 389-394

Shao-Cong, S. (2011) Non-canonical NF-κB signalling pathway. **Cell Research** *21*, 71-85

Sharma, M.,George, A. A.,Singh, B. N.,Sahoo, N. C. and Rao, K. V. S. (2007) Regulation of Transcript Elongation through Cooperative and Ordered Recruitment of Cofactors. **Journal of Biological Chemistry** *282*, 20887-20896

Shaw, G. and Kamen, R. (1986) A conserved AU sequence from the 3' untranslated region of GM-CSF mRNA mediates selective mRNA degradation. **Cell** *46*, 659-667

Shen, H.,Nelson, G.,Nelson, D. E.,Kennedy, S.,Spiller, D. G.,Griffiths, T.,Paton, N.,Oliver, S. G.,White, M. R. H. and Kell, D. B. (2006) Automated tracking of gene expression in individual cells and cell compartments. **Journal of The Royal Society Interface** *3*, 787-794

Shen, W.,Xu, C.,Huang, W.,Zhang, J.,Carlson, J. E.,Tu, X.,Wu, J. and Shi, Y. (2007) Solution Structure of Human Brg1 Bromodomain and Its Specific Binding to Acetylated Histone Tails. **Biochemistry** *46*, 2100-2110

Sheppard, K.-A.,Rose, D. W.,Haque, Z. K.,Kurokawa, R.,McInerney, E.,Westin, S.,Thanos, D.,Rosenfeld, M. G.,Glass, C. K. and Collins, T. (1999) Transcriptional Activation by NF-kappaB Requires Multiple Coactivators. **Molecular and Cellular Biology** *19*, 6367-6378

Shi, Y. (2007) Histone lysine demethylases: emerging roles in development, physiology and disease. **Nat Rev Genet** *8*, 829-833

Shim, E. Y.,Walker, A. K.,Shi, Y. and Blackwell, T. K. (2002) CDK-9/cyclin T (P-TEFb) is required in two postinitiation pathways for transcription in the C. elegans embryo. **Genes & Development** *16*, 2135-2146

Shizuya, H.,Birren, B.,Kim, U. J.,Mancino, V.,Slepak, T.,Tachiiri, Y. and Simon, M. (1992) Cloning and stable maintenance of 300-kilobase-pair fragments of human DNA in Escherichia coli using an F-factor-based vector. **Proceedings of the National Academy of Sciences** *89*, 8794-8797

Shu, U.,Demeure, C. E.,Byun, D. G.,Podlaski, F.,Stern, A. S. and Delespesse, G. (1994) Interleukin 12 exerts a differential effect on the maturation of neonatal and adult human CD45R0- CD4 T cells. **The Journal of Clinical Investigation** *94*, 1352-1358

Shuman, S. (2000) Structure, mechanism, and evolution of the mRNA capping apparatus. Volume 66, 1-40
Silkov, A.,Wolstein, O.,Shachar, I. and Dikstein, R. (2002) Enhanced Apoptosis of B and T Lymphocytes in TAFII105 Dominant-negative Transgenic Mice Is Linked to Nuclear Factor-kappaB. **Journal of Biological Chemistry** *277*, 17821-17829

Siller, E. N.,De Zwaan, D. C.,Anderson, J. F.,Freeman, B. C. and Barral, J. M. (2010) Slowing Bacterial Translation Speed Enhances Eukaryotic Protein Folding Efficiency. **Journal of Molecular Biology** *396*, 1310-1318

Sims, R. J.,Belotserkovskaya, R. and Reinberg, D. (2004) Elongation by RNA polymerase II: the short and long of it. **Genes & Development** *18*, 2437-2468

Smale, S. T. and Kadonaga, J. T. (2003) THE RNA POLYMERASE II CORE PROMOTER. **Annual Review of Biochemistry** *72*, 449-479

Smallie, T., Ricchetti, G., Horwood, N.J., Feldmann, M., Clark,. A.R. and Williams, L.M. (2010) IL-10 inhibtis transcription elongation of the human *TNF* gene in primary macrophages. **Journal Exp. Med.** 207, 2081-2088.

Smith, R. A. and Baglioni, C. (1987) The active form of tumor necrosis factor is a trimer. **Journal of Biological Chemistry** *262*, 6951-6954

Smith, R. S.,Smith, T. J.,Blieden, T. M. and Phipps, R. P. (1997) Fibroblasts as Sentinel Cells. **Am J Pathol** *151*, 317-322

Song, H. Y.,Ragnier, C. H.,Kirschning, C. J.,Goeddel, D. V. and Rothe, M. (1997) Tumor necrosis factor (TNF)-mediated kinase cascades: Bifurcation of Nuclear Factor-ÎºB and c-jun N-terminal kinase (JNK/SAPK) pathways at TNF receptor-associated factors. **Proceedings of the National Academy of Sciences** *94*, 9792-9796

Spence, J. R.,Mayhew, C. N.,Rankin, S. A.,Kuhar, M. F.,Vallance, J. E.,Tolle, K.,Hoskins, E. E.,Kalinichenko, V. V.,Wells, S. I.,Zorn, A. M.,Shroyer, N. F. and Wells, J. M. (2010) Directed differentiation of human pluripotent stem cells into intestinal tissue in vitro. **Nature** *470*, 105-109

Spiller, D. G.,Wood, C. D.,Rand, D. A. and White, M. R. H. (2010) Measurement of single-cell dynamics. **Nature** *465*, 736-745

Sterner, D. E. and Berger, S. L. (2000) Acetylation of Histones and Transcription-Related Factors. **Microbiology and Molecular Biology Reviews** *64*, 435-459

Stockley, P. and Persson, B. (2009) Surface Plasmon Resonance Assays of DNA-Protein Interactions. **Methods in Mol. Biol.** *543*, 653-669

Strebovsky, J.,Walker, P.,Lang, R. and Dalpke, A. H. (2011) Suppressor of cytokine signalling 1 (SOCS1) limits NFkappaB signalling by decreasing p65 stability within the cell nucleus. **The FASEB Journal** *25*, 863-874

Sullivan, D. E.,Ferris, M.,Nguyen, H.,Abboud, E. and Brody, A. R. (2009) TNF-α induces TGF-β1 expression in lung fibroblasts at the transcriptional level via AP-1 activation. **Journal of Cellular and Molecular Medicine** *13*, 1866-1876

Sun, M. and Fink, P. J. (2007) A New Class of Reverse Signalling Costimulators Belongs to the TNF Family. **The Journal of Immunology** *179*, 4307-4312

Sun, S. C.,Ganchi, P. A.,Ballard, D. W. and Greene, W. C. (1993) NF-kappa B controls expression of inhibitor IkappaB alpha: evidence for an inducible autoregulatory pathway. **Science** *259*, 1912-1915

Swinburne, I. A.,Miguez, D. G.,Landgraf, D. and Silver, P. A. (2008) Intron length increases oscillatory periods of gene expression in animal cells. **Genes & Development** *22*, 2342-2346

Szerlong, H. J.,Prenni, J. E.,Nyborg, J. K. and Hansen, J. C. (2010) Activator-dependent p300 Acetylation of Chromatin in Vitro. **Journal of Biological Chemistry** *285*, 31954-31964

Takada, H.,Chen, N.-J.,Mirtsos, C.,Suzuki, S.,Suzuki, N.,Wakeham, A.,Mak, T. W. and Yeh, W.-C. (2003) Role of SODD in Regulation of Tumor Necrosis Factor Responses. **Molecular and Cellular Biology** *23*, 4026-4033

Tang, H.,Liu, Y.,Madabusi, L. and Gilmour, D. S. (2000) Promoter-Proximal Pausing on the hsp70 Promoter in Drosophila melanogaster Depends on the Upstream Regulator. **Mol. Cell. Biol.** *20*, 2569-2580

Ten, R.,Paya, C.,Israel, N.,Le Bail, O.,Mattei, M.-G.,Virelizier, J.-L.,Kourilsky, P. and Israel, A. (1992) The characterisation of the promoter of the gene encoding the p50 subunit of NF-xB indicates that it participates in its own regulation. **EMBO J** *11*, 195-203

Thomas, J. O. and Travers, A. A. (2001) HMG1 and 2, and related architectural DNA-binding proteins. **Trends in Biochemical Sciences** *26*, 167-174

Tian, B.,Nowak, D. and Brasier, A. (2005) A TNF-induced gene expression program under oscillatory NF-kappaB control. **BMC Genomics** *6*, 137

Toualbi-Abed, K.,Daniel, F.,Galler, M. C.,Legrand, A. s.,Mauriz, J.-L.,Mauviel, A. and Bernuau, D. (2008) Jun D cooperates with p65 to activate the proximal kappaB site of the cyclin D1 promoter: role of PI3K/PDK-1. **Carcinogenesis** *29*, 536-543

Tsai, F. T. F. and Sigler, P. B. (2000) Structural basis of preinitiation complex assembly on human Pol II promoters. **EMBO J** *19*, 25-36

Tsien, R. Y. (1998) The green flurorescent protein. **Annual Review of Biochemistry** *67*, 509-544

Tsytsykova, A. V.,Falvo, J. V.,Schmidt-Supprian, M.,Courtois, G.,Thanos, D. and Goldfeld, A. E. (2007) Post-induction, Stimulus-specific Regulation of Tumor Necrosis Factor mRNA Expression. **Journal of Biological Chemistry** *282*, 11629-11638

Turner, D. A.,Paszek, P.,Woodcock, D. J.,Nelson, D. E.,Horton, C. A.,Wang, Y.,Spiller, D. G.,Rand, D. A.,White, M. R. H. and Harper, C. V. (2010) Physiological levels of TNFalpha stimulation induce stochastic dynamics of NF-kappaB responses in single living cells. **Journal of Cell Science** *123*, 2834-2843

Udalova, I. A.,Knight, J. C.,Vidal, V.,Nedospasov, S. A. and Kwiatkowski, D. (1998) Complex NF-kappaB Interactions at the Distal Tumor Necrosis Factor Promoter Region in Human Monocytes. **Journal of Biological Chemistry** *273*, 21178-21186

Udalova, I. A.,Richardson, A.,Denys, A.,Smith, C.,Ackerman, H.,Foxwell, B. and Kwiatkowski, D. (2000) Functional Consequences of a Polymorphism Affecting NF-kappa B p50-p50 Binding to the TNF Promoter Region. **Mol. Cell. Biol.** *20*, 9113-9119

Uhal, B. D.,Ramos, C.,Joshi, I.,Bifero, A.,Pardo, A. and Selman, M. (1998) Cell size, cell cycle, and smooth muscle actin expression by primary human lung fibroblasts. **American Journal of Physiology - Lung Cellular and Molecular Physiology** *275*, L998-L1005

Urban, M. B. and Baeuerle, P. A. (1990) The 65-kD subunit of NF-kappa B is a receptor for I kappa B and a modulator of DNA-binding specificity. **Genes & Development** *4*, 1975-1984

Utley, R. T.,Ikeda, K.,Grant, P. A.,Cote, J.,Steger, D. J.,Eberharter, A.,John, S. and Workman, J. L. (1998) Transcriptional activators direct histone acetyltransferase complexes to nucleosomes. **Nature** *394*, 498-502

Vallabhapurapu, S. and Karin, M. (2009) Regulation and Function of NF-kappaB Transcription Factors in the Immune System. **Annual Review of Immunology** *27*, 693-733

Van Antwerp, D. J.,Martin, S. J.,Kafri, T.,Green, D. R. and Verma, I. M. (1996) Suppression of TNF-alpha Induced Apoptosis by NF-kappaB. **Science** *274*, 787-789

Vassalli, P. (1992) The Pathophysiology of Tumor Necrosis Factors. **Annual Review of Immunology** *10*, 411-452

Vermeulen, M.,Mulder, K. W.,Denissov, S.,Pijnappel, W. W. M. P.,van Schaik, F. M. A.,Varier, R. A.,Baltissen, M. P. A.,Stunnenberg, H. G.,Mann, M. and Timmers, H. T. M. (2007) Selective Anchoring of TFIID to Nucleosomes by Trimethylation of Histone H3 Lysine 4. **Cell** *131*, 58-69

Viatour, P.,Dejardin, E.,Warnier, M.,Lair, F.,Claudio, E.,Bureau, F.,Marine, J.-C.,Merville, M.-P.,Maurer, U.,Green, D.,Piette, J.,Siebenlist, U.,Bours, V. and Chariot, A. (2004) GSK3-Mediated BCL-3 Phosphorylation Modulates Its Degradation and Its Oncogenicity. **Molecular Cell** *16*, 35-45

Voelkel, P. and Angrand, P.-O. (2007) The control of histone lysine methylation in epigenetic regulation. **Biochimie** *89*, 1-20

Wada, T.,Takagi, T.,Yamaguchi, Y.,Ferdous, A.,Imai, T.,Hirose, S.,Sugimoto, S.,Yano, K.,Hartzog, G. A.,Winston, F.,Buratowski, S. and Handa, H. (1998) DSIF, a novel transcription elongation factor that regulates RNA polymerase II processivity, is composed of human Spt4 and Spt5 homologs. **Genes & Development** *12*, 343-356

Wada, T.,Takagi, T.,Yamaguchi, Y.,Watanabe, D. and Handa, H. (1998) Evidence that P-TEFb alleviates the negative effect of DSIF on RNA polymerase II-dependent transcription in vitro. **EMBO J** *17*, 7395-7403

Wajant, H.,Pfizenmaier, K. and Scheurich, P. (2003) Tumor necrosis factor signalling. **Cell Death Differ** *10*, 45-65

Wan, F.,Anderson, D. E.,Barnitz, R. A.,Snow, A.,Bidere, N.,Zheng, L.,Hegde, V.,Lam, L. T.,Staudt, L. M.,Levens, D.,Deutsch, W. A. and Lenardo, M. J. (2007) Ribosomal Protein S3: A KH Domain Subunit in NF-kappaB Complexes that Mediates Selective Gene Regulation. **Cell** *131*, 927-939

Wang, C.-Y.,Mayo, M. W. and Baldwin, A. S. (1996) TNF- and Cancer Therapy-Induced Apoptosis: Potentiation by Inhibition of NF-kappaB. **Science** *274*, 784-787

Wang, C., Deng, L., Hong, M., Akkaraju, G.R., Inoue, J., and Chen, Z.J. (2001). TAK1 is a ubiquitin-dependent kinase of MKK and IKK. **Nature** 412, 346–351.

Wang, H. and Chong, S. (2003) Visualisation of coupled protein folding and binding in bacteria and purification of the heterodimeric complex. **Proceedings of the National Academy of Sciences** *100*, 478-483

Wang, H. and Ma, S. (2008) The cytokine storm and factors determining the sequence and severity of organ dysfunction in multiple organ dysfunction syndrome. **The American Journal of Emergency Medicine** *26*, 711-715

Wang, J. C. (1979) Helical repeat of DNA in solution. **Proceedings of the National Academy of Sciences** *76*, 200-203

Wanidworanun, C. and Strober, W. (1993) Predominant role of tumor necrosis factor-alpha in human monocyte IL-10 synthesis. **J Immunol** *151*, 6853-6861

Wen, Y. and Shatkin, A. J. (1999) Transcription elongation factor hSPT5 stimulates mRNA capping. **Genes & Development** *13*, 1774-1779

Wessells, J.,Baer, M.,Young, H. A.,Claudio, E.,Brown, K.,Siebenlist, U. and Johnson, P. F. (2004) BCL-3 and NF-kappaB p50 Attenuate Lipopolysaccharide-induced Inflammatory Responses in Macrophages. **Journal of Biological Chemistry** *279*, 49995-50003

Westerheide, S. D.,Mayo, M. W.,Anest, V.,Hanson, J. L. and Baldwin, A. S. (2001) The putative oncoprotein Bcl-3 induces cyclin d1 to stimulate G(1) transition. **Molecular and Cellular Biology** *21*, 8428-8436

Wiig, H.,Tenstad, O.,Iversen, P.,Kalluri, R. and Bjerkvig, R. (2010) Interstitial Fluid: the overlooked component of the tumour microenvironment? **Fibrogenesis & Tissue Repair** *3*, 3-12

Wong, J.,Shi, Y. B. and Wolffe, A. P. (1997) Determinants of chromatin disruption and transcriptional regulation instigated by the thyroid hormone receptor: hormone regulated chromatin disruption is not sufficient for transcriptional activation. **EMBO J** *16*, 3158-3171

Wu, C.-H.,Yamaguchi, Y.,Benjamin, L. R.,Horvat-Gordon, M.,Washinsky, J.,Enerly, E.,Larsson, J.,Lambertsson, A.,Handa, H. and Gilmour, D. (2003) NELF and DSIF cause promoter proximal pausing on the hsp70 promoter in Drosophila. **Genes & Development** *17*, 1402-1414

Wu, C. and Ghosh, S. (2003) Differential Phosphorylation of the Signal-responsive Domain of IÎºBÎ± and IÎºBÎ² by IÎºB Kinases. **Journal of Biological Chemistry** *278*, 31980-31987

Wu, H.,Min, J.,Lunin, V. V.,Antoshenko, T.,Dombrovski, L.,Zeng, H.,Allali-Hassani, A.,Campagna-Slater, V. R.,Vedadi, M.,Arrowsmith, C. H.,Plotnikov, A. N. and Schapira, M. (2010) Structural Biology of Human H3K9 Methyltransferases. **PLoS ONE** *5*, e8570

Wu, J. and Snyder, M. (2008) RNA polymerase II stalling: loading at the start prepares genes for a sprint. **Genome Biology** *9*, 220

Wulczyn, F. G.,Hataba, E. N.,Naumann, M.,Nieters, A.,Nucifora, G.,McKiethan, T. W. and Scheidereit, C. (1992) The ankyrin repeat domains of the NF-kappaB precursors p105 and the proto-oncogene BCL-3 act as specific inhibitors of NF-kappaB DNA binding. **Journal of Cellular Biochemistry Supplement** 195

Wysocka, J.,Swigut, T.,Xiao, H.,Milne, T. A.,Kwon, S. Y.,Landry, J.,Kauer, M.,Tackett, A. J.,Chait, B. T.,Badenhorst, P.,Wu, C. and Allis, C. D. (2006) A PHD finger of NURF couples histone H3 lysine 4 trimethylation with chromatin remodelling. **Nature** *442*, 86-90

Xiong, W. and Ferrell, J. E. (2003) A positive-feedback-based bistable `memory module' that governs a cell fate decision. **Nature** *426*, 460-465

Xu, F.,Zhang, K. and Grunstein, M. (2005) Acetylation in Histone H3 Globular Domain Regulates Gene Expression in Yeast. **Cell** *121*, 375-385

Yamada, T.,Yamaguchi, Y.,Inukai, N.,Okamoto, S.,Mura, T. and Handa, H. (2006) P-TEFb-Mediated Phosphorylation of hSpt5 C-Terminal Repeats Is Critical for Processive Transcription Elongation. **Molecular Cell** *21*, 227-237

Yamaguchi, Y.,Wada, T.,Watanabe, D.,Takagi, T.,Hasegawa, J. and Handa, H. (1999) Structure and Function of the Human Transcription Elongation Factor DSIF. **Journal of Biological Chemistry** *274*, 8085-8092

Yamit-Hezi, A.,Nir, S.,Wolstein, O. and Dikstein, R. (2000) Interaction of TAFII105 with Selected p65/RelA Dimers Is Associated with Activation of Subset of NF-kappaB Genes. **Journal of Biological Chemistry** *275*, 18180-18187

Yang, X.-J.,Ogryzko, V. V.,Nishikawa, J.-i.,Howard, B. H. and Nakatani, Y. (1996) A p300/CBP-associated factor that competes with the adenoviral oncoprotein E1A. **Nature** *382*, 319-324

Yang, X. W.,Model, P. and Heintz, N. (1997) Homologous recombination based modification in Esherichia coli and germline transmission in transgenic mice of a bacterial artificial chromsome. **Nat Biotech** *15*, 859-865

Yao, J.,Mackman, N.,Edgington, T. S. and Fan, S.-T. (1997) Lipopolysaccharide Induction of the Tumor Necrosis Factor-alpha Promoter in Human Monocytic Cells. **Journal of Biological Chemistry** *272*, 17795-17801

Yilmaz, Z. B.,Weih, D. S.,Sivakumar, V. and Weih, F. (2003) RelB is required for Peyer's patch development: differential regulation of p52-RelB by lymphotoxin and TNF. **EMBO J** *22*, 121-130

Youngchang Kim,James. H. Geiger,&, S. H. and Sigler, P. B. (1993) Crystal structure of a yeast TBP/TATA-box complex. **Nature** *365*, 312-320

Yu, D.,Ellis, H. M.,Lee, E. C.,Jenkins, N. A.,Copeland, N. G. and Court, D. L. (2000) An efficient recombination system for chromosome engineering in Escherichia coli. **Proceedings of the National Academy of Sciences of the United States of America** *97*, 5978-5983

Yu, J.,Li, Y.,Ishizuka, T.,Guenther, M. G. and Lazar, M. A. (2003) A SANT motif in the SMRT corepressor interprets the histone code and promotes histone deacetylation. **EMBO J** *22*, 3403-3410

Yuan, G.-C.,Liu, Y.-J.,Dion, M. F.,Slack, M. D.,Wu, L. F.,Altschuler, S. J. and Rando, O. J. (2005) Genome-Scale Identification of Nucleosome Positions in S. cerevisiae. **Science** *309*, 626-630

Yunger, S.,Rosenfeld, L.,Garini, Y. and Shav-Tal, Y. (2010) Single-allele analysis of transcription kinetics in living mammalian cells **Nat Methods** *7*, 631-633

Zabel, U. and Baeuerle, P. A. (1990) Purified human IkappaB can rapidly dissociate the complex of the NF-kappaB transcription factor with its cognate DNA. **Genes Dev** *61*, 255-265

Zandi, E.,Chen, Y. and Karin, M. (1998) Direct Phosphorylation of IkappaB by IKKalpha and IKKbeta Discrimination Between Free and NF-kappaB-Bound Substrate. **Science** *281*, 1360-1363

Zhang, H. and Reese, J. C. (2007) Exposing the core promoter is sufficient to activate transcription and alter coactivator requirement at RNR3. **Proceedings of the National Academy of Sciences** *104*, 8833-8838

Zhang, J. D.,Chang, C. C.,Lombardi, L. and Dallafavera, R. (1994) Rearranged NFKB2 gene in the HUT78 T-Lymphoma cell-line codes for a constitutively nuclear factor lacking transcriptional repressor functions. **Oncogene** *9*, 1931-1937

Zhang, Q.,Chakravarty, S.,Ghersi, D.,Zeng, L.,Plotnikov, A. N.,Sanchez, R. and Zhou, M.-M. (2010) Biochemical Profiling of Histone Binding Selectivity of the Yeast Bromodomain Family. **PLoS ONE** *5*, e8903

Zhang, Q.,Didonato, J. A.,Karin, M. and McKeithan, T. W. (1994) BCL3 encodes a nuclear protein which can alter the subcellular location of NF-kappaB proteins. **Molecular and Cellular Biology** *14*, 3915-3926

Zhang, Y.,Cao, H. J.,Graf, B.,Meekins, H.,Smith, T. J. and Phipps, R. P. (1998) Cutting Edge: CD40 Engagement Up-Regulates Cyclooxygenase-2 Expression and Prostaglandin E2 Production in Human Lung Fibroblasts. **The Journal of Immunology** *160*, 1053-1057

Zhao, W.,Wang, L.,Zhang, M.,Wang, P.,Zhang, L.,Yuan, C.,Qi, J.,Qiao, Y.,Kuo, P. C. and Gao, C. (2011) NF-kappaB and AP-1 Mediated DNA Looping Regulates Osteopontin Transcription in Endotoxin-Stimulated Murine Macrophages. **The Journal of Immunology** *186*, 3173-3179

Zheng, S.,Brown, M. C. and Taffet, S. M. (1993) Lipopolysaccharide stimulates both nuclear localisation of the nuclear factor kappa B 50-kDa subunit and loss of the 105-kDa precursor in RAW264 macrophage-like cells. **Journal of Biological Chemistry** *268*, 17233-17239

Zhong, H.,May, M. J.,Jimi, E. and Ghosh, S. (2002) The Phosphorylation Status of Nuclear NF-kappaB Determines Its Association with CBP/p300 or HDAC-1. **Molecular Cell** *9*, 625-636

Zhong, H.,Voll, R. E. and Ghosh, S. (1998) Phosphorylation of NF-kappaB p65 by PKA Stimulates Transcriptional Activity by Promoting a Novel Bivalent Interaction with the Coactivator CBP/p300. **Molecular Cell** *1*, 661-671

Zhu, W.,Brauchle, M. A.,Di Padova, F.,Gram, H.,New, L.,Ono, K.,Downey, J. S. and Han, J. (2001) Gene suppression by tristetraprolin and release by the p38 pathway. **American Journal of Physiology - Lung Cellular and Molecular Physiology** *281*, L499-L508

Zhu, Y. X.,Kang, L. Y.,Luo, W.,Li, C.-C. H.,Yang, L. and Yang, Y.-C. (1996) Multiple Transcription Factors Are Required for Activation of Human Interleukin 9 Gene in T Cells. **Journal of Biological Chemistry** *271*, 15815-15822

Ziegler-Heitbrock, H. W.,Sternsdorf, T.,Liese, J.,Belohradsky, B.,Weber, C.,Wedel, A.,Schreck, R.,Bauerle, P. and Strobel, M. (1993) Pyrrolidine dithiocarbamate inhibits NF-kappa B mobilisation and TNF production in human monocytes. **J Immunol** *151*, 6986-6993